



Discrete-time LPV Gain-scheduling Controllers for the Rejection of Harmonic Disturbances

Doctoral Thesis

to be awarded the degree
Doctor of Engineering (Dr.-Ing.)

Submitted by
Pablo Ballesteros Pazó
from Vigo (Spain)

Approved by the
Faculty of Mathematics/Computer Science
and Mechanical Engineering
Clausthal University of Technology

Date of oral examination
November 2, 2015

Chairperson of the Board of Examiners
Prof. Dr.-Ing. Stefan Hartmann

Chief Reviewer
Prof. Dr.-Ing. Christian Bohn

Reviewer
Prof. Dr.-Ing. Ferdinand Svaricek

Contents

Nomenclature	iii
1 Introduction and Motivation	1
1.1 Control Approaches	1
1.2 Stability Considerations	3
1.3 Implementation Aspects	4
1.4 Thesis Outline	5
2 Internal-model-principle-based Control	7
2.1 LTI Controller Structures	9
2.1.1 Observer Based Control Structures	9
2.1.2 Output Feedback Control Structure	19
3 LPV Gain-scheduling Control	29
3.1 pLPV Systems	30
3.2 pLPV Control Structure	32
3.2.1 pLPV Gain-scheduling Observer-Based Control Structure	33
3.2.2 pLPV Gain-scheduling Output-Feedback Control Structure	38
3.3 LFT Systems	39
3.4 LFT Control Structure	41
3.4.1 LFT Gain-scheduling Output Feedback Control Structure	41
4 LPV Gain-scheduling Control for Harmonic Disturbances with Time-varying Frequencies	45
4.1 LPV Disturbance Model	45
4.1.1 pLPV Disturbance Model	50
4.1.2 LFT Disturbance Model	58
4.1.3 Disturbance Observer Control Design	61
4.1.4 Error Filter Control Design	65
4.1.5 Output Feedback Control Design	68
4.1.6 Switching Control Strategy	75
4.1.7 LFT Control Design	85
5 Experimental Results	93
5.1 AVC Golf VI Experimental Setup	93
5.2 AVC Test Bed Experimental Setup	95
5.3 ANC Test Bed Experimental Setup	96
5.3.1 Golf VI Variant	97
5.3.2 AVC Test Bed	100
5.4 pLPV Error Filter Controller Experimental Results	102

Contents

5.5	LFT Controller Experimental Results	104
5.6	Switching Control Strategy Results	106
6	Summary and Conclusions	109
A	LTI Control Design	111
A.1	Linear Fractional Transformation	111
A.2	Schur Complement	112
A.3	H_2 -norm for discrete-time systems	112
A.4	H_2 state-feedback control for discrete-time systems	113
A.5	H_∞ -norm for discrete-time systems	115
References		119

Nomenclature

Acronyms

ANC	Active noise control.
AVC	Active vibration control.
do	Disturbance observer.
ef	Error filter.
FxLMS	Filtered-x least mean squares.
IMP	Internal model principle.
LFT	Linear fractional transformation.
LMI	Linear matrix inequality.
LPV	Linear parameter varying.
LQR	Linear quadratic regulator.
of	Output feedback.
pLPV	Polytopic linear parameter varying.

Variables

a	Constant scalar.
$a_{i,0}, \dots, a_{i,N_p}$	Constant scalars used for the polynomial approximation.
a_k	Time-varying scalar.
a_0, a_1, a_2, a_3	Constant scalars.
\mathbf{A}	Constant system matrix.
\mathbf{A}	Auxiliar matrix.
$\mathbf{A}_c(\boldsymbol{\theta}_k)$	Time-varying system matrix of the controller.
$\mathbf{A}_{c,v,j} = \mathbf{A}_c(\boldsymbol{\theta}_{v,j})$	System matrices of the vertices.
\mathbf{A}_{cl}	Closed-loop system matrix.
\mathbf{A}_d	Constant system matrix of the disturbance model.
$\mathbf{A}_{d,k} = \mathbf{A}_d(\boldsymbol{\theta}_k)$	Time-varying system matrix.
\mathbf{A}_{do}	Constant system matrix of the augmented system combining plant and disturbance model.
$\mathbf{A}_{d_{1,k}}, \dots, \mathbf{A}_{d_{n_d,k}}$	Auxiliar matrices to build the system matrix of the disturbance model.
$\tilde{\mathbf{A}}_{d_{1,k}}, \dots, \tilde{\mathbf{A}}_{d_{n_d,k}}$	Auxiliar matrices to build the system matrix of the disturbance model.
$\mathbf{A}_{do,k} = \mathbf{A}_{do}(\boldsymbol{\theta}_k)$	Time-varying system matrix of the augmented system built with plant and disturbance model.
$\mathbf{A}_{do,v,j} = \mathbf{A}_{do}(\boldsymbol{\theta}_{v,j})$	Vertex system matrices of the augmented system built with plant and disturbance model.

Nomenclature

\mathbf{A}_{doc}	Constant system matrix of the disturbance observer controller.
$\mathbf{A}_{\text{doc}, k} = \mathbf{A}_{\text{doc}}(\boldsymbol{\theta}_k)$	Time-varying system matrix of the disturbance observer controller.
$\mathbf{A}_{\text{doc, v}, j} = \mathbf{A}_{\text{doc}}(\boldsymbol{\theta}_{\text{v}, j})$	System matrices of the vertices for the disturbance observer controller.
\mathbf{A}_{ef}	System matrix of the error filter approach.
$\mathbf{A}_{\text{ef}, k} = \mathbf{A}_{\text{ef}}(\boldsymbol{\theta}_k)$	Time-varying system matrix of the error filter approach.
$\mathbf{A}_{\text{ef, v}, j} = \mathbf{A}_{\text{ef}}(\boldsymbol{\theta}_{\text{v}, j})$	System matrices of the vertices for the error filter approach.
\mathbf{A}_{efc}	Constant system matrix of the error-filter controller.
$\mathbf{A}_{\text{efc}, k} = \mathbf{A}_{\text{efc}}(\boldsymbol{\theta}_k)$	Time-varying system matrix of the error-filter controller.
$\mathbf{A}_{\text{efc, v}, j} = \mathbf{A}_{\text{efc}}(\boldsymbol{\theta}_{\text{v}, j})$	System matrices of the vertices for the error-filter controller.
$\mathbf{A}_k = \mathbf{A}(\boldsymbol{\theta}_k)$	Time-varying system matrix.
$\mathbf{A}_{\text{of, v}, j} = \mathbf{A}_{\text{of}}(\boldsymbol{\theta}_{\text{v}, j})$	System matrices of the vertices for the polytopic output feedback approach.
\mathbf{A}_p	Constant system matrix of the plant.
$\mathbf{A}_{\text{v}, j} = \mathbf{A}(\boldsymbol{\theta}_{\text{v}, j})$	System matrices of the vertices.
\mathbf{A}_{W_u}	System matrix of the weighting function for the input.
\mathbf{A}_{W_y}	System matrix of the weighting function for the output.
$\mathbf{A}^{(K)}$	System matrix of the output feedback controller.
\mathbf{A}_0	System matrix of the LFT state-space representation.
$\mathbf{A}_0^{(K)}$	System matrix of the LFT state-space representation of the controller.
\mathbf{A}_1	System matrix to obtain the closed-loop state representation.
$\mathcal{A}_0, \dots, \mathcal{A}_N$	Auxiliar constant matrices for a polytopic representation of a system.
$\mathbf{b}_{i, \min} = [b_{i, \min, 1} \dots b_{i, \min, N_p}]^T$	Auxiliar vector for the pLPV interpolation.
$b_{i, 0}, \dots, b_{i, N_p}$	Constant scalars used for the polynomial approximation.
b_1, b_2	Constant scalars.
$\mathbf{B}(\boldsymbol{\theta}_k)$	Time-varying state-space matrix.
$\underline{\mathbf{B}}, \underline{\mathbf{B}}$	Auxiliar matrices.
$\mathbf{B}_c(\boldsymbol{\theta}_k)$	Time-varying state-space matrix of the controller.
$\mathbf{B}_{c, \text{v}, j} = \mathbf{B}_c(\boldsymbol{\theta}_{\text{v}, j})$	Controller state-space matrices of the vertices.
\mathbf{B}_{cl}	State-space matrix of the closed-loop system.
\mathbf{B}_d	State-space matrix of the disturbance model.

$\mathbf{B}_{d_1}, \dots, \mathbf{B}_{d_n}$	Auxiliar matrices to build a state-space representation of the disturbance model.
$\mathbf{B}_{d,\theta}$	State-space matrix for the LFT representation of the disturbance model.
\mathbf{B}_{do}	State-space matrix of the augmented system built with plant and disturbance model.
\mathbf{B}_{doc}	State-space matrix of the disturbance observer controller.
$\mathbf{B}_{doc,k}$	Time-varying state-space matrix of the disturbance observer controller.
\mathbf{B}_{ef}	State-space matrix of the augmented system built with error filter and plant.
\mathbf{B}_{efc}	State-space matrix of the error-filter controller.
$\mathbf{B}_{of,v,j} = \mathbf{B}_{of}(\boldsymbol{\theta}_{v,j})$	State-space matrices of the vertices for the output-feedback approach.
\mathbf{B}_p	State-space matrix of the plant.
\mathbf{B}_u	State-space matrix of the generalized plant.
$\mathbf{B}_{v,j} = \mathbf{B}(\boldsymbol{\theta}_{v,j})$	State-space matrix of the vertices.
\mathbf{B}_w	State-space matrix of the generalized plant.
\mathbf{B}_{W_u}	State-space matrix of the weighting function for the input.
\mathbf{B}_{W_y}	State-space matrix of the weighting function for the output.
$\mathbf{B}_y^{(K)}$	State-space matrix of the output-feedback controller.
\mathbf{B}_θ	State-space matrix of the LFT generalized plant.
$\mathbf{B}_\theta^{(K)}$	State-space matrix of the LFT controller.
$\mathbf{B}_1, \mathbf{B}_2$	Auxiliar matrices to build the closed-loop system.
$\mathcal{B}_0, \dots, \mathcal{B}_N$	Auxiliar matrices to build a pLPV representation.
$c_{i,\max,k}, c_{i,\min,k}$	Auxiliar scalars to calculate the pLPV interpolation.
$\mathbf{C}(\boldsymbol{\theta}_k)$	Time-varying state-space matrix.
$\bar{\mathbf{C}}, \underline{\mathbf{C}}$	Auxiliar matrices.
$\mathbf{C}_c(\boldsymbol{\theta}_k)$	Time-varying state-space matrix of the controller.
$\mathbf{C}_{c,v,j} = \mathbf{C}_c(\boldsymbol{\theta}_{v,j})$	Controller state-space matrices of the vertices.
\mathbf{C}_{cl}	State-space matrix of the closed-loop system.
\mathbf{C}_d	State-space matrix of the disturbance model.
$\mathbf{C}_{d_1}, \dots, \mathbf{C}_{d_n}$	Auxiliar matrices to build a state-space representation of the disturbance model.
\mathbf{C}_{do}	State-space matrix of the augmented system built with plant and disturbance model.
\mathbf{C}_{doc}	State-space matrix of the disturbance observer controller.
\mathbf{C}_{ef}	State-space matrix of the augmented system built with error filter and plant.
\mathbf{C}_{efc}	State-space matrix of the error-filter controller.
$\mathbf{C}_{efc,k} = \mathbf{C}_{efc}(\boldsymbol{\theta}_k)$	Time-varying state-space matrix of the error-filter controller.

Nomenclature

$\mathbf{C}_{\text{efc}, \text{v}, j} = \mathbf{C}_{\text{efc}}(\boldsymbol{\theta}_{\text{v}, j})$	State-space matrices of the vertices for the error-filter controller.
$\mathbf{C}_{\text{of}, \text{v}, j} = \mathbf{C}_{\text{of}}(\boldsymbol{\theta}_{\text{v}, j})$	State-space matrices of the vertices for the output-feedback approach.
\mathbf{C}_p	State-space matrix of the plant.
$\mathbf{C}_q, \mathbf{C}_y$	State-space matrices of the generalized plant.
$\mathbf{C}_{\text{v}, j} = \mathbf{C}(\boldsymbol{\theta}_{\text{v}, j})$	State-space matrix of the vertices.
\mathbf{C}_{W_u}	State-space matrix of the weighting function for the input.
\mathbf{C}_{W_y}	State-space matrix of the weighting function for the output.
$\mathbf{C}_u^{(K)}$	State-space matrix of the output-feedback controller.
\mathbf{C}_θ	State-space matrix of the LFT generalized plant.
$\mathbf{C}_\theta^{(K)}$	State-space matrix of the LFT controller.
$\mathbf{C}_1, \mathbf{C}_2$	Auxiliar matrices to build the closed-loop system.
$\mathcal{C}_0, \dots, \mathcal{C}_N$	Auxiliar matrices to build a pLPV representation.
\mathbf{D}_{cl}	State-space matrix of the closed-loop system.
\mathbf{D}_d	State-space matrix of the disturbance model.
$\mathbf{D}_{\text{of}, \text{v}, j}$	State-space matrix of the vertices for the output-feedback pLPV approach.
\mathbf{D}_p	State-space matrix of the plant.
$\mathbf{D}_{qu}, \mathbf{D}_{qw}$	State-space matrices of the generalized plant.
$\underline{\mathbf{D}}_{qu}$	Auxiliar matrix.
$\mathbf{D}_{uy}^{(K)}, \mathbf{D}_{u\theta}^{(K)}$	State-space matrices for the LFT representation of the controller.
$\mathbf{D}_{wu}, \mathbf{D}_{wy}$	State-space matrices of the weighting functions.
$\mathbf{D}_{yw}, \mathbf{D}_{yu}$	State-space matrices of the generalized plant.
$\underline{\mathbf{D}}_{yw}$	Auxiliar matrix.
$\mathbf{D}_{y\theta}$	State-space matrix of the generalized plant.
$\mathbf{D}_{\theta u}, \mathbf{D}_{\theta\theta}, \mathbf{D}_{\theta w}$	State-space matrices of the generalized plant.
$\mathbf{D}_{\theta\theta}^{(K)}, \mathbf{D}_{\theta y}^{(K)}$	State-space matrices of the LFT controller.
$\mathbf{D}_{11}, \mathbf{D}_{12}, \mathbf{D}_{21}, \mathbf{D}_{22}$	Auxiliar matrices to obtain a state-space representation of the closed-loop system.
e_k	Error of the closed-loop system.
f	Constant frequency of the harmonic disturbance.
$f_{i,k}$	Time-varying i -component of the harmonic disturbance.
f_k	Time-varying frequency of the harmonic disturbance.
$f_{0,k}$	Fundamental frequency of the harmonic disturbance.
$G_d(z)$	Transfer function of the disturbance model.
$G_p(z)$	Transfer function of the plant.
$G_{yd}(z)$	Transfer function between disturbance and output of the system.
$\mathbf{J}_3, \underline{\mathbf{J}}$	Auxiliar matrices.

\mathbf{K}_d	State-feedback gain for the states of the disturbance model.
$\mathbf{K}_{d,k} = \mathbf{K}_d(\boldsymbol{\theta}_k)$	Time-varying state-feedback for the states of the disturbance.
\mathbf{K}_{do}	State-feedback gain of the disturbance observer approach.
$\mathbf{K}_{d,v,1}, \dots, \mathbf{K}_{d,v,M}$	State-feedback gain of the vertices for the states of the disturbance.
\mathbf{K}_{ef}	Constant state-feedback gain of the error-filter approach.
$\mathbf{K}_{ef,k} = \mathbf{K}_{ef}(\boldsymbol{\theta}_k)$	Time-varying state-feedback gain of the error-filter approach.
$\mathbf{K}_{ef,v,1}, \dots, \mathbf{K}_{ef,v,1}$	State-feedback gains of the vertices for the error-filter approach.
\mathbf{K}_p	State-feedback gain for the states of the plant.
$\mathbf{K}_{p,k} = \mathbf{K}_p(\boldsymbol{\theta}_k)$	Time-varying state-feedback gain for the states of the plant.
$\mathbf{K}_{p,v,1}, \dots, \mathbf{K}_{p,v,M}$	State-feedback gain of the vertices for the states of the plant.
$\mathbf{K}_{P_1}(\boldsymbol{\lambda}_{1,k})$	pLPV controller for the polytope of the Lyapunov function \mathbf{P}_1 .
$\mathbf{K}_{P_2}(\boldsymbol{\lambda}_{2,k})$	pLPV controller for the polytope of the Lyapunov function \mathbf{P}_2 .
$\mathbf{K}_{P_3}(\boldsymbol{\lambda}_{3,k})$	pLPV controller for the polytope of the Lyapunov function \mathbf{P}_3 .
$\mathbf{K}_{1,P_1}, \mathbf{K}_{2,P_1}, \mathbf{K}_{3,P_1}$	Controllers of the vertices for the Lyapunov function \mathbf{P}_1 .
$\mathbf{K}_{1,P_2}, \mathbf{K}_{2,P_2}, \mathbf{K}_{3,P_2}$	Controllers of the vertices for the Lyapunov function \mathbf{P}_2 .
$\mathbf{K}_{1,P_3}, \mathbf{K}_{2,P_3}, \mathbf{K}_{3,P_3}$	Controllers of the vertices for the Lyapunov function \mathbf{P}_3 .
$K(z)$	Transfer function of the controller.
\mathbf{L}	Auxiliar matrix.
\mathbf{L}_d	Observer gain for the disturbance.
\mathbf{L}_{do}	Observer gain for the augmented system combining plant and disturbance model.
$\mathbf{L}_{do,k}$	Time-varying observer gain for the disturbance model approach.
$\mathbf{L}_{do,v,j} = \mathbf{L}_{do}(\boldsymbol{\theta}_{v,j})$	Observer gain of the vertices for the disturbance observer approach.
$\mathbf{L}_{d,v,j}$	Observer gain of the vertices for the disturbance states.
$\mathbf{L}_{p,v,j}$	Observer gain of the vertices for the plant states.
\mathbf{L}_p	Observer gain for the plant.
$\mathbf{L}_1, \mathbf{L}_2, \mathbf{L}_3, \bar{\mathbf{L}}$	Auxiliar matrices.
m	Low pass filter parameter.
M	Number of vertices of the polytope.
m_u	Number of inputs of the system.

$m_{\mathbf{u}_p}$	Number of inputs of the plant.
m_w	Number of performance inputs for the generalized plant.
m_{w_d}	Number of performance inputs of the disturbance model.
m_θ	Number of parameter inputs for the LFT approach.
n_d	Number of frequencies contained in the harmonic disturbance.
n_K	Order of the system matrix of the output-feedback controller.
n_p	Order of the state-space representation of the plant.
$n_{\mathbf{W}_u}, n_{\mathbf{W}_y}$	Order of the state-space representations of the weighting functions for the input \mathbf{u}_k and the output \mathbf{y}_k .
N	Number of parameters of $\boldsymbol{\theta}_k$.
N_p	Maximal order of the polynom used for the polynomial approximation.
$N_{\mathbf{X}}, N_{\mathbf{Y}}$	Nullspaces of the matrices \mathbf{X} and \mathbf{Y} .
\mathbf{P}	Auxiliar matrix.
$\mathbf{P}_1, \mathbf{P}_2, \mathbf{P}_3$	Independent Lyapunov functions.
\mathbf{Q}	Weighting matrix for the LQR method and auxiliar matrix for the H_∞ problem.
$\tilde{\mathbf{Q}}$	Auxiliar matrix.
\mathbf{q}_k	Output of the weighting functions for the input \mathbf{u}_k and the output \mathbf{y}_k .
$\mathbf{q}_{u,k}$	Output of the weighting function for the input \mathbf{u}_k .
$\mathbf{q}_{y,k}$	Output of the weighting function for the output \mathbf{y}_k .
$\mathbf{q}_{\theta,k}, \tilde{\mathbf{q}}_{\theta,k}$	Outputs of the parameter matrix for the LFT approach.
r, r_0, r_1	Constant scalars.
\mathbf{R}	Weighting matrix for the LQR approach or to minimize the H_2 -norm.
r_q	Number of outputs of the weighting functions.
r_{q_u}	Number of outputs of the weighting function for the input \mathbf{u}_k .
r_{q_y}	Number of outputs of the weighting function for the output \mathbf{y}_k .
r_y	Number of outputs of the generalized plant.
r_{y_d}	Number of outputs of the disturbance model.
r_{y_p}	Number of outputs of the plant.
r_θ	Number of outputs of the parameter matrix.
s_0, s_1	Constant scalars.
T	Sampling time.
t_k	Time.
\mathbf{u}_k	Input of a general system.
$\mathbf{u}_{p,k}$	Input of the plant.

$\mathbf{U}_p(z)$	Z -Transformation of the plant input.
\mathbf{V}	Set of constant vertices.
$v_{j,i}$	Auxiliar scalar used to calculate the polytopic interpolation.
w_b	Low pass filter parameter.
$\mathbf{w}_{d,k}$	Input of the weighting functions for the model of the disturbance.
\mathbf{W}	Positive definite matrix.
\mathbf{w}_k	Input of the weighting functions for a general system.
$\mathbf{w}_{\theta,k}, \tilde{\mathbf{w}}_{\theta,k}$	Input of the parameter matrix.
$\mathbf{W}_P, \mathbf{W}_Q$	Nullspaces of the matrices \mathbf{P} and \mathbf{Q} .
$\mathbf{X}, \mathbf{X}_1, \mathbf{X}_2$	Lyapunov functions.
\mathbf{X}_{cl}	Lyapunov function of the closed-loop system.
$\mathbf{x}_{d,k}, \mathbf{x}_{d,k+1}$	State-space variable of the disturbance.
$\hat{\mathbf{x}}_{d,k}, \hat{\mathbf{x}}_{d,k+1}$	Estimated state-space variable of the disturbance.
$\mathbf{x}_{do,k}, \mathbf{x}_{do,k+1}$	State-space variable of the augmented system for the disturbance observer approach.
$\hat{\mathbf{x}}_{do,k}, \hat{\mathbf{x}}_{do,k+1}$	Estimated state-space variable of the augmented system for the disturbance observer approach.
$\mathbf{x}_{ef,k}, \mathbf{x}_{ef,k+1}$	State-space variable of the augmented system for the error-filter approach.
$\mathbf{x}_k, \mathbf{x}_{k+1}$	State-space variable of a general system.
$\mathbf{x}_{p,k}, \mathbf{x}_{p,k+1}$	State-space variable of the plant.
$\hat{\mathbf{x}}_{p,k}, \hat{\mathbf{x}}_{p,k+1}$	Estimated state-space variable of the plant.
$\tilde{\mathbf{x}}_{p,k}, \tilde{\mathbf{x}}_{p,k+1}$	Error of the estimated state-space variables and the state-space variables of the plant.
$\mathbf{x}_{W_u,k}, \mathbf{x}_{W_u,k+1}$	State-space variables of the weighting function for the input \mathbf{u}_k .
$\mathbf{x}_{W_y,k}, \mathbf{x}_{W_y,k+1}$	State-space variables of the weighting function for the input \mathbf{y}_k .
\mathbf{Y}	Auxiliar matrix.
\mathbf{y}_k	Output of a general system.
$\mathbf{y}_{p,k}$	Output of the plant.
γ	Bound of the H_2 - and the H_∞ -norm.
$\Delta_k, \Delta_{new,k}$	Matrices of the parameters.
$\boldsymbol{\theta}_k$	Vector of parameters.
$\boldsymbol{\theta}_{v,1}, \dots, \boldsymbol{\theta}_{v,M}$	Parameters of the vertices.
Θ	Convex polytope in \mathbb{R}^N .
$\boldsymbol{\lambda}_k = [\lambda_{1,k}, \dots, \lambda_{M,k}]$	Coordinate vector of the polytopic system.
$\tilde{\boldsymbol{\lambda}}_{1,k}, \tilde{\boldsymbol{\lambda}}_{2,k}, \dots$	Coordinate vector for the interpolation of the switching strategy.
Ψ	Auxiliar matrix.
$\Omega_k = 2\pi f_k T$	Time-varying angle of the cosine and sine functions.
$\Omega_{0,k} = 2\pi f_{0,k} T$	Time-varying angle of the cosine and sine functions for the fundamental frequency $f_{0,k}$.

Nomenclature

Chapter 1

Introduction and Motivation

The work of this thesis is focused on the rejection of harmonic disturbances with time-varying frequencies through gain-scheduling controllers. These disturbances can be found in industrial applications where rotating machinery operates with varying speed, e.g., vehicles and aircrafts. This control problem is shown in Fig. 1.1 where a harmonic disturbance with n_d harmonic components is acting at the output of a single input single output (SISO) linear time-invariant (LTI) plant. The state-space matrices are represented with $\mathbf{A}_p^{(n_p \times n_p)}$, $\mathbf{B}_p^{(n_p \times m_{u_p})}$ and $\mathbf{C}_p^{(r_{y_p} \times n_p)}$. The plant input is denoted by $u_{p,k}$, the plant output is $y_{p,k}$, the harmonic disturbance is $y_{d,k}$ and y_k is used for the addition of disturbance with the plant output. To solve this problem it is assumed that the frequencies of the disturbances are known or they can be measured.

Gain-scheduling controllers that are automatically adjusted to the disturbance frequencies are usually used for the rejection of disturbances with time-varying frequencies (Balini et al. (2011), Ballesteros & Bohn (2010, 2011a, 2011b), Ballesteros et al. (2012, 2013, 2014a, 2014b, 2014c), Bohn et al. (2003, 2004), Darengosse & Chevrel (2000), Du & Shi (2002), Du et al. (2003), Duarte et al. (2012, 2013b, 2013c), Füger et al. (2012, 2013), Heins et al. (2011, 2012a, 2012b), Karimi & Emedi (2013), Körögöl & Scherer (2008), Kinney & de Callafon (2006a, 2006b, 2007, 2009), Shu et al. (2011, 2013) and Witte et al. (2010)).

Four control approaches are presented in this thesis for the reduction of time-varying harmonic disturbances applying linear parameter varying (LPV) control design techniques. Two observer-based state-feedback controllers are designed based on the control structure proposed by Bohn et al. (2003, 2004) and Kinney & de Callafon (2006a). Two output-feedback controllers are also designed based on the control design of Gahinet & Apkarian (1994) and Apkarian & Gahinet (1995). All the LPV controllers are designed in discrete time and validated experimentally in three different test benches.

Control Approaches

The reduction of harmonic disturbances with time-varying frequencies can be achieved using adaptive active noise control (ANC) or active vibration control (AVC) techniques (Bein et al. (2012), Duan et al. (2013), Inoue et al. (2004), Kuo & Morgan (1996), Landau et al. (2013), Matsuoka et al. (2004), Sano et al. (2001, 2002), Shoureshi & Knurek (1996), Shoureshi et al. (1997) and Svaricek et al. (2010)). Adaptive filtering updating the filter weights through the filtered-x LMS (FxLMS) algorithm is the common approach in ANC/AVC (Bein et al. (2012), Duan et al. (2013), Kuo & Morgan (1996) and Svaricek et al. (2010)). The main disadvantage of this approach is that the analysis of the closed loop is difficult. The stability and transient behavior (convergence speed) depend on the system input. Also, to date, only approximate stability results are available for the FxLMS algorithm (Feintuch et al. (1993) and Kuo & Morgan (1996)).

1. Introduction and Motivation

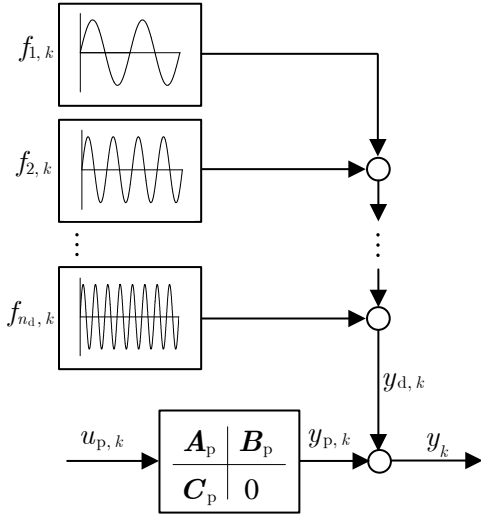


Figure 1.1: Control problem example for a harmonic disturbance with n_d harmonic components

Another approach is the use of gain-scheduling controllers for the rejection of periodic disturbances with time-varying frequencies. These controllers adjust their gain-scheduling parameters from the disturbance frequencies (Balini et al. (2011), Ballesteros & Bohn (2010, 2011a, 2011b), Ballesteros et al. (2012, 2013, 2014a, 2014b, 2014c), Bohn et al. (2003, 2004), Darengosse & Chevrel (2000), Du & Shi (2002), Du et al. (2003), Duarte et al. (2012, 2013b, 2013c), Füger et al. (2012, 2013), Heins et al. (2011, 2012a, 2012b), Karimi & Emedi (2013), Köroğlu & Scherer (2008), Kinney & de Callafon (2006a, 2006b, 2007, 2009), Shu et al. (2011, 2013) and Witte et al. (2010)). Depending on the method used for the calculation of the gain-scheduling parameters, the controllers can be further subdivided into indirect and direct scheduling.

In indirect scheduling, the controller or part of it, for example a state-feedback or observer gain, is determined from a set of pre-computed quantities through interpolation or switching. For example, for linear parameter-varying (LPV) systems, where the uncertain parameters are contained in a polytope (polytopic LPV (pLPV)), one controller or a feedback gain is calculated for each vertex and the resulting controller is obtained from interpolation (Ballesteros et al. (2012, 2013, 2014a, 2014b, 2014c), Darengosse & Chevrel (2000), Du & Shi (2002), Duarte et al. (2013c), Füger et al. (2012, 2013), Heins et al. (2011, 2012a, 2012b), Kinney & de Callafon (2006a), Köroğlu & Scherer (2008) and Shu et al. (2013)). In the approach of Bohn et al. (2003, 2004), the observer gain is selected from a set of pre-computed gains by switching. An interpolation between a grid of controllers is proposed by Karimi et al. (2013). Kinney & de Callafon (2006b) uses a look-up table to switch between state-feedback gains. A different approach is considered by Kinney & de Callafon (2007), where linear time-invariant (LTI) controllers are directly interpolated.

In direct scheduling, the dependence of the controller on the scheduling parameter does not correspond to a simple interpolation or switching law (Ballesteros & Bohn (2010, 2011a, 2011b), Du et al. (2003), Duarte et al. (2012, 2013b), Kinney & de Callafon (2007), Shu et al. (2011) and Witte et al. (2010)). For example, for LPV systems where the parameter dependence is expressed as an LFT, the uncertain parameters also

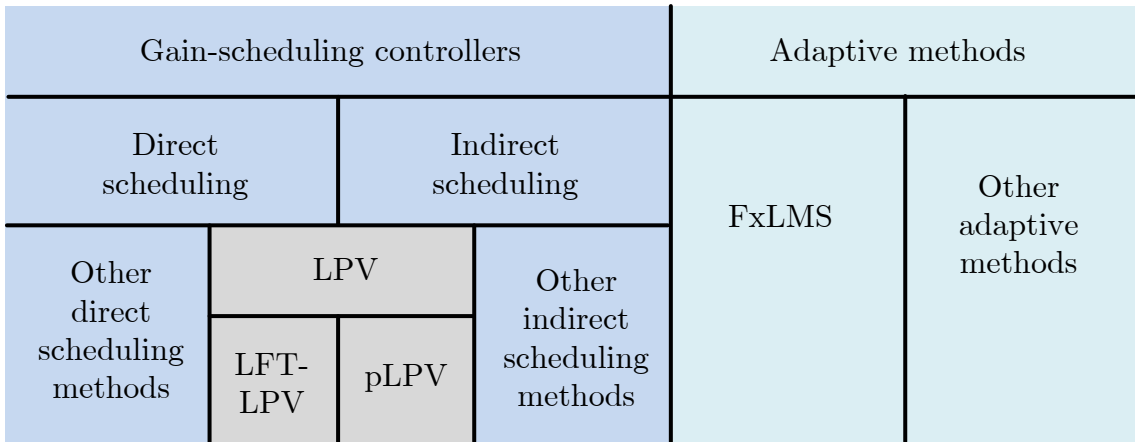


Figure 1.2: Overview of the control approaches used for the reduction of time-varying harmonic disturbances

enter the controller through an LFT (Ballesteros & Bohn (2010, 2011a, 2011b) and Shu et al. (2011)). Another example for direct scheduling is a controller based on a time-varying state estimator, for example a Kalman filter, where the scheduling parameters enter the controller through the recursive equations for the state estimation and the error covariance matrix. Such a controller is presented and compared to an indirect (interpolation) approach by Kinney & de Callafon (2007).

An overview and a classification¹ of all the control approaches is shown in Fig. 1.2. This thesis is focused on the control design of discrete-time LPV controllers (LFT and pLPV) for the reduction of time-varying harmonic disturbances. The advantages of applying discrete-time LPV techniques are discussed in Secs. 1.2 and 1.3.

Stability Considerations

For the reduction of time-varying harmonic disturbances there are approaches that take stability into consideration and such those do not. In indirect scheduling, for example, the controllers or gains are sometimes pre-computed for fixed operating points and then interpolated in an ad-hoc fashion (Bohn et al. (2003, 2004), Kinney & de Callafon (2006b)). Stability is then not guaranteed, although it might be expected that the system is stable for slow variations of the scheduling parameter. For the adaptive filtering approaches, only approximate stability results seem available to date (Feintuch & Bershad (1993), Kuo & Morgan (1996) and Ardekani (2012)).

To take stability into consideration, it is attractive to model the control problem as an LPV system and then use suitable gain-scheduling techniques. Linear parameter-varying (LPV) techniques are used by Apkarian & Gahinet (1995), Ballesteros & Bohn (2010, 2011a, 2011b), Ballesteros et al. (2012, 2013, 2014a, 2014b, 2014c), Cauet et al. (2013), Daafouz et al. (2000), Darengosse & Chevrel (2000), Du & Shi (2002), Du et al. (2003), Duarte et al. (2012, 2013b, 2013c), Füger et al. (2012, 2013), Heins et al. (2011, 2012a, 2012b), Kajiwara et al. (1999), Köroğlu & Scherer (2008), Kinney & de Callafon (2006a),

¹In Unbehauen (2011) gain-scheduling is considered as a feedforward adaptation (in German “gesteuerte Adaption”)

1. Introduction and Motivation

Rugh & Shamma (2000), Shu et al. (2011, 2013), Veenman & Scherer (2014), White et al. (2013) and Witte et al. (2010) and the stability is then guaranteed for arbitrarily fast changes in the gain-scheduling parameters. This work uses LPV techniques (LFT and pLPV) and independent Lyapunov functions for the design of gain-scheduling controllers for the rejection of time-varying harmonic disturbances.

In some applications, an LPV controller is not able to cover a range of the gain-scheduling parameter. A switch between pLPV controllers is in thesis presented to augment the actuation range of the controllers guaranteeing the stability at the same time. This method is based on independent Lyapunov functions. In Shimomura (2003), a switch between controllers based on parameter-dependent Lyapunov functions is proposed. A “smooth” switching is achieved in Hanifzadegan & Nagamune (2014) using also parameter-dependent Lyapunov functions. The main objective of the switching strategy presented in this thesis is to augment the actuation range of the controller, not to reduce the conservatism using parameter-dependent Lyapunov functions as in Shimomura (2003) and Hanifzadegan & Nagamune (2014).

Implementation Aspects

For a practical application, the controller obtained with the LPV control design has to be implemented in discrete time. In ANC/AVC applications, the plant model is often obtained through system identification. This usually gives a discrete-time plant model. It is therefore most natural to carry out the whole design in discrete time. If a continuous-time controller is computed, the controller has to be discretized. Since the controllers considered here are time-varying, the discretization would have to be carried out at each sampling instant. An exact discretization involves the calculation of a matrix exponential, which is computationally too expensive. Particularly in LPV gain-scheduling control, an approximate discretization is proposed by Apkarian (1997). However, this leads to a distortion of the frequency scale. Usually, this can be tolerated, but not for the suppression of harmonic disturbances. It is therefore not surprising that the continuous-time controllers of Darengosse & Chevrel (2000), Du et al. (2003), Kinney & de Callafon (2006a) and Körögöl & Scherer (2008) are only tested in simulations with a very simple system as a plant and a single frequency in the disturbance signal.

The design methods that are tested in real time are usually formulated in discrete time (Ballesteros & Bohn (2010, 2011a, 2011b), Ballesteros et al. (2012, 2013, 2014a, 2014b, 2014c), Bohn et al. (2003, 2004), Duarte et al. (2012, 2013a, 2013b, 2013c), Heins et al. (2011, 2012a, 2012b), Kinney & de Callafon (2006b, 2007), Shu et al. (2011, 2013)). Exceptions are Witte et al. (2010) and Balini et al. (2011), who designed continuous-time controllers which then are approximately discretized. However, Witte et al. (2010) use a very high sampling frequency of 40 kHz to reject a harmonic disturbance with a frequency up to 48 Hz (in fact, the authors state that they chose “the smallest [sampling time] available by the hardware” and Balini et al. (2011) use a maximal sampling frequency of 50 kHz. Another exception is Ruderman et al. (2014), they designed continuous-time observer-based LTI controllers for the reduction of a disturbance with a dominant frequency of 10 Hz using a sampling frequency of 11 kHz. It seems more natural to directly carry out the design in discrete time to avoid discretization issues.

All the controllers for the rejection of time-varying harmonic disturbances of this thesis are designed in discrete-time and validated experimentally in three different test benches. Discrete-time SISO gain-scheduling controllers are validated in an ANC headphone and an

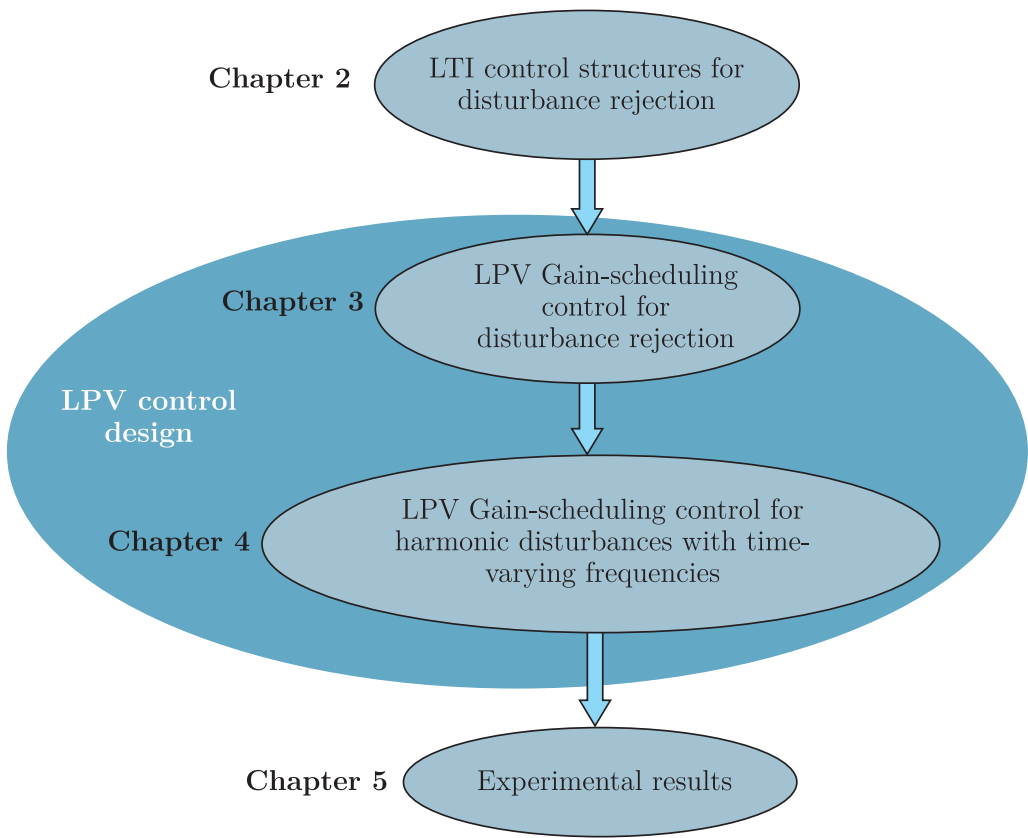


Figure 1.3: Structure representation of this work

AVC test bed and a multiple-input multiple-output (MIMO) LPV controller is validated experimentally in a Golf VI Variant for the rejection of nine time-varying frequency components induced by the engine vibration. To the best knowledge of the author, it is the first time that a discrete-time MIMO pLPV controller for the rejection of harmonic disturbances with time-varying frequencies is implemented and validated with experimental results. A switching strategy assuring the stability is used to augment the actuation range of the MIMO LPV controller.

Thesis Outline

Three pLPV control structures (Ballesteros et al. (2012, 2013, 2014a, 2014b, 2014c) and Heins et al. (2011, 2012a, 2012b)) and an LFT control structure (Ballesteros & Bohn (2010, 2011a, 2011b) and Shu et al. (2011)) for the reduction of harmonic disturbances with time-varying frequencies are presented in this thesis. The control structures are explained for the LTI case (constant disturbance frequencies) and then are extended to the LPV case (time-varying disturbance frequencies).

This thesis is organized as follows (see Fig 1.3). In Chapter 2, the internal model principle (IMP) (Francis and Wonham (1976)) is explained and three discrete-time LTI control structures fulfilling this principle are presented. Two observer-based control structures and an output-feedback control structure are considered for a general disturbance acting on a plant. These control structures are presented here for the LTI case and they achieve

1. Introduction and Motivation

disturbance rejection for a general disturbance acting on the plant. Chapter 3 extends the control structures of Chapter 2 to the LPV case and general pLPV and LFT control structures are presented. The rejection of harmonic time-varying disturbances through LPV gain-scheduling control is explained in Chapter 4. Different methods to model the disturbance are discussed and a polynomial approximation to reduce the gain-scheduling parameters is used. A pLPV or an LFT control structure is obtained depending on the technique used to model the disturbance. A switching control strategy is also presented to augment the actuation range of the controller. The LPV controllers obtained in Chapter 4 are validated with experimental results in Chapter 5. The conclusions are given in Chapter 6.

Chapter 2

Internal-model-principle-based Control

This thesis focuses on the rejection of disturbances acting on a plant. This problem is shown in Fig. 2.1. The discrete-time state-space representation of a plant is given by

$$\begin{bmatrix} \mathbf{x}_{p,k+1} \\ \mathbf{y}_{p,k} \end{bmatrix} = \begin{bmatrix} \mathbf{A}_p & \mathbf{B}_p \\ \mathbf{C}_p & \mathbf{D}_p \end{bmatrix} \begin{bmatrix} \mathbf{x}_{p,k} \\ \mathbf{u}_{p,k} \end{bmatrix} \quad (2.1)$$

with the plant state-space vector $\mathbf{x}_{p,k}$, the plant input $\mathbf{u}_{p,k}$ and output $\mathbf{y}_{p,k}$ and the plant state-space matrices $\mathbf{A}_p^{(n_p \times n_p)}$, $\mathbf{B}_p^{(n_p \times m_{u_p})}$, $\mathbf{C}_p^{(r_{y_p} \times n_p)}$ and $\mathbf{D}_p^{(r_{y_p} \times m_{u_p})}$. The state-space representation of a disturbance is described by

$$\begin{bmatrix} \mathbf{x}_{d,k+1} \\ \mathbf{y}_{d,k} \end{bmatrix} = \begin{bmatrix} \mathbf{A}_d & \mathbf{B}_d \\ \mathbf{C}_d & \mathbf{D}_d \end{bmatrix} \begin{bmatrix} \mathbf{x}_{d,k} \\ \mathbf{w}_{d,k} \end{bmatrix} \quad (2.2)$$

with the disturbance state-space vector $\mathbf{x}_{d,k}$, the disturbance model input $\mathbf{w}_{d,k}$, output $\mathbf{y}_{d,k}$ and the disturbance state-space matrices $\mathbf{A}_d^{(2n_d \times 2n_d)}$, $\mathbf{B}_d^{(2n_d \times m_{w_d})}$, $\mathbf{C}_d^{(r_{y_d} \times 2n_d)}$ and $\mathbf{D}_d^{(r_{y_d} \times m_{w_d})}$.

According to the well known IMP proposed by Francis and Wonham (1976), controllers designed for the rejection of a disturbance must contain a model of it. A trivial example illustrating this principle is shown for a harmonic disturbance $y_{d,k} = \sin(2\pi f t_k)$ acting on the output of a system described by the difference equation

$$y_{p,k+1} = ay_{p,k} + (1 - a)u_{p,k} + y_{d,k} \quad (2.3)$$

where the constant $a > 0$ and f is the frequency of the disturbance in Hz. A transfer function representation between input and output of the system is given by

$$G_p(z) = \frac{Y_p(z)}{U_p(z)} = \frac{1 - a}{z - a}. \quad (2.4)$$

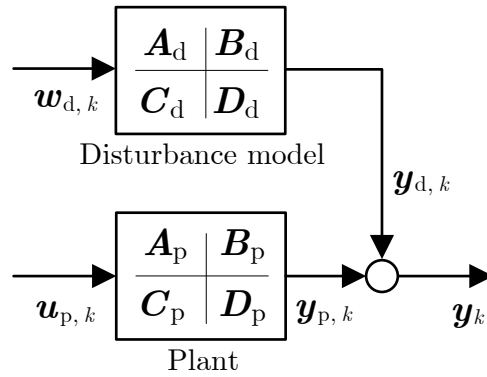


Figure 2.1: Plant and disturbance model

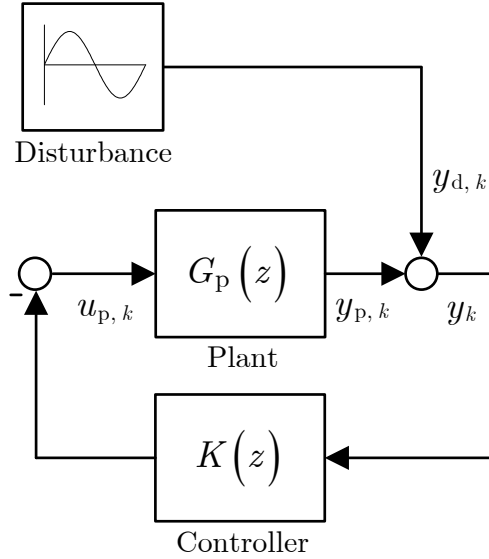


Figure 2.2: Control structure

In this example, the algebraic control design method is used to obtain a controller for the rejection of the disturbance.

The controller

$$K(z) = \frac{(z - a)(s_1 z + s_0)}{(1 - a)(z^2 - 2 \cos(2\pi fT)z + 1)(r_1 z + r_0)} \quad (2.5)$$

obtained with

$$r_1 = 1,$$

$$r_0 = -(a_1 + a_2 + a_3) + 2 \cos(2\pi fT)r_1,$$

$$s_1 = a_1 a_2 + a_3 a_1 + a_3 a_2 - r_1 + 2 \cos(2\pi fT)r_0$$

and

$$s_0 = -r_0 - a_1 a_2 a_3$$

is capable to place the poles in closed loop in $z = a_1$, $z = a_2$ and $z = a_3$ rejecting the harmonic disturbance at the same time. The control structure is shown in Fig. 2.2. The closed-loop transfer function between disturbance and output is given by

$$G_{yd}(z) = \frac{1}{1 + KG_p} = \frac{(z^2 - 2 \cos(2\pi fT)z + 1)(r_1 z + r_0)}{(z - a_1)(z - a_2)(z - a_3)}. \quad (2.6)$$

The pole-zero map and amplitude frequency response of the controller $K(z)$ and the closed-loop transfer function $G_{yd}(z)$ are shown in Fig. 2.3 for $T = 0.001$ s, $f = 20$ Hz, $a = 0.1$, $a_1 = 0.4$, $a_2 = 0.6$ and $a_3 = 0.8$. The controller poles at the frequency of the disturbance to be cancelled (20 Hz) show up as zeros in the closed-loop transfer function, as long as the model of the disturbance is contained in the controller the IMP is fulfilled. As a result of this, the controller is able to reject the harmonic disturbance.

In the next section three LTI controllers which contain a model of the disturbance are presented to achieve disturbance rejection.

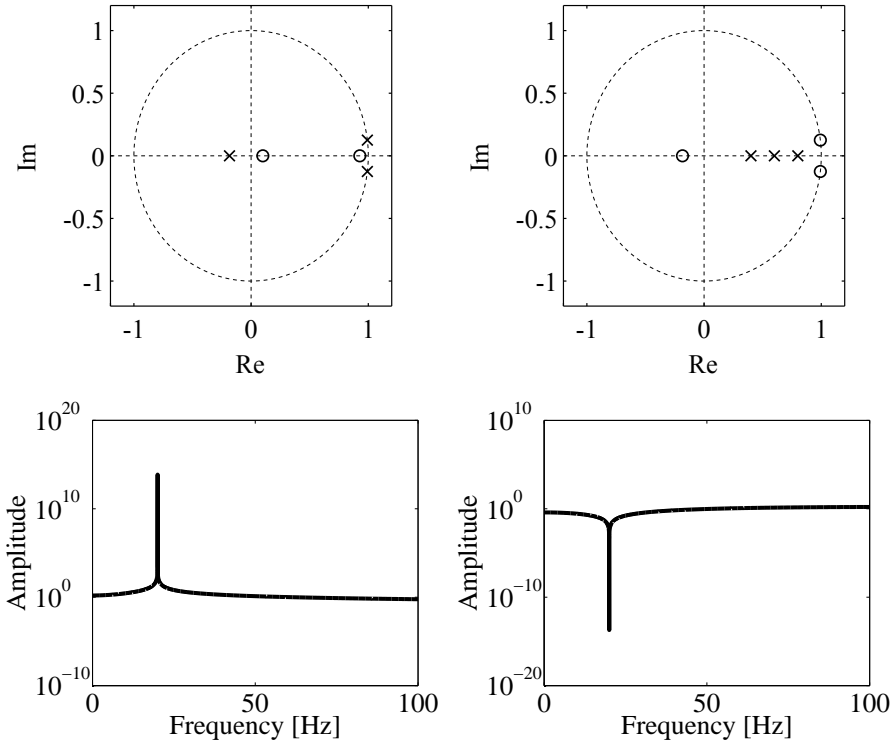


Figure 2.3: Pole-zero map (top) and amplitude frequency response (bottom) of controller (left) and closed-loop transfer function (right) for a sampling frequency of 1 kHz

LTI Controller Structures

This section presents LTI observer-based state-feedback and output-feedback control structures for the rejection of general disturbances acting on a plant (see Fig 2.4). It is assumed that the nature of the disturbance is known and therefore a model of it can be obtained. The controllers presented in these subsections reject the disturbances since they contain a model of the disturbance fulfilling the IMP.

Observer Based Control Structures

Two LTI observer-based state-feedback controller structures for the rejection of disturbances acting on a plant are explained in this section. The LTI disturbance-observer state-feedback control structure of Bohn et al. (2003, 2004) and the LTI error-filter observer-based control structure of Kinney and Callafon (2006a) are briefly reviewed. In the next chapters, these control structures are extended to LPV control structures. The LTI control design approaches presented here use state augmentation to add certain desired dynamics to the controller in order to fulfill the IMP.

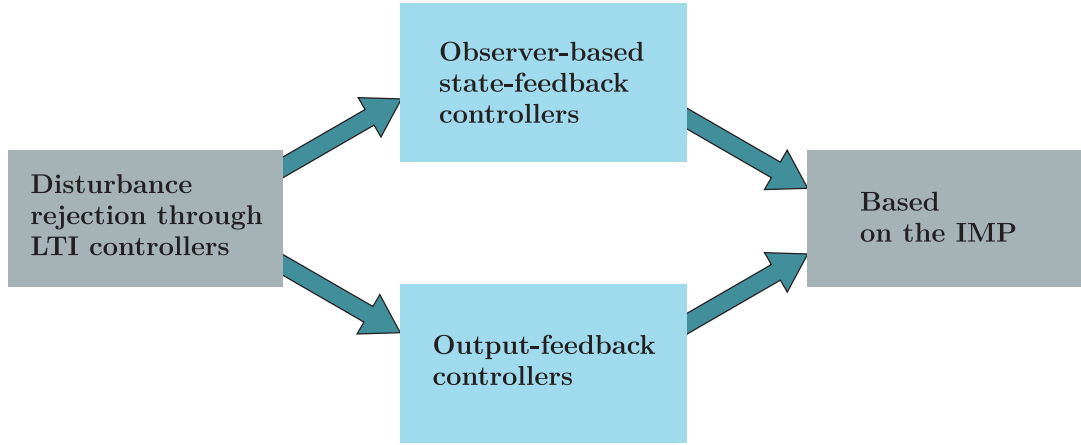


Figure 2.4: LTI controllers for the rejection of disturbances based on the IMP

Disturbance Observer Control Structure

In this control design, a disturbance $\mathbf{y}_{d,k}$ acting at the input of the plant

$$\begin{bmatrix} \mathbf{x}_{p,k+1} \\ \mathbf{y}_{p,k} \end{bmatrix} = \begin{bmatrix} \mathbf{A}_p & \mathbf{B}_p \\ \mathbf{C}_p & \mathbf{0} \end{bmatrix} \begin{bmatrix} \mathbf{x}_{p,k} \\ \mathbf{u}_{p,k} + \mathbf{y}_{d,k} \end{bmatrix} \quad (2.7)$$

is modeled as the output of an unforced LTI exo-system

$$\begin{bmatrix} \mathbf{x}_{d,k+1} \\ \mathbf{y}_{d,k} \end{bmatrix} = \begin{bmatrix} \mathbf{A}_d & \mathbf{0} \\ \mathbf{C}_d & \mathbf{0} \end{bmatrix} \begin{bmatrix} \mathbf{x}_{d,k} \\ \mathbf{w}_{d,k} \end{bmatrix} \quad (2.8)$$

as shown in Fig. 2.5. The dimensions of the system matrices for plant and disturbance are defined with $\mathbf{A}_p^{(n_p \times n_p)}$, $\mathbf{B}_p^{(n_p \times m_{u_p})}$, $\mathbf{C}_p^{(r_{y_p} \times n_p)}$, $\mathbf{A}_d^{(2n_d \times 2n_d)}$ and $\mathbf{C}_d^{(r_{y_d} \times 2n_d)}$.

To obtain a disturbance-observer controller, an augmented system is built combining plant and disturbance model through

$$\begin{bmatrix} \mathbf{x}_{d,k+1} \\ \mathbf{x}_{p,k+1} \\ \mathbf{y}_{p,k} \end{bmatrix} = \begin{bmatrix} \mathbf{A}_d & \mathbf{0} & \mathbf{0} \\ \mathbf{B}_p \mathbf{C}_d & \mathbf{A}_p & \mathbf{B}_p \\ \mathbf{0} & \mathbf{C}_p & \mathbf{0} \end{bmatrix} \begin{bmatrix} \mathbf{x}_{d,k} \\ \mathbf{x}_{p,k} \\ \mathbf{u}_{p,k} \end{bmatrix} \quad (2.9)$$

and it can be written in compact form as

$$\begin{bmatrix} \mathbf{x}_{do,k+1} \\ \mathbf{y}_{p,k} \end{bmatrix} = \begin{bmatrix} \mathbf{A}_{do} & \mathbf{B}_{do} \\ \mathbf{C}_{do} & \mathbf{0} \end{bmatrix} \begin{bmatrix} \mathbf{x}_{do,k} \\ \mathbf{u}_{p,k} \end{bmatrix} \quad (2.10)$$

with

$$\begin{aligned} \mathbf{x}_{do,k} &= \begin{bmatrix} \mathbf{x}_{d,k} \\ \mathbf{x}_{p,k} \end{bmatrix}, \quad \mathbf{A}_{do}^{((2n_d+n_p) \times (2n_d+n_p))} = \begin{bmatrix} \mathbf{A}_d & \mathbf{0} \\ \mathbf{B}_p \mathbf{C}_d & \mathbf{A}_p \end{bmatrix}, \\ \mathbf{B}_{do}^{((2n_d+n_p) \times m_{u_p})} &= \begin{bmatrix} \mathbf{0} \\ \mathbf{B}_p \end{bmatrix} \text{ and } \mathbf{C}_{do}^{(r_{y_p} \times (2n_d+n_p))} = [\mathbf{0} \quad \mathbf{C}_p] \end{aligned} \quad (2.11)$$

where the acronym “do” is used for disturbance observer approach.

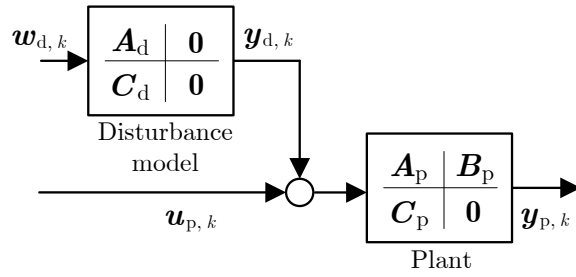


Figure 2.5: Disturbance modeled at the input of the plant

The control structure of this approach is a constant state-feedback gain $\mathbf{K}_{\text{do}}^{(m_{\mathbf{u}_p} \times (2n_d + n_p))}$

$$\mathbf{u}_{p,k} = -\mathbf{K}_{\text{do}} \hat{\mathbf{x}}_{\text{do},k} = -[\mathbf{K}_d \quad \mathbf{K}_p] \begin{bmatrix} \hat{\mathbf{x}}_{d,k} \\ \hat{\mathbf{x}}_{p,k} \end{bmatrix} \quad (2.12)$$

of the augmented system with the estimated states $\hat{\mathbf{x}}_{\text{do},k}$ calculated through an identity observer

$$\hat{\mathbf{x}}_{\text{do},k+1} = [\mathbf{A}_{\text{do}} - \mathbf{L}_{\text{do}} \mathbf{C}_{\text{do}} \mid \mathbf{B}_{\text{do}} \quad \mathbf{L}_{\text{do}}] \begin{bmatrix} \hat{\mathbf{x}}_{\text{do},k} \\ \mathbf{u}_{p,k} \\ \mathbf{y}_{p,k} \end{bmatrix} \quad (2.13)$$

with

$$\mathbf{L}_{\text{do}}^{((2n_d + n_p) \times r_{\mathbf{y}_p})} = \begin{bmatrix} \mathbf{L}_d \\ \mathbf{L}_p \end{bmatrix}. \quad (2.14)$$

The feedback gain \mathbf{K}_p can be chosen to change the dynamics of the plant, whereas \mathbf{K}_d can be chosen equal to \mathbf{C}_d to achieve disturbance rejection. This leads to the typical observer-based state-feedback control structure shown in Fig. 2.6. A state-space representation of the obtained controller is given by

$$\begin{bmatrix} \hat{\mathbf{x}}_{\text{do},k+1} \\ \mathbf{u}_{p,k} \end{bmatrix} = \left[\begin{array}{c|c} \mathbf{A}_{\text{do}} - \mathbf{L}_{\text{do}} \mathbf{C}_{\text{do}} - \mathbf{B}_{\text{do}} \mathbf{K}_{\text{do}} & \mathbf{L}_{\text{do}} \\ \hline \mathbf{K}_{\text{do}} & \mathbf{0} \end{array} \right] \begin{bmatrix} \hat{\mathbf{x}}_{\text{do},k} \\ \mathbf{y}_{p,k} \end{bmatrix}. \quad (2.15)$$

The controller is written in compact form as

$$\begin{bmatrix} \hat{\mathbf{x}}_{\text{do},k+1} \\ \mathbf{u}_{p,k} \end{bmatrix} = \begin{bmatrix} \mathbf{A}_{\text{doc}} & \mathbf{B}_{\text{doc}} \\ \hline \mathbf{C}_{\text{doc}} & \mathbf{0} \end{bmatrix} \begin{bmatrix} \hat{\mathbf{x}}_{\text{do},k} \\ \mathbf{y}_{p,k} \end{bmatrix} \quad (2.16)$$

with

$$\begin{aligned} \mathbf{A}_{\text{doc}}^{((2n_d + n_p) \times (2n_d + n_p))} &= \mathbf{A}_{\text{do}} - \mathbf{L}_{\text{do}} \mathbf{C}_{\text{do}} - \mathbf{B}_{\text{do}} \mathbf{K}_{\text{do}}, \\ \mathbf{B}_{\text{doc}}^{((2n_d + n_p) \times r_{\mathbf{y}_p})} &= \mathbf{L}_{\text{do}}, \quad \mathbf{C}_{\text{doc}}^{(m_{\mathbf{u}_p} \times (2n_d + n_p))} = \mathbf{K}_{\text{do}} \end{aligned} \quad (2.17)$$

and disturbance-observer controller is denoted by ‘‘doc’’. The controller is stable as long as the eigenvalues of \mathbf{A}_{doc} are contained inside the unitary circle. The gain \mathbf{L}_{do} can be calculated by means of a discrete-time linear quadratic regulator for the augmented system. This is equivalent to calculate the observer gain \mathbf{L}_{do} solving the LMIs

$$\begin{bmatrix} \mathbf{P} & \mathbf{PA}_{\text{do}} - \mathbf{Y}^T \mathbf{C}_{\text{do}} \\ (\mathbf{PA}_{\text{do}} - \mathbf{Y}^T \mathbf{C}_{\text{do}})^T & \mathbf{P} - \mathbf{I} \end{bmatrix} > 0, \quad (2.18)$$

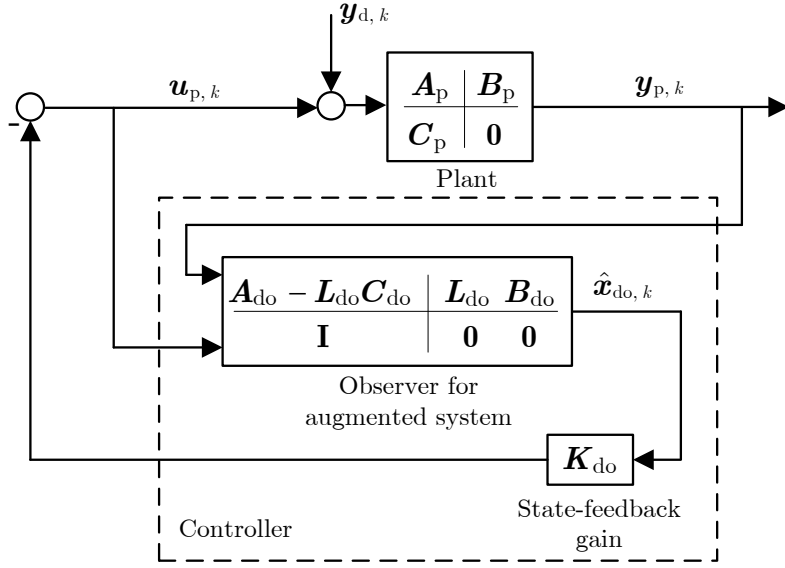


Figure 2.6: Disturbance-observer controller structure

$$\begin{bmatrix} \mathbf{W} & \tilde{\mathbf{Q}}\mathbf{P} - \tilde{\mathbf{R}}\mathbf{Y} \\ (\tilde{\mathbf{Q}}\mathbf{P} - \tilde{\mathbf{R}}\mathbf{Y})^T & \mathbf{P} \end{bmatrix} > 0, \quad (2.19)$$

$$\text{trace}(\mathbf{W}) < \gamma^2 \quad (2.20)$$

for $\mathbf{Y}^{(r_{y_p} \times (2n_d + n_p))}$ and for the positive definite matrices $\mathbf{P}^{((2n_d + n_p) \times (2n_d + n_p))}$ and $\mathbf{W}^{((r_{y_p} + 2n_d + n_p) \times (r_{y_p} + 2n_d + n_p))}$ with

$$\tilde{\mathbf{Q}}^{((r_{y_p} + 2n_d + n_p) \times (2n_d + n_p))} = \begin{bmatrix} \mathbf{Q}^{\frac{1}{2}} \\ \mathbf{0} \end{bmatrix}, \quad \tilde{\mathbf{R}}^{((r_{y_p} + 2n_d + n_p) \times r_{y_p})} = \begin{bmatrix} \mathbf{0} \\ \mathbf{R}^{\frac{1}{2}} \end{bmatrix} \quad (2.21)$$

and

$$\mathbf{Y}^T = \mathbf{P}\mathbf{L}_{\text{do}} \quad (2.22)$$

using the same weighting matrices $\mathbf{Q}^{((2n_d + n_p) \times (2n_d + n_p))}$ and $\mathbf{R}^{(r_{y_p} \times r_{y_p})}$ as the discrete-time linear quadratic regulator.

Finally the observer gain $\mathbf{L}_{\text{do}}^{((2n_d + n_p) \times r_{y_p})}$ is calculated through

$$\mathbf{L}_{\text{do}} = \mathbf{P}^{-1}\mathbf{Y}^T. \quad (2.23)$$

These LMIs are based on the H_2 -norm optimization problem, if solutions for \mathbf{P} , \mathbf{W} and \mathbf{Y} are found, the system has an H_2 -norm bounded by γ (see A.3 and A.4).

The stability analysis of the overall closed-loop system is obtained from the observer error for the plant states

$$\tilde{\mathbf{x}}_{p,k+1} = \hat{\mathbf{x}}_{p,k+1} - \mathbf{x}_{p,k+1} = \begin{bmatrix} \mathbf{B}_p \mathbf{C}_d & \mathbf{A}_p - \mathbf{L}_p \mathbf{C}_p & -\mathbf{B}_p \end{bmatrix} \begin{bmatrix} \hat{\mathbf{x}}_{d,k} \\ \tilde{\mathbf{x}}_{p,k} \\ \mathbf{y}_{d,k} \end{bmatrix} \quad (2.24)$$

and the plant states under state feedback

$$\mathbf{x}_{p,k+1} = \begin{bmatrix} -\mathbf{B}_p \mathbf{K}_d & -\mathbf{B}_p \mathbf{K}_p & \mathbf{A}_p - \mathbf{B}_p \mathbf{K}_p & \mathbf{B}_p \end{bmatrix} \begin{bmatrix} \hat{\mathbf{x}}_{d,k} \\ \tilde{\mathbf{x}}_{p,k} \\ \mathbf{x}_{p,k} \\ \mathbf{y}_{d,k} \end{bmatrix}. \quad (2.25)$$

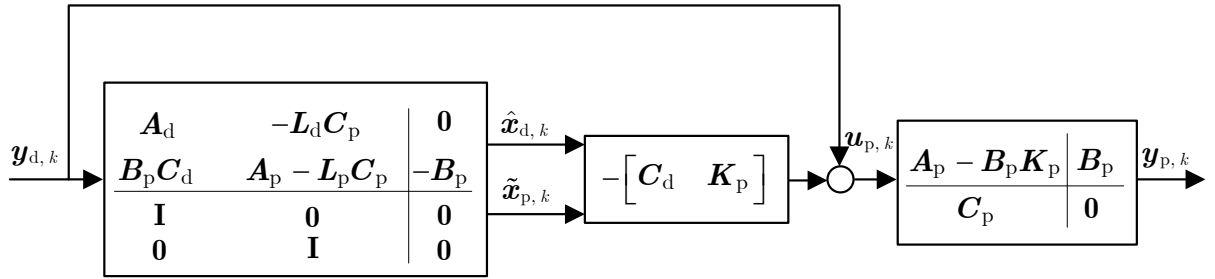


Figure 2.7: Dynamics of the overall closed-loop system

The overall closed loop dynamics of the system are given by

$$\begin{bmatrix} \hat{\mathbf{x}}_{d,k+1} \\ \tilde{\mathbf{x}}_{p,k+1} \\ \mathbf{x}_{p,k+1} \end{bmatrix} = \begin{bmatrix} \mathbf{A}_d & -\mathbf{L}_d \mathbf{C}_p & 0 \\ \mathbf{B}_p \mathbf{C}_d & \mathbf{A}_p - \mathbf{L}_p \mathbf{C}_p & -\mathbf{B}_p \\ \mathbf{I} & 0 & 0 \\ 0 & \mathbf{I} & 0 \end{bmatrix} \begin{bmatrix} \hat{\mathbf{x}}_{d,k} \\ \tilde{\mathbf{x}}_{p,k} \\ \mathbf{x}_{p,k} \\ \mathbf{y}_{d,k} \end{bmatrix}. \quad (2.26)$$

The structure of the overall system dynamics is shown in Fig. 2.7. The plant under state feedback is driven by the dynamics of the observer for the augmented system. From here it follows that as long as a stabilizing state-feedback gain \mathbf{K}_p for the LTI plant $(\mathbf{A}_p - \mathbf{B}_p \mathbf{K}_p)$ and a stabilizing observer gain \mathbf{L}_{do} for the augmented system $(\mathbf{A}_{do} - \mathbf{L}_{do} \mathbf{C}_{do})$ are found the closed loop system is stable. The feedback gain \mathbf{K}_d does not have influence on the eigenvalues of $(\mathbf{A}_p - \mathbf{B}_p \mathbf{K}_p)$ and $(\mathbf{A}_{do} - \mathbf{L}_{do} \mathbf{C}_{do})$ and therefore does not have influence on the overall closed loop system stability.

An example of this control design is shown for the simple system of (2.4) with the state-space representation given as

$$\begin{bmatrix} x_{p,k+1} \\ y_{p,k} \end{bmatrix} = \begin{bmatrix} a & 1 \\ (1-a) & 0 \end{bmatrix} \begin{bmatrix} x_{p,k} \\ u_{p,k} \end{bmatrix} \quad (2.27)$$

when a single harmonic disturbance $y_{d,k} = \sin(2\pi f t_k)$ ($n_d = 1$) is acting at the input of the plant for $a = 0.1$, $f = 20$ Hz and $t_k = T, 2T, \dots$ with $T = 0.001$ s. A model for a harmonic disturbance with a constant frequency f is given by

$$\begin{bmatrix} \mathbf{x}_{d,k+1} \\ y_{d,k} \end{bmatrix} = \begin{bmatrix} 0 & 1 & 0 \\ -r^2 & 2r \cos(2\pi f T) & 0 \\ 1 & 0 & 0 \end{bmatrix} \begin{bmatrix} \mathbf{x}_{d,k} \\ w_{d,k} \end{bmatrix} \quad (2.28)$$

with $r = 0.9999$. From (2.27) and (2.28) the values for $A_p^{(n_p \times n_p)} = a$, $B_p^{(n_p \times m_{u_p})} = 1$, $C_p^{(r_{y_p} \times n_p)} = (1-a)$,

$$\mathbf{A}_d^{(2n_d \times 2n_d)} = \begin{bmatrix} 0 & 1 \\ -r^2 & 2r \cos(2\pi f T) \end{bmatrix} \quad \text{and} \quad \mathbf{C}_d^{(r_{y_d} \times 2n_d)} = \begin{bmatrix} 1 & 0 \end{bmatrix} \quad (2.29)$$

are obtained with $n_p = m_{u_p} = r_{y_p} = n_d = r_{y_d} = 1$.

The augmented system of (2.10) is built with

$$\mathbf{A}_{do}^{((2n_d+n_p) \times (2n_d+n_p))} = \begin{bmatrix} \mathbf{A}_d & \mathbf{0} \\ \mathbf{B}_p \mathbf{C}_d & \mathbf{A}_p \end{bmatrix} = \begin{bmatrix} 0 & 1 & 0 \\ -r^2 & 2r \cos(2\pi f T) & 0 \\ 1 & 0 & a \end{bmatrix}, \quad (2.30)$$

2. Internal-model-principle-based Control

$$\mathbf{B}_{\text{do}}^{((2n_{\text{d}}+n_{\text{p}}) \times m_{u_{\text{p}}})} = \begin{bmatrix} \mathbf{0} \\ B_{\text{p}} \end{bmatrix} = \begin{bmatrix} 0 \\ 0 \\ 1 \end{bmatrix} \quad (2.31)$$

and

$$\mathbf{C}_{\text{do}}^{(r_{y_{\text{p}}} \times (2n_{\text{d}}+n_{\text{p}}))} = [\mathbf{0} \ C_{\text{p}}] = [0 \ 0 \ (1-a)] \quad (2.32)$$

to calculate the observer-feedback gain \mathbf{L}_{do} . The observer-feedback gain can be calculated using a discrete-time linear quadratic regulator for the augmented system or equivalently, solving the LMIs of (2.18)-(2.20). The matrices

$$\mathbf{Q}^{((2n_{\text{d}}+n_{\text{p}}) \times (2n_{\text{d}}+n_{\text{p}}))} = \begin{bmatrix} 0.01 & 0 & 0 \\ 0 & 0.01 & 0 \\ 0 & 0 & 0.01 \end{bmatrix} \quad \text{and} \quad R^{(r_{y_{\text{p}}} \times r_{y_{\text{p}}})} = 1000 \quad (2.33)$$

are chosen after trying different values to achieve a desired performance in the closed-loop system. The observer-feedback gain

$$\mathbf{L}_{\text{do}}^{((2n_{\text{d}}+n_{\text{p}}) \times r_{y_{\text{p}}})} = [0.0346 \ 0.0337 \ 0.0387]^T \quad (2.34)$$

is obtained.

The state-feedback gain

$$\mathbf{K}_{\text{do}}^{(m_{u_{\text{p}}} \times (2n_{\text{d}}+n_{\text{p}}))} = [\mathbf{C}_{\text{d}} \ 0] \quad (2.35)$$

is chosen to achieve disturbance rejection. The controller of (2.16) is obtained with

$$\begin{aligned} \mathbf{A}_{\text{doc}}^{((2n_{\text{d}}+n_{\text{p}}) \times (2n_{\text{d}}+n_{\text{p}}))} &= \mathbf{A}_{\text{do}} - \mathbf{L}_{\text{do}} \mathbf{C}_{\text{do}} - \mathbf{B}_{\text{do}} \mathbf{K}_{\text{do}} = \\ &= \mathbf{A}_{\text{doc}} = \begin{bmatrix} 0 & 1 & -0.0311 \\ -r^2 & 2r \cos(2\pi fT) & -0.0304 \\ 0 & 0 & 0.0652 \end{bmatrix}, \end{aligned} \quad (2.36)$$

$$\mathbf{B}_{\text{doc}}^{((2n_{\text{d}}+n_{\text{p}}) \times r_{y_{\text{p}}})} = \mathbf{L}_{\text{do}} = [0.0346 \ 0.0337 \ 0.0387]^T, \quad (2.37)$$

and

$$\mathbf{C}_{\text{doc}}^{(m_{u_{\text{p}}} \times (2n_{\text{d}}+n_{\text{p}}))} = \mathbf{K}_{\text{do}} = [1 \ 0 \ 0]. \quad (2.38)$$

The pole-zero map and the amplitude frequency response are shown in Fig. 2.8 for the controller and the closed-loop system. The closed-loop system is stable since $(A_{\text{p}} - B_{\text{p}} K_{\text{p}})$ is stable ($K_{\text{p}} = 0$) and the matrix $(\mathbf{A}_{\text{do}} - \mathbf{L}_{\text{do}} \mathbf{C}_{\text{do}})$ is stable (Fig. 2.7 and (2.26)). The gain $\mathbf{K}_{\text{d}} = \mathbf{C}_{\text{d}}$ does not have influence in the closed-loop stability.

Error Filter Observer-based Control Structure

Disturbance rejection is achieved in this approach including the dynamics of the disturbance into the controller through an error filter. A schema of this control structure is shown in Fig. 2.9. The error \mathbf{e}_k obtained with the output $\mathbf{y}_{\text{p},k}$ of the plant

$$\begin{bmatrix} \mathbf{x}_{\text{p},k+1} \\ \mathbf{y}_{\text{p},k} \end{bmatrix} = \left[\begin{array}{c|c} \mathbf{A}_{\text{p}} & \mathbf{B}_{\text{p}} \\ \hline \mathbf{C}_{\text{p}} & \mathbf{0} \end{array} \right] \begin{bmatrix} \mathbf{x}_{\text{p},k} \\ \mathbf{u}_{\text{p},k} \end{bmatrix} \quad (2.39)$$

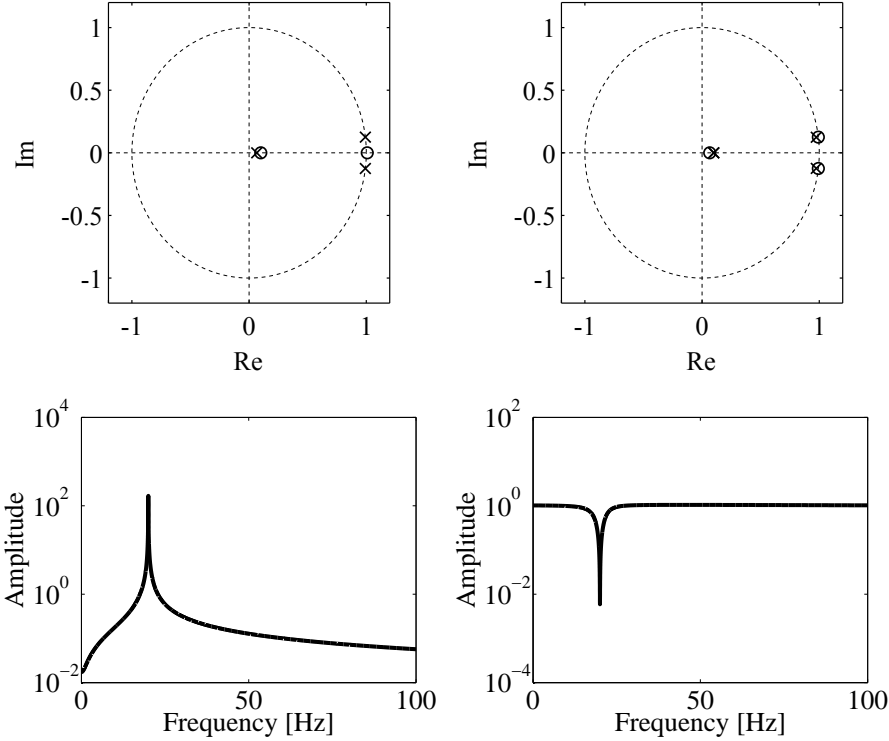


Figure 2.8: Pole-zero map (top) and amplitude frequency response (bottom) of controller (left) and closed-loop system (right) for a sampling frequency of 1 kHz

is filtered through a model of the disturbance

$$\begin{bmatrix} \mathbf{x}_{d,k+1} \\ \mathbf{y}_{d,k} \end{bmatrix} = \begin{bmatrix} \mathbf{A}_d & \mathbf{B}_d \\ \mathbf{I} & \mathbf{0} \end{bmatrix} \begin{bmatrix} \mathbf{x}_{d,k} \\ \mathbf{e}_k \end{bmatrix} \quad (2.40)$$

with $\mathbf{e}_k = -\mathbf{y}_{p,k}$. The dimensions of the system matrices for plant and disturbance are defined by $\mathbf{A}_p^{(n_p \times n_p)}$, $\mathbf{B}_p^{(n_p \times m_{u_p})}$, $\mathbf{C}_p^{(r_{y_p} \times n_p)}$, $\mathbf{A}_d^{(2n_d \times 2n_d)}$ and $\mathbf{B}_d^{(2n_d \times r_{y_p})}$.

The models of plant and error filter are combined in this control design to obtain a state-space representation

$$\begin{bmatrix} \mathbf{x}_{d,k+1} \\ \mathbf{x}_{p,k+1} \\ \mathbf{y}_{p,k} \end{bmatrix} = \begin{bmatrix} \mathbf{A}_d & -\mathbf{B}_d \mathbf{C}_p & \mathbf{0} \\ \mathbf{0} & \mathbf{A}_p & \mathbf{B}_p \\ \mathbf{0} & \mathbf{C}_p & \mathbf{0} \end{bmatrix} \begin{bmatrix} \mathbf{x}_{d,k} \\ \mathbf{x}_{p,k} \\ \mathbf{u}_{p,k} \end{bmatrix} \quad (2.41)$$

of the augmented system. In compact form the augmented system can be written as

$$\begin{bmatrix} \mathbf{x}_{ef,k+1} \\ \mathbf{y}_{p,k} \end{bmatrix} = \begin{bmatrix} \mathbf{A}_{ef} & \mathbf{B}_{ef} \\ \mathbf{C}_{ef} & \mathbf{0} \end{bmatrix} \begin{bmatrix} \mathbf{x}_{ef,k} \\ \mathbf{u}_{p,k} \end{bmatrix} \quad (2.42)$$

2. Internal-model-principle-based Control

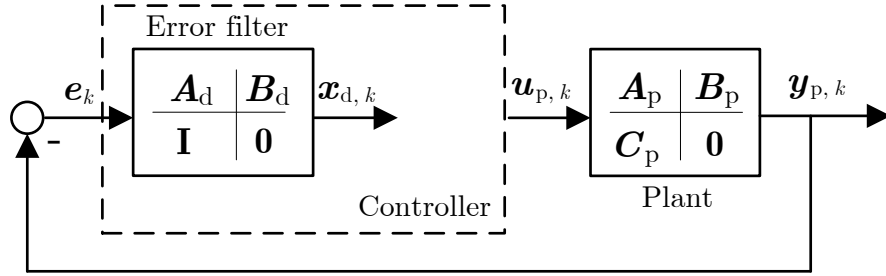


Figure 2.9: Error-filter controller structure

with

$$\begin{aligned} \mathbf{x}_{\text{ef}, k} &= \begin{bmatrix} \mathbf{x}_{d, k} \\ \mathbf{x}_{p, k} \end{bmatrix}, \quad \mathbf{A}_{\text{ef}}^{((2n_d+n_p) \times (2n_d+n_p))} = \begin{bmatrix} \mathbf{A}_d & -\mathbf{B}_d \mathbf{C}_p \\ \mathbf{0} & \mathbf{A}_p \end{bmatrix}, \\ \mathbf{B}_{\text{ef}}^{((2n_d+n_p) \times m_{\mathbf{u}_p})} &= \begin{bmatrix} \mathbf{0} \\ \mathbf{B}_p \end{bmatrix}, \quad \mathbf{C}_{\text{ef}}^{(r_{\mathbf{y}_p} \times (2n_d+n_p))} = [\mathbf{0} \quad \mathbf{C}_p] \end{aligned} \quad (2.43)$$

and “ef” is used for the error-filter approach.

The error-filter control structure is a state-feedback gain $\mathbf{K}_{\text{ef}}^{(m_{\mathbf{u}_p} \times (2n_d+n_p))}$ of the augmented system

$$\mathbf{u}_{p, k} = -\mathbf{K}_{\text{ef}} \mathbf{x}_{\text{ef}, k} = -[\mathbf{K}_d \quad \mathbf{K}_p] \begin{bmatrix} \mathbf{x}_{d, k} \\ \hat{\mathbf{x}}_{p, k} \end{bmatrix} \quad (2.44)$$

with the estimated plant states $\hat{\mathbf{x}}_{p, k}$ calculated using an identity observer

$$\hat{\mathbf{x}}_{p, k+1} = [\mathbf{A}_p - \mathbf{L}_p \mathbf{C}_p \mid \mathbf{B}_p \quad \mathbf{L}_p] \begin{bmatrix} \hat{\mathbf{x}}_{p, k} \\ \mathbf{u}_{p, k} \\ \mathbf{y}_{p, k} \end{bmatrix} \quad (2.45)$$

with an observer gain $\mathbf{L}_p^{(n_p \times r_{\mathbf{y}_p})}$.

A state-space representation of the controller is given by

$$\begin{bmatrix} \mathbf{x}_{d, k+1} \\ \hat{\mathbf{x}}_{p, k+1} \\ \mathbf{u}_{p, k} \end{bmatrix} = \left[\begin{array}{c|c} \mathbf{A}_d & \mathbf{0} \\ -\mathbf{B}_p \mathbf{K}_d & \mathbf{A}_p - \mathbf{B}_p \mathbf{K}_p - \mathbf{L}_p \mathbf{C}_p \\ \hline -\mathbf{K}_d & -\mathbf{K}_p \end{array} \right] \begin{bmatrix} \mathbf{x}_{d, k} \\ \hat{\mathbf{x}}_{p, k} \\ \mathbf{e}_k \end{bmatrix} \quad (2.46)$$

and the control structure is shown in Fig. 2.10. A state-representation of the controller in compact form is given by

$$\begin{bmatrix} \mathbf{x}_{\text{efc}, k+1} \\ \mathbf{u}_{p, k} \end{bmatrix} = \left[\begin{array}{c|c} \mathbf{A}_{\text{efc}} & \mathbf{B}_{\text{efc}} \\ \hline \mathbf{C}_{\text{efc}} & \mathbf{0} \end{array} \right] \begin{bmatrix} \mathbf{x}_{\text{efc}, k} \\ \mathbf{e}_k \end{bmatrix} \quad (2.47)$$

with

$$\begin{aligned} \mathbf{x}_{\text{efc}, k} &= \begin{bmatrix} \mathbf{x}_{d, k} \\ \hat{\mathbf{x}}_{p, k} \end{bmatrix}, \quad \mathbf{A}_{\text{efc}}^{((2n_d+n_p) \times (2n_d+n_p))} = \begin{bmatrix} \mathbf{A}_d & \mathbf{0} \\ -\mathbf{B}_p \mathbf{K}_d & \mathbf{A}_p - \mathbf{B}_p \mathbf{K}_p - \mathbf{L}_p \mathbf{C}_p \end{bmatrix}, \\ \mathbf{B}_{\text{efc}}^{((2n_d+n_p) \times r_{\mathbf{y}_p})} &= \begin{bmatrix} \mathbf{B}_d \\ \mathbf{L}_p \end{bmatrix} \end{aligned} \quad (2.48)$$

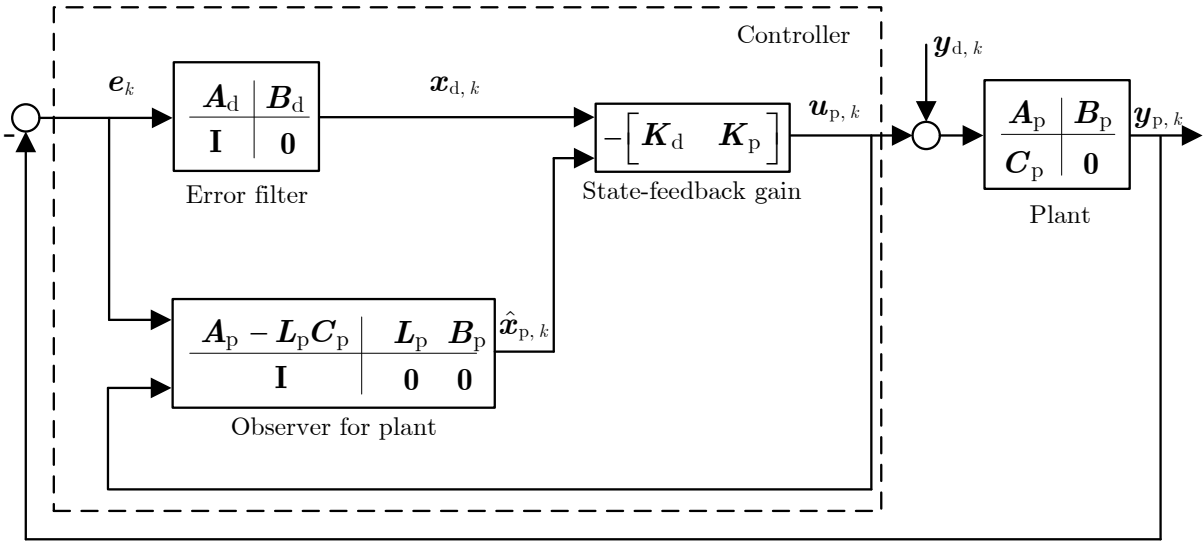


Figure 2.10: Error-filter control structure

and

$$C_{\text{efc}}^{(m_{u_p} \times (2n_d + n_p))} = [-K_d \quad -K_p]. \quad (2.49)$$

Error-filter controller is denoted by “efc”. The controller is stable if the eigenvalues of the matrix A_{efc} are placed inside the unitary circle. The constant state-feedback gain K_{ef} can be calculated solving the LMIs

$$\begin{bmatrix} P & (A_{\text{ef}}P - B_{\text{ef}}Y)^T \\ A_{\text{ef}}P - B_{\text{ef}}Y & P - I \end{bmatrix} > 0, \quad (2.50)$$

$$\begin{bmatrix} W & \tilde{Q}P - \tilde{R}Y \\ (\tilde{Q}P - \tilde{R}Y)^T & P \end{bmatrix} > 0, \quad (2.51)$$

$$\text{trace}(W) < \gamma^2 \quad (2.52)$$

for the positive definite matrix $P^{((2n_d + n_p) \times (2n_d + n_p))}$, $W^{((m_{u_p} + 2n_d + n_p) \times (m_{u_p} + 2n_d + n_p))}$ and for the matrix $Y^{(m_{u_p} \times (2n_d + n_p))}$ with

$$\tilde{Q}^{((m_{u_p} + 2n_d + n_p) \times (2n_d + n_p))} = \begin{bmatrix} Q^{\frac{1}{2}} \\ 0 \end{bmatrix} \text{ and } \tilde{R}^{((m_{u_p} + 2n_d + n_p) \times m_{u_p})} = \begin{bmatrix} 0 \\ R^{\frac{1}{2}} \end{bmatrix} \quad (2.53)$$

for the matrices $Q^{((2n_d + n_p) \times (2n_d + n_p))}$ and $R^{(m_{u_p} \times m_{u_p})}$.

The constant state-feedback $K_{\text{ef}}^{(m_{u_p} \times (2n_d + n_p))}$ gain is calculated as

$$K_{\text{ef}} = Y P^{-1}. \quad (2.54)$$

The closed-loop system has an H_2 -norm bounded by γ if solutions for these LMIs are found (see A.3 and A.4).

To study the stability of the closed-loop overall system, the observer error of the plant

$$\tilde{x}_{p,k+1} = \hat{x}_{p,k+1} - x_{p,k+1} = [A_p - L_p C_p \mid -B_p] \begin{bmatrix} \tilde{x}_{p,k} \\ y_{d,k} \end{bmatrix} \quad (2.55)$$

2. Internal-model-principle-based Control

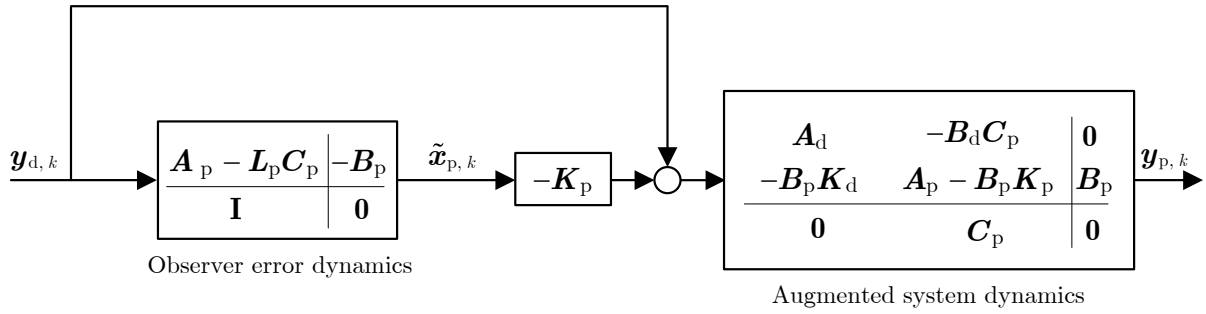


Figure 2.11: Overall closed-loop dynamics

and the plant under state feedback

$$\mathbf{x}_{p,k+1} = \begin{bmatrix} -\mathbf{B}_p \mathbf{K}_p & -\mathbf{B}_p \mathbf{K}_d & \mathbf{A}_p - \mathbf{B}_p \mathbf{K}_p & \mathbf{B}_p \end{bmatrix} \begin{bmatrix} \tilde{\mathbf{x}}_{p,k} \\ \mathbf{x}_{d,k} \\ \mathbf{x}_{p,k} \\ \mathbf{y}_{d,k} \end{bmatrix} \quad (2.56)$$

are combined to obtain the overall closed-loop system dynamics given by

$$\begin{bmatrix} \tilde{\mathbf{x}}_{p,k+1} \\ \mathbf{x}_{d,k+1} \\ \mathbf{x}_{p,k+1} \end{bmatrix} = \begin{bmatrix} \mathbf{A}_p - \mathbf{L}_p \mathbf{C}_p & \mathbf{0} & \mathbf{0} & -\mathbf{B}_p \\ \mathbf{0} & \mathbf{A}_d & -\mathbf{B}_d \mathbf{C}_p & \mathbf{0} \\ -\mathbf{B}_p \mathbf{K}_p & -\mathbf{B}_p \mathbf{K}_d & \mathbf{A}_p - \mathbf{B}_p \mathbf{K}_p & \mathbf{B}_p \end{bmatrix} \begin{bmatrix} \tilde{\mathbf{x}}_{p,k} \\ \mathbf{x}_{d,k} \\ \mathbf{x}_{p,k} \\ \mathbf{y}_{d,k} \end{bmatrix}. \quad (2.57)$$

The dynamics of the overall closed-loop system are shown in Fig. 2.11. From this representation it can be seen that the dynamics of the augmented plant under state feedback are driven by the dynamics of the observer error for the plant states. Choosing an observer gain \mathbf{L}_p for the plant and a state-feedback gain \mathbf{K}_{ef} for the augmented system such that $(\mathbf{A}_p - \mathbf{L}_p \mathbf{C}_p)$ and $(\mathbf{A}_{ef} - \mathbf{B}_{ef} \mathbf{K}_{ef})$ are stable; it guarantees overall stability of the closed-loop system.

A simple example of this control design is realized with the plant of (2.4)

$$\begin{bmatrix} \mathbf{x}_{p,k+1} \\ \mathbf{y}_{p,k} \end{bmatrix} = \begin{bmatrix} a & 1 \\ 1-a & 0 \end{bmatrix} \begin{bmatrix} \mathbf{x}_{p,k} \\ u_{p,k} \end{bmatrix} \quad (2.58)$$

for $a = 0.1$ and a disturbance $y_{d,k} = \sin(2\pi ft_k)$ with only one frequency component ($n_d = 1$), $f = 20$ Hz, $t_k = T, 2T, \dots$ and $T = 0.001$ s acting at the input of the plant. The plant matrices are given with $A_p^{(n_p \times n_p)} = a$, $B_p^{(n_p \times m_{u_p})} = 1$ and $C_p^{(r_{y_p} \times n_p)} = (1-a)$. The error $e_k = -y_{p,k}$ is filtered with the model of the disturbance as in (2.40). For a harmonic disturbance the error-filter is given as

$$\begin{bmatrix} \mathbf{x}_{d,k+1} \\ \mathbf{y}_{d,k} \end{bmatrix} = \begin{bmatrix} \mathbf{A}_d & \mathbf{B}_d \\ \mathbf{I} & \mathbf{0} \end{bmatrix} \begin{bmatrix} \mathbf{x}_{d,k} \\ e_k \end{bmatrix} \quad (2.59)$$

with

$$\mathbf{A}_d^{(2n_d \times 2n_d)} = \begin{bmatrix} 0 & 1 \\ -r^2 & 2r \cos(2\pi fT) \end{bmatrix}, \quad \mathbf{B}_d^{(2n_d \times r_{y_p})} = \begin{bmatrix} 1 \\ 0 \end{bmatrix} \quad \text{and} \quad r = 0.9999. \quad (2.60)$$

From these system matrices from plant and error filter the dimensions $n_p = m_{u_p} = r_{y_p} = n_d = r_{y_d} = 1$ are obtained.

For the calculation of the state-feedback gain $\mathbf{K}_{\text{ef}}^{(m_{u_p} \times (2n_d + n_p))}$ the augmented system

$$\left[\begin{array}{c} \mathbf{x}_{d,k+1} \\ \mathbf{x}_{p,k+1} \\ \hline \mathbf{y}_{p,k} \end{array} \right] = \left[\begin{array}{cc|c} \mathbf{A}_d & -\mathbf{B}_d C_p & \mathbf{0} \\ \mathbf{0} & A_p & B_p \\ \hline \mathbf{0} & C_p & 0 \end{array} \right] \left[\begin{array}{c} \mathbf{x}_{d,k} \\ \mathbf{x}_{p,k} \\ \hline \mathbf{u}_{p,k} \end{array} \right] \quad (2.61)$$

is built. A state-feedback gain

$$\mathbf{K}_{\text{ef}} = [\mathbf{K}_d \ K_p] = [-0.0346 \ 0.0337 \ 0.0348] \quad (2.62)$$

is obtained with a discrete-time linear quadratic regulator or using the LMIs from (2.50)-(2.52) with

$$\mathbf{Q}^{((2n_d + n_p) \times (2n_d + n_p))} = \left[\begin{array}{ccc} 0.01 & 0 & 0 \\ 0 & 0.01 & 0 \\ 0 & 0 & 0.01 \end{array} \right] \quad \text{and} \quad R^{(m_{u_p} \times m_{u_p})} = 1000 . \quad (2.63)$$

The matrices \mathbf{Q} and \mathbf{R} were chosen to satisfy a desired performance in closed loop after testing different values for them. The observer gain $L_p^{(n_p \times r_{y_p})} = 0.0499$ place the pole for the observer ($A_p - L_p C_p$) in 0.0551. A state-space representation of the controller obtained is given by (2.47) with

$$\begin{aligned} \mathbf{A}_{\text{efc}}^{((2n_d + n_p) \times (2n_d + n_p))} &= \left[\begin{array}{cc} \mathbf{A}_d & \mathbf{0} \\ -B_p \mathbf{K}_d & A_p - B_p K_p - L_p C_p \end{array} \right] = \\ &= \mathbf{A}_{\text{efc}} = \left[\begin{array}{ccc} 0 & 1 & 0 \\ -r^2 & 2r \cos(2\pi fT) & 0 \\ 0.0346 & -0.0337 & 0.0203 \end{array} \right], \end{aligned} \quad (2.64)$$

$$\mathbf{B}_{\text{efc}}^{((2n_d + n_p) \times r_{y_p})} = \left[\begin{array}{c} \mathbf{B}_d \\ L_p \end{array} \right] = \left[\begin{array}{c} 1 \\ 0 \\ 0.0499 \end{array} \right] \quad (2.65)$$

and

$$\mathbf{C}_{\text{efc}}^{(m_{u_p} \times (2n_d + n_p))} = [-\mathbf{K}_d \ -K_p] = [0.0346 \ -0.0337 \ -0.0348] . \quad (2.66)$$

Pole-zero map and amplitude frequency responses of controller and closed-loop system are shown in Fig. 2.12. The closed-loop system is stable since $(A_p - L_p C_p)$ and $(\mathbf{A}_{\text{ef}} - \mathbf{B}_{\text{ef}} \mathbf{K}_{\text{ef}})$ are stable (see Fig. 2.11 and (2.57)).

Output Feedback Control Structure

The control design techniques used here to obtain the output-feedback controller are based on the well-established H_∞ control framework (see A.5 and A.5). The basic idea is to use the generalized plant shown in Fig. 2.13 and minimize the H_∞ -norm between performance input \mathbf{w}_k and performance ouput \mathbf{q}_k using weighting functions. Here weighting functions

$$\left[\begin{array}{c} \mathbf{x}_{W_u,k+1} \\ \mathbf{q}_{u,k} \end{array} \right] = \left[\begin{array}{c|c} \mathbf{A}_{W_u} & \mathbf{B}_{W_u} \\ \hline \mathbf{C}_{W_u} & \mathbf{D}_{W_u} \end{array} \right] \left[\begin{array}{c} \mathbf{x}_{W_u,k} \\ \mathbf{u}_{p,k} \end{array} \right] \quad (2.67)$$

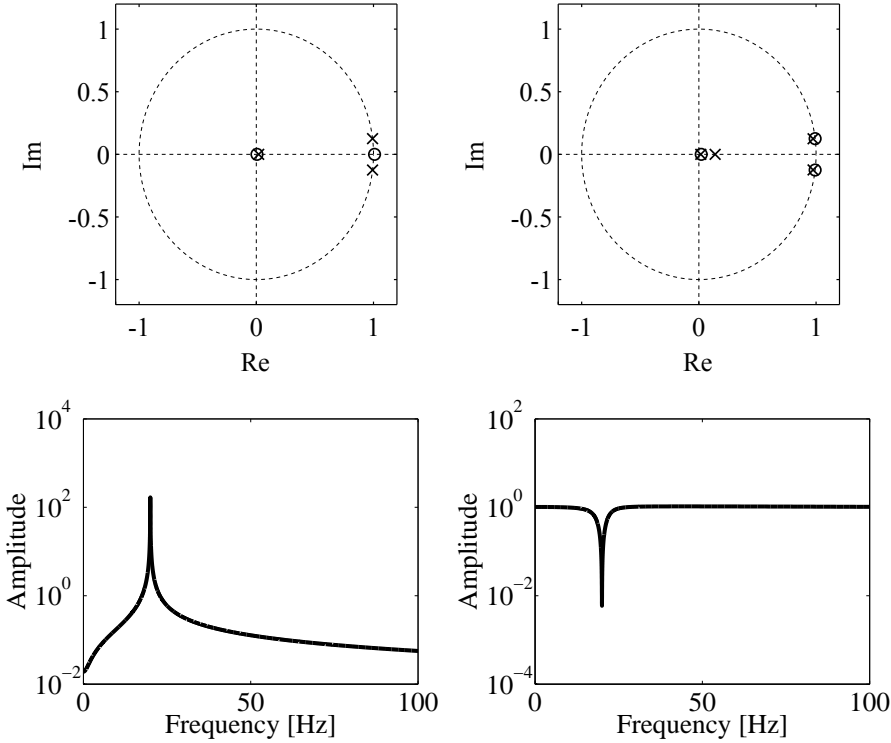


Figure 2.12: Pole-zero map (top) and amplitude frequency response (bottom) of controller (left) and closed-loop system (right) for a sampling frequency of 1 kHz

for the control input $\mathbf{u}_{p,k}$ with the matrices $\mathbf{A}_{\mathbf{W}_u}^{(n_{\mathbf{W}_u} \times n_{\mathbf{W}_u})}$, $\mathbf{B}_{\mathbf{W}_u}^{(n_{\mathbf{W}_u} \times m_u)}$, $\mathbf{C}_{\mathbf{W}_u}^{(r_{qu} \times n_{\mathbf{W}_u})}$, $\mathbf{D}_{\mathbf{W}_u}^{(r_{qu} \times m_u)}$ and

$$\begin{bmatrix} \mathbf{x}_{\mathbf{W}_y, k+1} \\ \mathbf{q}_{y, k} \end{bmatrix} = \begin{bmatrix} \mathbf{A}_{\mathbf{W}_y} & \mathbf{B}_{\mathbf{W}_y} \\ \mathbf{C}_{\mathbf{W}_y} & \mathbf{D}_{\mathbf{W}_y} \end{bmatrix} \begin{bmatrix} \mathbf{x}_{\mathbf{W}_y, k} \\ \mathbf{y}_{p, k} \end{bmatrix} \quad (2.68)$$

plant output $\mathbf{y}_{p,k}$ with $\mathbf{A}_{\mathbf{W}_y}^{(n_{\mathbf{W}_y} \times n_{\mathbf{W}_y})}$, $\mathbf{B}_{\mathbf{W}_y}^{(n_{\mathbf{W}_y} \times r_y)}$, $\mathbf{C}_{\mathbf{W}_y}^{(r_{qu} \times n_{\mathbf{W}_y})}$, $\mathbf{D}_{\mathbf{W}_y}^{(r_{qu} \times r_y)}$ are used. For disturbance rejection, additional dynamics are included in the generalized plant modeling the disturbance at the input of the plant (IMP). A state-space description of the generalized plant is given as

$$\begin{bmatrix} \mathbf{x}_{k+1} \\ \mathbf{q}_k \\ \mathbf{y}_{p, k} \end{bmatrix} = \begin{bmatrix} \mathbf{A} & \mathbf{B}_w & \mathbf{B}_u \\ \mathbf{C}_q & \mathbf{D}_{qw} & \mathbf{D}_{qu} \\ \mathbf{C}_y & \mathbf{D}_{yw} & \mathbf{D}_{yu} \end{bmatrix} \begin{bmatrix} \mathbf{x}_k \\ \mathbf{w}_k \\ \mathbf{u}_{p, k} \end{bmatrix} \quad (2.69)$$

assuming $\mathbf{D}_{yu} = \mathbf{0}$ (see Gahinet and Apkarian (1994)) with

$$\mathbf{x}_k = \begin{bmatrix} \mathbf{x}_{p, k} \\ \mathbf{x}_{d, k} \\ \mathbf{x}_{\mathbf{W}_u, k} \\ \mathbf{x}_{\mathbf{W}_y, k} \end{bmatrix}, \quad (2.70)$$

$$\mathbf{A}^{((n_p + 2n_d + n_{\mathbf{W}_u} + n_{\mathbf{W}_y}) \times (n_p + 2n_d + n_{\mathbf{W}_u} + n_{\mathbf{W}_y}))} = \begin{bmatrix} \mathbf{A}_p & \mathbf{B}_p \mathbf{C}_d & \mathbf{0} & \mathbf{0} \\ \mathbf{0} & \mathbf{A}_d & \mathbf{0} & \mathbf{0} \\ \mathbf{0} & \mathbf{0} & \mathbf{A}_{\mathbf{W}_u} & \mathbf{0} \\ \mathbf{B}_{\mathbf{W}_y} \mathbf{C}_p & \mathbf{0} & \mathbf{0} & \mathbf{A}_{\mathbf{W}_y} \end{bmatrix}, \quad (2.71)$$

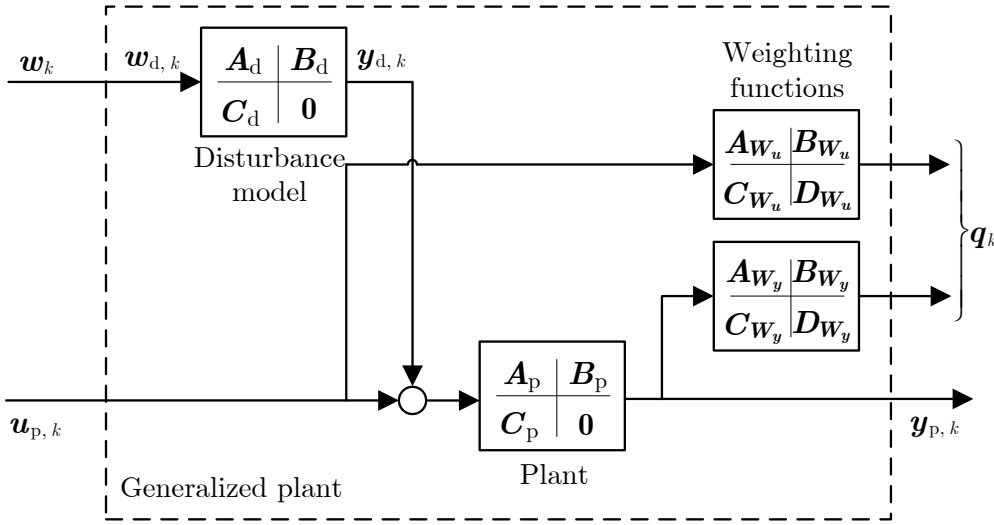


Figure 2.13: Generalized plant including weighting functions and model of the disturbance

$$[\mathbf{B}_w \quad \mathbf{B}_u]^{((n_p+2n_d+n_{W_u}+n_{W_y}) \times (m_w+m_u))} = \begin{bmatrix} \mathbf{0} & \mathbf{B}_p \\ \mathbf{B}_d & \mathbf{0} \\ \mathbf{0} & \mathbf{B}_{W_u} \\ \mathbf{0} & \mathbf{0} \end{bmatrix}, \quad (2.72)$$

$$\begin{bmatrix} \mathbf{C}_q \\ \mathbf{C}_y \end{bmatrix}^{((r_{qu}+r_{qy}+r_y) \times (n_p+2n_d+n_{W_u}+n_{W_y}))} = \begin{bmatrix} \mathbf{0} & \mathbf{0} & \mathbf{C}_{W_u} & \mathbf{0} \\ \mathbf{D}_{W_y} \mathbf{C}_p & \mathbf{0} & \mathbf{0} & \mathbf{C}_{W_y} \\ \hline \mathbf{C}_p & \mathbf{0} & \mathbf{0} & \mathbf{0} \end{bmatrix} \quad (2.73)$$

and

$$\begin{bmatrix} \mathbf{D}_{qw} & \mathbf{D}_{qu} \\ \mathbf{D}_{yw} & \mathbf{D}_{yu} \end{bmatrix}^{((r_{qu}+r_{qy}+r_y) \times (m_w+m_u))} = \begin{bmatrix} \mathbf{0} & \mathbf{D}_{W_u} \\ \mathbf{0} & \mathbf{0} \\ \hline \mathbf{0} & \mathbf{0} \end{bmatrix}. \quad (2.74)$$

The orders $n = n_p + 2n_d + n_{W_u} + n_{W_y}$ and $r_q = r_{qu} + r_{qy}$ are introduced for an easier representation of the generalized plant matrices.

Applying H_∞ control design techniques, the ouput-feedback controller of Fig. 2.14 is obtained. The procedure proposed by Gahinet and Apkarian (1994) for the calculation of a suboptimal controller is briefly explained.

The closed-loop system is obtained from the combination of controller

$$\begin{bmatrix} \mathbf{x}_{K,k+1} \\ \mathbf{u}_{p,k} \end{bmatrix} = \begin{bmatrix} \mathbf{A}^{(K)} & \mathbf{B}_y^{(K)} \\ \hline \mathbf{C}_u^{(K)} & \mathbf{D}_{uy}^{(K)} \end{bmatrix} \begin{bmatrix} \mathbf{x}_{K,k} \\ \mathbf{y}_{p,k} \end{bmatrix} \quad (2.75)$$

with $\mathbf{A}^{(K)(n \times n)}$, $\mathbf{B}_y^{(K)(n \times r_y)}$, $\mathbf{C}_u^{(K)(m_u \times n)}$, $\mathbf{D}_{uy}^{(K)(m_u \times r_y)}$ and generalized plant (2.69)

$$\begin{bmatrix} \mathbf{x}_{p,k+1} \\ \mathbf{x}_{K,k+1} \\ \hline \mathbf{q}_k \\ \hline \mathbf{u}_{p,k} \\ \mathbf{y}_{p,k} \end{bmatrix} = \begin{bmatrix} \mathbf{A} & \mathbf{0} & \mathbf{B}_w & \mathbf{B}_u & \mathbf{0} \\ \mathbf{0} & \mathbf{A}^{(K)} & \mathbf{0} & \mathbf{0} & \mathbf{B}_y^{(K)} \\ \hline \mathbf{C}_q & \mathbf{0} & \mathbf{D}_{qw} & \mathbf{D}_{qu} & \mathbf{0} \\ \hline \mathbf{0} & \mathbf{C}_u^{(K)} & \mathbf{0} & \mathbf{0} & \mathbf{D}_{uy}^{(K)} \\ \mathbf{C}_y & \mathbf{0} & \mathbf{D}_{yw} & \mathbf{D}_{yu} & \mathbf{0} \end{bmatrix} \begin{bmatrix} \mathbf{x}_{p,k} \\ \mathbf{w}_k \\ \hline \mathbf{x}_{K,k} \\ \hline \mathbf{u}_{p,k} \\ \mathbf{y}_{p,k} \end{bmatrix}. \quad (2.76)$$

2. Internal-model-principle-based Control

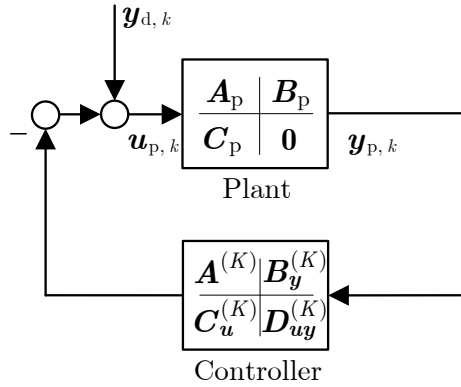


Figure 2.14: Output-feedback control structure

The equation (2.76) can be written as

$$\begin{bmatrix} \mathbf{x}_{p,k+1} \\ \mathbf{x}_{K,k+1} \\ \mathbf{q}_k \\ \mathbf{u}_{p,k} \\ \mathbf{y}_{p,k} \end{bmatrix} = \begin{bmatrix} \mathbf{A}_1 & \mathbf{B}_1 & \mathbf{B}_2 \\ \mathbf{C}_1 & \mathbf{D}_{11} & \mathbf{D}_{12} \\ \mathbf{C}_2 & \mathbf{D}_{21} & \mathbf{D}_{22} \end{bmatrix} \begin{bmatrix} \mathbf{x}_{p,k} \\ \mathbf{x}_{K,k} \\ \mathbf{w}_k \\ \mathbf{u}_{p,k} \\ \mathbf{y}_{p,k} \end{bmatrix} \quad (2.77)$$

with $\mathbf{A}_1^{(2n \times 2n)}$, $\mathbf{B}_1^{(2n \times m_w)}$, $\mathbf{B}_2^{(2n \times (m_u + r_y))}$, $\mathbf{C}_1^{(r_q \times 2n)}$, $\mathbf{D}_{11}^{(r_q \times m_w)}$, $\mathbf{D}_{12}^{(r_q \times (m_u + r_y))}$, $\mathbf{C}_2^{((m_u + r_y) \times 2n)}$, $\mathbf{D}_{21}^{((m_u + r_y) \times m_w)}$, $\mathbf{D}_{22}^{((m_u + r_y) \times (m_u + r_y))}$ and the LFT is applied here to obtain a representation of the closed-loop system

$$\begin{bmatrix} \mathbf{A}_1 & \mathbf{B}_1 \\ \mathbf{C}_1 & \mathbf{D}_{11} \end{bmatrix} + \begin{bmatrix} \mathbf{B}_2 \\ \mathbf{D}_{12} \end{bmatrix} (\mathbf{I} - \mathbf{D}_{22})^{-1} \begin{bmatrix} \mathbf{C}_2 & \mathbf{D}_{21} \end{bmatrix} \quad (2.78)$$

as

$$\begin{bmatrix} \mathbf{x}_{p,k+1} \\ \mathbf{x}_{K,k+1} \\ \mathbf{q}_k \end{bmatrix} = \begin{bmatrix} \mathbf{A}_{\text{cl}} & \mathbf{B}_{\text{cl}} \\ \mathbf{C}_{\text{cl}} & \mathbf{D}_{\text{cl}} \end{bmatrix} \begin{bmatrix} \mathbf{x}_{p,k} \\ \mathbf{x}_{K,k} \\ \mathbf{w}_k \end{bmatrix} \quad (2.79)$$

with

$$\mathbf{A}_{\text{cl}}^{(2n \times 2n)} = \begin{bmatrix} \mathbf{A} + \mathbf{B}_u \mathbf{D}_{uy}^{(K)} \mathbf{C}_y & \mathbf{B}_u \mathbf{C}_u^{(K)} \\ \mathbf{B}_y^{(K)} \mathbf{C}_y & \mathbf{A}^{(K)} \end{bmatrix}, \quad (2.80)$$

$$\mathbf{B}_{\text{cl}}^{(2n \times m_w)} = \begin{bmatrix} \mathbf{B}_w + \mathbf{B}_u \mathbf{D}_{uy}^{(K)} \mathbf{D}_{yw} \\ \mathbf{B}_y^{(K)} \mathbf{D}_{yw} \end{bmatrix}, \quad (2.81)$$

$$\mathbf{C}_{\text{cl}}^{(r_q \times 2n)} = \begin{bmatrix} \mathbf{C}_q + \mathbf{D}_{qu} \mathbf{D}_{uy}^{(K)} \mathbf{C}_y & \mathbf{D}_{qu} \mathbf{C}_u^{(K)} \end{bmatrix}, \quad (2.82)$$

$$\mathbf{D}_{\text{cl}}^{(r_q \times m_w)} = \begin{bmatrix} \mathbf{D}_{qw} + \mathbf{D}_{qu} \mathbf{D}_{uy}^{(K)} \mathbf{D}_{yw} \end{bmatrix} \quad (2.83)$$

and $\mathbf{D}_{yu} = \mathbf{0}$ (see Gahinet and Apkarian (1994)). Using the BRL this control problem is solvable if a solution for the positive definite matrix $\mathbf{X}_{\text{cl}}^{(2n \times 2n)}$ exists for the LMI

$$\begin{bmatrix} -\mathbf{X}_{\text{cl}}^{-1} & \mathbf{A}_{\text{cl}} & \mathbf{B}_{\text{cl}} & \mathbf{0} \\ \mathbf{A}_{\text{cl}}^T & -\mathbf{X}_{\text{cl}} & \mathbf{0} & \mathbf{C}_{\text{cl}}^T \\ \mathbf{B}_{\text{cl}}^T & \mathbf{0} & -\gamma \mathbf{I} & \mathbf{D}_{\text{cl}}^T \\ \mathbf{0} & \mathbf{C}_{\text{cl}} & \mathbf{D}_{\text{cl}} & -\gamma \mathbf{I} \end{bmatrix} < 0. \quad (2.84)$$

The LMI (2.84) can be rewritten as

$$\psi + \mathbf{P}^T \boldsymbol{\Omega} \mathbf{Q} + \mathbf{Q}^T \boldsymbol{\Omega}^T \mathbf{P} < 0 \quad (2.85)$$

with the matrices

$$\begin{aligned} \mathbf{P}^{((n+m_u) \times (4n+m_w+r_q))} &= [\underline{\mathbf{B}}^T \quad \mathbf{0} \quad \mathbf{0} \quad \underline{\mathbf{D}}_{qu}^T] \\ \mathbf{Q}^{((r_y+n) \times (4n+m_w+r_q))} &= [\mathbf{0} \quad \underline{\mathbf{C}} \quad \underline{\mathbf{D}}_{yw} \quad \mathbf{0}] \end{aligned} \quad (2.86)$$

defined with

$$\begin{aligned} \underline{\mathbf{B}}^{(2n \times (n+m_u))} &= \begin{bmatrix} \mathbf{0} & \mathbf{B}_u \\ \mathbf{I} & \mathbf{0} \end{bmatrix}, \quad \underline{\mathbf{C}}^{((n+r_y) \times 2n)} = \begin{bmatrix} \mathbf{0} & \mathbf{I} \\ \mathbf{C}_y & \mathbf{0} \end{bmatrix}, \\ \underline{\mathbf{D}}_{qu}^{(r_q \times (n+m_u))} &= [\mathbf{0} \quad \mathbf{D}_{qu}], \quad \underline{\mathbf{D}}_{yw}^{((n+r_y) \times m_w)} = \begin{bmatrix} \mathbf{0} \\ \mathbf{D}_{yw} \end{bmatrix} \end{aligned} \quad (2.87)$$

and the matrix

$$\psi^{((4n+m_w+r_q) \times (4n+m_w+r_q))} = \begin{bmatrix} -\mathbf{X}^{-1} & \bar{\mathbf{A}} & \bar{\mathbf{B}} & \mathbf{0} \\ \bar{\mathbf{A}}^T & -\mathbf{X} & \mathbf{0} & \bar{\mathbf{C}}^T \\ \bar{\mathbf{B}}^T & \mathbf{0} & -\gamma \mathbf{I} & \underline{\mathbf{D}}_{qw}^T \\ \mathbf{0} & \bar{\mathbf{C}} & \mathbf{D}_{qw} & -\gamma \mathbf{I} \end{bmatrix} \quad (2.88)$$

built with

$$\bar{\mathbf{A}}^{(2n \times 2n)} = [\mathbf{A} \quad \mathbf{0}], \quad \bar{\mathbf{B}}^{(2n \times m_w)} = [\mathbf{B}_w \quad \mathbf{0}] \quad \text{and} \quad \bar{\mathbf{C}}^{(r_q \times 2n)} = [\mathbf{C}_q \quad \mathbf{0}]. \quad (2.89)$$

Here it is important to notice that the controller $\boldsymbol{\Omega}$ can be calculated using (2.85) for a given positive definite matrix \mathbf{X} . A method to calculate the matrix \mathbf{X} will be explained later in this section.

Solvability conditions

$$\mathbf{W}_P^T \psi \mathbf{W}_P < 0 \quad (2.90)$$

and

$$\mathbf{W}_Q^T \psi \mathbf{W}_Q < 0 \quad (2.91)$$

are derived in Gahinet and Apkarian (1994) from (2.85) multiplying all the elements of this equation by the nullspaces \mathbf{W}_P and \mathbf{W}_Q of the matrices \mathbf{P} and \mathbf{Q} , respectively.

These conditions are equivalently expressed (see Apkarian and Gahinet (1994)) as

$$\begin{aligned} \begin{bmatrix} \mathbf{N}_X & \mathbf{0} \\ \mathbf{0} & \mathbf{I} \end{bmatrix}^T \begin{bmatrix} \mathbf{A}^T \mathbf{X}_1 \mathbf{A} - \mathbf{X}_1 & \mathbf{A}^T \mathbf{X}_1 \mathbf{B}_w & \mathbf{C}_q^T \\ \mathbf{B}_w^T \mathbf{X}_1 \mathbf{A} & -\gamma \mathbf{I} + \mathbf{B}_w^T \mathbf{X}_1 \mathbf{B}_w & \mathbf{D}_{qu}^T \\ \mathbf{C}_q & \mathbf{D}_{qu} & -\gamma \mathbf{I} \end{bmatrix} \begin{bmatrix} \mathbf{N}_X & \mathbf{0} \\ \mathbf{0} & \mathbf{I} \end{bmatrix} &< 0, \\ \begin{bmatrix} \mathbf{N}_Y & \mathbf{0} \\ \mathbf{0} & \mathbf{I} \end{bmatrix}^T \begin{bmatrix} \mathbf{A} \mathbf{Y}_1 \mathbf{A}^T - \mathbf{Y}_1 & \mathbf{A} \mathbf{Y}_1 \mathbf{C}_q^T & \mathbf{B}_w \\ \mathbf{C}_q \mathbf{Y}_1 \mathbf{A}^T & -\gamma \mathbf{I} + \mathbf{C}_q \mathbf{Y}_1 \mathbf{C}_q^T & \mathbf{D}_{qu} \\ \mathbf{B}_w^T & \mathbf{D}_{qu}^T & -\gamma \mathbf{I} \end{bmatrix} \begin{bmatrix} \mathbf{N}_Y & \mathbf{0} \\ \mathbf{0} & \mathbf{I} \end{bmatrix} &< 0, \\ \begin{bmatrix} \mathbf{X}_1 & \mathbf{I} \\ \mathbf{I} & \mathbf{Y}_1 \end{bmatrix} &\geq 0 \end{aligned} \quad (2.92)$$

2. Internal-model-principle-based Control

where

$$\mathbf{N}_X^{((n+m_w) \times (n+m_w))} = \text{null}([\mathbf{C}_y \quad \mathbf{D}_{yw}]) \quad (2.93)$$

and

$$\mathbf{N}_Y^{((n+r_q) \times (n+r_q))} = \text{null}([\mathbf{B}_u \quad \mathbf{D}_{qu}^T]). \quad (2.94)$$

If solutions $\mathbf{X}_1^{(n \times n)}$ and $\mathbf{Y}_1^{(n \times n)}$ for these LMIs exist, the control problem is feasible. Furthermore, the matrix

$$\mathbf{X}^{(2n \times 2n)} = \begin{bmatrix} \mathbf{X}_1 & \mathbf{X}_2 \\ \mathbf{X}_2^T & \mathbf{I} \end{bmatrix} \quad (2.95)$$

is built with the solutions \mathbf{X}_1 , \mathbf{Y}_1 and

$$\mathbf{X}_2^{(n \times n)} = (\mathbf{X}_1 - \mathbf{Y}_1^{-1})^{\frac{1}{2}}. \quad (2.96)$$

Once the matrix \mathbf{X} is built, the controller can be calculated from (2.85).

All the steps needed for the calculation of the controller are explained in the following in detail.

The dimensions of the matrices of the generalized plant are defined here as

$$\begin{array}{lll} \mathbf{A}^{n \times n} & \mathbf{B}_w^{n \times m_w} & \mathbf{B}_u^{n \times m_u} \\ \mathbf{C}_q^{r_q \times n} & \mathbf{D}_{qw}^{r_q \times m_w} & \mathbf{D}_{qu}^{r_q \times m_u} \\ \mathbf{C}_y^{r_y \times n} & \mathbf{D}_{yw}^{r_y \times m_w} & \mathbf{D}_{yu}^{r_y \times m_u} \end{array} \quad (2.97)$$

to make more clear the calculation of the controller.

First of all, three linear matrix inequalities (LMIs)

$$\begin{aligned} \begin{bmatrix} \mathbf{N}_X & \mathbf{0} \\ \mathbf{0} & \mathbf{I} \end{bmatrix}^T \begin{bmatrix} \mathbf{A}^T \mathbf{X}_1 \mathbf{A} - \mathbf{X}_1 & \mathbf{A}^T \mathbf{X}_1 \mathbf{B}_w & \mathbf{C}_q^T \\ \mathbf{B}_w^T \mathbf{X}_1 \mathbf{A} & -\gamma \mathbf{I} + \mathbf{B}_w^T \mathbf{X}_1 \mathbf{B}_w & \mathbf{D}_{qu}^T \\ \mathbf{C}_q & \mathbf{D}_{qu} & -\gamma \mathbf{I} \end{bmatrix} \begin{bmatrix} \mathbf{N}_X & \mathbf{0} \\ \mathbf{0} & \mathbf{I} \end{bmatrix} &< 0, \\ \begin{bmatrix} \mathbf{N}_Y & \mathbf{0} \\ \mathbf{0} & \mathbf{I} \end{bmatrix}^T \begin{bmatrix} \mathbf{A} \mathbf{Y}_1 \mathbf{A}^T - \mathbf{Y}_1 & \mathbf{A} \mathbf{Y}_1 \mathbf{C}_q^T & \mathbf{B}_w \\ \mathbf{C}_q \mathbf{Y}_1 \mathbf{A}^T & -\gamma \mathbf{I} + \mathbf{C}_q \mathbf{Y}_1 \mathbf{C}_q^T & \mathbf{D}_{qu} \\ \mathbf{B}_w^T & \mathbf{D}_{qu}^T & -\gamma \mathbf{I} \end{bmatrix} \begin{bmatrix} \mathbf{N}_Y & \mathbf{0} \\ \mathbf{0} & \mathbf{I} \end{bmatrix} &< 0, \\ \begin{bmatrix} \mathbf{X}_1 & \mathbf{I} \\ \mathbf{I} & \mathbf{Y}_1 \end{bmatrix} &\geq 0 \end{aligned} \quad (2.98)$$

are solved for $\mathbf{X}_1^{(n \times n)}$ and $\mathbf{Y}_1^{(n \times n)}$ with the matrices $\mathbf{N}_X^{((n+m_w) \times (n+m_w))}$ and $\mathbf{N}_Y^{((n+r_q) \times (n+r_q))}$ calculated through

$$\begin{aligned} \mathbf{N}_X &= \text{null}([\mathbf{C}_y \quad \mathbf{D}_{yw}]) \\ \mathbf{N}_Y &= \text{null}([\mathbf{B}_u \quad \mathbf{D}_{qu}^T]). \end{aligned} \quad (2.99)$$

Next, the auxiliary matrix is defined by

$$\psi^{((4n+m_w+r_q) \times (4n+m_w+r_q))} = \begin{bmatrix} -\mathbf{X}^{-1} & \bar{\mathbf{A}} & \bar{\mathbf{B}} & \mathbf{0} \\ \bar{\mathbf{A}}^T & -\mathbf{X} & \mathbf{0} & \bar{\mathbf{C}}^T \\ \bar{\mathbf{B}}^T & \mathbf{0} & -\gamma \mathbf{I} & \mathbf{D}_{qw}^T \\ \mathbf{0} & \bar{\mathbf{C}} & \mathbf{D}_{qu} & -\gamma \mathbf{I} \end{bmatrix} \quad (2.100)$$

with

$$\bar{\mathbf{A}}^{(2n \times 2n)} = \begin{bmatrix} \mathbf{A} & \mathbf{0} \\ \mathbf{0} & \mathbf{0} \end{bmatrix}, \quad \bar{\mathbf{B}}^{(2n \times m_w)} = \begin{bmatrix} \mathbf{B}_w \\ \mathbf{0} \end{bmatrix}, \quad \bar{\mathbf{C}}^{(r_q \times 2n)} = [\mathbf{C}_q \quad \mathbf{0}] \quad (2.101)$$

$$\mathbf{X}^{(2n \times 2n)} = \begin{bmatrix} \mathbf{X}_1 & \mathbf{X}_2 \\ \mathbf{X}_2^T & \mathbf{I} \end{bmatrix}, \quad (2.102)$$

and $\mathbf{X}_2^{(n \times n)}$ calculated through

$$\mathbf{X}_2 = (\mathbf{X}_1 - \mathbf{Y}_1^{-1})^{\frac{1}{2}}. \quad (2.103)$$

The matrices

$$\begin{aligned} \mathbf{P}^{((n+m_u) \times (4n+m_w+r_q))} &= [\underline{\mathbf{B}}^T \quad \mathbf{0} \quad \mathbf{0} \quad \underline{\mathbf{D}}_{qu}^T] \\ \mathbf{Q}^{((r_y+n) \times (4n+m_w+r_q))} &= [\mathbf{0} \quad \underline{\mathbf{C}} \quad \underline{\mathbf{D}}_{yw} \quad \mathbf{0}] \end{aligned} \quad (2.104)$$

are built with

$$\begin{aligned} \underline{\mathbf{B}}^{(2n \times (n+m_u))} &= \begin{bmatrix} \mathbf{0} & \mathbf{B}_u \\ \mathbf{I} & \mathbf{0} \end{bmatrix}, \quad \underline{\mathbf{C}}^{((n+r_y) \times 2n)} = \begin{bmatrix} \mathbf{0} & \mathbf{I} \\ \mathbf{C}_y & \mathbf{0} \end{bmatrix}, \\ \underline{\mathbf{D}}_{qu}^{(r_q \times (n+m_u))} &= [\mathbf{0} \quad \mathbf{D}_{qu}] \text{ and } \underline{\mathbf{D}}_{yw}^{((n+r_y) \times m_w)} = \begin{bmatrix} \mathbf{0} \\ \mathbf{D}_{yw} \end{bmatrix}. \end{aligned} \quad (2.105)$$

Finally, the basic LMI

$$\psi + \mathbf{P}^T \Omega \mathbf{Q} + \mathbf{Q}^T \Omega^T \mathbf{P} < 0 \quad (2.106)$$

is solved for $\Omega^{((n+m_u) \times (n+r_y))}$ with the matrices ψ , \mathbf{P} and \mathbf{Q} . The controller matrices are extracted from Ω with

$$\Omega = \left[\begin{array}{c|c} \mathbf{A}^{(K)} & \mathbf{B}_y^{(K)} \\ \hline \mathbf{C}_u^{(K)} & \mathbf{D}_{uy}^{(K)} \end{array} \right] \quad (2.107)$$

and a state-space representation of the controller is written as

$$\begin{bmatrix} \mathbf{x}_{K,k+1} \\ \mathbf{u}_{p,k} \end{bmatrix} = \left[\begin{array}{c|c} \mathbf{A}^{(K)} & \mathbf{B}_y^{(K)} \\ \hline \mathbf{C}_u^{(K)} & \mathbf{D}_{uy}^{(K)} \end{array} \right] \begin{bmatrix} \mathbf{x}_{K,k} \\ \mathbf{y}_{p,k} \end{bmatrix}. \quad (2.108)$$

This control design guarantees the stability in closed loop ($\mathbf{X} = \mathbf{X}^T > 0$).

An example to obtain an output-feedback controller for the rejection of a disturbance $y_{d,k} = \sin(2\pi f t_k)$ ($n_d = 1$) acting at the input of the plant

$$\begin{bmatrix} x_{p,k+1} \\ y_{p,k} \end{bmatrix} = \left[\begin{array}{c|c} a & 1 \\ \hline 1-a & 0 \end{array} \right] \begin{bmatrix} x_{p,k} \\ u_{p,k} \end{bmatrix} \quad (2.109)$$

for $a = 0.1$ is here made using the control design explained in this section, where $f = 20 \text{ Hz}$, $t_k = T, 2T, \dots$ and $T = 0.001 \text{ s}$.

The plant matrices are obtained from (2.109) as $A_p^{(n_p \times n_p)} = a$, $B_p^{(n_p \times m_u)} = 1$ and $C_p^{(r_y \times n_p)} = (1-a)$ with $n_p = m_u = r_y = 1$. The disturbance is modelled as the ouput $y_{d,k}$ of a system given by

$$\begin{bmatrix} \mathbf{x}_{d,k+1} \\ y_{d,k} \end{bmatrix} = \left[\begin{array}{c|c} \mathbf{A}_d & \mathbf{B}_d \\ \hline \mathbf{C}_d & 0 \end{array} \right] \begin{bmatrix} \mathbf{x}_{d,k} \\ w_{d,k} \end{bmatrix} \quad (2.110)$$

with $r = 0.9999$ and

$$\begin{aligned} \mathbf{A}_d^{(2n_d \times 2n_d)} &= \begin{bmatrix} 0 & 1 \\ -r^2 & 2r \cos(2\pi f T) \end{bmatrix}, \quad \mathbf{B}_d^{(2n_d \times m_{w_d})} = \begin{bmatrix} 0.01 \\ 0.01 \end{bmatrix}, \\ \mathbf{C}_d^{(r_{y_d} \times 2n_d)} &= [1 \quad 0]. \end{aligned} \quad (2.111)$$

2. Internal-model-principle-based Control

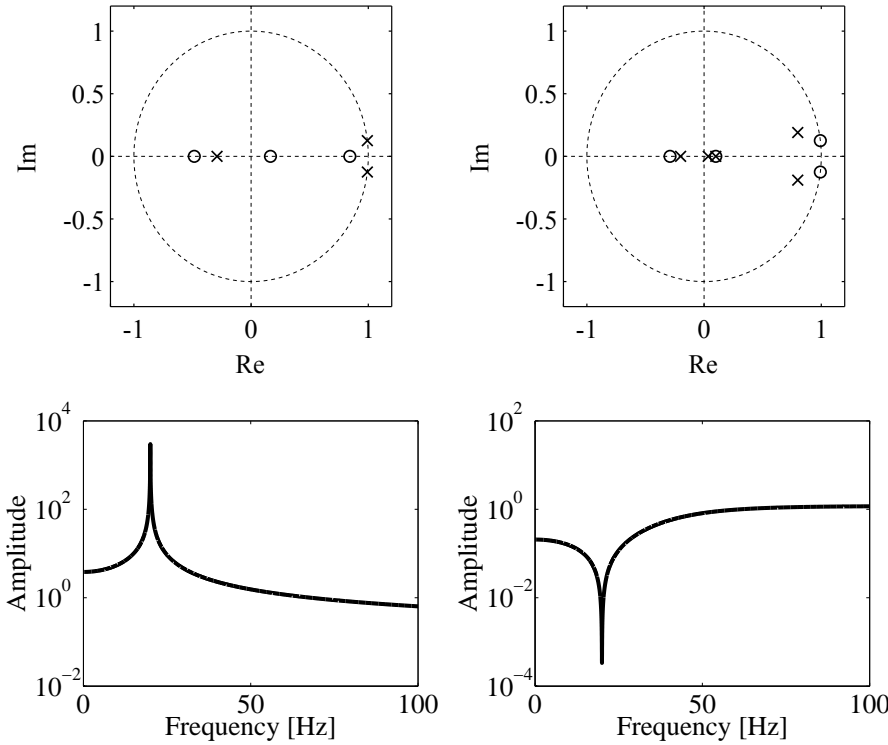


Figure 2.15: Pole-zero map (top) and amplitude frequency response (bottom) of controller (left) and closed-loop system (right) for a sampling frequency of 1 kHz

The weighting functions are chosen as constant gains with the state-space matrices

$$A_{W_u}^{(n_{W_u} \times n_{W_u})} = B_{W_u}^{(n_{W_u} \times m_u)} = C_{W_u}^{(r_{qu} \times n_{W_u})} = 0 \text{ and } D_{W_u}^{(r_{qu} \times m_u)} = 0.001 \quad (2.112)$$

with $r_{qu} = m_u = 1$, $n_{W_u} = 0$

for the input $u_{p,k}$ and

$$A_{W_y}^{(n_{W_y} \times n_{W_y})} = B_{W_y}^{(n_{W_y} \times r_y)} = C_{W_y}^{(r_{qy} \times n_{W_y})} = 0 \text{ and } D_{W_y}^{(r_{qy} \times r_y)} = 1 \quad (2.113)$$

for the output $y_{p,k}$ with $r_{qy} = r_y = 1$ and $n_{W_y} = 0$. Different weighting functions were tested, these functions satisfied a desired performance for the closed loop system.

The generalized plant from (2.69) is built with the matrices

$$\mathbf{A}^{(n \times n)} = \begin{bmatrix} A_p & B_p C_d & 0 & 0 \\ 0 & A_d & 0 & 0 \\ 0 & 0 & A_{W_u} & 0 \\ -B_{W_y} C_p & 0 & 0 & A_{W_y} \end{bmatrix} = \begin{bmatrix} 0.1 & 1 & 0 \\ 0 & 0 & 1 \\ 0 & -0.9998 & 1.9840 \end{bmatrix}, \quad (2.114)$$

$$[\mathbf{B}_w \quad \mathbf{B}_u]^{(n \times (m_w + m_u))} = \begin{bmatrix} 0 & B_p \\ \mathbf{B}_d & 0 \\ 0 & B_{W_u} \\ 0 & 0 \end{bmatrix} = \begin{bmatrix} 0 & 1 \\ 0.01 & 0 \\ 0.01 & 0 \end{bmatrix}, \quad (2.115)$$

$$\begin{bmatrix} C_q \\ C_y \end{bmatrix}^{((r_q + r_y) \times n)} = \begin{bmatrix} 0 & 0 & C_{W_u} & 0 \\ D_{W_y} C_p & 0 & 0 & C_{W_y} \\ C_p & 0 & 0 & 0 \end{bmatrix} = \begin{bmatrix} 0 & 0 & 0 \\ 0.9 & 0 & 0 \\ 0.9 & 0 & 0 \end{bmatrix} \text{ and} \quad (2.116)$$

$$\begin{bmatrix} \mathbf{D}_{qw} & \mathbf{D}_{qu} \\ \mathbf{D}_{yw} & \mathbf{D}_{yu} \end{bmatrix}^{((r_q+r_y) \times (m_w+m_u))} = \begin{bmatrix} 0 & D_{W_u} \\ 0 & 0 \\ \hline 0 & 0 \end{bmatrix} = \begin{bmatrix} 0 & 0.001 \\ 0 & 0 \\ \hline 0 & 0 \end{bmatrix}. \quad (2.117)$$

The controller is obtained applying the control-design and solving the LMIs from (2.98)-(2.106). A state-space representation of the obtained output-feedback controller is given with

$$\begin{bmatrix} \mathbf{x}_{K,k+1} \\ u_p \end{bmatrix} = \left[\begin{array}{ccc|c} -0.4810 & -0.8350 & -1.2496 & -7.9756 \\ 0.3135 & 1.1488 & 0.7014 & -18.6391 \\ 0.0072 & -0.0286 & 1.0256 & -9.8357 \\ \hline 0.0043 & 0.0155 & 0.0148 & -0.3994 \end{array} \right] \begin{bmatrix} \mathbf{x}_{K,k} \\ y_p \end{bmatrix} \quad (2.118)$$

and pole-zero map and amplitude frequency response of controller and closed loop system in Fig. 2.15. Once more, the controller has poles at the disturbance frequency to be cancelled.

2. Internal-model-principle-based Control

Chapter 3

LPV Gain-scheduling Control

Disturbances acting on a system may vary with the time. The LTI control structures presented in chapter 2 do not reject time-varying disturbances. Gain-scheduling controllers obtained by switching or interpolation between LTI controllers could be a solution but then the stability is not guaranteed for changes in the gain-scheduling parameters.

An LPV disturbance model can be used since the disturbances are time-varying. Then LPV gain-scheduling control design techniques can be used to achieve disturbance rejection and assure the stability for changes of the gain-scheduling parameters. This chapter is the LPV extension for all the LTI controllers presented in the previous chapter. Different LPV techniques are used for the reduction of nonstationary harmonic disturbances depending on how the disturbance is modeled (polytopic LPV (pLPV) or linear fractional transformation (LFT)) as shown in Fig. 3.1.

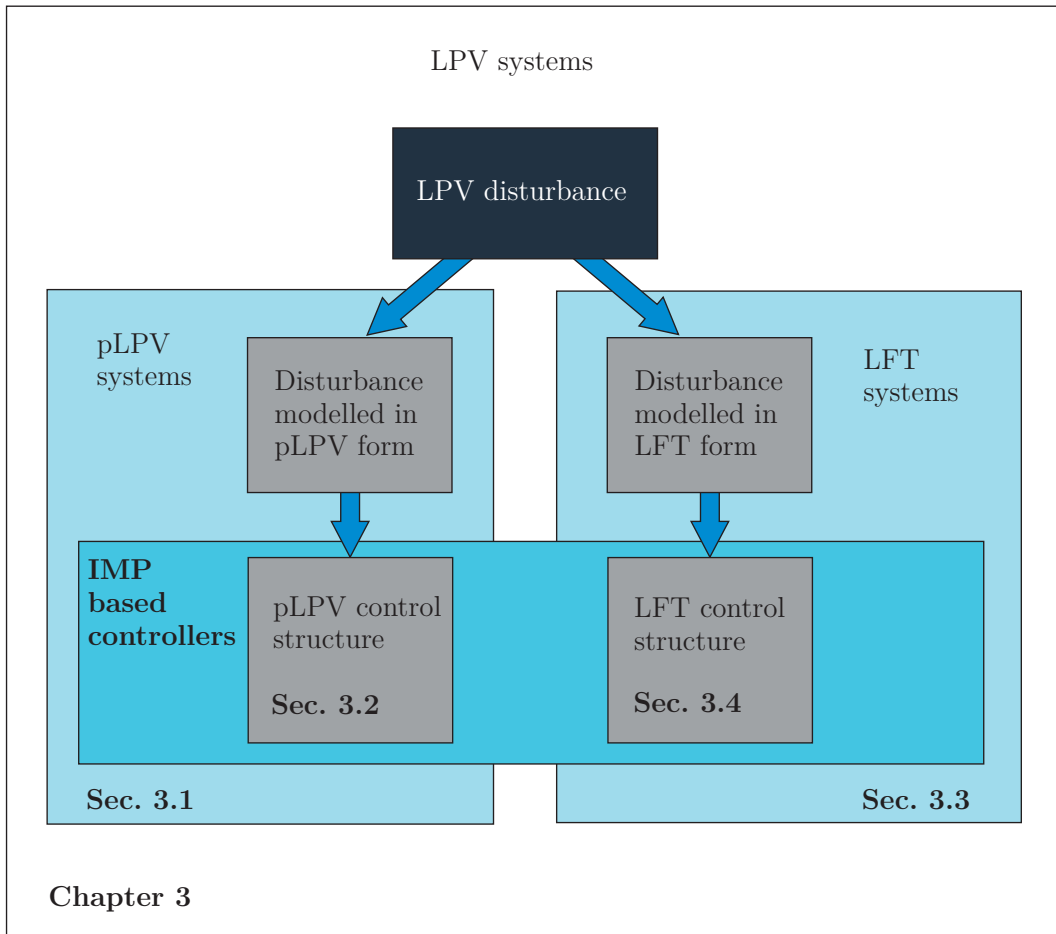


Figure 3.1: Schema of the chapter outline

3. LPV Gain-scheduling Control

This chapter introduces pLPV and LFT systems and the corresponding pLPV and LFT control structures for the reduction of time-varying disturbances. General pLPV systems are explained in Sec. 3.1 and the pLPV control structures in Sec. 3.2. Sec. 3.3 explains LPV systems in LFT form and Sec. 3.4 their control structures.

pLPV Systems

An LPV state-space representation of a system given by

$$\begin{bmatrix} \mathbf{x}_{k+1} \\ \mathbf{y}_k \end{bmatrix} = \begin{bmatrix} \mathbf{A}(\boldsymbol{\theta}_k) & \mathbf{B}(\boldsymbol{\theta}_k) \\ \mathbf{C}(\boldsymbol{\theta}_k) & \mathbf{0} \end{bmatrix} \begin{bmatrix} \mathbf{x}_k \\ \mathbf{u}_k \end{bmatrix} \quad (3.1)$$

is called a pLPV system (Amato (2006) and Heins et al. (2011, 2012a, 2012b)) if the matrices

$$\begin{aligned} \mathbf{A}(\boldsymbol{\theta}_k)^{(n_{\text{pLPV}} \times n_{\text{pLPV}})} &= \mathbf{A}_0 + \mathbf{A}_1 \theta_{1,k} + \mathbf{A}_2 \theta_{2,k} + \dots + \mathbf{A}_N \theta_{N,k} \\ \mathbf{B}(\boldsymbol{\theta}_k)^{(n_{\text{pLPV}} \times m_{\text{pLPV}})} &= \mathbf{B}_0 + \mathbf{B}_1 \theta_{1,k} + \mathbf{B}_2 \theta_{2,k} + \dots + \mathbf{B}_N \theta_{N,k} \\ \mathbf{C}(\boldsymbol{\theta}_k)^{(r_{\text{pLPV}} \times n_{\text{pLPV}})} &= \mathbf{C}_0 + \mathbf{C}_1 \theta_{1,k} + \mathbf{C}_2 \theta_{2,k} + \dots + \mathbf{C}_N \theta_{N,k} \end{aligned} \quad (3.2)$$

depend affinely on the parameters $\boldsymbol{\theta}_k = [\theta_{1,k} \ \theta_{2,k} \ \dots \ \theta_{N,k}]$ where Θ is a convex polytope in \mathbb{R}^N and $\mathbf{A}_0, \mathbf{A}_1, \mathbf{A}_2, \dots, \mathbf{A}_N, \mathbf{B}_0, \mathbf{B}_1, \mathbf{B}_2, \dots, \mathbf{B}_N$ and $\mathbf{C}_0, \mathbf{C}_1, \mathbf{C}_2, \dots, \mathbf{C}_N$ are constant matrices. The convex polytope Θ has a finite set of constant vertices $\mathbf{V} = [\boldsymbol{\theta}_{v,1} \ \boldsymbol{\theta}_{v,2} \ \dots \ \boldsymbol{\theta}_{v,M}]$ with $\boldsymbol{\theta}_{v,j} \in \mathbb{R}^N$ for $j = 1, \dots, M$. A point $\boldsymbol{\theta}_k \in \Theta$ can be written as a convex combination of the constant vertices, which means there exist a coordinate vector $\boldsymbol{\lambda}_k = [\lambda_{1,k} \ \lambda_{2,k} \ \dots \ \lambda_{M,k}] \in \mathbb{R}^M$ such that $\boldsymbol{\theta}_k$ can be written as

$$\boldsymbol{\theta}_k = \sum_{j=1}^M \lambda_{j,k} \boldsymbol{\theta}_{v,j} \quad (3.3)$$

with

$$\lambda_{j,k} \geq 0 \ \forall j \text{ and } \sum_{j=1}^M \lambda_{j,k} = 1. \quad (3.4)$$

The state-space matrices of (3.1) can be written in the same way as (3.3)

$$\begin{aligned} \mathbf{A}(\boldsymbol{\theta}_k) &= \lambda_{1,k} \mathbf{A}_{v,1} + \lambda_{2,k} \mathbf{A}_{v,2} + \dots + \lambda_{M,k} \mathbf{A}_{v,M} \\ \mathbf{B}(\boldsymbol{\theta}_k) &= \lambda_{1,k} \mathbf{B}_{v,1} + \lambda_{2,k} \mathbf{B}_{v,2} + \dots + \lambda_{M,k} \mathbf{B}_{v,M} \\ \mathbf{C}(\boldsymbol{\theta}_k) &= \lambda_{1,k} \mathbf{C}_{v,1} + \lambda_{2,k} \mathbf{C}_{v,2} + \dots + \lambda_{M,k} \mathbf{C}_{v,M} \end{aligned} \quad (3.5)$$

with

$$\mathbf{A}_{v,j}^{(n_{\text{pLPV}} \times n_{\text{pLPV}})} = \mathbf{A}(\boldsymbol{\theta}_{v,j}), \quad \mathbf{B}_{v,j}^{(n_{\text{pLPV}} \times m_{\text{pLPV}})} = \mathbf{B}(\boldsymbol{\theta}_{v,j}) \quad (3.6)$$

and

$$\mathbf{C}_{v,j}^{(r_{\text{pLPV}} \times n_{\text{pLPV}})} = \mathbf{C}(\boldsymbol{\theta}_{v,j}) \text{ for } j = 1, \dots, M. \quad (3.7)$$

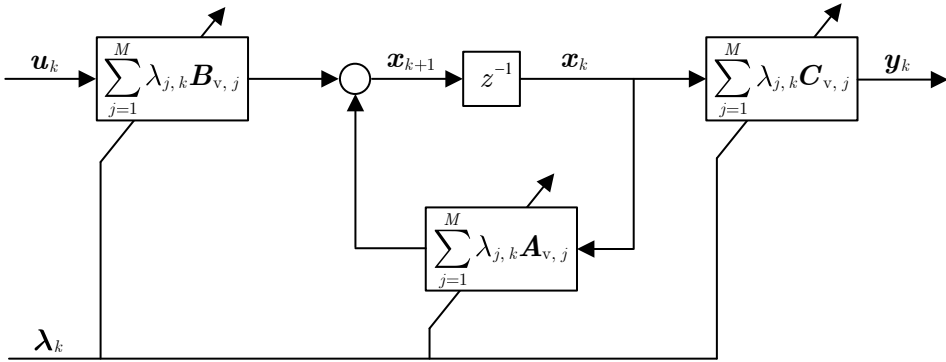


Figure 3.2: Schema of the pLPV system

A state-space pLPV representation of the system is given by (3.1) with

$$\mathbf{A}(\boldsymbol{\theta}_k) = \sum_{j=1}^M \lambda_{j,k} \mathbf{A}_{v,j}, \quad \mathbf{B}(\boldsymbol{\theta}_k) = \sum_{j=1}^M \lambda_{j,k} \mathbf{B}_{v,j} \text{ and } \mathbf{C}(\boldsymbol{\theta}_k) = \sum_{j=1}^M \lambda_{j,k} \mathbf{C}_{v,j} \quad (3.8)$$

and the coordinate vector $\boldsymbol{\lambda}_k$ calculated from (3.3) and (3.4) with $\boldsymbol{\theta}_k$ and the M vertices $\boldsymbol{\theta}_{v,j}$. A schema of a pLPV state-space representation is shown in Fig. 3.2.

A pLPV system is stable (Amato (2006)) if exists a positive definite matrix $\mathbf{P}^{(n_{\text{pLPV}} \times n_{\text{pLPV}})}$ such that

$$\mathbf{A}(\boldsymbol{\theta}_{v,j})^T \mathbf{P} \mathbf{A}(\boldsymbol{\theta}_{v,j}) - \mathbf{P} < 0 \text{ for } j = 1, \dots, M \quad (3.9)$$

for all the vertices of $\boldsymbol{\theta}_{v,j}$. These LMIs can be written as

$$\mathbf{P} - \mathbf{A}(\boldsymbol{\theta}_{v,j})^T \mathbf{P} \mathbf{P}^{-1} \mathbf{P} \mathbf{A}(\boldsymbol{\theta}_{v,j}) > 0 \text{ for } j = 1, \dots, M. \quad (3.10)$$

The Schur complement (Horn and Johnson (1985)) is then applied to obtain an equivalent expression

$$\begin{bmatrix} \mathbf{P} & \mathbf{P} \mathbf{A}(\boldsymbol{\theta}_{v,j}) \\ \mathbf{A}(\boldsymbol{\theta}_{v,j})^T \mathbf{P} & \mathbf{P} \end{bmatrix} > 0 \text{ for } j = 1, \dots, M \quad (3.11)$$

for the LMIs (3.9). The stability is guaranteed for the whole parameter space if a positive definite matrix \mathbf{P} exists solving the LMIs for all the vertices of $\boldsymbol{\theta}_{v,j}$.

A very simple example of an LPV system is given by the system of (2.4) written as a state-space representation

$$\begin{bmatrix} x_{p,k+1} \\ y_{p,k} \end{bmatrix} = \begin{bmatrix} a_k & 1 \\ 1 - a_k & 0 \end{bmatrix} \begin{bmatrix} x_{p,k} \\ u_{p,k} \end{bmatrix} \quad (3.12)$$

with $a_k \in [0.2 \ 0.8]$. In this case, $A(\theta_k)^{(n_p \times n_p)} = a_k$, $B^{(n_p \times m_{u_p})} = 1$ and $C(\theta_k)^{(r_{y_p} \times n_p)} = 1 - a_k$ with $n_p = m_{u_p} = r_{y_p} = 1$. The objective is to obtain a pLPV representation of this system.

The parameter $\theta_k = a_k$ and therefore the vertices of the system are given by $\theta_{v,1} = 0.2$ and $\theta_{v,2} = 0.8$. For a given θ_k the coordinate vector $\boldsymbol{\lambda}_k$ can be calculated using (3.3) and (3.4). These conditions are expresed by the following equation

$$\begin{bmatrix} \theta_k \\ 1 \end{bmatrix} = \begin{bmatrix} \theta_{v,1} & \theta_{v,2} \\ 1 & 1 \end{bmatrix} \begin{bmatrix} \lambda_{1,k} \\ \lambda_{2,k} \end{bmatrix} \quad (3.13)$$

3. LPV Gain-scheduling Control

written in matrix form. Knowing the value θ_k , the coordinate vector $\boldsymbol{\lambda}_k$ is calculated

$$\begin{bmatrix} \lambda_{1,k} \\ \lambda_{2,k} \end{bmatrix} = \begin{bmatrix} \theta_{v,1} & \theta_{v,2} \\ 1 & 1 \end{bmatrix}^{-1} \begin{bmatrix} \theta_k \\ 1 \end{bmatrix} \quad (3.14)$$

as a simple matrix multiplication. For example, with $a_k = 0.4$ the values of $\lambda_{1,k} = 0.6667$ and $\lambda_{2,k} = 0.3333$ are obtained and θ_k is given by

$$\theta_k = \lambda_{1,k}\theta_{v,1} + \lambda_{2,k}\theta_{v,2} = 0.6667 \cdot 0.2 + 0.3333 \cdot 0.8 = 0.4. \quad (3.15)$$

The matrices $A(\theta_k)$ and $C(\theta_k)$ depend on the parameter θ_k and they can be written for this reason in the same way as

$$\begin{aligned} A(\theta_k) &= \lambda_{1,k}A(\theta_{v,1}) + \lambda_{2,k}A(\theta_{v,2}) &= 0.4 \\ C(\theta_k) &= \lambda_{1,k}C(\theta_{v,1}) + \lambda_{2,k}C(\theta_{v,2}) &= 0.6. \end{aligned} \quad (3.16)$$

A pLPV representation is obtained for the system of (3.12) as

$$\begin{bmatrix} x_{p,k+1} \\ y_{p,k} \end{bmatrix} = \begin{bmatrix} A(\theta_k) & B \\ C(\theta_k) & 0 \end{bmatrix} \begin{bmatrix} x_{p,k} \\ u_{p,k} \end{bmatrix} \quad (3.17)$$

with

$$A(\theta_k) = \sum_{j=1}^2 \lambda_{j,k}A_{v,j}, \quad C(\theta_k) = \sum_{j=1}^2 \lambda_{j,k}C_{v,j}, \quad A_{v,j} = A(\theta_{v,j}) \text{ and } C_{v,j} = C(\theta_{v,j}).$$

The stability of this system is checked using (3.9) for all the vertices. The system is then stable if for the two vertices $A(\theta_{v,1}) = A_{v,1} = 0.2$ and $A(\theta_{v,2}) = A_{v,2} = 0.8$ a constant P is found such that

$$\begin{aligned} A(\theta_{v,1})^T P A(\theta_{v,1}) - P &< 0 \\ A(\theta_{v,2})^T P A(\theta_{v,2}) - P &< 0 \\ P > 0. \end{aligned} \quad (3.18)$$

From here it follows, that any matrix $P > 0$ fullfills all the three inequalities and therefore the pLPV system is stable.

pLPV Control Structure

This section focuses on pLPV control structures for the rejection of disturbances. pLPV controllers are obtained using control design techniques for LPV systems written in pLPV form. The controller for a given $\boldsymbol{\theta}_k$ is calculated from the M vertex controllers using the coordinate vector $\boldsymbol{\lambda}_k$. Similar to (3.1) the pLPV controller can be written as

$$\begin{bmatrix} x_{c,k+1} \\ \mathbf{u}_k \end{bmatrix} = \begin{bmatrix} \mathbf{A}_c(\boldsymbol{\theta}_k) & \mathbf{B}_c(\boldsymbol{\theta}_k) \\ \mathbf{C}_c(\boldsymbol{\theta}_k) & \mathbf{0} \end{bmatrix} \begin{bmatrix} x_{c,k} \\ \mathbf{y}_k \end{bmatrix} \quad (3.19)$$

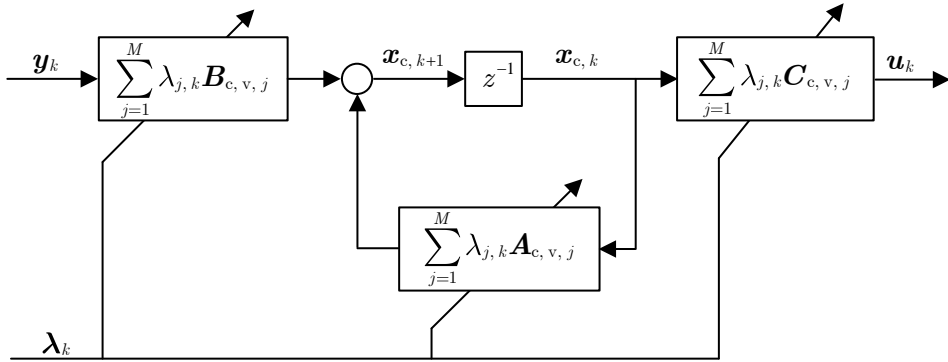


Figure 3.3: Schema of the pLPV controller

with

$$\begin{aligned}
 \mathbf{A}_c(\boldsymbol{\theta}_k)^{(n_c \times n_c)} &= \sum_{j=1}^M \mathbf{A}_{c,v,j} \lambda_{j,k}, \\
 \mathbf{B}_c(\boldsymbol{\theta}_k)^{(n_c \times m_c)} &= \sum_{j=1}^M \mathbf{B}_{c,v,j} \lambda_{j,k}, \\
 \mathbf{C}_c(\boldsymbol{\theta}_k)^{(r_c \times n_c)} &= \sum_{j=1}^M \mathbf{C}_{c,v,j} \lambda_{j,k}
 \end{aligned} \tag{3.20}$$

and $\mathbf{A}_{c,v,j}^{(n_c \times n_c)} = \mathbf{A}_c(\boldsymbol{\theta}_{v,j})$, $\mathbf{B}_{c,v,j}^{(n_c \times m_c)} = \mathbf{B}_c(\boldsymbol{\theta}_{v,j})$ and $\mathbf{C}_{c,v,j}^{(r_c \times n_c)} = \mathbf{C}_c(\boldsymbol{\theta}_{v,j})$. A schema of this control structure is given in Fig. 3.3. The control structures of the previous section are in the next sections extended to the pLPV case.

pLPV Gain-scheduling Observer-Based Control Structure

The control structures of the subsections 2.1.1 and 2.1.2 are extended here to pLPV control structures. This section is focused on the pLPV control structure. The calculation of the feedback gains (observer-based approach) and the controller matrices (output-feedback approach) is considered in the next chapter.

pLPV Disturbance Observer Control Structure

The disturbance observer control structure was briefly reviewed in Sec. 2.1.1 for an LTI disturbance. In most industrial applications, the disturbance is time varying, therefore to guarantee the stability for changes in the parameters pLPV design techniques are used in this section.

A state-space representation of the augmented system for time-varying disturbances is given by

$$\left[\begin{array}{c} \mathbf{x}_{d,k+1} \\ \mathbf{x}_{p,k+1} \\ \hline \mathbf{y}_{p,k} \end{array} \right] = \left[\begin{array}{cc|c} \mathbf{A}_{d,k} & \mathbf{0} & \mathbf{0} \\ \mathbf{B}_p \mathbf{C}_d & \mathbf{A}_p & \mathbf{B}_p \\ \hline \mathbf{0} & \mathbf{C}_p & \mathbf{0} \end{array} \right] \left[\begin{array}{c} \mathbf{x}_{d,k} \\ \mathbf{x}_{p,k} \\ \hline \mathbf{u}_{p,k} \end{array} \right] \tag{3.21}$$

where $\mathbf{A}_{d,k}^{(2n_d \times 2n_d)} = \mathbf{A}_d(\boldsymbol{\theta}_k)$. A representation of this system can be written in compact

3. LPV Gain-scheduling Control

form as

$$\begin{bmatrix} \mathbf{x}_{\text{do}, k+1} \\ \mathbf{y}_{\text{p}, k} \end{bmatrix} = \left[\begin{array}{c|c} \mathbf{A}_{\text{do}, k} & \mathbf{B}_{\text{do}} \\ \mathbf{C}_{\text{do}} & \mathbf{0} \end{array} \right] \begin{bmatrix} \mathbf{x}_{\text{do}, k} \\ \mathbf{u}_{\text{p}, k} \end{bmatrix} \quad (3.22)$$

with $\mathbf{A}_{\text{do}, k}^{((2n_{\text{d}}+n_{\text{p}}) \times (2n_{\text{d}}+n_{\text{p}}))} = \mathbf{A}_{\text{do}}(\boldsymbol{\theta}_k)$, $\mathbf{B}_{\text{do}}^{((2n_{\text{d}}+n_{\text{p}}) \times m_{\text{u}_{\text{p}}})}$ and $\mathbf{C}_{\text{do}}^{(r_{\text{y}_{\text{p}}} \times (2n_{\text{d}}+n_{\text{p}}))}$. Knowing $\boldsymbol{\theta}_k$ and their M vertices

$$\boldsymbol{\theta}_{\text{v}, j}, \text{ for } j = 1, \dots, M \quad (3.23)$$

the coordinate vector $\boldsymbol{\lambda}_k$ can be calculated using (3.3) and (3.4). The LPV system of (3.22) is represented in pLPV form with the matrix $\mathbf{A}_{\text{do}, k}$ written as

$$\mathbf{A}_{\text{do}, k} = \mathbf{A}_{\text{do}}(\boldsymbol{\theta}_k) = \sum_{j=1}^M \lambda_{j, k} \mathbf{A}_{\text{do}, \text{v}, j} = \sum_{j=1}^M \lambda_{j, k} \mathbf{A}_{\text{do}}(\boldsymbol{\theta}_{\text{v}, j}). \quad (3.24)$$

The disturbance-observer control structure is a combination of a state-feedback gain and an identity observer. A state-space representation of the controller is given for LTI systems by (2.16) and here is written as

$$\begin{bmatrix} \hat{\mathbf{x}}_{\text{do}, k+1} \\ \mathbf{u}_{\text{p}, k} \end{bmatrix} = \left[\begin{array}{c|c} \mathbf{A}_{\text{doc}, k} & \mathbf{B}_{\text{doc}, k} \\ \mathbf{C}_{\text{doc}} & \mathbf{0} \end{array} \right] \begin{bmatrix} \hat{\mathbf{x}}_{\text{do}, k} \\ \mathbf{y}_{\text{p}, k} \end{bmatrix} \quad (3.25)$$

with

$$\begin{aligned} \mathbf{A}_{\text{doc}, k}^{((2n_{\text{d}}+n_{\text{p}}) \times (2n_{\text{d}}+n_{\text{p}}))} &= (\mathbf{A}_{\text{do}, k} - \mathbf{L}_{\text{do}, k} \mathbf{C}_{\text{do}} - \mathbf{B}_{\text{do}} \mathbf{K}_{\text{do}}) = \\ &= \mathbf{A}_{\text{doc}}(\boldsymbol{\theta}_k) = (\mathbf{A}_{\text{do}}(\boldsymbol{\theta}_k) - \mathbf{L}_{\text{do}}(\boldsymbol{\theta}_k) \mathbf{C}_{\text{do}} - \mathbf{B}_{\text{do}} \mathbf{K}_{\text{do}}) \\ \mathbf{B}_{\text{doc}, k}^{((2n_{\text{d}}+n_{\text{p}}) \times r_{\text{y}_{\text{p}}})} &= \mathbf{B}_{\text{doc}}(\boldsymbol{\theta}_k) = \mathbf{L}_{\text{do}, k} = \mathbf{L}_{\text{do}}(\boldsymbol{\theta}_k), \\ \mathbf{C}_{\text{doc}}^{(m_{\text{u}_{\text{p}}} \times (2n_{\text{d}}+n_{\text{p}}))} &= \mathbf{K}_{\text{do}} = [\mathbf{C}_{\text{d}} \quad \mathbf{K}_{\text{p}}] \end{aligned} \quad (3.26)$$

for an LPV system.

The same procedure to study the stability can be here realized as in (2.26) by simply changing \mathbf{L}_{do} with $\mathbf{L}_{\text{do}, k}$ and \mathbf{A}_{do} with $\mathbf{A}_{\text{do}, k}$. The overall closed-loop dynamics of the LPV system is given by

$$\begin{bmatrix} \hat{\mathbf{x}}_{\text{d}, k+1} \\ \tilde{\mathbf{x}}_{\text{p}, k+1} \\ \mathbf{x}_{\text{p}, k+1} \end{bmatrix} = \left[\begin{array}{ccc|c} \mathbf{A}_{\text{d}, k} & -\mathbf{L}_{\text{d}, k} \mathbf{C}_{\text{p}} & \mathbf{0} & \mathbf{0} \\ \mathbf{B}_{\text{p}} \mathbf{C}_{\text{d}} & \mathbf{A}_{\text{p}} - \mathbf{L}_{\text{p}, k} \mathbf{C}_{\text{p}} & \mathbf{0} & -\mathbf{B}_{\text{p}} \\ -\mathbf{B}_{\text{p}} \mathbf{C}_{\text{d}} & \mathbf{B}_{\text{p}} \mathbf{K}_{\text{p}} & \mathbf{A}_{\text{p}} - \mathbf{B}_{\text{p}} \mathbf{K}_{\text{p}} & \mathbf{B}_{\text{p}} \end{array} \right] \begin{bmatrix} \hat{\mathbf{x}}_{\text{d}, k} \\ \tilde{\mathbf{x}}_{\text{p}, k} \\ \mathbf{x}_{\text{p}, k} \\ \mathbf{y}_{\text{d}, k} \end{bmatrix}. \quad (3.27)$$

The structure of the closed-loop dynamics for the LPV system is shown in Fig. 3.4. From here it follows that the stability of the closed-loop system depends on the stability of two systems in series. An LTI system (plant under state feedback) and an LPV system (dynamics of the observer for the augmented system). The system is stable if a stabilizing state-feedback gain \mathbf{K}_{p} for the LTI system ($\mathbf{A}_{\text{p}} - \mathbf{B}_{\text{p}} \mathbf{K}_{\text{p}}$) and a stabilizing observer-gain $\mathbf{L}_{\text{do}, k}$ for the LPV augmented system ($\mathbf{A}_{\text{do}, k} - \mathbf{L}_{\text{do}, k} \mathbf{C}_{\text{do}}$) are found. That is, if a common positive definite matrix $\mathbf{P}^{((2n_{\text{d}}+n_{\text{p}}) \times (2n_{\text{d}}+n_{\text{p}}))}$ is found for

$$(\mathbf{A}_{\text{do}, k} - \mathbf{L}_{\text{do}, k} \mathbf{C}_{\text{do}})^T \mathbf{P} (\mathbf{A}_{\text{do}, k} - \mathbf{L}_{\text{do}, k} \mathbf{C}_{\text{do}}) - \mathbf{P} < 0 \quad (3.28)$$

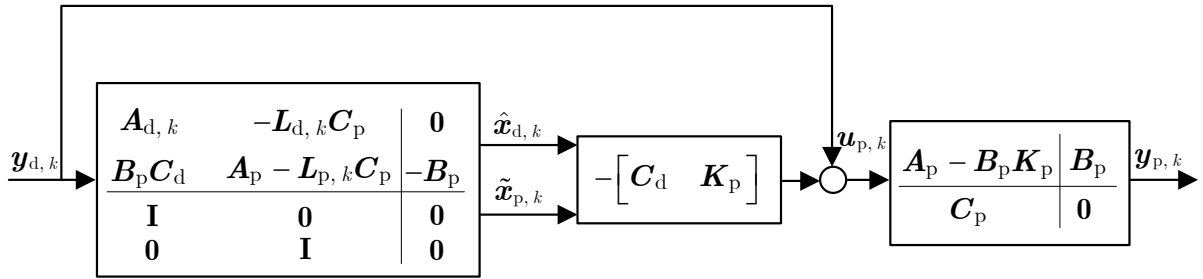


Figure 3.4: Dynamics of the overall closed-loop LPV system

or equivalently using the Schur complement

$$\begin{bmatrix} \mathbf{P} & \mathbf{P}(\mathbf{A}_{\text{do},k} - \mathbf{L}_{\text{do},k}\mathbf{C}_{\text{do}}) \\ (\mathbf{A}_{\text{do},k} - \mathbf{L}_{\text{do},k}\mathbf{C}_{\text{do}})^T \mathbf{P} & \mathbf{P} \end{bmatrix} > 0 \quad (3.29)$$

for the whole parameter space $\boldsymbol{\theta}_k \in \Theta$.

This infinite set of LMIs is reduced to a finite set of LMIs if the system is written in pLPV form. Using (3.9) the pLPV system is stable if a positive definite matrix \mathbf{P} is found such that

$$\begin{aligned} & \left(\mathbf{A}_{\text{do}}(\boldsymbol{\theta}_{v,j}) - \mathbf{L}_{\text{do}}(\boldsymbol{\theta}_{v,j})\mathbf{C}_{\text{do}} \right)^T \mathbf{P} \left(\mathbf{A}_{\text{do}}(\boldsymbol{\theta}_{v,j}) - \mathbf{L}_{\text{do}}(\boldsymbol{\theta}_{v,j})\mathbf{C}_{\text{do}} \right) - \mathbf{P} < 0 \\ & j = 1, \dots, M \end{aligned} \quad (3.30)$$

or

$$\begin{bmatrix} \mathbf{P} & \mathbf{P}(\mathbf{A}_{\text{do}}(\boldsymbol{\theta}_{v,j}) - \mathbf{L}_{\text{do}}(\boldsymbol{\theta}_{v,j})\mathbf{C}_{\text{do}}) \\ \left(\mathbf{A}_{\text{do}}(\boldsymbol{\theta}_{v,j}) - \mathbf{L}_{\text{do}}(\boldsymbol{\theta}_{v,j})\mathbf{C}_{\text{do}} \right)^T \mathbf{P} & \mathbf{P} \end{bmatrix} > 0 \quad (3.31)$$

$$j = 1, \dots, M$$

for all the vertices $\boldsymbol{\theta}_{v,j}$.

The vertex observer gains $\mathbf{L}_{\text{do}}(\boldsymbol{\theta}_{v,j})^{((2n_d+n_p) \times r_{y_p})} = \mathbf{L}_{\text{do},v,j}$ will be obtained in the next chapter. A pLPV representation of the controller is given as in (3.19) and (3.20) with

$$\begin{aligned} \mathbf{A}_{c,v,j}^{((2n_d+n_p) \times (2n_d+n_p))} &= \mathbf{A}_{\text{do},v,j} - \mathbf{L}_{\text{do},v,j}\mathbf{C}_{\text{do}} - \mathbf{B}_{\text{do}}\mathbf{K}_{\text{do}}, \\ \mathbf{B}_{c,v,j}^{((2n_d+n_p) \times r_{y_p})} &= \mathbf{L}_{\text{do},v,j}, \\ \mathbf{C}_{c,v,j}^{(m_{u_p} \times (2n_d+n_p))} &= \mathbf{K}_{\text{do}} \end{aligned} \quad (3.32)$$

and the coordinate vector $\boldsymbol{\lambda}_k$ calculated through (3.3) and (3.4).

pLPV Error Filter Control Structure

The augmented system for this control design is a combination of an LTI plant and a time-varying disturbance model. A state-space representation of the LPV augmented

3. LPV Gain-scheduling Control

system is given with

$$\begin{bmatrix} \mathbf{x}_{d,k+1} \\ \mathbf{x}_{p,k+1} \\ \mathbf{y}_{p,k} \end{bmatrix} = \left[\begin{array}{cc|c} \mathbf{A}_{d,k} & -\mathbf{B}_d \mathbf{C}_p & \mathbf{0} \\ \mathbf{0} & \mathbf{A}_p & \mathbf{B}_p \\ \mathbf{0} & \mathbf{C}_p & \mathbf{0} \end{array} \right] \begin{bmatrix} \mathbf{x}_{d,k} \\ \mathbf{x}_{p,k} \\ \mathbf{u}_{p,k} \end{bmatrix} \quad (3.33)$$

and

$$\begin{bmatrix} \mathbf{x}_{ef,k+1} \\ \mathbf{y}_{p,k} \end{bmatrix} = \left[\begin{array}{c|c} \mathbf{A}_{ef,k} & \mathbf{B}_{ef} \\ \mathbf{C}_{ef} & \mathbf{0} \end{array} \right] \begin{bmatrix} \mathbf{x}_{ef,k} \\ \mathbf{u}_{p,k} \end{bmatrix} \quad (3.34)$$

is an LPV state-space representation in compact form with $\mathbf{A}_{ef,k}^{((2n_d+n_p) \times (2n_d+n_p))}$, $\mathbf{B}_{ef}^{((2n_d+n_p) \times m_{u_p})}$ and $\mathbf{C}_{ef}^{(r_{y_p} \times (2n_d+n_p))}$.

If the matrix $\mathbf{A}_{d,k}^{(2n_d \times 2n_d)}$ depends on the parameter $\boldsymbol{\theta}_k$

$$\mathbf{A}_{d,k} = \mathbf{A}(\boldsymbol{\theta}_k) \quad (3.35)$$

then the matrix $\mathbf{A}_{ef,k}$ depends also on $\boldsymbol{\theta}_k$

$$\mathbf{A}_{ef,k} = \mathbf{A}_{ef}(\boldsymbol{\theta}_k). \quad (3.36)$$

A pLPV representation of this system is given with the matrix $\mathbf{A}_{ef,k}$ written as

$$\mathbf{A}_{ef,k} = \mathbf{A}_{ef}(\boldsymbol{\theta}_k) = \sum_{j=1}^M \lambda_{j,k} \mathbf{A}_{ef,v,j} = \sum_{j=1}^M \lambda_{j,k} \mathbf{A}_{ef}(\boldsymbol{\theta}_{v,j}). \quad (3.37)$$

It is assumed that the vector $\boldsymbol{\theta}_k$ is known or can be measured and it is also known the range variations of $\boldsymbol{\theta}_k$ to calculate the M vertices $\boldsymbol{\theta}_{v,j}$ of the polytope. The coordinate vector $\boldsymbol{\lambda}_k$ is calculated as in (3.3) and (3.4) with $\boldsymbol{\theta}_k$ and the M vertices $\boldsymbol{\theta}_{v,j}$.

The control structure of (2.46) is here written as an LPV system

$$\begin{bmatrix} \mathbf{x}_{d,k+1} \\ \hat{\mathbf{x}}_{p,k+1} \\ \mathbf{u}_{p,k} \end{bmatrix} = \left[\begin{array}{cc|c} \mathbf{A}_{d,k} & \mathbf{0} & \mathbf{B}_d \\ -\mathbf{B}_p \mathbf{K}_{d,k} & \mathbf{A}_p - \mathbf{B}_p \mathbf{K}_{p,k} - \mathbf{L}_p \mathbf{C}_p & \mathbf{L}_p \\ -\mathbf{K}_{d,k} & -\mathbf{K}_{p,k} & \mathbf{0} \end{array} \right] \begin{bmatrix} \mathbf{x}_{d,k} \\ \hat{\mathbf{x}}_{p,k} \\ \mathbf{e}_k \end{bmatrix} \quad (3.38)$$

and this LPV system is written in compact form as

$$\begin{bmatrix} \mathbf{x}_{efc,k+1} \\ \mathbf{u}_{p,k} \end{bmatrix} = \left[\begin{array}{c|c} \mathbf{A}_{efc,k} & \mathbf{B}_{efc} \\ \mathbf{C}_{efc,k} & \mathbf{0} \end{array} \right] \begin{bmatrix} \mathbf{x}_{efc,k} \\ \mathbf{e}_k \end{bmatrix} \quad (3.39)$$

with

$$\begin{aligned} \mathbf{A}_{efc,k}^{((2n_d+n_p) \times (2n_d+n_p))} &= \left[\begin{array}{cc} \mathbf{A}_{d,k} & \mathbf{0} \\ -\mathbf{B}_p \mathbf{K}_{d,k} & \mathbf{A}_p - \mathbf{B}_p \mathbf{K}_{p,k} - \mathbf{L}_p \mathbf{C}_p \end{array} \right] = \\ &= \mathbf{A}_{efc}(\boldsymbol{\theta}_k) = \left[\begin{array}{cc} \mathbf{A}_d(\boldsymbol{\theta}_k) & \mathbf{0} \\ -\mathbf{B}_p \mathbf{K}_d(\boldsymbol{\theta}_k) & \mathbf{A}_p - \mathbf{B}_p \mathbf{K}_p(\boldsymbol{\theta}_k) - \mathbf{L}_p \mathbf{C}_p \end{array} \right], \\ \mathbf{B}_{efc}^{((2n_d+n_p) \times r_{y_p})} &= \left[\begin{array}{c} \mathbf{B}_d \\ \mathbf{L}_p \end{array} \right] \end{aligned} \quad (3.40)$$

$$\mathbf{C}_{efc,k}^{(m_{u_p} \times (2n_d+n_p))} = \left[\begin{array}{cc} -\mathbf{K}_{d,k} & -\mathbf{K}_{p,k} \end{array} \right] =$$

$$= \mathbf{C}_{efc}(\boldsymbol{\theta}_k) = \left[\begin{array}{cc} -\mathbf{K}_d(\boldsymbol{\theta}_k) & -\mathbf{K}_p(\boldsymbol{\theta}_k) \end{array} \right].$$

The closed-loop stability is studied as in (2.57) but here for the LPV case. The overall closed-loop dynamics are described by

$$\begin{bmatrix} \tilde{\mathbf{x}}_{p,k+1} \\ \mathbf{x}_{d,k+1} \\ \mathbf{x}_{p,k+1} \end{bmatrix} = \left[\begin{array}{ccc|c} \mathbf{A}_p - \mathbf{L}_p \mathbf{C}_p & \mathbf{0} & \mathbf{0} & -\mathbf{B}_p \\ \mathbf{0} & \mathbf{A}_{d,k} & -\mathbf{B}_d \mathbf{C}_p & \mathbf{0} \\ -\mathbf{B}_p \mathbf{K}_{p,k} & -\mathbf{B}_p \mathbf{K}_{d,k} & \mathbf{A}_p - \mathbf{B}_p \mathbf{K}_{p,k} & \mathbf{B}_p \end{array} \right] \begin{bmatrix} \tilde{\mathbf{x}}_{p,k} \\ \mathbf{x}_{d,k} \\ \mathbf{x}_{p,k} \\ \mathbf{y}_{d,k} \end{bmatrix}. \quad (3.41)$$

The structure of the closed-loop dynamics is shown in Fig. 3.5. The closed-loop stability depends on two systems in series, an LTI system (observer error for the plant states) and an LPV system (augmented system under state feedback). The system is stable if an observer gain \mathbf{L}_p that stabilizes $(\mathbf{A}_p - \mathbf{L}_p \mathbf{C}_p)$ and a state-feedback gain $\mathbf{K}_{ef,k}^{(m_{u_p} \times (2n_d + n_p))}$ that stabilizes $(\mathbf{A}_{ef,k} - \mathbf{B}_{ef} \mathbf{K}_{ef,k})$ are found. The system is stable if a positive definite matrix $\mathbf{P}^{((2n_d + n_p) \times (2n_d + n_p))}$ is found with

$$(\mathbf{A}_{ef,k} - \mathbf{B}_{ef} \mathbf{K}_{ef,k})^T \mathbf{P} (\mathbf{A}_{ef,k} - \mathbf{B}_{ef} \mathbf{K}_{ef,k}) - \mathbf{P} < 0 \quad (3.42)$$

or

$$\begin{bmatrix} \mathbf{P} & \mathbf{P}(\mathbf{A}_{ef,k} - \mathbf{B}_{ef} \mathbf{K}_{ef,k}) \\ (\mathbf{A}_{ef,k} - \mathbf{B}_{ef} \mathbf{K}_{ef,k})^T \mathbf{P} & \mathbf{P} \end{bmatrix} > 0 \quad (3.43)$$

for the whole parameter space $\boldsymbol{\theta}_k \in \Theta$. If the LPV system can be written in pLPV form, the infinite set of LMIs is converted in a finite set using (3.9). The stability is guaranteed if a positive definite matrix \mathbf{P} is found such that

$$\begin{aligned} & \left(\mathbf{A}_{ef}(\boldsymbol{\theta}_{v,j}) - \mathbf{B}_{ef} \mathbf{K}_{ef}(\boldsymbol{\theta}_{v,j}) \right)^T \mathbf{P} \left(\mathbf{A}_{ef}(\boldsymbol{\theta}_{v,j}) - \mathbf{B}_{ef} \mathbf{K}_{ef}(\boldsymbol{\theta}_{v,j}) \right) - \mathbf{P} < 0 \\ & j = 1, \dots, M \end{aligned} \quad (3.44)$$

or

$$\begin{bmatrix} \mathbf{P} & \mathbf{P}(\mathbf{A}_{ef}(\boldsymbol{\theta}_{v,j}) - \mathbf{B}_{ef} \mathbf{K}_{ef}(\boldsymbol{\theta}_{v,j})) \\ \left(\mathbf{A}_{ef}(\boldsymbol{\theta}_{v,j}) - \mathbf{B}_{ef} \mathbf{K}_{ef}(\boldsymbol{\theta}_{v,j}) \right)^T \mathbf{P} & \mathbf{P} \end{bmatrix} > 0 \quad (3.45)$$

$$j = 1, \dots, M$$

for all the vertices $\boldsymbol{\theta}_{v,j}$.

If the vector $\boldsymbol{\theta}_k$ varies inside of a polytope with M vertices $\boldsymbol{\theta}_{v,j}$, a pLPV representation of the controller is given as in (3.19) and (3.20) with

$$\begin{aligned} \mathbf{A}_{c,v,j}^{((2n_d + n_p) \times (2n_d + n_p))} &= \mathbf{A}_{efc,v,j} \\ \mathbf{B}_{c,v,j}^{((2n_d + n_p) \times r_{u_p})} &= \mathbf{B}_{efc}, \\ \mathbf{C}_{c,v,j}^{(m_{u_p} \times (2n_d + n_p))} &= \mathbf{C}_{efc,v,j} \end{aligned} \quad (3.46)$$

and $\boldsymbol{\lambda}_k$ calculated through (3.3) and (3.4) with $\boldsymbol{\theta}_k$ and the M vertices $\boldsymbol{\theta}_{v,j}$.

3. LPV Gain-scheduling Control

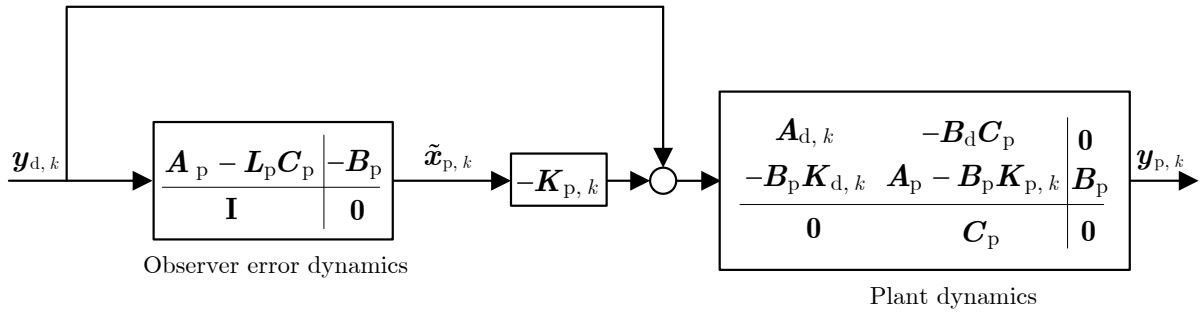


Figure 3.5: Dynamics of the overall closed-loop LPV system

pLPV Gain-scheduling Output-Feedback Control Structure

The output-feedback control structure presented in this thesis is based on H_∞ control design techniques. Before solving the LMIs to calculate the output-feedback controller the generalized plant (2.69) is built with the weighting functions and the desired additional dynamics (model of the disturbance). The generalized plant is here written

$$\begin{bmatrix} \mathbf{x}_{k+1} \\ \mathbf{q}_k \\ \mathbf{y}_{p,k} \end{bmatrix} = \begin{bmatrix} \mathbf{A}_k & \mathbf{B}_w & \mathbf{B}_u \\ \mathbf{C}_q & \mathbf{D}_{qw} & \mathbf{D}_{qu} \\ \mathbf{C}_y & \mathbf{D}_{yw} & \mathbf{D}_{yu} \end{bmatrix} \begin{bmatrix} \mathbf{x}_k \\ \mathbf{w}_k \\ \mathbf{u}_{p,k} \end{bmatrix} \quad (3.47)$$

with

$$\mathbf{x}_k = \begin{bmatrix} \mathbf{x}_{p,k} \\ \mathbf{x}_{d,k} \\ \mathbf{x}_{W_u,k} \\ \mathbf{x}_{W_y,k} \end{bmatrix}, \quad (3.48)$$

$$\mathbf{A}_k^{((n_p+2n_d+n_{W_u}+n_{W_y}) \times (n_p+2n_d+n_{W_u}+n_{W_y}))} = \begin{bmatrix} \mathbf{A}_p & \mathbf{B}_p C_d & \mathbf{0} & \mathbf{0} \\ \mathbf{0} & \mathbf{A}_{d,k} & \mathbf{0} & \mathbf{0} \\ \mathbf{0} & \mathbf{0} & \mathbf{A}_{W_u} & \mathbf{0} \\ \mathbf{B}_{W_y} C_p & \mathbf{0} & \mathbf{0} & \mathbf{A}_{W_y} \end{bmatrix},$$

$$[\mathbf{B}_w \quad \mathbf{B}_u]^{((n_p+2n_d+n_{W_u}+n_{W_y}) \times (m_w+m_u))} = \begin{bmatrix} \mathbf{0} & \mathbf{B}_p \\ \mathbf{B}_d & \mathbf{0} \\ \mathbf{0} & \mathbf{B}_{W_u} \\ \mathbf{0} & \mathbf{0} \end{bmatrix}, \quad (3.49)$$

$$\begin{bmatrix} \mathbf{C}_q \\ \mathbf{C}_y \end{bmatrix}^{((r_{qu}+r_{qy}+r_y) \times (n_p+2n_d+n_{W_u}+n_{W_y}))} = \begin{bmatrix} \mathbf{0} & \mathbf{0} & \mathbf{C}_{W_u} & \mathbf{0} \\ \mathbf{D}_{W_y} C_p & \mathbf{0} & \mathbf{0} & \mathbf{C}_{W_y} \\ \mathbf{C}_p & \mathbf{0} & \mathbf{0} & \mathbf{0} \end{bmatrix} \quad (3.50)$$

and

$$\begin{bmatrix} \mathbf{D}_{qw} & \mathbf{D}_{qu} \\ \mathbf{D}_{yw} & \mathbf{D}_{yu} \end{bmatrix}^{((r_{qu}+r_{qy}+r_y) \times (n_p+2n_d+n_{W_u}+n_{W_y}))} = \begin{bmatrix} \mathbf{0} & \mathbf{D}_{W_u} \\ \mathbf{0} & \mathbf{0} \\ \hline \mathbf{0} & \mathbf{0} \end{bmatrix} \quad (3.51)$$

in LPV form. This system can be written in pLPV form if the matrix \mathbf{A}_k depends on the parameter $\boldsymbol{\theta}_k$ and this parameter varies inside a polytope with M vertices $\boldsymbol{\theta}_{v,j}$. The matrix

$$\mathbf{A}_k = \mathbf{A}(\boldsymbol{\theta}_k) \quad (3.52)$$

is written in pLPV form as

$$\mathbf{A}_k = \mathbf{A}(\boldsymbol{\theta}_k) = \sum_{j=1}^M \lambda_{j,k} \mathbf{A}_{v,j} = \sum_{j=1}^M \lambda_{j,k} \mathbf{A}(\boldsymbol{\theta}_{v,j}) \quad (3.53)$$

with the coordinate vector $\boldsymbol{\lambda}_k$ calculated through (3.3)-(3.4) with $\boldsymbol{\theta}_k$ and the M vertices $\boldsymbol{\theta}_{v,j}$. Applying to this system pLPV control design techniques an output-feedback controller is found for each vertex of the polytope. These controllers are written here

$$\begin{bmatrix} \mathbf{x}_{of,k+1} \\ \mathbf{u}_p \end{bmatrix} = \left[\begin{array}{c|c} \mathbf{A}_{of,v,j} & \mathbf{B}_{of,v,j} \\ \mathbf{C}_{of,v,j} & \mathbf{D}_{of,v,j} \end{array} \right] \begin{bmatrix} \mathbf{x}_{of,k} \\ \mathbf{y}_p \end{bmatrix} \quad (3.54)$$

for $j = 1, \dots, M$, $\mathbf{A}_{of,v,j}^{((n_p+2n_d+n_{W_u}+n_{W_y}) \times (n_p+2n_d+n_{W_u}+n_{W_y}))}$, $\mathbf{B}_{of,v,j}^{((n_p+2n_d+n_{W_u}+n_{W_y}) \times m_u)}$, $\mathbf{C}_{of,v,j}^{(r_y \times (n_p+2n_d+n_{W_u}+n_{W_y}))}$ and $\mathbf{D}_{of,v,j}^{(r_y \times m_u)}$. This system is written in pLPV form as

$$\begin{bmatrix} \mathbf{x}_{c,k+1} \\ \mathbf{u}_k \end{bmatrix} = \left[\begin{array}{c|c} \mathbf{A}_c(\boldsymbol{\theta}_k) & \mathbf{B}_c(\boldsymbol{\theta}_k) \\ \mathbf{C}_c(\boldsymbol{\theta}_k) & \mathbf{D}_c(\boldsymbol{\theta}_k) \end{array} \right] \begin{bmatrix} \mathbf{x}_{c,k} \\ \mathbf{y}_k \end{bmatrix} \quad (3.55)$$

with

$$\begin{aligned} \mathbf{A}_c(\boldsymbol{\theta}_k)^{((n_p+2n_d+n_{W_u}+n_{W_y}) \times (n_p+2n_d+n_{W_u}+n_{W_y}))} &= \sum_{j=1}^M \mathbf{A}_{of,v,j} \lambda_{j,k}, \\ \mathbf{B}_c(\boldsymbol{\theta}_k)^{((n_p+2n_d+n_{W_u}+n_{W_y}) \times m_u)} &= \sum_{j=1}^M \mathbf{B}_{of,v,j} \lambda_{j,k}, \\ \mathbf{C}_c(\boldsymbol{\theta}_k)^{(r_y \times (n_p+2n_d+n_{W_u}+n_{W_y}))} &= \sum_{j=1}^M \mathbf{C}_{of,v,j} \lambda_{j,k} \end{aligned} \quad (3.56)$$

and

$$\mathbf{D}_c(\boldsymbol{\theta}_k)^{(r_y \times m_u)} = \sum_{j=1}^M \mathbf{D}_{of,v,j} \lambda_{j,k}. \quad (3.57)$$

Knowing the value of $\boldsymbol{\theta}_k$ and the vertices $\boldsymbol{\theta}_{v,j}$ the coordinate vector $\boldsymbol{\lambda}_k$ is calculated fulfilling the conditions (3.3) and (3.4).

LFT Systems

An LPV system given by the equations

$$\begin{bmatrix} \mathbf{x}_{k+1} \\ \mathbf{y}_k \end{bmatrix} = \left[\begin{array}{c|c} \mathbf{A}(\boldsymbol{\theta}_k) & \mathbf{B}(\boldsymbol{\theta}_k) \\ \mathbf{C}(\boldsymbol{\theta}_k) & \mathbf{0} \end{array} \right] \begin{bmatrix} \mathbf{x}_k \\ \mathbf{u}_k \end{bmatrix} \quad (3.58)$$

3. LPV Gain-scheduling Control

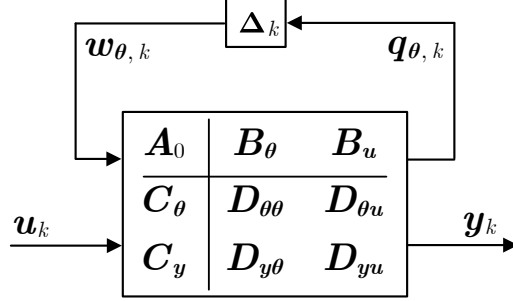


Figure 3.6: LPV system in LFT form

and the matrices $\mathbf{A}(\boldsymbol{\theta}_k)^{(n \times n)}$, $\mathbf{B}(\boldsymbol{\theta}_k)^{(n \times m_u)}$, $\mathbf{C}(\boldsymbol{\theta}_k)^{(m_y \times n)}$ can be written in LFT form if a representation of the LPV system is obtained as a lower LFT (see A.1) of the system defined by

$$\begin{bmatrix} \mathbf{x}_{k+1} \\ \mathbf{q}_{\theta,k} \\ \mathbf{y}_k \end{bmatrix} = \begin{bmatrix} \mathbf{A}_0 & \mathbf{B}_\theta & \mathbf{B}_u \\ \mathbf{C}_\theta & \mathbf{D}_{\theta\theta} & \mathbf{D}_{\theta u} \\ \mathbf{C}_y & \mathbf{D}_{y\theta} & \mathbf{D}_{yu} \end{bmatrix} \begin{bmatrix} \mathbf{x}_k \\ \mathbf{w}_{\theta,k} \\ \mathbf{u}_k \end{bmatrix} \quad (3.59)$$

with $\mathbf{A}_0^{(n \times n)}$, $\mathbf{B}_\theta^{(n \times m_\theta)}$, $\mathbf{B}_u^{(n \times m_u)}$, $\mathbf{C}_\theta^{(r_\theta \times n)}$, $\mathbf{D}_{\theta\theta}^{(r_\theta \times m_\theta)}$, $\mathbf{D}_{\theta u}^{(r_\theta \times m_u)}$, $\mathbf{C}_y^{(r_y \times n)}$, $\mathbf{D}_{y\theta}^{(r_y \times m_\theta)}$, $\mathbf{D}_{yu}^{(r_y \times m_u)}$ and the matrix

$$\Delta_k^{(m_\theta \times r_\theta)} = \begin{bmatrix} \theta_{1,k} & & \mathbf{0} \\ & \ddots & \\ \mathbf{0} & & \theta_{N,k} \end{bmatrix} \quad (3.60)$$

defined with the parameter $\boldsymbol{\theta}_k = [\theta_{1,k}, \dots, \theta_{N,k}]$. For a disturbance with n_d harmonic components the dimension $N = n_d$. A representation of an LPV system in LFT form is shown in Fig. 3.6. As this figure shows, the parametric uncertainty Δ_k is “pulled out” of the system.

An example to obtain an LFT model is here realized for the LPV system example

$$\begin{bmatrix} x_{p,k+1} \\ y_{p,k} \end{bmatrix} = \begin{bmatrix} a_k & 1 \\ 1 - a_k & 0 \end{bmatrix} \begin{bmatrix} x_{p,k} \\ u_{p,k} \end{bmatrix} \quad (3.61)$$

with $a_k \in [0.2 \ 0.8]$, $A(\theta_k)^{(n \times n)} = a_k$, $B^{(n \times m_u)} = 1$ and $C(\theta_k)^{(r_y \times n)} = 1 - a_k$ for $n = m_u = r_y = 1$.

An LFT representation of the LPV system can be obtained by simply doing $\theta_k = a_k$. The relation between a_k and θ_k can be written as

$$a_k = a_0 + b_1 \theta_k b_2 \quad (3.62)$$

for $\theta_k \in [a_{\min} \ a_{\max}]$ with $a_0 = 0$, $b_1 = b_2 = 1$. The matrix $A(\theta_k)^{(n \times n)}$ can be written as

$$A(\theta_k) = a_k = A_0 + B_\theta \theta_k C_\theta \quad (3.63)$$

with $A_0^{(n \times n)} = 0$, $B_\theta^{(n \times m_\theta)} = 1$, $C_\theta^{(r_\theta \times n)} = 1$ and $m_\theta = r_\theta = 1$. The same procedure is realized for the matrix $C(\theta_k)$ written as

$$C(\theta_k) = 1 - a_k = C_y + D_{y\theta} \theta_k C_\theta \quad (3.64)$$

with $C_y^{(r_y \times n)} = 1$ and $D_{y\theta}^{(r_y \times m_\theta)} = -1$. Finally the system is written in LFT form as

$$\begin{bmatrix} x_{k+1} \\ q_{\theta, k} \\ y_k \end{bmatrix} = \left[\begin{array}{c|cc} 0 & 1 & 1 \\ 1 & 0 & 0 \\ 1 & -1 & 0 \end{array} \right] \begin{bmatrix} x_k \\ w_{\theta, k} \\ u_k \end{bmatrix} \quad (3.65)$$

with $A_0 = 0$, $B_\theta = 1$, $B_u = 1$, $C_\theta = 1$, $D_{\theta\theta} = 0$, $D_{\theta u} = 0$, $C_y = 1$, $D_{y\theta} = -1$, $D_{yu} = 0$ and $\theta_k \in [0.2 \ 0.8]$. For $a_k = \theta_k = 0.4$ the lower LFT (see A.1) results in the system given with the state-space representation

$$\begin{bmatrix} x_{k+1} \\ y_k \end{bmatrix} = \left[\begin{array}{c|c} 0.4 & 1 \\ 0.6 & 0 \end{array} \right] \begin{bmatrix} x_k \\ u_k \end{bmatrix}. \quad (3.66)$$

LFT Control Structure

An LPV system in LFT form was shown in Fig. 3.6. For the control design, a generalized plant $G(z)$ in LFT form is built with input and output weighting functions and a parametric uncertainty block

$$\Delta_k = \begin{bmatrix} \theta_{1,k} & & \mathbf{0} \\ & \ddots & \\ \mathbf{0} & & \theta_{N,k} \end{bmatrix}. \quad (3.67)$$

For this general system, a gain-scheduling controller $K(z)$ can be calculated following the method presented in Apkarian and Gahinet (1995). In this method, two sets of LMIs are solved. The first set of LMIs determines the feasibility of the problem which means that a bound on the control system performance in the sense of the H_∞ can be satisfied. With the second set of LMIs, the controller matrices are calculated from the solution of the first set of LMIs.

As a result of applying this control design method, the gain-scheduling control structure of Fig. 3.7 is obtained. The time-varying plant parameter is directly used as the gain-scheduling parameter of the controller.

LFT Gain-scheduling Output Feedback Control Structure

The control structure presented in this section is obtained modeling the disturbance acting at the input of the plant as an LFT system. The system matrix $\mathbf{A}_d(\theta_k)$ of the disturbance can be written as

$$\mathbf{A}_d(\theta_k) = \mathbf{A}_{d,0} + \mathbf{B}_{d,\theta} \Delta_k \mathbf{C}_{d,\theta} \quad (3.68)$$

and a state-space representation of the disturbance model in LFT form is written as

$$\begin{bmatrix} \mathbf{x}_{d,k+1} \\ \mathbf{q}_{\theta,k} \\ \mathbf{y}_{d,k} \end{bmatrix} = \left[\begin{array}{c|cc} \mathbf{A}_{d,0} & \mathbf{B}_{d,\theta} & \mathbf{B}_d \\ \mathbf{C}_{d,\theta} & \mathbf{D}_{\theta\theta} & \mathbf{D}_{\theta w} \\ \mathbf{C}_d & \mathbf{D}_{y\theta} & \mathbf{D}_{yw} \end{array} \right] \begin{bmatrix} \mathbf{x}_{d,k} \\ \mathbf{w}_{\theta,k} \\ \mathbf{w}_{d,k} \end{bmatrix} \quad (3.69)$$

with

$$\begin{aligned} & \mathbf{A}_{d,0}^{(2n_d \times 2n_d)} \quad \mathbf{B}_{d,\theta}^{(2n_d \times m_\theta)} \quad \mathbf{B}_d^{(2n_d \times m_w)} \\ & \mathbf{C}_{d,\theta}^{(r_\theta \times 2n_d)} \quad \mathbf{D}_{\theta\theta}^{(r_\theta \times m_\theta)} \quad \mathbf{D}_{\theta w}^{(r_\theta \times m_w)} \\ & \mathbf{C}_d^{(r_{y_d} \times 2n_d)} \quad \mathbf{D}_{y\theta}^{(r_{y_d} \times m_\theta)} \quad \mathbf{D}_{yw}^{(r_{y_d} \times m_w)}. \end{aligned} \quad (3.70)$$

3. LPV Gain-scheduling Control

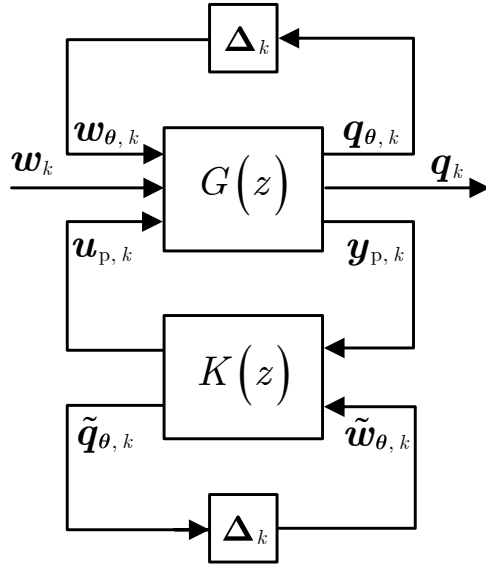


Figure 3.7: LFT control structure

Then the combination of plant and disturbance results in the LFT system shown in Fig. 3.8. A state-space representation of the LFT system is given as

$$\begin{bmatrix} \mathbf{x}_{k+1} \\ \mathbf{q}_{\theta, k} \\ \mathbf{y}_{p, k} \end{bmatrix} = \left[\begin{array}{c|ccc} \mathbf{A}_0 & \mathbf{B}_\theta & \mathbf{B}_w & \mathbf{B}_u \\ \mathbf{C}_\theta & \mathbf{D}_{\theta\theta} & \mathbf{D}_{\theta w} & \mathbf{D}_{\theta u} \\ \mathbf{C}_y & \mathbf{D}_{y\theta} & \mathbf{D}_{yw} & \mathbf{D}_{yu} \end{array} \right] \begin{bmatrix} \mathbf{x}_k \\ \mathbf{w}_{\theta, k} \\ \mathbf{w}_{d, k} \\ \mathbf{u}_{p, k} \end{bmatrix} \quad (3.71)$$

with

$$\mathbf{x}_k = \begin{bmatrix} \mathbf{x}_{p, k} \\ \mathbf{x}_{d, k} \end{bmatrix}, \quad \mathbf{A}_0^{((n_p+2n_d) \times (n_p+2n_d))} = \begin{bmatrix} \mathbf{A}_p & \mathbf{B}_p \mathbf{C}_d \\ \mathbf{0} & \mathbf{A}_{d, 0} \end{bmatrix}, \quad (3.72)$$

$$[\mathbf{B}_\theta \quad \mathbf{B}_w \quad \mathbf{B}_u]^{((n_p+2n_d) \times (m_\theta+m_w+m_u))} = \begin{bmatrix} \mathbf{0} & \mathbf{0} & \mathbf{B}_p \\ \mathbf{B}_{d, \theta} & \mathbf{B}_d & \mathbf{0} \end{bmatrix}, \quad (3.73)$$

$$\begin{bmatrix} \mathbf{C}_\theta \\ \mathbf{C}_y \end{bmatrix}^{((r_\theta+r_y) \times (n_p+2n_d))} = \begin{bmatrix} \mathbf{0} & \mathbf{C}_{d, \theta} \\ \mathbf{C}_p & \mathbf{0} \end{bmatrix} \quad (3.74)$$

and

$$\begin{bmatrix} \mathbf{D}_{\theta\theta} & \mathbf{D}_{\theta w} & \mathbf{D}_{\theta u} \\ \mathbf{D}_{y\theta} & \mathbf{D}_{yw} & \mathbf{D}_{yu} \end{bmatrix}^{((r_\theta+r_y) \times (m_\theta+m_w+m_u))} = \begin{bmatrix} \mathbf{0} & \mathbf{0} & \mathbf{0} \\ \mathbf{0} & \mathbf{0} & \mathbf{0} \end{bmatrix}. \quad (3.75)$$

Additional weighting functions for the control input $\mathbf{u}_{p, k}$

$$\begin{bmatrix} \mathbf{x}_{W_u, k+1} \\ \mathbf{q}_{u, k} \end{bmatrix} = \left[\begin{array}{c|c} \mathbf{A}_{W_u} & \mathbf{B}_{W_u} \\ \mathbf{C}_{W_u} & \mathbf{D}_{W_u} \end{array} \right] \begin{bmatrix} \mathbf{x}_{W_u, k} \\ \mathbf{u}_{p, k} \end{bmatrix} \quad (3.76)$$

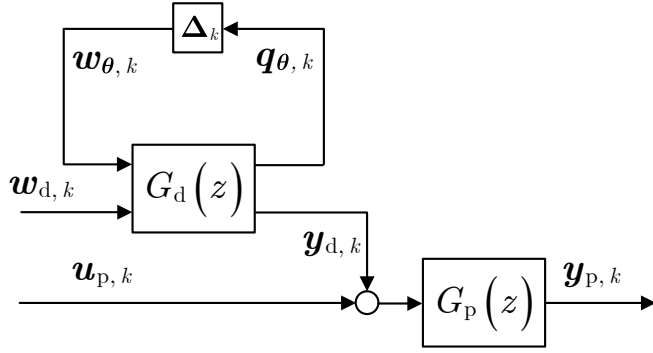


Figure 3.8: LFT disturbance model acting at the input of the plant

with

$$\begin{array}{ll} \mathbf{A}_{W_u}^{(n_{W_u} \times n_{W_u})} & \mathbf{B}_{W_u}^{(n_{W_u} \times m_u)} \\ \mathbf{C}_{W_u}^{(r_{qu} \times n_{W_u})} & \mathbf{D}_{W_u}^{(r_{qu} \times m_u)} \end{array} \quad (3.77)$$

and for the plant output $\mathbf{y}_{p, k}$

$$\left[\begin{array}{c} \mathbf{x}_{W_y, k+1} \\ \mathbf{q}_{y, k} \end{array} \right] = \left[\begin{array}{c|c} \mathbf{A}_{W_y} & \mathbf{B}_{W_y} \\ \hline \mathbf{C}_{W_y} & \mathbf{D}_{W_y} \end{array} \right] \left[\begin{array}{c} \mathbf{x}_{W_y, k} \\ \mathbf{y}_{p, k} \end{array} \right] \quad (3.78)$$

with

$$\begin{array}{ll} \mathbf{A}_{W_y}^{(n_{W_y} \times n_{W_y})} & \mathbf{B}_{W_y}^{(n_{W_y} \times r_y)} \\ \mathbf{C}_{W_y}^{(r_{qu} \times n_{W_y})} & \mathbf{D}_{W_y}^{(r_{qu} \times r_y)} \end{array} \quad (3.79)$$

are added to apply the H_∞ control design techniques of Apkarian and Gahinet (1995). The generalized system with plant, disturbance model and weighting functions is shown in Fig. 3.9 and can be written as a state-space representation

$$\left[\begin{array}{c} \mathbf{x}_{k+1} \\ \mathbf{q}_{\theta, k} \\ \mathbf{q}_k \\ \mathbf{y}_{p, k} \end{array} \right] = \left[\begin{array}{c|ccc} \mathbf{A}_0 & \mathbf{B}_\theta & \mathbf{B}_w & \mathbf{B}_u \\ \hline \mathbf{C}_\theta & \mathbf{D}_{\theta\theta} & \mathbf{D}_{\theta w} & \mathbf{D}_{\theta u} \\ \mathbf{C}_q & \mathbf{D}_{q\theta} & \mathbf{D}_{qw} & \mathbf{D}_{qu} \\ \mathbf{C}_y & \mathbf{D}_{y\theta} & \mathbf{D}_{yw} & \mathbf{D}_{yu} \end{array} \right] \left[\begin{array}{c} \mathbf{x}_k \\ \mathbf{w}_{\theta, k} \\ \mathbf{w}_k \\ \mathbf{u}_{p, k} \end{array} \right] \quad (3.80)$$

with

$$\mathbf{x}_k = \left[\begin{array}{c} \mathbf{x}_{p, k} \\ \mathbf{x}_{d, k} \\ \mathbf{x}_{W_u, k} \\ \mathbf{x}_{W_y, k} \end{array} \right], \quad n = n_p + n_d + n_{W_u} + n_{W_y} \quad (3.81)$$

$$\mathbf{A}^{(n \times n)} = \left[\begin{array}{cccc} \mathbf{A}_p & \mathbf{B}_p \mathbf{C}_d & \mathbf{0} & \mathbf{0} \\ \mathbf{0} & \mathbf{A}_{d, 0} & \mathbf{0} & \mathbf{0} \\ \mathbf{0} & \mathbf{0} & \mathbf{A}_{W_u} & \mathbf{0} \\ \mathbf{B}_{W_y} \mathbf{C}_p & \mathbf{0} & \mathbf{0} & \mathbf{A}_{W_y} \end{array} \right], \quad (3.82)$$

3. LPV Gain-scheduling Control

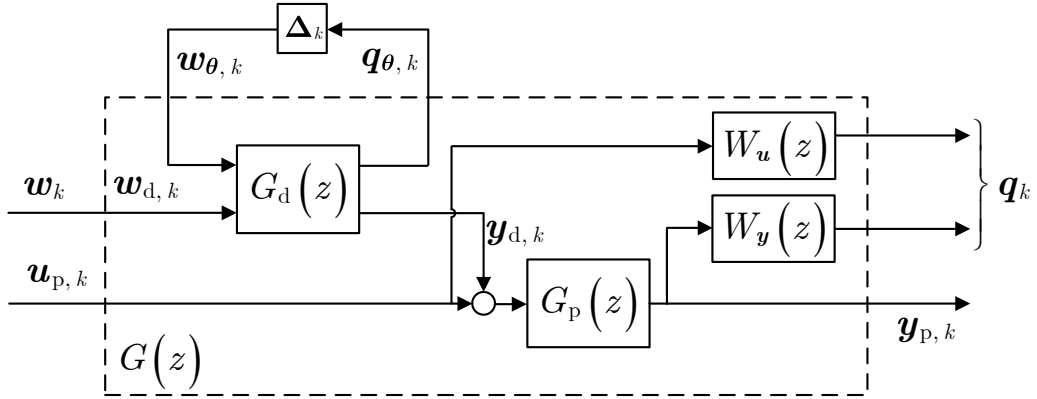


Figure 3.9: Generalized plant with disturbance model in LFT form and weighting functions

$$[\mathbf{B}_\theta \quad \mathbf{B}_w \quad \mathbf{B}_u]^{(n \times (m_\theta + m_w + m_u))} = \begin{bmatrix} \mathbf{0} & \mathbf{0} & \mathbf{B}_p \\ \mathbf{B}_{d,\theta} & \mathbf{B}_d & \mathbf{0} \\ \mathbf{0} & \mathbf{0} & \mathbf{B}_{W_u} \\ \mathbf{0} & \mathbf{0} & \mathbf{0} \end{bmatrix}, \quad (3.83)$$

$$\begin{bmatrix} \mathbf{C}_\theta \\ \mathbf{C}_q \\ \mathbf{C}_y \end{bmatrix}^{((r_\theta + r_q + r_y) \times n)} = \begin{bmatrix} \mathbf{0} & \mathbf{C}_{d,\theta} & \mathbf{0} & \mathbf{0} \\ \mathbf{0} & \mathbf{0} & \mathbf{C}_{W_u} & \mathbf{0} \\ \mathbf{D}_{W_y} \mathbf{C}_p & \mathbf{0} & \mathbf{0} & \mathbf{C}_{W_y} \\ \mathbf{C}_p & \mathbf{0} & \mathbf{0} & \mathbf{0} \end{bmatrix} \quad (3.84)$$

and

$$\begin{bmatrix} \mathbf{D}_{\theta\theta} & \mathbf{D}_{\theta w} & \mathbf{D}_{\theta u} \\ \mathbf{D}_{q\theta} & \mathbf{D}_{qw} & \mathbf{D}_{qu} \\ \mathbf{D}_{y\theta} & \mathbf{D}_{yw} & \mathbf{D}_{yu} \end{bmatrix}^{((r_\theta + r_q + r_y) \times (m_\theta + m_w + m_u))} = \begin{bmatrix} \mathbf{0} & \mathbf{0} & \mathbf{0} \\ \mathbf{0} & \mathbf{0} & \mathbf{D}_{W_u} \\ \mathbf{0} & \mathbf{0} & \mathbf{0} \\ \hline \mathbf{0} & \mathbf{0} & \mathbf{0} \end{bmatrix} \quad (3.85)$$

in LFT form with the parameter Δ_k .

Applying H_∞ control design techniques a LFT controller

$$\begin{bmatrix} \mathbf{x}_{K,k+1} \\ \mathbf{u}_{p,k} \\ \tilde{\mathbf{q}}_{\theta,k} \end{bmatrix} = \begin{bmatrix} \mathbf{A}_0^{(K)} & \mathbf{B}_y^{(K)} & \mathbf{B}_\theta^{(K)} \\ \mathbf{C}_u^{(K)} & \mathbf{D}_{uy}^{(K)} & \mathbf{D}_{u\theta}^{(K)} \\ \mathbf{C}_\theta^{(K)} & \mathbf{D}_{\theta y}^{(K)} & \mathbf{D}_{\theta\theta}^{(K)} \end{bmatrix} \begin{bmatrix} \mathbf{x}_{K,k} \\ \mathbf{y}_{p,k} \\ \tilde{\mathbf{w}}_{\theta,k} \end{bmatrix} \quad (3.86)$$

is obtained for

$$\begin{aligned} & \mathbf{A}_0^{(K)(n_K \times n_K)} \quad \mathbf{B}_y^{(K)(n_K \times r_y)} \quad \mathbf{B}_\theta^{(K)(n_K \times r_\theta)} \\ & \mathbf{C}_u^{(K)(m_u \times n_K)} \quad \mathbf{D}_{uy}^{(K)(m_u \times r_y)} \quad \mathbf{D}_{u\theta}^{(K)(m_u \times r_\theta)} \\ & \mathbf{C}_\theta^{(K)(m_\theta \times n_K)} \quad \mathbf{D}_{\theta y}^{(K)(m_\theta \times r_y)} \quad \mathbf{D}_{\theta\theta}^{(K)(m_\theta \times r_\theta)} \end{aligned} \quad (3.87)$$

and $n_K = n$ with the same gain-scheduling parameter as the generalized plant. The calculation of the controller will be explained in the next chapter.

Chapter 4

LPV Gain-scheduling Control for Harmonic Disturbances with Time-varying Frequencies

Harmonic disturbances with time-varying frequencies appear in industrial applications with rotating machinery (e.g., aircrafts and automotive applications). In this thesis, this problem is considered and solved through the use of LPV gain-scheduling controllers for the reduction of harmonic disturbances. The complete control design is explained in this chapter resulting in LPV controllers with the frequency of the disturbance as the gain-scheduling parameter.

According to the IMP, the controller must contain a model of the harmonic disturbance to achieve disturbance rejection. Since the harmonic disturbance is time varying, the disturbance is modelled as an LPV system using the models explained in Sec. 4.1. As shown in Fig. 4.1, depending on how the LPV disturbance is modelled a pLPV or LFT system is obtained and approximations to reduce the gain-scheduling parameters are presented. The control structures from the previous chapters are used with pLPV control design techniques to obtain pLPV gain-scheduling controllers in Sec. 4.1.2. The LFT control design techniques for the calculation of an LFT gain-scheduling controller are presented in Sec. 4.1.6.

LPV Disturbance Model

An MIMO state-space representation of a disturbance with n_d components of constant frequencies, n inputs and n outputs ($n \times n$) is given as

$$\begin{bmatrix} \mathbf{x}_{d,k+1} \\ \mathbf{y}_{d,k} \end{bmatrix} = \left[\begin{array}{c|c} \mathbf{A}_{d,k} & \mathbf{B}_d \\ \hline \mathbf{C}_d & \mathbf{0} \end{array} \right] \begin{bmatrix} \mathbf{x}_{d,k} \\ \mathbf{w}_{d,k} \end{bmatrix} \quad (4.1)$$

with

$$\mathbf{A}_{d,k}^{(2n_d n \times 2n_d n)} = \begin{bmatrix} \mathbf{A}_{d_1,k} & \dots & \mathbf{0} \\ \vdots & \ddots & \vdots \\ \mathbf{0} & \dots & \mathbf{A}_{d_n,k} \end{bmatrix}, \quad (4.2)$$

$$\mathbf{A}_{d_1,k}^{(2n_d \times 2n_d)} = \dots = \mathbf{A}_{d_n,k}^{(2n_d \times 2n_d)} = \begin{bmatrix} \tilde{\mathbf{A}}_{d_1,k} & \dots & \mathbf{0} \\ \vdots & \ddots & \vdots \\ \mathbf{0} & \dots & \tilde{\mathbf{A}}_{d_n,k} \end{bmatrix}, \quad (4.3)$$

$$\tilde{\mathbf{A}}_{d_i,k}^{(2 \times 2)} = \begin{bmatrix} 0 & 1 \\ -r^2 & 2r \cos(\Omega_{i,k}) \end{bmatrix}, \quad (4.4)$$

4. LPV Gain-scheduling Control for Harmonic Disturbances with Time-varying Frequencies

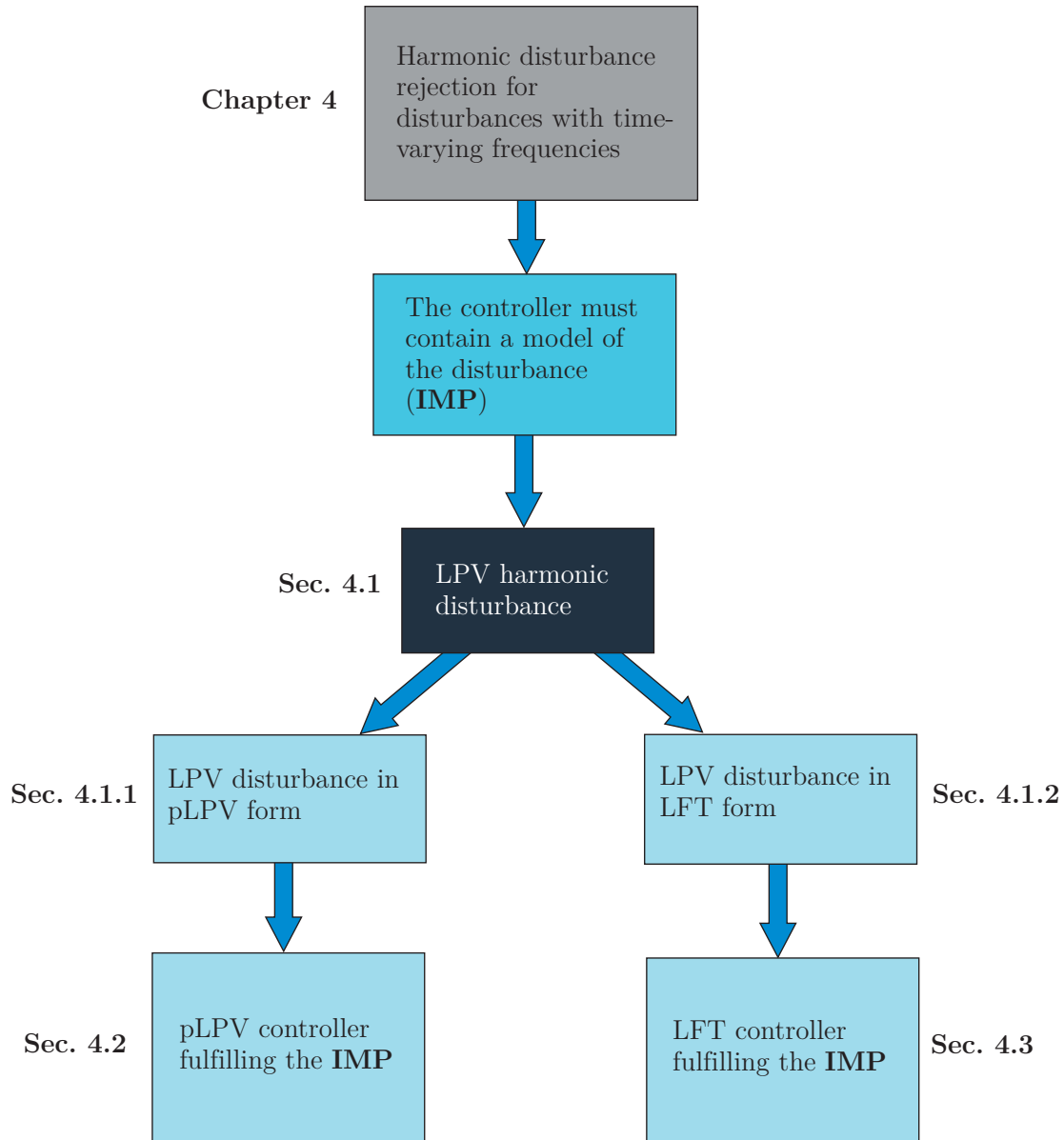


Figure 4.1: Chapter schema

$$\mathbf{B}_d^{(2n_d n \times m_{w_d})} = \begin{bmatrix} \mathbf{B}_{d_1} & \dots & \mathbf{0} \\ \vdots & \ddots & \vdots \\ \mathbf{0} & \dots & \mathbf{B}_{d_n} \end{bmatrix}, \quad \mathbf{B}_{d_1}^{(2n_d \times 1)} = \dots = \mathbf{B}_{d_n}^{(2n_d \times 1)} = \begin{bmatrix} 1 \\ 0 \\ \vdots \\ 1 \\ 0 \end{bmatrix} \quad (4.5)$$

and

$$\mathbf{C}_d^{(r_{y_d} \times 2n_d n)} = \begin{bmatrix} \mathbf{C}_{d_1} & \dots & \mathbf{0} \\ \vdots & \ddots & \vdots \\ \mathbf{0} & \dots & \mathbf{C}_{d_n} \end{bmatrix}, \quad (4.6)$$

$$\mathbf{C}_{d_1}^{(1 \times 2n_d)} = \dots = \mathbf{C}_{d_n}^{(1 \times 2n_d)} = [1 \ 0 \ \dots \ 1 \ 0]$$

with $\Omega_{i,k} = 2\pi f_{i,k}T$ for $i = 1, \dots, n_d$. This model is only correct for constant frequencies, but this model was used to obtain controllers for the rejection of time-varying frequencies in Ballesteros and Bohn (2010, 2011a, 2011b), Ballesteros et al. (2012, 2013), Duarte et al. (2012, 2013, 2013a, 2013b), Heins et al. (2011, 2012, 2012a), Shu et al. (2011, 2013) and they were validated with experimental results. The main advantage of this model is that only one parameter per frequency is needed. The system described with the state-space representation of (4.1) and (4.2)-(4.4) needs n_d parameters.

For time-varying frequencies the disturbance model is as in (4.1) with the matrix $\tilde{\mathbf{A}}_{d_i,k}$ from (4.2)-(4.3) given as

$$\tilde{\mathbf{A}}_{d_i,k}^{(2 \times 2)} = \begin{bmatrix} r \cos(\Omega_{i,k}) & r \sin(\Omega_{i,k}) \\ -r \sin(\Omega_{i,k}) & r \cos(\Omega_{i,k}) \end{bmatrix} \quad (4.7)$$

for $\Omega_{i,k} = 2\pi f_{i,k}T$ and $i = 1, \dots, n_d$. This model is correct for time-varying frequencies but it has the disadvantage that it needs $2n_d$ gain-scheduling parameters to obtain an LPV representation of the disturbance model. This model needs twice as many number of gain-scheduling parameters as the disturbance model for constant frequencies of (4.1)-(4.4).

A very useful idea was introduced in Füger et al. (2012, 2013) that uses a polynomial approximation to reduce the number of gain-scheduling parameters if the components of frequency are harmonically related and the range of variation of the fundamental frequency

$$f_{0,k} \in [f_{0,\min}, f_{0,\max}] \quad (4.8)$$

is known. The polynomial approximation was used in Füger et al. (2012, 2013) with the model of constant frequencies for the rejection of time-varying harmonic disturbances for a SISO system. This thesis and the work realized in Ballesteros et al. (2014a, 2014b, 2014c) uses the polynomial approximation for a MIMO model of time-varying disturbance frequencies (4.7). The cosine function and the sine function can be written as

$$\begin{aligned} r \cos(\Omega_{i,k}) &\approx a_{i,0} + a_{i,1}\Omega_{0,k} + \dots + a_{i,N_p}\Omega_{0,k}^{N_p} \\ r \sin(\Omega_{i,k}) &\approx b_{i,0} + b_{i,1}\Omega_{0,k} + \dots + b_{i,N_p}\Omega_{0,k}^{N_p} \end{aligned} \quad (4.9)$$

for n_d harmonically related time-varying frequencies

$$\mathbf{f}_k = [f_{1,k} \ f_{2,k} \ \dots \ f_{n_d,k}] = [h_1 \ h_2 \ \dots \ h_{n_d}]f_{0,k} \text{ and } \Omega_{0,k} = 2\pi f_{0,k}T \quad (4.10)$$

for $f_{0,k} \in [f_{0,\min}, f_{0,\max}]$. A least square fit can be used to calculate the coefficients $a_{i,0}, \dots, a_{i,N_p}$ and $b_{i,0}, \dots, b_{i,N_p}$. Simulations and experiments achieved a very good approximation with only three coefficients. Therefore here the sine and cosine function are approximated as

$$\begin{aligned} r \cos(\Omega_{i,k}) &\approx a_{i,0} + a_{i,2}\Omega_{0,k}^2 + a_{i,4}\Omega_{0,k}^4 \\ r \sin(\Omega_{i,k}) &\approx b_{i,0} + b_{i,2}\Omega_{0,k}^2 + b_{i,4}\Omega_{0,k}^4. \end{aligned} \quad (4.11)$$

The time-varying parameters

$$\begin{aligned} \theta_{1,k} &= \Omega_{0,k}^2 = (2\pi f_{0,k})^2, \\ \theta_{2,k} &= \Omega_{0,k}^4 = (2\pi f_{0,k})^4 \end{aligned} \quad (4.12)$$

4. LPV Gain-scheduling Control for Harmonic Disturbances with Time-varying Frequencies

are introduced and the matrix $\tilde{\mathbf{A}}_{d_i,k}$ can be written as

$$\tilde{\mathbf{A}}_{d_i,k}^{(2 \times 2)} = \begin{bmatrix} a_{i,0} & b_{i,0} \\ -b_{i,0} & a_{i,0} \end{bmatrix} + \begin{bmatrix} a_{i,2} & b_{i,2} \\ -b_{i,2} & a_{i,2} \end{bmatrix} \theta_{1,k} + \begin{bmatrix} a_{i,4} & b_{i,4} \\ -b_{i,4} & a_{i,4} \end{bmatrix} \theta_{2,k} \quad (4.13)$$

with only two gain-scheduling parameters independently of the number of frequencies. An LPV representation of the matrix $\mathbf{A}_{d_i,k}$ with two gain-scheduling parameters is possible since the matrices $\tilde{\mathbf{A}}_{d_i,k}$ are included in the matrix $\mathbf{A}_{d_i,k}$.

Through an example, the three LPV models presented in this section are compared. The objective is to obtain the three LPV disturbance models for a harmonic disturbance with two components of frequency $n_d = 2$

$$\mathbf{f}_k = f_{0,k} [1 \ 2] = [f_{1,k} \ f_{2,k}] \quad (4.14)$$

harmonically related with $f_{0,k} \in [80, 85]$ Hz with a sampling time of $T = 0.001$ s.

Using the disturbance model for constant frequencies from (4.1)-(4.4) the matrix

$$\mathbf{A}_{d,k}^{(2n_d \times 2n_d)} = \begin{bmatrix} 0 & 1 & 0 & 0 \\ -r^2 & 2r \cos(2\pi f_{1,k} T) & 0 & 0 \\ 0 & 0 & 0 & 1 \\ 0 & 0 & -r^2 & 2r \cos(2\pi f_{2,k} T) \end{bmatrix} \quad (4.15)$$

can be written in LPV form defining $\boldsymbol{\theta}_k = [\theta_{1,k} \ \theta_{2,k}]$ as

$$\theta_{1,k} = 2r \cos(2\pi f_{1,k} T), \ \theta_{2,k} = 2r \cos(2\pi f_{2,k} T) \quad (4.16)$$

and then the matrix

$$\mathbf{A}_{d,k} = \mathbf{A}_d(\boldsymbol{\theta}_k) = \mathcal{A}_0 + \mathcal{A}_1 \theta_{1,k} + \mathcal{A}_2 \theta_{2,k} \quad (4.17)$$

is written as an LPV representation with

$$\begin{aligned} \mathcal{A}_0^{(2n_d \times 2n_d)} &= \begin{bmatrix} 0 & 1 & 0 & 0 \\ -r^2 & 0 & 0 & 0 \\ 0 & 0 & 0 & 1 \\ 0 & 0 & -r^2 & 0 \end{bmatrix}, \quad \mathcal{A}_1^{(2n_d \times 2n_d)} = \begin{bmatrix} 0 & 0 & 0 & 0 \\ 0 & 1 & 0 & 0 \\ 0 & 0 & 0 & 0 \\ 0 & 0 & 0 & 0 \end{bmatrix} \\ \mathcal{A}_2^{(2n_d \times 2n_d)} &= \begin{bmatrix} 0 & 0 & 0 & 0 \\ 0 & 0 & 0 & 0 \\ 0 & 0 & 0 & 0 \\ 0 & 0 & 0 & 1 \end{bmatrix}. \end{aligned} \quad (4.18)$$

The disturbance model for time-varying frequencies (4.1)-(4.3) and (4.7) is used now to obtain an LPV representation for the harmonic disturbance of the example. The matrix

$$\mathbf{A}_{d,k} = \begin{bmatrix} r \cos(2\pi f_{1,k} T) & r \sin(2\pi f_{1,k} T) & 0 & 0 \\ -r \sin(2\pi f_{1,k} T) & r \cos(2\pi f_{1,k} T) & 0 & 0 \\ 0 & 0 & r \cos(2\pi f_{2,k} T) & r \sin(2\pi f_{2,k} T) \\ 0 & 0 & -r \sin(2\pi f_{2,k} T) & r \cos(2\pi f_{2,k} T) \end{bmatrix} \quad (4.19)$$

is written using

$$\begin{aligned} \theta_{1,k} &= r \cos(2\pi f_{1,k} T), \ \theta_{2,k} = r \sin(2\pi f_{1,k} T), \ \theta_{3,k} = r \cos(2\pi f_{2,k} T), \\ \theta_{4,k} &= r \sin(2\pi f_{2,k} T) \end{aligned} \quad (4.20)$$

in LPV form as

$$\mathbf{A}_{d,k}^{(2n_d \times 2n_d)} = \mathbf{A}_d(\theta_k) = \mathbf{A}_0 + \mathbf{A}_1\theta_{1,k} + \mathbf{A}_2\theta_{2,k} + \mathbf{A}_3\theta_{3,k} + \mathbf{A}_4\theta_{4,k} \quad (4.21)$$

with

$$\begin{aligned} \mathbf{A}_0^{(2n_d \times 2n_d)} &= \begin{bmatrix} 0 & 0 & 0 & 0 \\ 0 & 0 & 0 & 0 \\ 0 & 0 & 0 & 0 \\ 0 & 0 & 0 & 0 \end{bmatrix}, \quad \mathbf{A}_1^{(2n_d \times 2n_d)} = \begin{bmatrix} 1 & 0 & 0 & 0 \\ 0 & 1 & 0 & 0 \\ 0 & 0 & 0 & 0 \\ 0 & 0 & 0 & 0 \end{bmatrix} \\ \mathbf{A}_2^{(2n_d \times 2n_d)} &= \begin{bmatrix} 0 & 1 & 0 & 0 \\ -1 & 0 & 0 & 0 \\ 0 & 0 & 0 & 0 \\ 0 & 0 & 0 & 0 \end{bmatrix}, \quad \mathbf{A}_3^{(2n_d \times 2n_d)} = \begin{bmatrix} 0 & 0 & 0 & 0 \\ 0 & 0 & 0 & 0 \\ 0 & 0 & 1 & 0 \\ 0 & 0 & 0 & 1 \end{bmatrix} \quad (4.22) \\ \text{and } \mathbf{A}_4^{(2n_d \times 2n_d)} &= \begin{bmatrix} 0 & 0 & 0 & 0 \\ 0 & 0 & 0 & 0 \\ 0 & 0 & 0 & 1 \\ 0 & 0 & -1 & 0 \end{bmatrix}. \end{aligned}$$

This LPV model needs double gain-scheduling parameters as the LPV model for constant frequencies.

A reduction of the gain-scheduling parameters is done using the polynomial approximation for the frequency range of $f_{0,k} \in [80 \text{--} 85] \text{ Hz}$. The cosine function is approximated as

$$\begin{aligned} r \cos(2\pi f_{0,k} T) &\approx a_{0,1} + a_{2,1}(2\pi f_{0,k} T)^2 + a_{4,1}(2\pi f_{0,k} T)^4 \\ r \cos(2\pi 2f_{0,k} T) &\approx a_{0,2} + a_{2,2}(2\pi f_{0,k} T)^2 + a_{4,2}(2\pi f_{0,k} T)^4 \end{aligned} \quad (4.23)$$

with $r = 0.9999$, $T = 0.001 \text{ s}$ and the coefficients

$$\begin{aligned} a_{0,1} &= 0.9999, \quad a_{2,1} = -0.4997, \quad a_{4,1} = 0.0406 \\ a_{0,2} &= 0.9983, \quad a_{2,2} = -1.9815, \quad a_{4,2} = 0.5976 \end{aligned} \quad (4.24)$$

calculated through a least square fit. For $f_{0,k} = 82 \text{ Hz}$, $r \cos(2\pi f_{0,k} T) = 0.87012$ and the value obtained using the polynomial approximation is 0.87009. The absolute error obtained in this case is 0.00003. The same approximation is realized for the sine function doing

$$\begin{aligned} r \sin(2\pi f_{0,k} T) &\approx b_{0,1} + b_{2,1}(2\pi f_{0,k} T)^2 + b_{4,1}(2\pi f_{0,k} T)^4 \\ r \sin(2\pi 2f_{0,k} T) &\approx b_{0,2} + b_{2,2}(2\pi f_{0,k} T)^2 + b_{4,2}(2\pi f_{0,k} T)^4 \end{aligned} \quad (4.25)$$

obtaining the coefficients

$$\begin{aligned} b_{0,1} &= 0.1973, \quad b_{2,1} = 1.3807, \quad b_{4,1} = -1.0098 \\ b_{0,2} &= 0.4151, \quad b_{2,2} = 2.3339, \quad b_{4,2} = -2.5146 \end{aligned} \quad (4.26)$$

4. LPV Gain-scheduling Control for Harmonic Disturbances with Time-varying Frequencies

with a least square fit. Finally the matrix

$$\begin{aligned} \mathbf{A}_{d,k} = & \begin{bmatrix} a_{0,1} & b_{0,1} & 0 & 0 \\ -b_{0,1} & a_{0,1} & 0 & 0 \\ 0 & 0 & a_{0,2} & b_{0,2} \\ 0 & 0 & -b_{0,2} & a_{0,2} \end{bmatrix} + \begin{bmatrix} a_{2,1} & b_{2,1} & 0 & 0 \\ -b_{2,1} & a_{2,1} & 0 & 0 \\ 0 & 0 & a_{2,2} & b_{2,2} \\ 0 & 0 & -b_{2,2} & a_{2,2} \end{bmatrix} \theta_{1,k} + \\ & + \begin{bmatrix} a_{4,1} & b_{4,1} & 0 & 0 \\ -b_{4,1} & a_{4,1} & 0 & 0 \\ 0 & 0 & a_{4,2} & b_{4,2} \\ 0 & 0 & -b_{4,2} & a_{4,2} \end{bmatrix} \theta_{2,k} \end{aligned} \quad (4.27)$$

is written with the coefficients calculated before with the gain-scheduling parameters $\theta_{1,k}$ and $\theta_{2,k}$. Independently of the number of frequencies contained in the disturbance, if the frequencies are harmonically related this model requires only two gain-scheduling parameters.

The pLPV and LFT disturbance models are explained and obtained from the LPV form in the next subsections.

pLPV Disturbance Model

Substituting $2r \cos(\Omega_{i,k})$ with $\theta_{i,k}$ and knowing the range of variation $\theta_{i,k} \in [\theta_{i,\min}, \theta_{i,\max}]$ with

$$\begin{aligned} \theta_{i,\min} &= 2r \cos(\Omega_{i,\min}) = 2r \cos(2\pi f_{i,\min} T), \\ \theta_{i,\max} &= 2r \cos(\Omega_{i,\max}) = 2r \cos(2\pi f_{i,\max} T) \end{aligned} \quad (4.28)$$

for $i = 1, \dots, n_d$, the LPV model for constant frequencies (4.1)-(4.4) can be written in pLPV form if the parameters $\boldsymbol{\theta}_k = [\theta_{1,k} \ \theta_{2,k} \ \dots \ \theta_{n_d,k}]$ varies inside a convex polytope $\boldsymbol{\Theta}$. The vertices $\mathbf{V} = [\boldsymbol{\theta}_{v,1} \ \boldsymbol{\theta}_{v,2} \ \dots \ \boldsymbol{\theta}_{v,M}]$ with $\boldsymbol{\theta}_{v,j} \in \mathbb{R}^{n_d}$ for $j = 1, \dots, M$ with all the possible combinations of $f_{i,\min}$ and $f_{i,\max}$ form a convex polytope $\boldsymbol{\Theta}$. The parameters $\boldsymbol{\theta}_k$ are calculated with the coordinate vector $\boldsymbol{\lambda}_k = [\lambda_{1,k} \ \lambda_{2,k} \ \dots \ \lambda_{M,k}]$ as in (3.3) and (3.4). These conditions can be expressed in matrix form as

$$\begin{bmatrix} \boldsymbol{\theta}_{v,1} & \dots & \boldsymbol{\theta}_{v,M} \\ 1 & \dots & 1 \end{bmatrix} \boldsymbol{\lambda}_k^T = \begin{bmatrix} \boldsymbol{\theta}_k^T \\ 1 \end{bmatrix} \quad \text{with } \lambda_{j,k} \geq 0 \text{ for } j = 1, \dots, M. \quad (4.29)$$

The disturbance model of (4.1)-(4.4) is written in pLPV form as

$$\begin{bmatrix} \mathbf{x}_{d,k+1} \\ \mathbf{y}_{d,k} \end{bmatrix} = \begin{bmatrix} \mathbf{A}_{d,k} & \mathbf{B}_d \\ \mathbf{C}_d & \mathbf{0} \end{bmatrix} \begin{bmatrix} \mathbf{x}_{d,k} \\ \mathbf{u}_{d,k} \end{bmatrix} = \begin{bmatrix} \mathbf{A}_d(\boldsymbol{\theta}_k) & \mathbf{B}_d \\ \mathbf{C}_d & \mathbf{0} \end{bmatrix} \begin{bmatrix} \mathbf{x}_{d,k} \\ \mathbf{u}_{d,k} \end{bmatrix} \quad (4.30)$$

with

$$\mathbf{A}_d(\boldsymbol{\theta}_k)^{(2n_d n \times 2n_d n)} = \lambda_{1,k} \mathbf{A}_{d,v,1} + \lambda_{2,k} \mathbf{A}_{d,v,2} + \dots + \lambda_{M,k} \mathbf{A}_{d,v,M} \quad (4.31)$$

and

$$\mathbf{A}_{d,v,j}^{(2n_d n \times 2n_d n)} = \mathbf{A}(\boldsymbol{\theta}_{v,j}). \quad (4.32)$$

As an example, a disturbance model with two frequencies $f_{1,k} \in [70, 80]$ Hz, $f_{2,k} \in [140, 160]$ Hz, $n_d = 2$, $T = 0.001$ s and $r = 0.9999$ will be written in pLPV using

the coordinate vector $\boldsymbol{\lambda}_k$ fulfilling the conditions of (4.29). The disturbance model is represented now as

$$\begin{aligned} \mathbf{A}_{d,k}^{(2n_d \times 2n_d)} &= \begin{bmatrix} 0 & 1 & 0 & 0 \\ -r^2 & 2r \cos(2\pi f_{1,k} T) & 0 & 0 \\ 0 & 0 & 0 & 1 \\ 0 & 0 & -r^2 & 2r \cos(2\pi f_{2,k} T) \end{bmatrix} = \\ &= \begin{bmatrix} 0 & 1 & 0 & 0 \\ -r^2 & \theta_{1,k} & 0 & 0 \\ 0 & 0 & 0 & 1 \\ 0 & 0 & -r^2 & \theta_{2,k} \end{bmatrix} \end{aligned} \quad (4.33)$$

with

$$\left[\begin{array}{c} \mathbf{x}_{d,k+1} \\ \mathbf{y}_{d,k} \end{array} \right] = \left[\begin{array}{c|c} \mathbf{A}_{d,k} & \mathbf{B}_d \\ \hline \mathbf{C}_d & \mathbf{0} \end{array} \right] \left[\begin{array}{c} \mathbf{x}_{d,k} \\ \mathbf{u}_{d,k} \end{array} \right]. \quad (4.34)$$

The vertices of the disturbance model are defined with

$$\begin{aligned} \theta_{1,\min} &= 2r \cos(2\pi f_{1,\min} T) = 1.8095, \quad \theta_{1,\max} = 2r \cos(2\pi f_{1,\max} T) = 1.7524 \\ \theta_{2,\min} &= 2r \cos(2\pi f_{2,\min} T) = 1.2747, \quad \theta_{2,\max} = 2r \cos(2\pi f_{2,\max} T) = 1.0715 \end{aligned} \quad (4.35)$$

and then the disturbance model is written in pLPV form as

$$\mathbf{A}_d(\boldsymbol{\theta}_k)^{(2n_d \times 2n_d)} = \lambda_{1,k} \mathbf{A}_d(\boldsymbol{\theta}_{v,1}) + \lambda_{2,k} \mathbf{A}_d(\boldsymbol{\theta}_{v,2}) + \lambda_{3,k} \mathbf{A}_d(\boldsymbol{\theta}_{v,3}) + \lambda_{4,k} \mathbf{A}_d(\boldsymbol{\theta}_{v,4}) \quad (4.36)$$

The difficulty to calculate the coordinate vector increases with the number of vertices of the pLPV system. For the calculation of the coordinate vector, the method presented in Heins et al. (2012, 2012a) based on Daafouz et al. (2000) can be used. Here, this method is briefly reviewed. The following steps are then carried out for the calculation of the coordinate vector $\boldsymbol{\lambda}_k$.

1. $\theta_{i,k} = \cos(2\pi f_{i,k} T), i = 1, \dots, n_d,$
2. $c_{i_{\max},k} = \theta_{i,k} - \theta_{i,\min}, \quad c_{i_{\min},k} = \theta_{i,\max} - \theta_{i,k}, i = 1, \dots, n_d,$
3. $\lambda_{j,k} = \prod_{i=1}^{n_d} (b_{i_{\max},j} c_{i_{\max},k} + b_{i_{\min},j} c_{i_{\min},k}), j = 1, \dots, M$

with

$$\mathbf{b}_{i_{\min}} = \begin{bmatrix} b_{i_{\min},1} \\ \vdots \\ b_{i_{\min},M} \end{bmatrix}, \quad \mathbf{b}_{i_{\max}} = \begin{bmatrix} b_{i_{\max},1} \\ \vdots \\ b_{i_{\max},M} \end{bmatrix} \quad (4.38)$$

are pre-computed such that

$$b_{i_{\max},j} = \begin{cases} \frac{1}{\theta_{i,\max} - \theta_{i,\min}}, & \text{if } v_{j,i} = \theta_{i,\max}, \\ 0, & \text{if } v_{j,i} = \theta_{i,\min}, \end{cases} \quad (4.39)$$

$$b_{i_{\min},j} = \begin{cases} \frac{1}{\theta_{i,\max} - \theta_{i,\min}}, & \text{if } v_{j,i} = \theta_{i,\min}, \\ 0, & \text{if } v_{j,i} = \theta_{i,\max} \end{cases} \quad (4.40)$$

4. LPV Gain-scheduling Control for Harmonic Disturbances with Time-varying Frequencies

where $v_{j,i}$ is an element of the matrix

$$\begin{bmatrix} \boldsymbol{\theta}_{v,1} \\ \vdots \\ \boldsymbol{\theta}_{v,M} \end{bmatrix}. \quad (4.41)$$

Applying these steps to our example the following auxiliar matrices

$$b_{1\max} = \begin{bmatrix} 0 \\ 0 \\ \frac{1}{\theta_{1,\max} - \theta_{1,\min}} \\ \frac{1}{\theta_{1,\max} - \theta_{1,\min}} \end{bmatrix} = \begin{bmatrix} 0 \\ 0 \\ -17.5331 \\ -17.5331 \end{bmatrix}, \quad b_{2\max} = \begin{bmatrix} 0 \\ \frac{1}{\theta_{2,\max} - \theta_{2,\min}} \\ 0 \\ \frac{1}{\theta_{2,\max} - \theta_{2,\min}} \end{bmatrix} = \begin{bmatrix} 0 \\ -4.9219 \\ 0 \\ -4.9219 \end{bmatrix},$$

$$b_{1\min} = \begin{bmatrix} \frac{1}{\theta_{1,\max} - \theta_{1,\min}} \\ \frac{1}{\theta_{1,\max} - \theta_{1,\min}} \\ 0 \\ 0 \end{bmatrix} = \begin{bmatrix} -17.5331 \\ -17.5331 \\ 0 \\ 0 \end{bmatrix}, \quad b_{2\min} = \begin{bmatrix} \frac{1}{\theta_{2,\max} - \theta_{2,\min}} \\ 0 \\ \frac{1}{\theta_{2,\max} - \theta_{2,\min}} \\ 0 \end{bmatrix} = \begin{bmatrix} -4.9219 \\ 0 \\ -4.9219 \\ 0 \end{bmatrix} \quad (4.42)$$

are calculated. For the frequencies $f_{1,k} = 75$ Hz and $f_{2,k} = 150$ Hz the coefficients

$$c_{1\max,k} = \theta_{1,k} - \theta_{1,\min} = -0.0276, \quad c_{2\max,k} = \theta_{2,k} - \theta_{2,\min} = -0.0993 \quad (4.43)$$

$$c_{1\min,k} = \theta_{1,\max} - \theta_{1,k} = -0.0294, \quad c_{2\min,k} = \theta_{2,\max} - \theta_{2,k} = -0.1039.$$

The coordinate vector $\boldsymbol{\lambda}_k$

$$\lambda_{1,k} = (b_{1\max,1}c_{1\max,k} + b_{1\min,1}c_{1\min,k})(b_{2\max,1}c_{2\max,k} + b_{2\min,1}c_{2\min,k}) = 0.2636$$

$$\lambda_{2,k} = (b_{1\max,2}c_{1\max,k} + b_{1\min,2}c_{1\min,k})(b_{2\max,2}c_{2\max,k} + b_{2\min,2}c_{2\min,k}) = 0.2518 \quad (4.44)$$

$$\lambda_{3,k} = (b_{1\max,3}c_{1\max,k} + b_{1\min,3}c_{1\min,k})(b_{2\max,3}c_{2\max,k} + b_{2\min,3}c_{2\min,k}) = 0.2478$$

$$\lambda_{4,k} = (b_{1\max,4}c_{1\max,k} + b_{1\min,4}c_{1\min,k})(b_{2\max,4}c_{2\max,k} + b_{2\min,4}c_{2\min,k}) = 0.2368$$

is obtained as in (4.37) for the frequencies $f_{1,k} = 75$ Hz, $f_{2,k} = 150$ Hz with $f_{1,k} \in [70, 80]$ Hz and $f_{2,k} \in [140, 160]$ Hz. The pLPV disturbance model is written as

$$\begin{bmatrix} \mathbf{x}_{d,k+1} \\ \mathbf{y}_{d,k} \end{bmatrix} = \left[\begin{array}{c|c} \mathbf{A}_{d,k} & \mathbf{B}_d \\ \hline \mathbf{C}_d & \mathbf{0} \end{array} \right] \begin{bmatrix} \mathbf{x}_{d,k} \\ \mathbf{u}_{d,k} \end{bmatrix} \quad (4.45)$$

with

$$\mathbf{A}_{d,k} = \lambda_{1,k} \mathbf{A}_d(\boldsymbol{\theta}_{v,1}) + \lambda_{2,k} \mathbf{A}_d(\boldsymbol{\theta}_{v,2}) + \lambda_{3,k} \mathbf{A}_d(\boldsymbol{\theta}_{v,3}) + \lambda_{4,k} \mathbf{A}_d(\boldsymbol{\theta}_{v,4}). \quad (4.46)$$

This equation can also be written as

$$\begin{aligned} \mathbf{A}_{d,k} = & \lambda_{1,k} \begin{bmatrix} 0 & 1 & 0 & 0 \\ -r^2 & \theta_{1,\min} & 0 & 0 \\ 0 & 0 & 0 & 1 \\ 0 & 0 & -r^2 & \theta_{2,\min} \end{bmatrix} + \lambda_{2,k} \begin{bmatrix} 0 & 1 & 0 & 0 \\ -r^2 & \theta_{1,\min} & 0 & 0 \\ 0 & 0 & 0 & 1 \\ 0 & 0 & -r^2 & \theta_{2,\max} \end{bmatrix} + \\ & + \lambda_{3,k} \begin{bmatrix} 0 & 1 & 0 & 0 \\ -r^2 & \theta_{1,\max} & 0 & 0 \\ 0 & 0 & 0 & 1 \\ 0 & 0 & -r^2 & \theta_{2,\min} \end{bmatrix} + \lambda_{4,k} \begin{bmatrix} 0 & 1 & 0 & 0 \\ -r^2 & \theta_{1,\max} & 0 & 0 \\ 0 & 0 & 0 & 1 \\ 0 & 0 & -r^2 & \theta_{2,\max} \end{bmatrix} \end{aligned} \quad (4.47)$$

and it is equal to

$$\mathbf{A}_{d,k} = \begin{bmatrix} 0 & 1 & 0 & 0 \\ -r^2 & \theta_{1,k} & 0 & 0 \\ 0 & 0 & 0 & 1 \\ 0 & 0 & -r^2 & \theta_{2,k} \end{bmatrix} = \begin{bmatrix} 0 & 1 & 0 & 0 \\ -0.9998 & 1.7818 & 0 & 0 \\ 0 & 0 & 0 & 1 \\ 0 & 0 & -0.9998 & 1.1755 \end{bmatrix} \quad (4.48)$$

for the frequencies $f_{1,k} = 75$ Hz, $f_{2,k} = 150$ Hz.

The use of the polynomial approximation if the frequencies are harmonically related can reduce the complexity of the interpolation, the number of vertices and the number of gain-scheduling parameters.

The polynomial approach of the previous section is used here with the disturbance model for constant frequencies by simply doing

$$2r \cos(2\pi f_{i,k} T) \approx a_{i,0} + a_{i,2}(2\pi f_{0,k} T)^2 + a_{i,4}(2\pi f_{0,k} T)^4 \quad (4.49)$$

for $i = 1, 2$ with

$$\begin{aligned} \theta_{1,k} &= (2\pi f_{0,k} T)^2 \\ \theta_{2,k} &= (2\pi f_{0,k} T)^4 = \theta_{1,k}^2 \end{aligned} \quad (4.50)$$

where $f_{0,k} \in [70, 80]$ Hz is the fundamental frequency of the harmonic disturbance that is $[f_{1,k} \ f_{2,k}] = [f_{0,k} \ 2f_{0,k}]$. An LPV representation of the disturbance model is obtained as

$$\begin{aligned} \mathbf{A}_{d,k}^{(2n_d \times 2n_d)} = & \begin{bmatrix} 0 & 0 & 0 & 0 \\ 0 & a_{1,0} & 0 & 0 \\ 0 & 0 & 0 & 0 \\ 0 & 0 & 0 & a_{2,0} \end{bmatrix} + \begin{bmatrix} 0 & 0 & 0 & 0 \\ 0 & a_{1,2}\theta_{1,k} & 0 & 0 \\ 0 & 0 & 0 & 0 \\ 0 & 0 & 0 & a_{2,2}\theta_{1,k} \end{bmatrix} + \\ & + \begin{bmatrix} 0 & 1 & 0 & 0 \\ -r^2 & a_{1,4}\theta_{2,k} & 0 & 0 \\ 0 & 0 & 0 & 1 \\ 0 & 0 & -r^2 & a_{2,4}\theta_{2,k} \end{bmatrix} \end{aligned} \quad (4.51)$$

with

$$\begin{aligned} a_{1,0} &= 1.9998, \quad a_{1,2} = -0.9995, \quad a_{1,4} = 0.0815, \\ a_{2,0} &= 1.9979, \quad a_{2,2} = -3.9743, \quad a_{2,4} = 1.2181. \end{aligned} \quad (4.52)$$

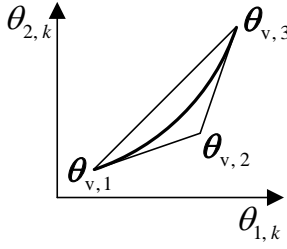


Figure 4.2: Triangle as polytope

The gain-scheduling parameters vary inside a triangle in \mathbb{R}^2 as shown in Fig. 4.2 with vertices

$$\begin{aligned}\boldsymbol{\theta}_{v,1} &= [\theta_{1,\min} \quad \theta_{1,\min}^2]^T \\ \boldsymbol{\theta}_{v,2} &= \left[\frac{\theta_{1,\min} + \theta_{1,\max}}{2} \quad \theta_{1,\min}\theta_{1,\max} \right]^T \\ \boldsymbol{\theta}_{v,3} &= [\theta_{1,\max} \quad \theta_{1,\max}^2]^T\end{aligned}\tag{4.53}$$

for

$$\begin{aligned}\theta_{1,\min} &= (2\pi f_{0,\min} T)^2 = (2\pi 70 T)^2 \\ \theta_{1,\max} &= (2\pi f_{0,\max} T)^2 = (2\pi 80 T)^2\end{aligned}\tag{4.54}$$

since the relation between the two gain-scheduling parameters $\theta_{1,k}$ and $\theta_{2,k}$ is known ($\theta_{2,k} = \theta_{1,k}^2$). A pLPV representation of the disturbance model with the polynomial approximation is obtained as

$$\begin{bmatrix} \mathbf{x}_{d,k+1} \\ \mathbf{y}_{d,k} \end{bmatrix} = \begin{bmatrix} \mathbf{A}_{d,k} & \mathbf{B}_d \\ \mathbf{C}_d & \mathbf{0} \end{bmatrix} \begin{bmatrix} \mathbf{x}_{d,k} \\ \mathbf{u}_{d,k} \end{bmatrix}\tag{4.55}$$

with

$$\mathbf{A}_{d,k}^{(2n_d \times 2n_d)} = \lambda_{1,k} \mathbf{A}_d(\boldsymbol{\theta}_{v,1}) + \lambda_{2,k} \mathbf{A}_d(\boldsymbol{\theta}_{v,2}) + \lambda_{3,k} \mathbf{A}_d(\boldsymbol{\theta}_{v,3}).\tag{4.56}$$

The calculation of the coordinate vector is fairly simple using the polynomial approximation and a triangle as polytope. From (4.29) the coordinate vector $\boldsymbol{\lambda}_k$ is calculated through

$$\begin{bmatrix} \lambda_{1,k} \\ \lambda_{2,k} \\ \lambda_{3,k} \end{bmatrix} = \begin{bmatrix} \boldsymbol{\theta}_{v,1} & \boldsymbol{\theta}_{v,2} & \boldsymbol{\theta}_{v,3} \\ 1 & 1 & 1 \end{bmatrix}^{-1} \begin{bmatrix} \theta_{1,k} \\ \theta_{2,k} \\ 1 \end{bmatrix}.\tag{4.57}$$

The matrix inverse can be calculated offline and the calculation of the coordinate vector $\boldsymbol{\lambda}_k$ at each sampling time is only the result of a matrix multiplication. For a fundamental frequency $f_{0,k} = 75$ Hz the coordinate vector

$$\boldsymbol{\lambda}_k = [\lambda_{1,k} \quad \lambda_{2,k} \quad \lambda_{3,k}] = [0.2669 \quad 0.4994 \quad 0.2336]\tag{4.58}$$

is obtained and the matrix $\mathbf{A}_{d,k}$ is written in pLPV form as in (4.56) with

$$\mathbf{A}_d(\boldsymbol{\theta}_{v,1}) = \begin{bmatrix} 0 & 0 & 0 & 0 \\ 0 & a_{1,0} & 0 & 0 \\ 0 & 0 & 0 & 0 \\ 0 & 0 & 0 & a_{2,0} \end{bmatrix} + \begin{bmatrix} 0 & 0 & 0 & 0 \\ 0 & a_{1,2}\theta_{1,\min} & 0 & 0 \\ 0 & 0 & 0 & 0 \\ 0 & 0 & 0 & a_{2,2}\theta_{1,\min} \end{bmatrix} + \quad (4.59)$$

$$+ \begin{bmatrix} 0 & 1 & 0 & 0 \\ -r^2 & a_{1,4}\theta_{1,\min}^2 & 0 & 0 \\ 0 & 0 & 0 & 1 \\ 0 & 0 & -r^2 & a_{2,4}\theta_{1,\min}^2 \end{bmatrix} = \begin{bmatrix} 0 & 1 & 0 & 0 \\ -r^2 & 1.8095 & 0 & 0 \\ 0 & 0 & 0 & 1 \\ 0 & 0 & -r^2 & 1.2747 \end{bmatrix}$$

$$\mathbf{A}_d(\boldsymbol{\theta}_{v,2}) = \begin{bmatrix} 0 & 0 & 0 & 0 \\ 0 & a_{1,0} & 0 & 0 \\ 0 & 0 & 0 & 0 \\ 0 & 0 & 0 & a_{2,0} \end{bmatrix} + \begin{bmatrix} 0 & 0 & 0 & 0 \\ 0 & a_{1,2}\theta_{v,2}^{(1)} & 0 & 0 \\ 0 & 0 & 0 & 0 \\ 0 & 0 & 0 & a_{2,2}\theta_{v,2}^{(1)} \end{bmatrix} +$$

$$+ \begin{bmatrix} 0 & 1 & 0 & 0 \\ -r^2 & a_{1,4}\theta_{1,\min}\theta_{1,\max} & 0 & 0 \\ 0 & 0 & 0 & 1 \\ 0 & 0 & -r^2 & a_{2,4}\theta_{1,\min}\theta_{1,\max} \end{bmatrix} = \begin{bmatrix} 0 & 1 & 0 & 0 \\ -r^2 & 1.7808 & 0 & 0 \\ 0 & 0 & 0 & 1 \\ 0 & 0 & -r^2 & 1.1710 \end{bmatrix} \quad (4.60)$$

$$\mathbf{A}_d(\boldsymbol{\theta}_{v,3}) = \begin{bmatrix} 0 & 0 & 0 & 0 \\ 0 & a_{1,0} & 0 & 0 \\ 0 & 0 & 0 & 0 \\ 0 & 0 & 0 & a_{2,0} \end{bmatrix} + \begin{bmatrix} 0 & 0 & 0 & 0 \\ 0 & a_{1,2}\theta_{1,\max} & 0 & 0 \\ 0 & 0 & 0 & 0 \\ 0 & 0 & 0 & a_{2,2}\theta_{1,\max} \end{bmatrix} + \quad (4.61)$$

$$+ \begin{bmatrix} 0 & 1 & 0 & 0 \\ -r^2 & a_{1,4}\theta_{1,\max}^2 & 0 & 0 \\ 0 & 0 & 0 & 1 \\ 0 & 0 & -r^2 & a_{2,4}\theta_{1,\max}^2 \end{bmatrix} = \begin{bmatrix} 0 & 1 & 0 & 0 \\ -r^2 & 1.7524 & 0 & 0 \\ 0 & 0 & 0 & 1 \\ 0 & 0 & -r^2 & 1.0715 \end{bmatrix}$$

with

$$\theta_{v,2}^{(1)} = \frac{\theta_{1,\min} + \theta_{1,\max}}{2} \quad (4.62)$$

resulting in

$$\mathbf{A}_{d,k} = \begin{bmatrix} 0 & 1 & 0 & 0 \\ -r^2 & 1.7818 & 0 & 0 \\ 0 & 0 & 0 & 1 \\ 0 & 0 & -r^2 & 1.1755 \end{bmatrix}. \quad (4.63)$$

An LPV disturbance model representation for time-varying frequencies of (4.7) needs two parameters per frequency as shown in the previous section. There are two alternatives to obtain a pLPV model. The first alternative is to use the interpolation used by Heins et al. (2012, 2012a) and Daafouz et al. (2000). This approach results in a pLPV model with 2^{2n_d} vertices, complicating significantly the calculation of the coordinate vector at each sampling time. The second alternative is to use the polynomial approximation if the frequencies are harmonically related. The use of this approach simplifies the coordinate

4. LPV Gain-scheduling Control for Harmonic Disturbances with Time-varying Frequencies

vector calculation and reduces the number of gain-scheduling parameters to two, independently of the amount of frequencies contained in the disturbance.

A disturbance model for time-varying frequencies is in the following example written in pLPV form using the polynomial approximation for a disturbance with two components of frequency $f_{1,k} \in [70, 80]$ Hz and $f_{2,k} \in [140, 160]$ Hz. The disturbance model for time-varying frequencies is given by

$$\begin{bmatrix} \mathbf{x}_{d,k+1} \\ \mathbf{y}_{d,k} \end{bmatrix} = \left[\begin{array}{c|c} \mathbf{A}_{d,k} & \mathbf{B}_d \\ \hline \mathbf{C}_d & \mathbf{0} \end{array} \right] \begin{bmatrix} \mathbf{x}_{d,k} \\ \mathbf{u}_{d,k} \end{bmatrix} \quad (4.64)$$

with

$$\mathbf{A}_{d,k} = \begin{bmatrix} r \cos(2\pi f_{1,k} T) & r \sin(2\pi f_{1,k} T) & 0 & 0 \\ -r \sin(2\pi f_{1,k} T) & r \cos(2\pi f_{1,k} T) & 0 & 0 \\ 0 & 0 & r \cos(2\pi f_{2,k} T) & r \sin(2\pi f_{2,k} T) \\ 0 & 0 & -r \sin(2\pi f_{2,k} T) & r \cos(2\pi f_{2,k} T) \end{bmatrix}. \quad (4.65)$$

The cosine and the sine function are approximated with

$$\begin{aligned} r \cos(2\pi f_{0,k} T) &\approx a_{0,1} + a_{2,1}(2\pi f_{0,k} T)^2 + a_{4,1}(2\pi f_{0,k} T)^4 \\ r \cos(2\pi 2f_{0,k} T) &\approx a_{0,2} + a_{2,2}(2\pi f_{0,k} T)^2 + a_{4,2}(2\pi f_{0,k} T)^4 \\ r \sin(2\pi f_{0,k} T) &\approx b_{0,1} + b_{2,1}(2\pi f_{0,k} T)^2 + b_{4,1}(2\pi f_{0,k} T)^4 \\ r \sin(2\pi 2f_{0,k} T) &\approx b_{0,2} + b_{2,2}(2\pi f_{0,k} T)^2 + b_{4,2}(2\pi f_{0,k} T)^4 \end{aligned} \quad (4.66)$$

obtaining the coefficients

$$\begin{bmatrix} a_{0,1} & a_{2,1} & a_{4,1} \\ a_{0,2} & a_{2,2} & a_{4,2} \end{bmatrix} = \begin{bmatrix} 0.9999 & -0.4997 & 0.0407 \\ 0.9990 & -1.9872 & 0.6090 \end{bmatrix} \quad (4.67)$$

and

$$\begin{bmatrix} b_{0,1} & b_{2,1} & b_{4,1} \\ b_{0,2} & b_{2,2} & b_{4,2} \end{bmatrix} = \begin{bmatrix} 0.1787 & 1.5324 & -1.3187 \\ 0.3723 & 2.6817 & -3.2224 \end{bmatrix}. \quad (4.68)$$

The matrix

$$\begin{aligned} \mathbf{A}_{d,k}^{(2n_d \times 2n_d)} &= \begin{bmatrix} a_{0,1} & b_{0,1} & 0 & 0 \\ -b_{0,1} & a_{0,1} & 0 & 0 \\ 0 & 0 & a_{0,2} & b_{0,2} \\ 0 & 0 & -b_{0,2} & a_{0,2} \end{bmatrix} + \begin{bmatrix} a_{2,1} & b_{2,1} & 0 & 0 \\ -b_{2,1} & a_{2,1} & 0 & 0 \\ 0 & 0 & a_{2,2} & b_{2,2} \\ 0 & 0 & -b_{2,2} & a_{2,2} \end{bmatrix} \theta_{1,k} + \\ &+ \begin{bmatrix} a_{4,1} & b_{4,1} & 0 & 0 \\ -b_{4,1} & a_{4,1} & 0 & 0 \\ 0 & 0 & a_{4,2} & b_{4,2} \\ 0 & 0 & -b_{4,2} & a_{4,2} \end{bmatrix} \theta_{2,k} \end{aligned} \quad (4.69)$$

is written in LPV form with $\theta_{1,k} = (2\pi f_{0,k} T)^2$ and $\theta_{2,k} = (2\pi f_{0,k} T)^4$. The same procedure as before is here realized since the relation between the two gain-scheduling parameters is known $\theta_{2,k} = \theta_{1,k}^2$. A triangle as polytope is used here as in (4.53) with the same vertices since the range of variation of the fundamental frequency is $f_{0,k} \in [70, 80]$ Hz.

The coordinate vector depends only on $\theta_{1,\min}$ and $\theta_{1,\max}$ and the pLPV model for time-varying frequencies can be written as

$$\begin{bmatrix} \mathbf{x}_{d,k+1} \\ \mathbf{y}_{d,k} \end{bmatrix} = \left[\begin{array}{c|c} \mathbf{A}_{d,k} & \mathbf{B}_d \\ \hline \mathbf{C}_d & \mathbf{0} \end{array} \right] \begin{bmatrix} \mathbf{x}_{d,k} \\ \mathbf{u}_{d,k} \end{bmatrix} \quad (4.70)$$

with

$$\mathbf{A}_{d,k}^{(2n_d \times 2n_d)} = \lambda_{1,k} \mathbf{A}_d(\boldsymbol{\theta}_{v,1}) + \lambda_{2,k} \mathbf{A}_d(\boldsymbol{\theta}_{v,2}) + \lambda_{3,k} \mathbf{A}_d(\boldsymbol{\theta}_{v,3}). \quad (4.71)$$

and

$$\begin{aligned} \mathbf{A}_{d,v,1}^{(2n_d \times 2n_d)} = & \begin{bmatrix} a_{0,1} & b_{0,1} & 0 & 0 \\ -b_{0,1} & a_{0,1} & 0 & 0 \\ 0 & 0 & a_{0,2} & b_{0,2} \\ 0 & 0 & -b_{0,2} & a_{0,2} \end{bmatrix} + \begin{bmatrix} a_{2,1} & b_{2,1} & 0 & 0 \\ -b_{2,1} & a_{2,1} & 0 & 0 \\ 0 & 0 & a_{2,2} & b_{2,2} \\ 0 & 0 & -b_{2,2} & a_{2,2} \end{bmatrix} \theta_{1,\min} + \\ & + \begin{bmatrix} a_{4,1} & b_{4,1} & 0 & 0 \\ -b_{4,1} & a_{4,1} & 0 & 0 \\ 0 & 0 & a_{4,2} & b_{4,2} \\ 0 & 0 & -b_{4,2} & a_{4,2} \end{bmatrix} \theta_{1,\min}^2, \end{aligned} \quad (4.72)$$

$$\begin{aligned} \mathbf{A}_{d,v,2}^{(2n_d \times 2n_d)} = & \begin{bmatrix} a_{0,1} & b_{0,1} & 0 & 0 \\ -b_{0,1} & a_{0,1} & 0 & 0 \\ 0 & 0 & a_{0,2} & b_{0,2} \\ 0 & 0 & -b_{0,2} & a_{0,2} \end{bmatrix} + \begin{bmatrix} a_{2,1} & b_{2,1} & 0 & 0 \\ -b_{2,1} & a_{2,1} & 0 & 0 \\ 0 & 0 & a_{2,2} & b_{2,2} \\ 0 & 0 & -b_{2,2} & a_{2,2} \end{bmatrix} \theta_{v,2}^{(1)} + \\ & + \begin{bmatrix} a_{4,1} & b_{4,1} & 0 & 0 \\ -b_{4,1} & a_{4,1} & 0 & 0 \\ 0 & 0 & a_{4,2} & b_{4,2} \\ 0 & 0 & -b_{4,2} & a_{4,2} \end{bmatrix} \theta_{1,\min} \theta_{1,\max}, \end{aligned} \quad (4.73)$$

$$\begin{aligned} \mathbf{A}_{d,v,3}^{(2n_d \times 2n_d)} = & \begin{bmatrix} a_{0,1} & b_{0,1} & 0 & 0 \\ -b_{0,1} & a_{0,1} & 0 & 0 \\ 0 & 0 & a_{0,2} & b_{0,2} \\ 0 & 0 & -b_{0,2} & a_{0,2} \end{bmatrix} + \begin{bmatrix} a_{2,1} & b_{2,1} & 0 & 0 \\ -b_{2,1} & a_{2,1} & 0 & 0 \\ 0 & 0 & a_{2,2} & b_{2,2} \\ 0 & 0 & -b_{2,2} & a_{2,2} \end{bmatrix} \theta_{1,\max} + \\ & + \begin{bmatrix} a_{4,1} & b_{4,1} & 0 & 0 \\ -b_{4,1} & a_{4,1} & 0 & 0 \\ 0 & 0 & a_{4,2} & b_{4,2} \\ 0 & 0 & -b_{4,2} & a_{4,2} \end{bmatrix} \theta_{1,\max}^2 \end{aligned} \quad (4.74)$$

with

$$\theta_{v,2}^{(1)} = \frac{\theta_{1,\min} + \theta_{1,\max}}{2}. \quad (4.75)$$

The coordinate vector is calculated with (4.57). For example for $f_{1,k} = 75$ Hz and $f_{2,k} = 150$ Hz the values of

$$\boldsymbol{\lambda}_k = [\lambda_{1,k} \ \lambda_{2,k} \ \lambda_{3,k}] = [0.2669 \ 0.4994 \ 0.2336] \quad (4.76)$$

are obtained. The use of the polynomial approximation reduces the number of gain-scheduling parameters to two if the frequencies are harmonically related and a triangle as polytope simplifies the calculation of the coordinate vector to a matrix multiplication.

4. LPV Gain-scheduling Control for Harmonic Disturbances with Time-varying Frequencies

Experimental results will show later the effectiveness of these models for the rejection of harmonic disturbances. Results will be shown for controllers using the model for constant frequencies without polynomial approximation and the use of the model for time-varying frequencies with the polynomial approximation.

LFT Disturbance Model

An $(n \times n)$ MIMO LPV disturbance model for constant frequencies is given as

$$\begin{bmatrix} \mathbf{x}_{d,k+1} \\ \mathbf{y}_{d,k} \end{bmatrix} = \left[\begin{array}{c|c} \mathbf{A}_d(\mathbf{a}_k) & \mathbf{B}_d \\ \hline \mathbf{C}_d & \mathbf{0} \end{array} \right] \begin{bmatrix} \mathbf{x}_{d,k} \\ \mathbf{w}_{d,k} \end{bmatrix} \quad (4.77)$$

with

$$\mathbf{A}_d(\mathbf{a}_k)^{(2n_d n \times 2n_d n)} = \begin{bmatrix} \mathbf{A}_{d_1}(\mathbf{a}_k) & \dots & \mathbf{0} \\ \vdots & \ddots & \vdots \\ \mathbf{0} & \dots & \mathbf{A}_{d_n}(\mathbf{a}_k) \end{bmatrix}, \quad (4.78)$$

$$\mathbf{A}_{d_1}(\mathbf{a}_k)^{(2n_d \times 2n_d)} = \dots = \mathbf{A}_{d_n}(\mathbf{a}_k)^{(2n_d \times 2n_d)} = \begin{bmatrix} \tilde{\mathbf{A}}_{d_1}(a_{1,k}) & \dots & \mathbf{0} \\ \vdots & \ddots & \vdots \\ \mathbf{0} & \dots & \tilde{\mathbf{A}}_{d_n}(a_{n,k}) \end{bmatrix}, \quad (4.79)$$

$$\tilde{\mathbf{A}}_{d_i}(a_{i,k})^{(2 \times 2)} = \begin{bmatrix} 0 & 1 \\ -r^2 & a_{i,k} \end{bmatrix}, \quad (4.80)$$

$$\mathbf{B}_d^{(2n_d n \times m_w)} = \begin{bmatrix} \mathbf{B}_{d_1} & \dots & \mathbf{B}_{d_n} \\ \vdots & \ddots & \vdots \\ \mathbf{B}_{d_1} & \dots & \mathbf{B}_{d_n} \end{bmatrix}, \quad \mathbf{B}_{d_1}^{(2n_d \times 1)} = \dots = \mathbf{B}_{d_n}^{(2n_d \times 1)} = \begin{bmatrix} 1 \\ 0 \\ \vdots \\ 1 \\ 0 \end{bmatrix} \quad (4.81)$$

and

$$\mathbf{C}_d^{(r_y \times 2n_d n)} = \begin{bmatrix} \mathbf{C}_{d_1} & \dots & \mathbf{0} \\ \vdots & \ddots & \vdots \\ \mathbf{0} & \dots & \mathbf{C}_{d_n} \end{bmatrix}, \quad (4.82)$$

$$\mathbf{C}_{d_1}^{(1 \times 2n_d)} = \dots = \mathbf{C}_{d_n}^{(1 \times 2n_d)} = [1 \ 0 \ \dots \ 1 \ 0]$$

with $a_{i,k} = 2r \cos(\Omega_{i,k})$, $\Omega_{i,k} = 2\pi f_{i,k} T$ for $i = 1, \dots, n_d$.

Knowing the range of variation of the frequencies $f_{i,k} \in [f_{i,\min}, f_{i,\max}]$, the parameter $a_{i,k}$ can be represented for given frequencies $f_{i,k}$ as

$$a_{i,k} = a_{0,i} + a_{1,i}\theta_{i,k} \quad (4.83)$$

with

$$\begin{aligned} a_{0,i} &= \frac{a_{\max,i} + a_{\min,i}}{2}, & a_{1,i} &= \frac{a_{\max,i} - a_{\min,i}}{2}, \\ \theta_{i,k} &= \frac{a_{i,k} - a_{0,i}}{a_{1,i}}, & \theta_{i,k} &\in [-1, 1], \end{aligned} \quad (4.84)$$

for

$$a_{\max,i} = 2r \cos(2\pi f_{\min,i} T) \text{ and } a_{\min,i} = 2r \cos(2\pi f_{\max,i} T). \quad (4.85)$$

The disturbance model is written in LFT form as

$$\begin{bmatrix} \mathbf{x}_{d,k+1} \\ \mathbf{q}_{\theta,k} \\ \mathbf{y}_{d,k} \end{bmatrix} = \left[\begin{array}{c|cc} \mathbf{A}_{d,0} & \mathbf{B}_{d,\theta} & \mathbf{B}_d \\ \mathbf{C}_{d,\theta} & \mathbf{D}_{\theta\theta} & \mathbf{D}_{\theta w} \\ \mathbf{C}_d & \mathbf{D}_{y\theta} & \mathbf{D}_{yw} \end{array} \right] \begin{bmatrix} \mathbf{x}_{d,k} \\ \mathbf{w}_{\theta,k} \\ \mathbf{w}_{d,k} \end{bmatrix} \quad (4.86)$$

with

$$\mathbf{A}_{d,0}^{(2n_d n \times 2n_d n)} = \begin{bmatrix} \mathbf{A}_{d_1}(\mathbf{a}_0) & \dots & \mathbf{0} \\ \vdots & \ddots & \vdots \\ \mathbf{0} & \dots & \mathbf{A}_{d_n}(\mathbf{a}_0) \end{bmatrix}, \quad (4.87)$$

$$\mathbf{A}_{d_1}(\mathbf{a}_0)^{(2n_d \times 2n_d)} = \dots = \mathbf{A}_{d_n}(\mathbf{a}_0)^{(2n_d \times 2n_d)} = \begin{bmatrix} \tilde{\mathbf{A}}_{d_1}(a_{0,1}) & \dots & \mathbf{0} \\ \vdots & \ddots & \vdots \\ \mathbf{0} & \dots & \tilde{\mathbf{A}}_{d_{n_d}}(a_{0,n_d}) \end{bmatrix}, \quad (4.88)$$

$$\tilde{\mathbf{A}}_{d_i}(a_{0,i})^{(2 \times 2)} = \begin{bmatrix} 0 & 1 \\ -r^2 & a_{0,i} \end{bmatrix}, \quad (4.89)$$

$$\mathbf{B}_{d,\theta}^{(2n_d n \times nm_\theta)} = \begin{bmatrix} \mathbf{B}_{d,\theta_1} & \dots & \mathbf{0} \\ \vdots & \ddots & \vdots \\ \mathbf{0} & \dots & \mathbf{B}_{d,\theta_n} \end{bmatrix}, \quad \mathbf{B}_{d,\theta_i}^{(2n_d \times m_\theta)} = \begin{bmatrix} \tilde{\mathbf{B}}_{d,\theta_1} & \dots & \mathbf{0} \\ \vdots & \ddots & \vdots \\ \mathbf{0} & \dots & \tilde{\mathbf{B}}_{d,\theta_{n_d}} \end{bmatrix}, \quad (4.90)$$

$$\tilde{\mathbf{B}}_{d,\theta_i}^{(2 \times 1)} = \begin{bmatrix} 0 \\ a_{1,i} \end{bmatrix}, \quad (4.91)$$

$$\mathbf{C}_{d,\theta}^{(nr_\theta \times 2n_d n)} = \begin{bmatrix} \mathbf{C}_{d,\theta_1} & \dots & \mathbf{0} \\ \vdots & \ddots & \vdots \\ \mathbf{0} & \dots & \mathbf{C}_{d,\theta_n} \end{bmatrix}, \quad \mathbf{C}_{d,\theta_i}^{(r_\theta \times 2n_d)} = \begin{bmatrix} \tilde{\mathbf{C}}_{d,\theta_1} & \dots & \mathbf{0} \\ \vdots & \ddots & \vdots \\ \mathbf{0} & \dots & \tilde{\mathbf{C}}_{d,\theta_{n_d}} \end{bmatrix}, \quad (4.92)$$

$$\tilde{\mathbf{C}}_{d,\theta_i}^{(1 \times 2)} = [0 \ 1], \quad (4.93)$$

$$\boldsymbol{\theta}_k^{(n_d n \times n_d n)} = \begin{bmatrix} \theta_{1,k} & \dots & \mathbf{0} \\ \vdots & \ddots & \vdots \\ \mathbf{0} & \dots & \theta_{n,k} \end{bmatrix} \quad (4.94)$$

and

$$\boldsymbol{\theta}_{1,k}^{(n_d \times n_d)} = \dots = \boldsymbol{\theta}_{n,k}^{(n_d \times n_d)} = \begin{bmatrix} \theta_{1,k} & \dots & \mathbf{0} \\ \vdots & \ddots & \vdots \\ \mathbf{0} & \dots & \theta_{n_d,k} \end{bmatrix} \quad (4.95)$$

for $m_\theta = r_\theta = n_d$.

As an example, a 2×2 MIMO ($n = 2$) harmonic disturbance with two frequencies $n_d = 2$, $f_{1,k} \in [70, 80]$ Hz and $f_{2,k} \in [140, 160]$ Hz can be modelled in LFT form as

$$\begin{bmatrix} \mathbf{x}_{d,k+1} \\ \mathbf{q}_{\theta,k} \\ \mathbf{y}_{d,k} \end{bmatrix} = \left[\begin{array}{c|cc} \mathbf{A}_{d,0} & \mathbf{B}_{d,\theta} & \mathbf{B}_d \\ \mathbf{C}_{d,\theta} & \mathbf{D}_{\theta\theta} & \mathbf{D}_{\theta w} \\ \mathbf{C}_d & \mathbf{D}_{y\theta} & \mathbf{D}_{yw} \end{array} \right] \begin{bmatrix} \mathbf{x}_{d,k} \\ \mathbf{w}_{\theta,k} \\ \mathbf{w}_{d,k} \end{bmatrix} \quad (4.96)$$

with

$$\mathbf{A}_{d,0}^{(2n_d n \times 2n_d n)} = \begin{bmatrix} \mathbf{A}_{d_1}(\mathbf{a}_0) & \mathbf{0} \\ \mathbf{0} & \mathbf{A}_{d_2}(\mathbf{a}_0) \end{bmatrix}, \quad (4.97)$$

4. LPV Gain-scheduling Control for Harmonic Disturbances with Time-varying Frequencies

$$\mathbf{A}_{d_1}(\mathbf{a}_0)^{(2n_d \times 2n_d)} = \mathbf{A}_{d_2}(\mathbf{a}_0)^{(2n_d \times 2n_d)} = \begin{bmatrix} \tilde{\mathbf{A}}_{d_1}(a_{0,1}) & \mathbf{0} \\ \mathbf{0} & \tilde{\mathbf{A}}_{d_2}(a_{0,2}) \end{bmatrix}, \quad (4.98)$$

$$\tilde{\mathbf{A}}_{d_1}(a_{0,1})^{(2 \times 2)} = \begin{bmatrix} 0 & 1 \\ -r^2 & a_{0,1} \end{bmatrix}, \quad \tilde{\mathbf{A}}_{d_2}(a_{0,2})^{(2 \times 2)} = \begin{bmatrix} 0 & 1 \\ -r^2 & a_{0,2} \end{bmatrix}, \quad (4.99)$$

$$\mathbf{B}_{d,\theta}^{(2n_dn \times nm_{\theta})} = \begin{bmatrix} \mathbf{B}_{d,\theta_1} & \mathbf{0} \\ \mathbf{0} & \mathbf{B}_{d,\theta_2} \end{bmatrix}, \quad \mathbf{B}_{d,\theta_1}^{(2n_d \times m_{\theta})} = \mathbf{B}_{d,\theta_2}^{(2n_d \times m_{\theta})} = \begin{bmatrix} \tilde{\mathbf{B}}_{d,\theta_1} & \mathbf{0} \\ \mathbf{0} & \tilde{\mathbf{B}}_{d,\theta_2} \end{bmatrix}, \quad (4.100)$$

$$\tilde{\mathbf{B}}_{d,\theta_1}^{(2 \times 1)} = \begin{bmatrix} 0 \\ a_{1,1} \end{bmatrix}, \quad \tilde{\mathbf{B}}_{d,\theta_2}^{(2 \times 1)} = \begin{bmatrix} 0 \\ a_{1,2} \end{bmatrix}, \quad (4.101)$$

$$\mathbf{B}_d^{(2n_dn \times m_{w_d})} = \begin{bmatrix} \mathbf{B}_{d_1} & \mathbf{B}_{d_2} \\ \mathbf{B}_{d_1} & \mathbf{B}_{d_2} \end{bmatrix}, \quad \mathbf{B}_{d_1}^{(2n_d \times 1)} = \mathbf{B}_{d_2}^{(2n_d \times 1)} = \begin{bmatrix} 1 \\ 0 \\ 1 \\ 0 \end{bmatrix}, \quad (4.102)$$

$$\mathbf{C}_{d,\theta}^{(nr_{\theta} \times 2n_dn)} = \begin{bmatrix} \mathbf{C}_{d,\theta_1} & \mathbf{0} \\ \mathbf{0} & \mathbf{C}_{d,\theta_2} \end{bmatrix}, \quad \mathbf{C}_{d,\theta_1}^{(r_{\theta} \times 2n_d)} = \mathbf{C}_{d,\theta_2}^{(r_{\theta} \times 2n_d)} = \begin{bmatrix} \tilde{\mathbf{C}}_{d,\theta_1} & \mathbf{0} \\ \mathbf{0} & \tilde{\mathbf{C}}_{d,\theta_2} \end{bmatrix}, \quad (4.103)$$

$$\tilde{\mathbf{C}}_{d,\theta_1}^{(1 \times 2)} = \tilde{\mathbf{C}}_{d,\theta_2}^{(1 \times 2)} = [0 \ 1], \quad (4.104)$$

$$\mathbf{C}_d^{(r_{y_d} \times 2n_dn)} = \begin{bmatrix} \mathbf{C}_{d_1} & \mathbf{0} \\ \mathbf{0} & \mathbf{C}_{d_2} \end{bmatrix}, \quad \mathbf{C}_{d_1}^{(1 \times 2n_d)} = \mathbf{C}_{d_2}^{(1 \times 2n_d)} = [1 \ 0 \ 1 \ 0], \quad (4.105)$$

$$\begin{bmatrix} \mathbf{D}_{\theta\theta} & \mathbf{D}_{\theta w} \\ \mathbf{D}_{y\theta} & \mathbf{D}_{yw} \end{bmatrix}^{((nr_{\theta} + r_{y_d}) \times (nm_{\theta} + m_{w_d}))} = \begin{bmatrix} \mathbf{0} & \mathbf{0} \\ \mathbf{0} & \mathbf{0} \end{bmatrix}, \quad (4.106)$$

$$\boldsymbol{\theta}_k^{(n_dn \times n_dn)} = \begin{bmatrix} \boldsymbol{\theta}_{1,k} & \mathbf{0} \\ \mathbf{0} & \boldsymbol{\theta}_{2,k} \end{bmatrix}, \quad (4.107)$$

$$\boldsymbol{\theta}_{1,k}^{(n_d \times n_d)} = \boldsymbol{\theta}_{2,k}^{(n_d \times n_d)} = \begin{bmatrix} \theta_{1,k} & 0 \\ 0 & \theta_{2,k} \end{bmatrix}, \quad (4.108)$$

$$[a_{0,1} \ a_{0,2}] = [1.7810 \ 1.1731] \quad (4.109)$$

and

$$[a_{1,1} \ a_{1,2}] = [-0.0285 \ -0.1016] \quad (4.110)$$

for $n = n_d = m_{\theta} = r_{\theta} = 2$.

The matrix $\mathbf{A}_d(\mathbf{a}_k)^{(2n_dn \times 2n_dn)}$ of the disturbance model is given for $f_{1,k} = 75$ Hz and $f_{2,k} = 150$ Hz as

$$\mathbf{A}_d(\mathbf{a}_k) = \mathbf{A}_{d,0} + \mathbf{B}_{d,\theta} \boldsymbol{\theta}_k \mathbf{C}_{d,\theta} \quad (4.111)$$

for

$$\boldsymbol{\theta}_k = \begin{bmatrix} \boldsymbol{\theta}_{1,k} & \mathbf{0} \\ \mathbf{0} & \boldsymbol{\theta}_{2,k} \end{bmatrix}, \quad (4.112)$$

$$\boldsymbol{\theta}_{1,k} = \boldsymbol{\theta}_{2,k} = \begin{bmatrix} \theta_{1,k} & 0 \\ 0 & \theta_{2,k} \end{bmatrix} \quad (4.113)$$

with

$$\theta_{1,k} = \frac{a_{1,k} - a_{0,1}}{a_{1,1}} = -0.0308, \quad (4.114)$$

$$\theta_{2,k} = \frac{a_{2,k} - a_{0,2}}{a_{1,2}} = -0.0228, \quad (4.115)$$

$$a_{1,k} = 2r \cos(2\pi 75 T) \text{ and } a_{2,k} = 2r \cos(2\pi 150 T). \quad (4.116)$$

pLPV Gain-scheduling Control for Harmonic Disturbances with Time-varying Frequencies

In this section, LPV gain-scheduling design techniques are applied to the LPV control structures of the previous chapter. The controllers achieved with these techniques are gain-scheduling with some functions of the disturbance frequency as gain-scheduling parameter. It is assumed that the frequency of the disturbance is known or can be measured.

Disturbance Observer Control Design

A complete representation of the pLPV disturbance observer controller was obtained in Sec. 3.2.1. In this section the vertex observer gains $\mathbf{L}_{\text{do}, v, j}$ are calculated.

For a pLPV augmented system with M vertices

$$\left[\begin{array}{c} \mathbf{x}_{\text{d}, k+1} \\ \mathbf{x}_{\text{p}, k+1} \\ \mathbf{y}_{\text{p}, k} \end{array} \right] = \left[\begin{array}{cc|c} \mathbf{A}_{\text{d}, v, j} & \mathbf{0} & \mathbf{0} \\ \mathbf{B}_{\text{p}} \mathbf{C}_{\text{d}} & \mathbf{A}_{\text{p}} & \mathbf{B}_{\text{p}} \\ \mathbf{0} & \mathbf{C}_{\text{p}} & \mathbf{0} \end{array} \right] \left[\begin{array}{c} \mathbf{x}_{\text{d}, k} \\ \mathbf{x}_{\text{p}, k} \\ \mathbf{u}_{\text{p}, k} \end{array} \right] \quad (4.117)$$

or in compact form

$$\left[\begin{array}{c} \mathbf{x}_{\text{do}, k+1} \\ \mathbf{y}_{\text{p}, k} \end{array} \right] = \left[\begin{array}{c|c} \mathbf{A}_{\text{do}, v, j} & \mathbf{B}_{\text{do}} \\ \mathbf{C}_{\text{do}} & \mathbf{0} \end{array} \right] \left[\begin{array}{c} \mathbf{x}_{\text{do}, k} \\ \mathbf{u}_{\text{p}, k} \end{array} \right] \quad (4.118)$$

with $\mathbf{A}_{\text{do}, v, j}^{((2n_{\text{d}}+n_{\text{p}}) \times (2n_{\text{d}}+n_{\text{p}}))}$, $\mathbf{B}_{\text{do}}^{((2n_{\text{d}}+n_{\text{p}}) \times m_{\text{u}_{\text{p}}})}$ and $\mathbf{C}_{\text{do}}^{(r_{\text{y}_{\text{p}}} \times (2n_{\text{d}}+n_{\text{p}}))}$, M vertex observer gains are calculated solving the LMIs for the positive definite matrix $\mathbf{X}^{((2n_{\text{d}}+n_{\text{p}}) \times (2n_{\text{d}}+n_{\text{p}}))}$, $\mathbf{Z}^{((r_{\text{y}_{\text{p}}}+2n_{\text{d}}+n_{\text{p}}) \times (r_{\text{y}_{\text{p}}}+2n_{\text{d}}+n_{\text{p}}))}$ and for the matrix $\mathbf{Y}_{v, j}^{(r_{\text{y}_{\text{p}}} \times (2n_{\text{d}}+n_{\text{p}}))}$ (see A.4)

$$\left[\begin{array}{cc} \mathbf{X} & \mathbf{X} \mathbf{A}_{\text{do}, v, j} - \mathbf{Y}_{v, j}^{\text{T}} \mathbf{C}_{\mathbf{y}} \\ (\mathbf{X} \mathbf{A}_{\text{do}, v, j} - \mathbf{Y}_{v, j}^{\text{T}} \mathbf{C}_{\mathbf{y}})^{\text{T}} & \mathbf{X} - \mathbf{C}_{\mathbf{q}}^{\text{T}} \mathbf{C}_{\mathbf{q}} \end{array} \right] > 0, \quad (4.119)$$

$$\left[\begin{array}{cc} \mathbf{Z} & \mathbf{B}_{\mathbf{w}} \mathbf{X} - \mathbf{D}_{\mathbf{y}_{\mathbf{w}}} \mathbf{Y}_{v, j} \\ (\mathbf{B}_{\mathbf{w}} \mathbf{X} - \mathbf{D}_{\mathbf{y}_{\mathbf{w}}} \mathbf{Y}_{v, j})^{\text{T}} & \mathbf{X} \end{array} \right] > 0, \quad (4.120)$$

$$\text{trace}(\mathbf{Z}) < \gamma^2 \quad (4.121)$$

for $j = 1, \dots, M$ with

$$\mathbf{B}_{\mathbf{w}}^{((r_{\text{y}_{\text{p}}}+2n_{\text{d}}+n_{\text{p}}) \times (2n_{\text{d}}+n_{\text{p}}))} = \left[\begin{array}{c} \mathbf{Q}^{\frac{1}{2}} \\ \mathbf{0} \end{array} \right], \quad \mathbf{D}_{\mathbf{y}_{\mathbf{w}}}^{((r_{\text{y}_{\text{p}}}+2n_{\text{d}}+n_{\text{p}}) \times r_{\text{y}_{\text{p}}})} = \left[\begin{array}{c} \mathbf{0} \\ \mathbf{R}^{\frac{1}{2}} \end{array} \right], \quad (4.122)$$

$$\mathbf{C}_{\mathbf{y}}^{(r_{\text{y}_{\text{p}}} \times (2n_{\text{d}}+n_{\text{p}}))} = \mathbf{C}_{\text{do}},$$

$$\mathbf{C}_{\mathbf{q}}^{((2n_{\text{d}}+n_{\text{p}}) \times (2n_{\text{d}}+n_{\text{p}}))} = \mathbf{I}, \quad \mathbf{Q}^{((2n_{\text{d}}+n_{\text{p}}) \times (2n_{\text{d}}+n_{\text{p}}))} \text{ and } \mathbf{R}^{(r_{\text{y}_{\text{p}}} \times r_{\text{y}_{\text{p}}})}.$$

Finally, the vertex observer gains are calculated through

$$\mathbf{L}_{\text{do}, v, j}^{((2n_{\text{d}}+n_{\text{p}}) \times r_{\text{y}_{\text{p}}})} = \mathbf{X}^{-1} \mathbf{Y}_{v, j}^{\text{T}}. \quad (4.123)$$

The matrices of the pLPV disturbance observer controller are written then as

$$\left[\begin{array}{c|c} \mathbf{A}_{\text{doc}}(\boldsymbol{\theta}_k) & \mathbf{B}_{\text{doc}}(\boldsymbol{\theta}_k) \\ \mathbf{C}_{\text{doc}} & \mathbf{0} \end{array} \right] = \sum_{j=1}^M \lambda_{j, k} \left[\begin{array}{c|c} \mathbf{A}_{\text{do}, v, j} & \mathbf{B}_{\text{do}, v, j} \\ \mathbf{C}_{\text{do}} & \mathbf{0} \end{array} \right] \quad (4.124)$$

4. LPV Gain-scheduling Control for Harmonic Disturbances with Time-varying Frequencies

with

$$\begin{aligned} \mathbf{A}_{\text{doc}, v, j}^{((2n_d+n_p) \times (2n_d+n_p))} &= \mathbf{A}_{\text{do}, v, j} - \mathbf{L}_{v, j} \mathbf{C}_{\text{do}} - \mathbf{B}_{\text{do}} \mathbf{K}_{\text{do}}, \\ \mathbf{B}_{\text{doc}, v, j}^{((2n_d+n_p) \times r_{y_p})} &= \mathbf{L}_{\text{do}, v, j}, \\ \mathbf{C}_{\text{doc}}^{(m_{u_p} \times (2n_d+n_p))} &= \mathbf{K}_{\text{do}} \end{aligned} \quad (4.125)$$

and the coordinate vector $\lambda_{j, k}$ calculated fulfilling

$$\left[\begin{array}{ccc} \boldsymbol{\theta}_{v, 1} & \dots & \boldsymbol{\theta}_{v, M} \\ 1 & \dots & 1 \end{array} \right] \left[\begin{array}{c} \lambda_{1, k} \\ \vdots \\ \lambda_{M, k} \end{array} \right] = \left[\begin{array}{c} \theta_{1, k} \\ \vdots \\ \theta_{n_d, k} \\ 1 \end{array} \right] \quad \text{with } \lambda_{j, k} \geq 0 \text{ for } j = 1, \dots, M. \quad (4.126)$$

The vector $\boldsymbol{\theta}_k = [\theta_{1, k} \dots \theta_{n_d, k}]$ is obtained using the frequencies measured from the disturbance and it is used to calculate the coordinate vector. The pLPV controller is written as

$$\left[\begin{array}{c} \mathbf{x}_{\text{doc}, k+1} \\ \mathbf{u}_{p, k} \end{array} \right] = \sum_{j=1}^M \lambda_{j, k} \left[\begin{array}{c|c} \mathbf{A}_{\text{doc}, v, j} & \mathbf{B}_{\text{doc}, v, j} \\ \hline \mathbf{C}_{\text{doc}} & \mathbf{0} \end{array} \right] \left[\begin{array}{c} \mathbf{x}_{\text{doc}, k} \\ \mathbf{y}_{p, k} \end{array} \right] \quad (4.127)$$

depending on the coordinate vector $\boldsymbol{\lambda}_k$ calculated at each sampling time.

As an example, a controller is calculated for the rejection of a harmonic disturbance with two harmonically related frequencies ($n_d = 2$) acting at the output of the plant

$$\left[\begin{array}{c} x_{p, k+1} \\ y_{p, k} \end{array} \right] = \left[\begin{array}{c|c} a & 1 \\ \hline (1-a) & 0 \end{array} \right] \left[\begin{array}{c} x_{p, k} \\ u_{p, k} \end{array} \right] \quad (4.128)$$

for $T = 0.001$ s, $a = 0.1$ and $[f_{1, k} \ f_{2, k}] = f_{0, k}[1 \ 2]$ with $f_{0, k} \in [40, 50]$ Hz. Since in this example the frequencies of the disturbance are harmonically related, the polynomial approximation of (4.11) is used to obtain an LPV representation of the disturbance using the model for time-varying frequencies (4.7) as

$$\begin{aligned} \mathbf{A}_{d, k}^{(2n_d \times 2n_d)} &= \left[\begin{array}{cccc} a_{0, 1} & b_{0, 1} & 0 & 0 \\ -b_{0, 1} & a_{0, 1} & 0 & 0 \\ 0 & 0 & a_{0, 2} & b_{0, 2} \\ 0 & 0 & -b_{0, 2} & a_{0, 2} \end{array} \right] + \left[\begin{array}{cccc} a_{2, 1} & b_{2, 1} & 0 & 0 \\ -b_{2, 1} & a_{2, 1} & 0 & 0 \\ 0 & 0 & a_{2, 2} & b_{2, 2} \\ 0 & 0 & -b_{2, 2} & a_{2, 2} \end{array} \right] \theta_{1, k} + \\ &+ \left[\begin{array}{cccc} a_{4, 1} & b_{4, 1} & 0 & 0 \\ -b_{4, 1} & a_{4, 1} & 0 & 0 \\ 0 & 0 & a_{4, 2} & b_{4, 2} \\ 0 & 0 & -b_{4, 2} & a_{4, 2} \end{array} \right] \theta_{2, k} \end{aligned} \quad (4.129)$$

with

$$a_{0, 1} = 0.9999, \ a_{2, 1} = -0.4999, \ a_{4, 1} = 0.0413 \quad (4.130)$$

$$a_{0, 2} = 0.9999, \ a_{2, 2} = -1.9981, \ a_{4, 2} = 0.6453$$

and

$$b_{0, 1} = 0.1060, \ b_{2, 1} = 2.6214, \ b_{4, 1} = -5.7339 \quad (4.131)$$

$$b_{0, 2} = 0.2150, \ b_{2, 2} = 5.0239, \ b_{4, 2} = -12.6601$$

for $r = 0.9999$, $\theta_{1,k} = (2\pi f_{0,k}T)^2$ and $\theta_{2,k} = (2\pi f_{0,k}T)^4$. A triangle as polytope is used in the same way as (4.53) with the vertices

$$\boldsymbol{\theta}_{v,1} = [\theta_{1,\min} \quad \theta_{1,\min}^2]^T = [0.0632 \quad 0.0040]^T$$

$$\boldsymbol{\theta}_{v,2} = \left[\frac{\theta_{1,\min} + \theta_{1,\max}}{2} \quad \theta_{1,\min}\theta_{1,\max} \right]^T = [0.0809 \quad 0.0062]^T \quad (4.132)$$

$$\boldsymbol{\theta}_{v,3} = [\theta_{1,\max} \quad \theta_{1,\max}^2]^T = [0.0987 \quad 0.0097]^T$$

for

$$\theta_{1,\min} = (2\pi f_{0,\min}T)^2 = (2\pi 40 T)^2, \quad (4.133)$$

$$\theta_{1,\max} = (2\pi f_{0,\max}T)^2 = (2\pi 50 T)^2$$

resulting in a pLPV representation of the disturbance

$$\begin{bmatrix} \mathbf{x}_{d,k+1} \\ y_{d,k} \end{bmatrix} = \sum_{j=1}^3 \lambda_{j,k} \begin{bmatrix} \mathbf{A}_{d,v,j} & \mathbf{0} \\ \mathbf{C}_d & 0 \end{bmatrix} \begin{bmatrix} \mathbf{x}_{d,k} \\ w_{d,k} \end{bmatrix} \quad (4.134)$$

with

$$\begin{aligned} \mathbf{A}_{d,v,1}^{(2n_d \times 2n_d)} &= \begin{bmatrix} 0.9685 & 0.2487 & 0 & 0 \\ -0.2487 & 0.9685 & 0 & 0 \\ 0 & 0 & 0.8762 & 0.4819 \\ 0 & 0 & -0.4819 & 0.8762 \end{bmatrix}, \\ \mathbf{A}_{d,v,2}^{(2n_d \times 2n_d)} &= \begin{bmatrix} 0.9597 & 0.2824 & 0 & 0 \\ -0.2824 & 0.9597 & 0 & 0 \\ 0 & 0 & 0.8422 & 0.5427 \\ 0 & 0 & -0.5427 & 0.8422 \end{bmatrix}, \\ \mathbf{A}_{d,v,3}^{(2n_d \times 2n_d)} &= \begin{bmatrix} 0.9510 & 0.3089 & 0 & 0 \\ -0.3089 & 0.9510 & 0 & 0 \\ 0 & 0 & 0.8089 & 0.5876 \\ 0 & 0 & -0.5876 & 0.8089 \end{bmatrix} \end{aligned} \quad (4.135)$$

and the coordinate vector calculated through

$$\begin{bmatrix} \lambda_{1,k} \\ \lambda_{2,k} \\ \lambda_{3,k} \end{bmatrix} = \begin{bmatrix} \boldsymbol{\theta}_{v,1} & \boldsymbol{\theta}_{v,2} & \boldsymbol{\theta}_{v,3} \\ 1 & 1 & 1 \end{bmatrix}^{-1} \begin{bmatrix} \theta_{1,k} \\ \theta_{2,k} \\ 1 \end{bmatrix}. \quad (4.136)$$

A pLPV augmented system is built

$$\begin{bmatrix} \mathbf{x}_{do,k+1} \\ y_{p,k} \end{bmatrix} = \sum_{j=1}^3 \lambda_{j,k} \begin{bmatrix} \mathbf{A}_{do,v,j} & \mathbf{B}_{do} \\ \mathbf{C}_{do} & 0 \end{bmatrix} \begin{bmatrix} \mathbf{x}_{do,k} \\ u_{p,k} \end{bmatrix} \quad (4.137)$$

with

$$\begin{aligned} \mathbf{A}_{do,v,j}^{((2n_d+n_p) \times (2n_d+n_p))} &= \begin{bmatrix} \mathbf{A}_{d,v,j} & \mathbf{0} \\ B_p \mathbf{C}_d & A_p \end{bmatrix}, \quad \mathbf{B}_{do}^{((2n_d+n_p) \times m_{u_p})} = \begin{bmatrix} \mathbf{0} \\ B_p \end{bmatrix}, \\ \mathbf{C}_{do}^{(r_{y_p} \times (2n_d+n_p))} &= [\mathbf{0} \quad C_p] \end{aligned} \quad (4.138)$$

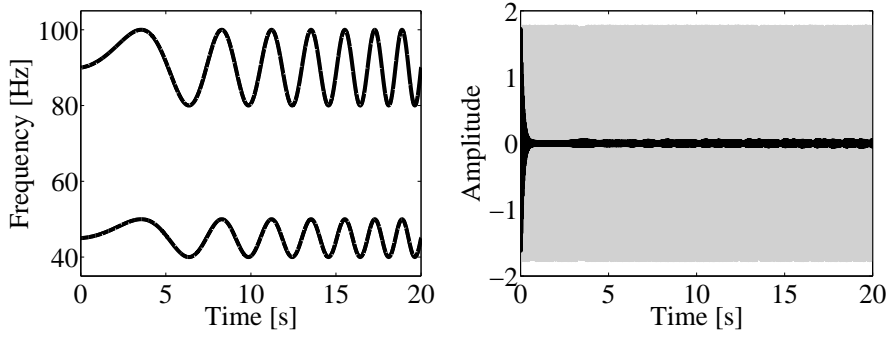


Figure 4.3: Variations of the disturbance frequencies (left) and simulation results (right) in closed loop (black) and open loop (gray)

for $j = 1, \dots, 3$, $A_p^{(n_p \times n_p)} = a$, $B_p^{(n_p \times m_{u_p})} = 1$, $C_p^{(r_{y_p} \times n_p)} = (1 - a)$, $n_p = m_{u_p} = r_{y_p} = 1$, $n_d = 2$ combining the pLPV disturbance model and the LTI plant.

Finally, three vertex observer gains

$$\begin{aligned} \mathbf{L}_{\text{do}, v, 1}^{((2n_d+n_p) \times r_{y_p})} &= \mathbf{X}^{-1} \mathbf{Y}_{v, 1}^T = [0.0115 \quad -0.0076 \quad 0.0065 \quad -0.0162 \quad 0.0131]^T \\ \mathbf{L}_{\text{do}, v, 2}^{((2n_d+n_p) \times r_{y_p})} &= \mathbf{X}^{-1} \mathbf{Y}_{v, 2}^T = [0.0115 \quad -0.0077 \quad 0.0070 \quad -0.0168 \quad 0.0307]^T \quad (4.139) \\ \mathbf{L}_{\text{do}, v, 3}^{((2n_d+n_p) \times r_{y_p})} &= \mathbf{X}^{-1} \mathbf{Y}_{v, 3}^T = [0.0118 \quad -0.0079 \quad 0.0068 \quad -0.0165 \quad 0.0338]^T \end{aligned}$$

are calculated solving the LMIs of (4.119)-(4.121) for \mathbf{X} , \mathbf{Z} and $\mathbf{Y}_{v, j}$ for all the vertices of the pLPV augmented system with

$$\mathbf{Q}^{((2n_d+n_p) \times (2n_d+n_p))} = \begin{bmatrix} \mathbf{I} & \mathbf{0} \\ \mathbf{0} & 0 \end{bmatrix} \quad \text{and} \quad R^{(r_{y_p} \times r_{y_p})} = 10^4. \quad (4.140)$$

These values of \mathbf{Q} and \mathbf{R} achieved the desired performance of the closed loop system. The controller is written in pLPV form as

$$\begin{bmatrix} \mathbf{x}_{\text{doc}, k+1} \\ u_{p, k} \end{bmatrix} = \sum_{j=1}^M \lambda_{j, k} \begin{bmatrix} \mathbf{A}_{\text{doc}, v, j} & \mathbf{B}_{\text{doc}, v, j} \\ \mathbf{C}_{\text{doc}} & 0 \end{bmatrix} \begin{bmatrix} \mathbf{x}_{\text{doc}, k} \\ y_{p, k} \end{bmatrix} \quad (4.141)$$

with

$$\mathbf{A}_{\text{doc}, v, j}^{((2n_d+n_p) \times (2n_d+n_p))} = \mathbf{A}_{\text{do}, v, j} - \mathbf{L}_{\text{do}, v, j} \mathbf{C}_{\text{do}} - \mathbf{B}_{\text{do}} \mathbf{K}_{\text{do}},$$

$$\mathbf{B}_{\text{doc}, v, j}^{((2n_d+n_p) \times r_{y_p})} = \mathbf{L}_{\text{do}, v, j}, \quad (4.142)$$

$$\mathbf{C}_{\text{doc}}^{(m_{u_p} \times (2n_d+n_p))} = \mathbf{K}_{\text{do}} = [\mathbf{C}_d \quad 0] = [1 \quad 0 \quad 1 \quad 0 \quad 0]$$

and the coordinate vector $\boldsymbol{\lambda}_k$ calculated from (4.136).

Simulation results for the system in closed loop and open loop are shown in Fig. 4.3 for a disturbance acting at the output of the plant with time-varying disturbance frequencies. The stability is guaranteed since pLPV control design techniques and independent Lyapunov functions are used.

Error Filter Control Design

This control structure is a state-feedback gain of plant and disturbance model combined with an observer to estimate the states of the plant. A state-space representation for all the M vertices of the augmented system is given with

$$\left[\begin{array}{c} \mathbf{x}_{d,k+1} \\ \mathbf{x}_{p,k+1} \\ \mathbf{y}_{p,k} \end{array} \right] = \left[\begin{array}{cc|c} \mathbf{A}_{d,v,j} & -\mathbf{B}_d \mathbf{C}_p & \mathbf{0} \\ \mathbf{0} & \mathbf{A}_p & \mathbf{B}_p \\ \hline \mathbf{0} & \mathbf{C}_p & \mathbf{0} \end{array} \right] \left[\begin{array}{c} \mathbf{x}_{d,k} \\ \mathbf{x}_{p,k} \\ \mathbf{u}_{p,k} \end{array} \right] \quad (4.143)$$

or in compact form as

$$\left[\begin{array}{c} \mathbf{x}_{ef,k+1} \\ \mathbf{y}_{p,k} \end{array} \right] = \left[\begin{array}{c|c} \mathbf{A}_{ef,v,j} & \mathbf{B}_{ef} \\ \mathbf{C}_{ef} & \mathbf{0} \end{array} \right] \left[\begin{array}{c} \mathbf{x}_{ef,k} \\ \mathbf{u}_{p,k} \end{array} \right] \quad (4.144)$$

with $\mathbf{A}_{ef,v,j}^{((2n_d+n_p) \times (2n_d+n_p))}$, $\mathbf{B}_{ef}^{((2n_d+n_p) \times m_{u_p})}$ and $\mathbf{C}_{ef}^{(r_{y_p} \times (2n_d+n_p))}$.

The state-feedback gains $\mathbf{K}_{ef,v,j}^{(m_{u_p} \times (2n_d+n_p))}$ are calculated solving the LMIs

$$\left[\begin{array}{cc} \mathbf{P} & (\mathbf{A}_{ef,v,j} \mathbf{P} - \mathbf{B}_u \mathbf{Y}_{v,j})^T \\ \mathbf{A}_{ef,v,j} \mathbf{P} - \mathbf{B}_u \mathbf{Y}_{v,j} & \mathbf{P} - \mathbf{B}_w \mathbf{B}_w^T \end{array} \right] > 0, \quad (4.145)$$

$$\left[\begin{array}{cc} \mathbf{W} & \mathbf{C}_q \mathbf{P} - \mathbf{D}_{qu} \mathbf{Y}_{v,j} \\ (\mathbf{C}_q \mathbf{P} - \mathbf{D}_{qu} \mathbf{Y}_{v,j})^T & \mathbf{P} \end{array} \right] > 0, \quad (4.146)$$

$$\text{trace}(\mathbf{W}) < \gamma^2 \quad (4.147)$$

for the positive definite matrices $\mathbf{P}^{((2n_d+n_p) \times (2n_d+n_p))}$, $\mathbf{W}^{((m_{u_p}+2n_d+n_p) \times (m_{u_p}+2n_d+n_p))}$ and for the matrix $\mathbf{Y}_{v,j}^{(m_{u_p} \times (2n_d+n_p))}$ with

$$\begin{aligned} \mathbf{C}_q^{((m_{u_p}+2n_d+n_p) \times (2n_d+n_p))} &= \left[\begin{array}{c} \mathbf{Q}^{\frac{1}{2}} \\ \mathbf{0} \end{array} \right], \quad \mathbf{D}_{qu}^{((m_{u_p}+2n_d+n_p) \times m_{u_p})} = \left[\begin{array}{c} \mathbf{0} \\ \mathbf{R}^{\frac{1}{2}} \end{array} \right], \\ \mathbf{B}_u^{((2n_d+n_p) \times m_{u_p})} &= \mathbf{B}_{ef}, \quad \mathbf{B}_w^{((2n_d+n_p) \times (2n_d+n_p))} = \mathbf{I}, \end{aligned} \quad (4.148)$$

$$\mathbf{Q}^{((2n_d+n_p) \times (2n_d+n_p))} \quad \text{and} \quad \mathbf{R}^{(m_{u_p} \times m_{u_p})}.$$

The state-feedback gains are calculated through

$$\mathbf{K}_{ef,v,j}^{(m_{u_p} \times (2n_d+n_p))} = \mathbf{Y}_{v,j} \mathbf{P}^{-1} \quad (4.149)$$

for $j = 1, \dots, M$.

The error filter controller matrices are written in pLPV form as

$$\left[\begin{array}{c|c} \mathbf{A}_{efc}(\boldsymbol{\theta}_k) & \mathbf{B}_{efc} \\ \hline \mathbf{C}_{efc}(\boldsymbol{\theta}_k) & \mathbf{0} \end{array} \right] = \sum_{j=1}^M \lambda_{j,k} \left[\begin{array}{c|c} \mathbf{A}_{efc,v,j} & \mathbf{B}_{efc} \\ \hline \mathbf{C}_{efc,v,j} & \mathbf{0} \end{array} \right] \quad (4.150)$$

with

$$\begin{aligned} \mathbf{A}_{efc,v,j}^{((2n_d+n_p) \times (2n_d+n_p))} &= \left[\begin{array}{cc} \mathbf{A}_{d,v,j} & \mathbf{0} \\ -\mathbf{B}_p \mathbf{K}_{d,v,j} & \mathbf{A}_p - \mathbf{B}_p \mathbf{K}_{p,v,j} - \mathbf{L}_p \mathbf{C}_p \end{array} \right], \\ \mathbf{B}_{efc}^{((2n_d+n_p) \times r_{y_p})} &= \left[\begin{array}{c} \mathbf{B}_d \\ \mathbf{L}_p \end{array} \right], \end{aligned} \quad (4.151)$$

$$\mathbf{C}_{efc,v,j}^{(m_{u_p} \times (2n_d+n_p))} = -\mathbf{K}_{ef,v,j} = \left[\begin{array}{cc} -\mathbf{K}_{d,v,j} & -\mathbf{K}_{p,v,j} \end{array} \right]$$

4. LPV Gain-scheduling Control for Harmonic Disturbances with Time-varying Frequencies

for $j = 1, \dots, M$.

The coordinate vector $\lambda_{j,k}$ is calculated at each sampling time using the conditions of (4.126) using the parameter vector θ_k .

The pLPV error filter controller representation is obtained as

$$\begin{bmatrix} \mathbf{x}_{\text{efc},k+1} \\ \mathbf{u}_{\text{p},k} \end{bmatrix} = \sum_{j=1}^M \lambda_{j,k} \left[\begin{array}{c|c} \mathbf{A}_{\text{efc},v,j} & \mathbf{B}_{\text{efc}} \\ \mathbf{C}_{\text{efc},v,j} & \mathbf{0} \end{array} \right] \begin{bmatrix} \mathbf{x}_{\text{efc},k} \\ \mathbf{e}_k \end{bmatrix}. \quad (4.152)$$

A controller is calculated as an example with this control design for the rejection of a harmonic disturbance with two harmonically related frequencies ($n_d = 2$) acting at the output of the plant

$$\begin{bmatrix} x_{\text{p},k+1} \\ y_{\text{p},k} \end{bmatrix} = \left[\begin{array}{c|c} a & 1 \\ (1-a) & 0 \end{array} \right] \begin{bmatrix} x_{\text{p},k} \\ u_{\text{p},k} \end{bmatrix} \quad (4.153)$$

for $T = 0.001$ s, $a = 0.1$, $A_p^{(n_p \times n_p)} = a$, $B_p^{(n_p \times m_{u_p})} = 1$, $C_p^{(r_{y_p} \times n_p)} = (1-a)$ and $[f_{1,k} \ f_{2,k}] = f_{0,k}[1 \ 2]$ with $f_{0,k} \in [40, 50]$ Hz. The frequencies are harmonically related and therefore the polynomial approximation is used to obtain an LPV disturbance model. Since the number of frequencies and the range of variation of these frequencies is the same as in the previous section the same LPV disturbance model of (4.129) is used. A triangle as polytope is used to reduce the number of vertices to three.

The pLPV augmented system

$$\begin{bmatrix} \mathbf{x}_{\text{d},k+1} \\ \frac{x_{\text{p},k+1}}{y_{\text{p},k}} \end{bmatrix} = \sum_{j=1}^3 \lambda_{j,k} \left[\begin{array}{c|c} \mathbf{A}_{\text{d},v,j} & -\mathbf{B}_{\text{d}} C_{\text{p}} \\ \mathbf{0} & A_{\text{p}} \\ \hline \mathbf{0} & C_{\text{p}} \end{array} \right] \begin{bmatrix} \mathbf{x}_{\text{d},k} \\ \frac{x_{\text{p},k}}{u_{\text{p},k}} \end{bmatrix} \quad (4.154)$$

or

$$\begin{bmatrix} \mathbf{x}_{\text{ef},k+1} \\ y_{\text{p},k} \end{bmatrix} = \sum_{j=1}^3 \lambda_{j,k} \left[\begin{array}{c|c} \mathbf{A}_{\text{ef},v,j} & \mathbf{B}_{\text{ef}} \\ \mathbf{C}_{\text{ef}} & \mathbf{0} \end{array} \right] \begin{bmatrix} \mathbf{x}_{\text{ef},k} \\ u_{\text{p},k} \end{bmatrix} \quad (4.155)$$

is built with the same vertices (4.132) and coordinate vector (4.136) combining pLPV disturbance model and plant with

$$\mathbf{A}_{\text{ef},v,1}^{((2n_d+n_p) \times (2n_d+n_p))} = \begin{bmatrix} 0.9685 & 0.2487 & 0 & 0 & 0 \\ -0.2487 & 0.9685 & 0 & 0 & -0.9 \\ 0 & 0 & 0.8762 & 0.4819 & 0 \\ 0 & 0 & -0.4819 & 0.8762 & -0.9 \\ 0 & 0 & 0 & 0 & 0.1 \end{bmatrix}, \quad (4.156)$$

$$\mathbf{A}_{\text{ef},v,2}^{((2n_d+n_p) \times (2n_d+n_p))} = \begin{bmatrix} 0.9597 & 0.2824 & 0 & 0 & 0 \\ -0.2824 & 0.9597 & 0 & 0 & -0.9 \\ 0 & 0 & 0.8422 & 0.5427 & 0 \\ 0 & 0 & -0.5427 & 0.8422 & -0.9 \\ 0 & 0 & 0 & 0 & 0.1 \end{bmatrix} \quad (4.157)$$

and

$$\mathbf{A}_{\text{ef},v,3}^{((2n_d+n_p) \times (2n_d+n_p))} = \begin{bmatrix} 0.9510 & 0.3089 & 0 & 0 & 0 \\ -0.3089 & 0.9510 & 0 & 0 & -0.9 \\ 0 & 0 & 0.8089 & 0.5876 & 0 \\ 0 & 0 & -0.5876 & 0.8089 & -0.9 \\ 0 & 0 & 0 & 0 & 0.1 \end{bmatrix}. \quad (4.158)$$

Three state-feedback gains are calculated solving the LMIs of (4.145)-(4.147) for the three vertex obtaining

$$\begin{aligned} \mathbf{K}_{\text{ef}, v, 1}^{(m_{u_p} \times (2n_d + n_p))} &= \mathbf{Y}_{v, 1} \mathbf{P}^{-1} = \left[\begin{array}{cc} \mathbf{K}_{d, v, 1} & K_{p, v, 1} \end{array} \right] \\ \mathbf{K}_{\text{ef}, v, 1} &= \left[\begin{array}{ccccc} 0.0235 & -0.0340 & 0.0383 & -0.0207 & 0.0700 \end{array} \right], \end{aligned} \quad (4.159)$$

$$\begin{aligned} \mathbf{K}_{\text{ef}, v, 2}^{(m_{u_p} \times (2n_d + n_p))} &= \mathbf{Y}_{v, 2} \mathbf{P}^{-1} = \left[\begin{array}{cc} \mathbf{K}_{d, v, 2} & K_{p, v, 2} \end{array} \right] \\ \mathbf{K}_{\text{ef}, v, 2} &= \left[\begin{array}{ccccc} 0.0238 & -0.0342 & 0.0391 & -0.0204 & 0.0748 \end{array} \right] \end{aligned} \quad (4.160)$$

and

$$\begin{aligned} \mathbf{K}_{\text{ef}, v, 3}^{(m_{u_p} \times (2n_d + n_p))} &= \mathbf{Y}_{v, 3} \mathbf{P}^{-1} = \left[\begin{array}{cc} \mathbf{K}_{d, v, 3} & K_{p, v, 3} \end{array} \right] \\ \mathbf{K}_{\text{ef}, v, 3} &= \left[\begin{array}{ccccc} 0.0242 & -0.0349 & 0.0394 & -0.0204 & 0.0824 \end{array} \right] \end{aligned} \quad (4.161)$$

with

$$\mathbf{Q}^{((2n_d + n_p) \times (2n_d + n_p))} = \left[\begin{array}{ccccc} 1 & 0 & 0 & 0 & 0 \\ 0 & 1 & 0 & 0 & 0 \\ 0 & 0 & 1 & 0 & 0 \\ 0 & 0 & 0 & 1 & 0 \\ 0 & 0 & 0 & 0 & 0.82 \end{array} \right] \quad \text{and} \quad \mathbf{R}^{(m_{u_p} \times m_{u_p})} = 1000 \quad (4.162)$$

and the observer gain of the plant

$$L_p^{(n_p \times r_{y_p})} = 0.1098 \quad (4.163)$$

obtained solving the LMIs of A.4 for $Q = 100$ and $R = 1$. The dimension of the matrices are given with $n_p = m_{u_p} = r_{y_p} = 1$ and $n_d = 2$.

The controller is then written in pLPV form as

$$\left[\begin{array}{c} \mathbf{x}_{\text{efc}, k+1} \\ u_{p, k} \end{array} \right] = \sum_{j=1}^3 \lambda_{j, k} \left[\begin{array}{c|c} \mathbf{A}_{\text{efc}, v, j} & \mathbf{B}_{\text{efc}} \\ \hline \mathbf{C}_{\text{efc}, v, j} & 0 \end{array} \right] \left[\begin{array}{c} \mathbf{x}_{\text{efc}, k} \\ e_k \end{array} \right] \quad (4.164)$$

with

$$\mathbf{A}_{\text{efc}, v, j}^{((2n_d + n_p) \times (2n_d + n_p))} = \left[\begin{array}{cc} \mathbf{A}_{d, v, j} & \mathbf{0} \\ -B_p \mathbf{K}_{d, v, j} & A_p - B_p K_{p, v, j} - L_p C_p \end{array} \right], \quad (4.165)$$

$$\mathbf{C}_{\text{efc}, v, j}^{(m_{u_p} \times (2n_d + n_p))} = -\mathbf{K}_{\text{efc}, v, j} = \left[\begin{array}{cc} -\mathbf{K}_{d, v, j} & -K_{p, v, j} \end{array} \right] \quad (4.166)$$

4. LPV Gain-scheduling Control for Harmonic Disturbances with Time-varying Frequencies

for $j = 1, \dots, 3$

$$\begin{aligned} \mathbf{A}_{\text{efc}, v, 1}^{((2n_d+n_p) \times (2n_d+n_p))} &= \begin{bmatrix} 0.9685 & 0.2487 & 0 & 0 & 0 \\ -0.2487 & 0.9685 & 0 & 0 & 0 \\ 0 & 0 & 0.8762 & 0.4819 & 0 \\ 0 & 0 & -0.4819 & 0.8762 & 0 \\ -0.0235 & 0.0340 & -0.0383 & 0.0207 & -0.0688 \end{bmatrix}, \\ \mathbf{A}_{\text{efc}, v, 2}^{((2n_d+n_p) \times (2n_d+n_p))} &= \begin{bmatrix} 0.9597 & 0.2824 & 0 & 0 & 0 \\ -0.2824 & 0.9597 & 0 & 0 & 0 \\ 0 & 0 & 0.8422 & 0.5427 & 0 \\ 0 & 0 & -0.5427 & 0.8422 & 0 \\ -0.0238 & 0.0342 & -0.0391 & 0.0204 & -0.0736 \end{bmatrix}, \\ \mathbf{A}_{\text{efc}, v, 3}^{((2n_d+n_p) \times (2n_d+n_p))} &= \begin{bmatrix} 0.9510 & 0.3089 & 0 & 0 & 0 \\ -0.3089 & 0.9510 & 0 & 0 & 0 \\ 0 & 0 & 0.8089 & 0.5876 & 0 \\ 0 & 0 & -0.5876 & 0.8089 & 0 \\ -0.0242 & 0.0349 & -0.0394 & 0.0204 & -0.0812 \end{bmatrix}, \end{aligned} \quad (4.167)$$

$$\mathbf{B}_{\text{efc}}^{((2n_d+n_p) \times r_{y_p})} = \begin{bmatrix} \mathbf{B}_d \\ L_p \end{bmatrix} = \begin{bmatrix} 0 \\ 1 \\ 0 \\ 1 \\ 0.1098 \end{bmatrix}, \quad (4.168)$$

$$\begin{aligned} \mathbf{C}_{\text{efc}, v, 1}^{(m_{u_p} \times (2n_d+n_p))} &= -\mathbf{K}_{\text{ef}, v, 1} = \begin{bmatrix} -\mathbf{K}_{d, v, 1} & -K_{p, v, 1} \end{bmatrix} = \\ &= \begin{bmatrix} -0.0235 & 0.0340 & -0.0383 & 0.0207 & -0.0700 \end{bmatrix}, \end{aligned} \quad (4.169)$$

$$\begin{aligned} \mathbf{C}_{\text{efc}, v, 2}^{(m_{u_p} \times (2n_d+n_p))} &= -\mathbf{K}_{\text{ef}, v, 2} = \begin{bmatrix} -\mathbf{K}_{d, v, 2} & -K_{p, v, 2} \end{bmatrix} = \\ &= \begin{bmatrix} -0.0238 & 0.0342 & -0.0391 & 0.0204 & -0.0748 \end{bmatrix}, \end{aligned} \quad (4.170)$$

and

$$\begin{aligned} \mathbf{C}_{\text{efc}, v, 3}^{(m_{u_p} \times (2n_d+n_p))} &= -\mathbf{K}_{\text{ef}, v, 3} = \begin{bmatrix} -\mathbf{K}_{d, v, 3} & -K_{p, v, 3} \end{bmatrix} = \\ &= \begin{bmatrix} -0.0242 & 0.0349 & -0.0394 & 0.0204 & -0.0824 \end{bmatrix}. \end{aligned} \quad (4.171)$$

Simulation results are shown in closed loop and open loop for a disturbance acting with time-varying frequencies acting at the ouput of the plant in Fig. 4.4.

Output Feedback Control Design

In this section pLPV design techniques are applied to obtain a pLPV gain-scheduling controller with the frequency of the disturbance as gain-scheduling parameter. The generalized plant with disturbance model, plant and weighting functions for a polytopic system with M vertices is written as

$$\begin{bmatrix} \mathbf{x}_{k+1} \\ \mathbf{q}_k \\ \mathbf{y}_{p, k} \end{bmatrix} = \begin{bmatrix} \mathbf{A}_{v, j} & \mathbf{B}_w & \mathbf{B}_u \\ \mathbf{C}_q & \mathbf{D}_{qw} & \mathbf{D}_{qu} \\ \mathbf{C}_y & \mathbf{D}_{yw} & \mathbf{D}_{yu} \end{bmatrix} \begin{bmatrix} \mathbf{x}_k \\ \mathbf{w}_k \\ \mathbf{u}_{p, k} \end{bmatrix} \quad (4.172)$$

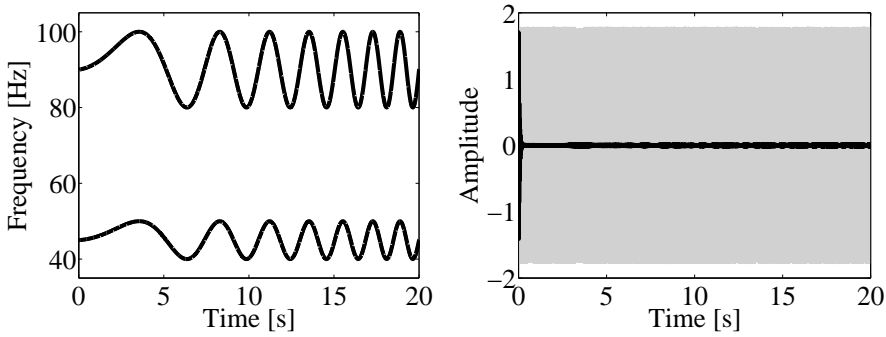


Figure 4.4: Variations of the disturbance frequencies (left) and simulation results (right) in closed loop (black) and open loop (gray)

with

$$\boldsymbol{x}_k = \begin{bmatrix} \boldsymbol{x}_{p,k} \\ \boldsymbol{x}_{d,k} \\ \boldsymbol{x}_{W_u,k} \\ \boldsymbol{x}_{W_y,k} \end{bmatrix}, \quad (4.173)$$

$$\boldsymbol{A}_{v,j}^{((n_p+2n_d+n_{W_u}+n_{W_y})) \times (n_p+2n_d+n_{W_u}+n_{W_y})} = \begin{bmatrix} \boldsymbol{A}_p & \boldsymbol{B}_p \boldsymbol{C}_d & \boldsymbol{0} & \boldsymbol{0} \\ \boldsymbol{0} & \boldsymbol{A}_{d,v,j} & \boldsymbol{0} & \boldsymbol{0} \\ \boldsymbol{0} & \boldsymbol{0} & \boldsymbol{A}_{W_u} & \boldsymbol{0} \\ \boldsymbol{B}_{W_y} \boldsymbol{C}_p & \boldsymbol{0} & \boldsymbol{0} & \boldsymbol{A}_{W_y} \end{bmatrix}, \quad (4.174)$$

$$[\boldsymbol{B}_w \quad \boldsymbol{B}_u]^{((n_p+2n_d+n_{W_u}+n_{W_y})) \times (m_w+m_u)} = \begin{bmatrix} \boldsymbol{0} & \boldsymbol{B}_p \\ \boldsymbol{B}_d & \boldsymbol{0} \\ \boldsymbol{0} & \boldsymbol{B}_{W_u} \\ \boldsymbol{0} & \boldsymbol{0} \end{bmatrix}, \quad (4.175)$$

$$\begin{bmatrix} \boldsymbol{C}_q \\ \boldsymbol{C}_y \end{bmatrix}^{((r_{qu}+r_{qy}+r_y)) \times (n_p+2n_d+n_{W_u}+n_{W_y})} = \begin{bmatrix} \boldsymbol{0} & \boldsymbol{0} & \boldsymbol{C}_{W_u} & \boldsymbol{0} \\ \boldsymbol{D}_{W_y} \boldsymbol{C}_p & \boldsymbol{0} & \boldsymbol{0} & \boldsymbol{C}_{W_y} \\ \hline \boldsymbol{C}_p & \boldsymbol{0} & \boldsymbol{0} & \boldsymbol{0} \end{bmatrix} \quad (4.176)$$

and

$$\begin{bmatrix} \boldsymbol{D}_{qw} & \boldsymbol{D}_{qu} \\ \boldsymbol{D}_{yw} & \boldsymbol{D}_{yu} \end{bmatrix}^{((r_{qu}+r_{qy}+r_y)) \times (m_w+m_u)} = \begin{bmatrix} \boldsymbol{0} & \boldsymbol{D}_{W_u} \\ \boldsymbol{0} & \boldsymbol{0} \\ \hline \boldsymbol{0} & \boldsymbol{0} \end{bmatrix} \quad (4.177)$$

for $j = 1, \dots, M$.

Then, the LMIs

$$\begin{aligned} \begin{bmatrix} \boldsymbol{N}_X & \boldsymbol{0} \\ \boldsymbol{0} & \mathbf{I} \end{bmatrix}^T \begin{bmatrix} \boldsymbol{A}_{v,j}^T \boldsymbol{X}_1 \boldsymbol{A}_{v,j} - \boldsymbol{X}_1 & \boldsymbol{A}_{v,j}^T \boldsymbol{X}_1 \boldsymbol{B}_w & \boldsymbol{C}_q^T \\ \boldsymbol{B}_w^T \boldsymbol{X}_1 \boldsymbol{A}_{v,j} & -\gamma \mathbf{I} + \boldsymbol{B}_w^T \boldsymbol{X}_1 \boldsymbol{B}_w & \boldsymbol{D}_{qu}^T \\ \boldsymbol{C}_q & \boldsymbol{D}_{qu} & -\gamma \mathbf{I} \end{bmatrix} \begin{bmatrix} \boldsymbol{N}_X & \boldsymbol{0} \\ \boldsymbol{0} & \mathbf{I} \end{bmatrix} &< 0, \\ \begin{bmatrix} \boldsymbol{N}_Y & \boldsymbol{0} \\ \boldsymbol{0} & \mathbf{I} \end{bmatrix}^T \begin{bmatrix} \boldsymbol{A}_{v,j} \boldsymbol{Y}_1 \boldsymbol{A}_{v,j}^T - \boldsymbol{Y}_1 & \boldsymbol{A}_{v,j} \boldsymbol{Y}_1 \boldsymbol{C}_q^T & \boldsymbol{B}_w \\ \boldsymbol{C}_q \boldsymbol{Y}_1 \boldsymbol{A}_{v,j}^T & -\gamma \mathbf{I} + \boldsymbol{C}_q \boldsymbol{Y}_1 \boldsymbol{C}_q^T & \boldsymbol{D}_{qu} \\ \boldsymbol{B}_w^T & \boldsymbol{D}_{qu}^T & -\gamma \mathbf{I} \end{bmatrix} \begin{bmatrix} \boldsymbol{N}_Y & \boldsymbol{0} \\ \boldsymbol{0} & \mathbf{I} \end{bmatrix} &< 0, \\ \begin{bmatrix} \boldsymbol{X}_1 & \mathbf{I} \\ \mathbf{I} & \boldsymbol{Y}_1 \end{bmatrix} &\geq 0 \end{aligned} \quad (4.178)$$

4. LPV Gain-scheduling Control for Harmonic Disturbances with Time-varying Frequencies

for feasibility and optimality are solved for $\mathbf{X}_1^{(n \times n)}$ and $\mathbf{Y}_1^{(n \times n)}$, for every $\mathbf{A}_{v,j}$. The dimension $n = n_p + 2n_d + n_{W_u} + n_{W_y}$ is used for the system matrix of the generalized plant and $r_q = r_{qu} + r_{qy}$ for the performance outputs.

With \mathbf{X}_1 and \mathbf{Y}_1 , the matrix

$$\mathbf{X}^{(2n \times 2n)} = \begin{bmatrix} \mathbf{X}_1 & \mathbf{X}_2 \\ \mathbf{X}_2^T & \mathbf{I} \end{bmatrix} \quad (4.179)$$

is built and $\mathbf{X}_2^{(n \times n)}$ is calculated through

$$\mathbf{X}_2 = (\mathbf{X}_1 - \mathbf{Y}_1^{-1})^{\frac{1}{2}}. \quad (4.180)$$

Let

$$\bar{\mathbf{A}}_{v,j}^{(2n \times 2n)} = \begin{bmatrix} \mathbf{A}_{v,j} & \mathbf{0} \\ \mathbf{0} & \mathbf{0} \end{bmatrix}, \bar{\mathbf{B}}^{(2n \times m_w)} = \begin{bmatrix} \mathbf{B}_w \\ \mathbf{0} \end{bmatrix}, \bar{\mathbf{C}}^{(r_q \times 2n)} = [\mathbf{C}_q \quad \mathbf{0}] \quad (4.181)$$

and \mathbf{X} define the auxiliar matrix

$$\psi_{v,j}^{((4n+m_w+r_q) \times (4n+m_w+r_q))} = \begin{bmatrix} -\mathbf{X}^{-1} & \bar{\mathbf{A}}_{v,j} & \bar{\mathbf{B}} & \mathbf{0} \\ \bar{\mathbf{A}}_{v,j}^T & -\mathbf{X} & \mathbf{0} & \bar{\mathbf{C}}^T \\ \bar{\mathbf{B}}^T & \mathbf{0} & -\gamma \mathbf{I} & \mathbf{D}_{qw}^T \\ \mathbf{0} & \bar{\mathbf{C}} & \mathbf{D}_{qw} & -\gamma \mathbf{I} \end{bmatrix}. \quad (4.182)$$

Build

$$\begin{aligned} \mathbf{P}^{((n+m_u) \times (4n+m_w+r_q))} &= [\underline{\mathbf{B}}^T \quad \mathbf{0} \quad \mathbf{0} \quad \underline{\mathbf{D}}_{qu}^T] \\ \mathbf{Q}^{((r_y+n) \times (4n+m_w+r_q))} &= [\mathbf{0} \quad \underline{\mathbf{C}} \quad \underline{\mathbf{D}}_{yw} \quad \mathbf{0}] \end{aligned} \quad (4.183)$$

with the following matrices

$$\begin{aligned} \underline{\mathbf{B}}^{(2n \times (n+m_u))} &= \begin{bmatrix} \mathbf{0} & \mathbf{B}_u \\ \mathbf{I} & \mathbf{0} \end{bmatrix}, \underline{\mathbf{C}}^{((n+r_y) \times 2n)} = \begin{bmatrix} \mathbf{0} & \mathbf{I} \\ \mathbf{C}_y & \mathbf{0} \end{bmatrix}, \\ \underline{\mathbf{D}}_{qu}^{(r_q \times (n+m_u))} &= [\mathbf{0} \quad \mathbf{D}_{qu}] \text{ and } \underline{\mathbf{D}}_{yw}^{((n+r_y) \times m_w)} = \begin{bmatrix} \mathbf{0} \\ \mathbf{D}_{yw} \end{bmatrix}. \end{aligned} \quad (4.184)$$

Finally, the basic LMIs

$$\psi_{v,j} + \mathbf{P}^T \Omega_{v,j}^T \mathbf{Q} + \mathbf{Q}^T \Omega_{v,j} \mathbf{P} < 0 \quad (4.185)$$

are solved for $\Omega_{v,j}^{((n+m_u) \times (n+r_y))}$ with the matrices $\psi_{v,j}$, \mathbf{P} and \mathbf{Q} . The M controller matrices are extracted from $\Omega_{v,j}$ with

$$\Omega_{v,j} = \left[\begin{array}{c|c} \mathbf{A}_{of,v,j} & \mathbf{B}_{of,v,j} \\ \hline \mathbf{C}_{of,v,j} & \mathbf{D}_{of,v,j} \end{array} \right] \quad (4.186)$$

and a pLPV state-space representation of the controller is written as

$$\begin{bmatrix} \mathbf{x}_{of,k+1} \\ \mathbf{u}_{p,k} \end{bmatrix} = \sum_{j=1}^M \lambda_{j,k} \left[\begin{array}{c|c} \mathbf{A}_{of,v,j} & \mathbf{B}_{of,v,j} \\ \hline \mathbf{C}_{of,v,j} & \mathbf{D}_{of,v,j} \end{array} \right] \begin{bmatrix} \mathbf{x}_{of,k} \\ \mathbf{y}_{p,k} \end{bmatrix} \quad (4.187)$$

with the coordinate vector calculated from (4.126).

A pLPV output-feedback controller for the rejection of a harmonic disturbance with two frequency components $[f_{1,k} \ f_{2,k}] = f_{0,k}[1 \ 2]$, $n_d = 2$ and $f_{0,k} \in [45, 50]$ Hz acting at the ouput of the plant

$$\left[\begin{array}{c} x_{p,k+1} \\ y_{p,k} \end{array} \right] = \left[\begin{array}{c|c} a & 1 \\ \hline 1-a & 0 \end{array} \right] \left[\begin{array}{c} x_{p,k} \\ u_{p,k} \end{array} \right] \quad (4.188)$$

with $a = 0.1$, $A_p^{(n_p \times n_p)} = a$, $B_p^{(n_p \times m_{u_p})} = 1$, $C_p^{(r_{y_p} \times n_p)} = (1-a)$, $n_p = m_{u_p} = r_{y_p} = 1$ and $T = 0.001$ s is calculated here to illustrate this control design.

The same procedure is here realized as in the previous sections to obtain a pLPV representation of the disturbance. The frequencies contained in the disturbance are harmonically related and then the polynomial approximation is used to reduce the number of scheduling parameters. The LPV disturbance model is approximated as

$$\begin{aligned} A_{d,k}^{(2n_d \times 2n_d)} &= \left[\begin{array}{cccc} a_{0,1} & b_{0,1} & 0 & 0 \\ -b_{0,1} & a_{0,1} & 0 & 0 \\ 0 & 0 & a_{0,2} & b_{0,2} \\ 0 & 0 & -b_{0,2} & a_{0,2} \end{array} \right] + \left[\begin{array}{cccc} a_{2,1} & b_{2,1} & 0 & 0 \\ -b_{2,1} & a_{2,1} & 0 & 0 \\ 0 & 0 & a_{2,2} & b_{2,2} \\ 0 & 0 & -b_{2,2} & a_{2,2} \end{array} \right] \theta_{1,k} + \\ &+ \left[\begin{array}{cccc} a_{4,1} & b_{4,1} & 0 & 0 \\ -b_{4,1} & a_{4,1} & 0 & 0 \\ 0 & 0 & a_{4,2} & b_{4,2} \\ 0 & 0 & -b_{4,2} & a_{4,2} \end{array} \right] \theta_{2,k} \end{aligned} \quad (4.189)$$

with

$$\left[\begin{array}{ccc} a_{0,1} & a_{2,1} & a_{4,1} \\ a_{0,2} & a_{2,2} & a_{4,2} \end{array} \right] = \left[\begin{array}{ccc} 0.9980 & -0.4990 & 0.0412 \\ 0.9979 & -1.9939 & 0.6419 \end{array} \right] \quad (4.190)$$

and

$$\left[\begin{array}{ccc} b_{0,1} & b_{2,1} & b_{4,1} \\ b_{0,2} & b_{2,2} & b_{4,2} \end{array} \right] = \left[\begin{array}{ccc} 0.1121 & 2.4714 & -4.8947 \\ 0.2278 & 4.7115 & -10.9058 \end{array} \right] \quad (4.191)$$

for $r = 0.998$, $\theta_{1,k} = (2\pi f_{0,k} T)^2$ and $\theta_{2,k} = (2\pi f_{0,k} T)^4$.

A triangle is used as polytope to reduce the number of vertices. A pLPV representation of the disturbance is obtained as

$$\left[\begin{array}{c} x_{d,k+1} \\ y_{d,k} \end{array} \right] = \sum_{j=1}^3 \lambda_{j,k} \left[\begin{array}{c|c} A_{d,v,j} & B_d \\ \hline C_d & 0 \end{array} \right] \left[\begin{array}{c} x_{d,k} \\ w_{d,k} \end{array} \right] \quad (4.192)$$

4. LPV Gain-scheduling Control for Harmonic Disturbances with Time-varying Frequencies

with

$$\begin{aligned}
\mathbf{A}_{d,v,1}^{(2n_d \times 2n_d)} &= \begin{bmatrix} 0.9584 & 0.2784 & 0 & 0 \\ -0.2784 & 0.9584 & 0 & 0 \\ 0 & 0 & 0.8426 & 0.5348 \\ 0 & 0 & -0.5348 & 0.8426 \end{bmatrix}, \\
\mathbf{A}_{d,v,2}^{(2n_d \times 2n_d)} &= \begin{bmatrix} 0.9538 & 0.2943 & 0 & 0 \\ -0.2943 & 0.9538 & 0 & 0 \\ 0 & 0 & 0.8249 & 0.5626 \\ 0 & 0 & -0.5626 & 0.8249 \end{bmatrix}, \\
\mathbf{A}_{d,v,3}^{(2n_d \times 2n_d)} &= \begin{bmatrix} 0.9492 & 0.3084 & 0 & 0 \\ -0.3084 & 0.9492 & 0 & 0 \\ 0 & 0 & 0.8074 & 0.5866 \\ 0 & 0 & -0.5866 & 0.8074 \end{bmatrix}, \\
\mathbf{B}_d^{(2n_d \times m_{w_d})} &= 10^{-3} \begin{bmatrix} 1 \\ 1 \\ 1 \\ 1 \end{bmatrix}, \quad \mathbf{C}_d^{(r_{y_d} \times 2n_d)} = [1 \ 0 \ 1 \ 0]
\end{aligned} \tag{4.193}$$

for the vertices

$$\begin{aligned}
\boldsymbol{\theta}_{v,1} &= [\theta_{1,\min} \ \theta_{1,\max}^2]^T = [0.0799 \ 0.0064]^T \\
\boldsymbol{\theta}_{v,2} &= \left[\frac{\theta_{1,\min} + \theta_{1,\max}}{2} \ \theta_{1,\min}\theta_{1,\max} \right]^T = [0.0893 \ 0.0079]^T \\
\boldsymbol{\theta}_{v,3} &= [\theta_{1,\max} \ \theta_{1,\max}^2]^T = [0.0987 \ 0.0097]^T
\end{aligned} \tag{4.194}$$

with $\theta_{1,\min} = (2\pi f_{0,\min} T)^2 = 0.0799$, $\theta_{1,\max} = (2\pi f_{0,\max} T)^2 = 0.0987$, $n_d = 2$, $m_{w_d} = r_{y_d} = 1$ and the coordinate vector $\boldsymbol{\lambda}_k$ calculated through

$$\begin{bmatrix} \lambda_{1,k} \\ \lambda_{2,k} \\ \lambda_{3,k} \end{bmatrix} = \begin{bmatrix} \boldsymbol{\theta}_{v,1} & \boldsymbol{\theta}_{v,2} & \boldsymbol{\theta}_{v,3} \\ 1 & 1 & 1 \end{bmatrix}^{-1} \begin{bmatrix} \theta_{1,k} \\ \theta_{2,k} \\ 1 \end{bmatrix}. \tag{4.195}$$

Before applying the control design explained in this section to calculate the output-feedback controller, the weighting functions

$$\begin{bmatrix} x_{W_u,k+1} \\ q_{u,k} \end{bmatrix} = \begin{bmatrix} A_{W_u} & B_{W_u} \\ C_{W_u} & D_{W_u} \end{bmatrix} \begin{bmatrix} x_{W_u,k} \\ u_{p,k} \end{bmatrix} = \begin{bmatrix} 0 & 0 \\ 0 & 0.01 \end{bmatrix} \begin{bmatrix} x_{W_u,k} \\ u_{p,k} \end{bmatrix} \tag{4.196}$$

with $A_{W_u}^{(n_{W_u} \times n_{W_u})}$, $B_{W_u}^{(n_{W_u} \times m_u)}$, $C_{W_u}^{(r_{q_u} \times n_{W_u})}$, $D_{W_u}^{(r_{q_u} \times m_u)}$, $n_{W_u} = 0$, $m_u = r_{q_u} = 1$ for the control input $u_{p,k}$ and

$$\begin{bmatrix} x_{W_y,k+1} \\ q_{y,k} \end{bmatrix} = \begin{bmatrix} A_{W_y} & B_{W_y} \\ C_{W_y} & D_{W_y} \end{bmatrix} \begin{bmatrix} x_{W_y,k} \\ y_{p,k} \end{bmatrix} = \begin{bmatrix} 0 & 0 \\ 0 & 1 \end{bmatrix} \begin{bmatrix} x_{W_y,k} \\ y_{p,k} \end{bmatrix} \tag{4.197}$$

for the plant output $y_{p,k}$ are chosen to build the generalized plant

$$\begin{bmatrix} \mathbf{x}_{k+1} \\ \mathbf{q}_k \\ y_{p,k} \end{bmatrix} = \begin{bmatrix} \mathbf{A}_{v,j} & \mathbf{B}_w & \mathbf{B}_u \\ \mathbf{C}_q & \mathbf{D}_{qw} & \mathbf{D}_{qu} \\ \mathbf{C}_y & \mathbf{D}_{yw} & \mathbf{D}_{yu} \end{bmatrix} \begin{bmatrix} \mathbf{x}_k \\ \mathbf{w}_k \\ u_{p,k} \end{bmatrix} \tag{4.198}$$

with

$$\mathbf{x}_k = \begin{bmatrix} x_{p,k} \\ x_{d,k} \end{bmatrix}, \quad \mathbf{A}_{v,j}^{((n_p+2n_d) \times (n_p+2n_d))} = \begin{bmatrix} A_p & B_p C_d \\ \mathbf{0} & \mathbf{A}_{d,v,j} \end{bmatrix}, \quad (4.199)$$

$$[\mathbf{B}_w \quad \mathbf{B}_u]^{((n_p+2n_d) \times (m_w+m_u))} = \begin{bmatrix} 0 & B_p \\ \mathbf{B}_d & \mathbf{0} \end{bmatrix}, \quad (4.200)$$

$$\begin{bmatrix} \mathbf{C}_q \\ \mathbf{C}_y \end{bmatrix}^{((r_{qu}+r_{qy}+r_y) \times (n_p+2n_d))} = \begin{bmatrix} 0 & \mathbf{0} \\ \frac{D_{W_y} C_p}{C_p} & \mathbf{0} \end{bmatrix} \quad (4.201)$$

and

$$\begin{bmatrix} \mathbf{D}_{qw} & \mathbf{D}_{qu} \\ D_{yw} & D_{yu} \end{bmatrix}^{((r_{qu}+r_{qy}+r_y) \times (m_w+m_u))} = \begin{bmatrix} 0 & D_{W_u} \\ 0 & 0 \\ \hline 0 & 0 \end{bmatrix} \quad (4.202)$$

for $j = 1, \dots, 3$. The control design explained in this section (4.178)-(4.187) is applied to the generalized plant to obtain three vertex controllers. A polytopic representation of the output-feedback controller is written as

$$\begin{bmatrix} \mathbf{x}_{of,k+1} \\ u_{p,k} \end{bmatrix} = \sum_{j=1}^3 \lambda_{j,k} \begin{bmatrix} \mathbf{A}_{of,v,j} & \mathbf{B}_{of,v,j} \\ \mathbf{C}_{of,v,j} & D_{of,v,j} \end{bmatrix} \begin{bmatrix} \mathbf{x}_{of,k} \\ y_{p,k} \end{bmatrix} \quad (4.203)$$

with

$$\begin{aligned} \mathbf{A}_{of,v,1}^{((n_p+2n_d) \times (n_p+2n_d))} &= \begin{bmatrix} -0.5864 & -0.5386 & -0.0660 & -0.5006 & -0.2040 \\ 0.4642 & 1.2119 & 0.2825 & 0.2997 & 0.0652 \\ -0.1405 & -0.3506 & 0.8653 & -0.0598 & -0.0593 \\ 0.4477 & 0.2784 & 0.0082 & 1.0810 & 0.5602 \\ -0.2208 & -0.1697 & -0.0604 & -0.6469 & 0.7149 \end{bmatrix}, \\ \mathbf{B}_{of,v,1}^{((n_p+2n_d) \times r_y)} &= \begin{bmatrix} -20.3266 \\ -24.1712 \\ 12.8255 \\ -8.7139 \\ 32.2004 \end{bmatrix}, \quad \mathbf{C}_{of,v,1}^{(m_u \times (n_p+2n_d))} = \begin{bmatrix} 0.0051 \\ 0.0079 \\ 0.0006 \\ 0.0076 \\ 0.0024 \end{bmatrix}^T, \\ D_{of,v,1}^{(m_u \times r_y)} &= -0.2944, \end{aligned} \quad (4.204)$$

$$\begin{aligned} \mathbf{A}_{\text{of}, v, 2}^{((n_p+2n_d) \times (n_p+2n_d))} &= \begin{bmatrix} -0.6010 & -0.5460 & -0.0711 & -0.5034 & -0.2142 \\ 0.4540 & 1.2116 & 0.2993 & 0.3055 & 0.0705 \\ -0.1417 & -0.3686 & 0.8553 & -0.0616 & -0.0627 \\ 0.4389 & 0.2830 & 0.0095 & 1.0659 & 0.5888 \\ -0.2157 & -0.1760 & -0.0646 & -0.6757 & 0.6901 \end{bmatrix}, \\ \mathbf{B}_{\text{of}, v, 2}^{((n_p+2n_d) \times r_y)} &= \begin{bmatrix} -21.8338 \\ -25.5352 \\ 13.6657 \\ -8.6885 \\ 34.3218 \end{bmatrix}, \quad \mathbf{C}_{\text{of}, v, 2}^{(m_u \times (n_p+2n_d))} = \begin{bmatrix} 0.0050 \\ 0.0079 \\ 0.0006 \\ 0.0075 \\ 0.0024 \end{bmatrix}^T, \\ D_{\text{of}, v, 2}^{(m_u \times r_y)} &= -0.3016 \end{aligned} \quad (4.205)$$

and

$$\begin{aligned} \mathbf{A}_{\text{of}, v, 3}^{((n_p+2n_d) \times (n_p+2n_d))} &= \begin{bmatrix} -2.3084 & -1.0534 & -0.0482 & -1.0157 & -0.2479 \\ 0.8855 & 1.3411 & 0.3072 & 0.4432 & 0.0821 \\ -0.1078 & -0.3744 & 0.8453 & -0.0528 & -0.0654 \\ 0.8824 & 0.4203 & 0.0034 & 1.1866 & 0.6200 \\ -0.2438 & -0.1917 & -0.0680 & -0.7103 & 0.6658 \end{bmatrix}, \\ \mathbf{B}_{\text{of}, v, 3}^{((n_p+2n_d) \times r_y)} &= \begin{bmatrix} -183.1849 \\ 14.8782 \\ 17.7157 \\ 34.0517 \\ 33.0778 \end{bmatrix}, \quad \mathbf{C}_{\text{of}, v, 3}^{(m_u \times (n_p+2n_d))} = \begin{bmatrix} 0.0185 \\ 0.0119 \\ 0.0004 \\ 0.0116 \\ 0.0026 \end{bmatrix}^T, \\ D_{\text{of}, v, 3}^{(m_u \times r_y)} &= 0.9757 \end{aligned} \quad (4.206)$$

with the coordinate vector calculated with (4.195). Results for the pLPV controller are shown for time-varying frequencies in Fig.4.5 in open loop and closed loop. All LPV the techniques presented in this thesis guarantee the stability in closed loop since Lyapunov independent functions are used in the control design.

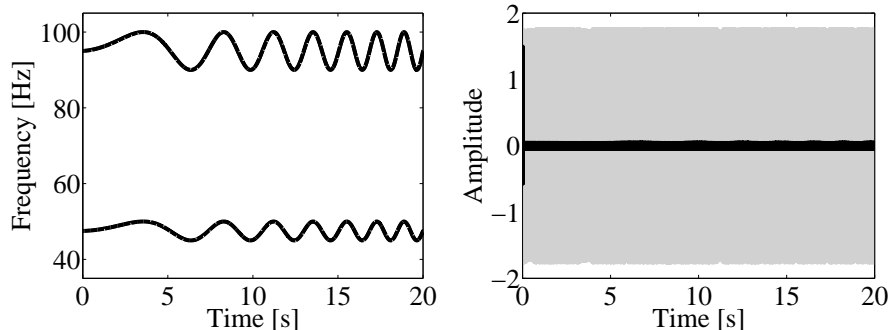


Figure 4.5: Variations of the disturbance frequencies (left) and simulation results (right) in closed loop (black) and open loop (gray)

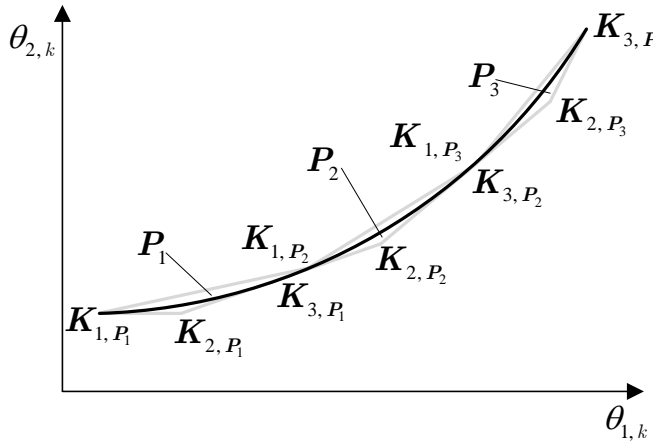


Figure 4.6: Triangle division to switch between controllers

Switching Control Strategy

All the pLPV controllers presented in this section are able to reject harmonic disturbances with time-varying frequencies for a given range of frequencies or in case where the frequencies are harmonically related for a given range of the fundamental frequency. The main objective of this section is to augment the range of actuation through a switching control strategy between controllers guaranteeing the stability at the same time. This control strategy can be applied for a general pLPV system where the variations of a parameter are enclosed in a triangle, or where a triangle is used as polytope. Therefore here the polynomial approximation is used to model the harmonic disturbance (4.11) and a triangle is used as polytope (see Fig. 4.2).

For a given range of frequencies, three controllers are calculated for each vertex of the system. The range of actuation can be augmented here combining pLPV controllers. As an approach, three triangles can be used as polytopes placed consecutively as shown in Fig. 4.6. The controllers $\mathbf{K}_{1,P_1}^{((n_K+m_u)\times(n_K+r_y))}$, $\mathbf{K}_{2,P_1}^{((n_K+m_u)\times(n_K+r_y))}$ and $\mathbf{K}_{3,P_1}^{((n_K+m_u)\times(n_K+r_y))}$ are calculated for the first triangle using one of the pLPV control designs explained in this section. For the next triangle one controller is fixed as $\mathbf{K}_{1,P_2} = \mathbf{K}_{3,P_1}$ and two new controllers \mathbf{K}_{2,P_2} and \mathbf{K}_{3,P_2} are calculated solving the LMIs from one of the pLPV control designs. The same procedure is carried out for further triangles.

This approach uses the same controller at each union point of the triangles. This switching strategy guarantees the stability if the parameters vary continuously. The stability is not guaranteed if the parameters vary from one triangle to another triangle region. For variations inside the triangle of the gain-scheduling parameters the stability is guaranteed. This approach was implemented in test drives in a Golf VI Variant and excellent results were achieved for three consecutive triangles covering a region of 1200 rpm for the reduction of nine frequency components of the engine-induced vibration.

The main objective is to switch between controllers guaranteeing the stability. Therefore an extension of this approach is realized finding a Lyapunov function $\mathbf{X}^{(n_{cl}\times n_{cl})}$ for all the closed loop matrices $\mathbf{A}_{cl,1}^{(n_{cl}\times n_{cl})}$, $\mathbf{A}_{cl,2}^{(n_{cl}\times n_{cl})}$, $\mathbf{A}_{cl,3}^{(n_{cl}\times n_{cl})}$, $\mathbf{A}_{cl,4}^{(n_{cl}\times n_{cl})}$ and $\mathbf{A}_{cl,5}^{(n_{cl}\times n_{cl})}$ of the vertex systems obtained from \mathbf{K}_{1,P_1} , \mathbf{K}_{2,P_1} , \mathbf{K}_{2,P_2} , \mathbf{K}_{2,P_3} and \mathbf{K}_{3,P_3} shown in Fig. 4.7.

Stability is then guaranteed if a common Lyapunov function $\mathbf{X} = \mathbf{X}^T > 0$

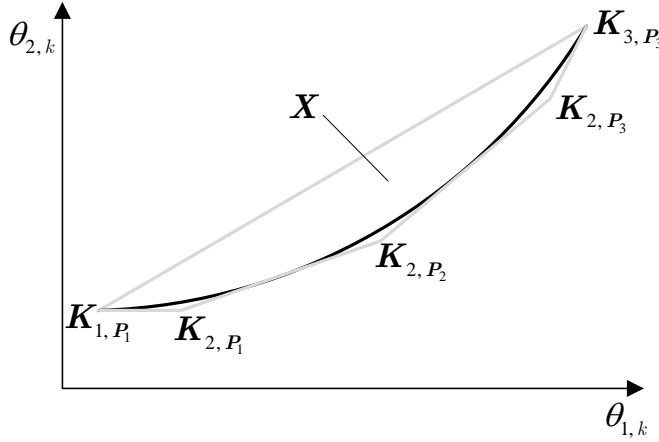


Figure 4.7: Polygon to guarantee the stability of the controllers

$$\begin{bmatrix} \mathbf{X} & \mathbf{X}\mathbf{A}_{\text{cl},j} \\ \mathbf{A}_{\text{cl},j}^T \mathbf{X} & \mathbf{X} \end{bmatrix} > 0, \quad j = 1, \dots, 5 \quad (4.207)$$

is found for all the five vertices of the polytope.

In a similar way as (4.53), the simple matrix multiplication to obtain the pLPV controller can be used if the polygon is further subdivided in triangles. A pLPV controller is used for the triangle (\mathbf{K}_{1,P_1} , \mathbf{K}_{2,P_1} and \mathbf{K}_{2,P_2}) and another pLPV controller for the triangle (\mathbf{K}_{2,P_2} , \mathbf{K}_{2,P_3} and \mathbf{K}_{3,P_3}). A switch between controllers is realized in the middle of the polygon and the controllers are initialized with the same state spaces. The stability is guaranteed since a common Lyapunov function was found for the five vertices and the switch is done between the vertices of the polytope.

It is important to notice that this switching control strategy can be applied for n -number of triangles, finding a common Lyapunov function for the polygon fixes the number of triangles used and establishes the range of the frequencies variations covered by the pLPV controllers.

A controller for the rejection of a harmonic disturbance with two frequencies $f_{1,k} \in [40, 150]$ Hz and $f_{2,k} \in [80, 300]$ Hz acting at the output of the plant

$$\begin{bmatrix} x_{p,k+1} \\ y_{p,k} \end{bmatrix} = \begin{bmatrix} a & 1 \\ 1-a & 0 \end{bmatrix} \begin{bmatrix} x_{p,k} \\ u_{p,k} \end{bmatrix} \quad (4.208)$$

with $a = 0.1$ and $T = 0.0005$ s is calculated as an example to explain in detail the switching control strategy. From the size of the frequency variation range $f_{1,k}$ and $f_{2,k}$ it is clear that a switching control strategy is needed since only one controller is not capable to cover all this range.

The disturbance observer approach will be used here to illustrate this control strategy. Since the disturbance frequencies are harmonically related $f_{0,k}[1 \ 2] = [f_{1,k} \ f_{2,k}]$ the polynomial approximation can be used. Eleven pLPV controllers are calculated using triangles as polytopes for intervals of 10 Hz of the fundamental frequency $f_{0,k} \in [40, 150]$. The controllers

$$\mathbf{K}_{P_1}(\lambda_{1,k})^{((n_K+m_{u_p}) \times (n_K+r_{y_p}))} = \mathbf{K}_{1,P_1}\lambda_{1,P_1,k} + \mathbf{K}_{2,P_1}\lambda_{2,P_1,k} + \mathbf{K}_{3,P_1}\lambda_{3,P_1,k} \quad (4.209)$$

for $f_{0,k} \in [40, 50]$ Hz,

$$\mathbf{K}_{P_2}(\lambda_{2,k})^{((n_K+m_{u_p}) \times (n_K+r_{y_p}))} = \mathbf{K}_{1,P_2}\lambda_{1,P_2,k} + \mathbf{K}_{2,P_2}\lambda_{2,P_2,k} + \mathbf{K}_{3,P_2}\lambda_{3,P_2,k} \quad (4.210)$$

for $f_{0,k} \in [50, 60]$ Hz,

⋮

$$\mathbf{K}_{\mathbf{P}_{11}}(\boldsymbol{\lambda}_{11,k})^{((n_K+m_{u_p}) \times (n_K+r_{y_p}))} = \mathbf{K}_{1,\mathbf{P}_{11}}\lambda_{1,\mathbf{P}_{11},k} + \mathbf{K}_{2,\mathbf{P}_{11}}\lambda_{2,\mathbf{P}_{11},k} + \mathbf{K}_{3,\mathbf{P}_{11}}\lambda_{3,\mathbf{P}_{11},k} \quad (4.211)$$

for $f_{0,k} \in [140, 150]$ Hz are calculated with the control design of Sec. 4.1.3 for the values of

$$\mathbf{Q}^{((2n_d+n_p) \times (2n_d+n_p))} = \begin{bmatrix} \mathbf{I} & \mathbf{0} \\ \mathbf{0} & 0 \end{bmatrix}, \quad R^{(r_y \times r_y)} = 10^4 \text{ and } r = 0.9999 \quad (4.212)$$

used for all the eleven polytopic triangles. A polygon is built with the vertices $\mathbf{K}_{1,\mathbf{P}_1}$, $\mathbf{K}_{2,\mathbf{P}_1}$, $\mathbf{K}_{2,\mathbf{P}_2}$, $\mathbf{K}_{2,\mathbf{P}_3}$, ..., $\mathbf{K}_{2,\mathbf{P}_9}$, $\mathbf{K}_{2,\mathbf{P}_{10}}$, $\mathbf{K}_{2,\mathbf{P}_{11}}$ and $\mathbf{K}_{3,\mathbf{P}_{11}}$ (see Fig. 4.7). A Lyapunov function $\mathbf{X} = \mathbf{X}^T > 0$ is found

$$\mathbf{X} = \begin{bmatrix} 1.5684 & 1.8057 & -0.4448 & 1.7025 & -0.9069 & -0.5962 \\ 1.8057 & 23.7308 & -0.7145 & 1.2733 & -1.4462 & -0.3522 \\ -0.4448 & -0.7145 & 22.4853 & -0.1408 & 0.2274 & -0.028 \\ 1.7025 & 1.2733 & -0.1408 & 26.1455 & -0.918 & -0.4995 \\ -0.9069 & -1.4462 & 0.2274 & -0.918 & 25.4096 & 0.0342 \\ -0.5962 & -0.3522 & -0.028 & -0.4995 & 0.0342 & 26.7855 \end{bmatrix} \quad (4.213)$$

solving the LMIs

$$\begin{bmatrix} \mathbf{X} & \mathbf{X}\mathbf{A}_{\text{cl},1,\mathbf{P}_1} \\ \mathbf{A}_{\text{cl},1,\mathbf{P}_1}^T \mathbf{X} & \mathbf{X} \end{bmatrix} > 0,$$

$$\begin{bmatrix} \mathbf{X} & \mathbf{X}\mathbf{A}_{\text{cl},2,\mathbf{P}_1} \\ \mathbf{A}_{\text{cl},2,\mathbf{P}_1}^T \mathbf{X} & \mathbf{X} \end{bmatrix} > 0,$$

⋮

$$\begin{bmatrix} \mathbf{X} & \mathbf{X}\mathbf{A}_{\text{cl},2,\mathbf{P}_{11}} \\ \mathbf{A}_{\text{cl},2,\mathbf{P}_{11}}^T \mathbf{X} & \mathbf{X} \end{bmatrix} > 0,$$

$$\begin{bmatrix} \mathbf{X} & \mathbf{X}\mathbf{A}_{\text{cl},3,\mathbf{P}_{11}} \\ \mathbf{A}_{\text{cl},3,\mathbf{P}_{11}}^T \mathbf{X} & \mathbf{X} \end{bmatrix} > 0$$

for the closed loop system matrices defined with the vertices of the polygon.

A very simple calculation of the coordinate vectors is obtained using triangles as polytopes. Therefore the polygon is further subdivided in triangles with vertices

$$\mathbf{K}_{1,\mathbf{P}_1}, \mathbf{K}_{2,\mathbf{P}_1}, \mathbf{K}_{2,\mathbf{P}_2},$$

$$\mathbf{K}_{2,\mathbf{P}_1}, \mathbf{K}_{2,\mathbf{P}_2}, \mathbf{K}_{2,\mathbf{P}_3},$$

⋮

$$\mathbf{K}_{2,\mathbf{P}_9}, \mathbf{K}_{2,\mathbf{P}_{10}}, \mathbf{K}_{2,\mathbf{P}_{11}},$$

$$\mathbf{K}_{2,\mathbf{P}_{10}}, \mathbf{K}_{2,\mathbf{P}_{11}}, \mathbf{K}_{3,\mathbf{P}_{11}}. \quad (4.215)$$

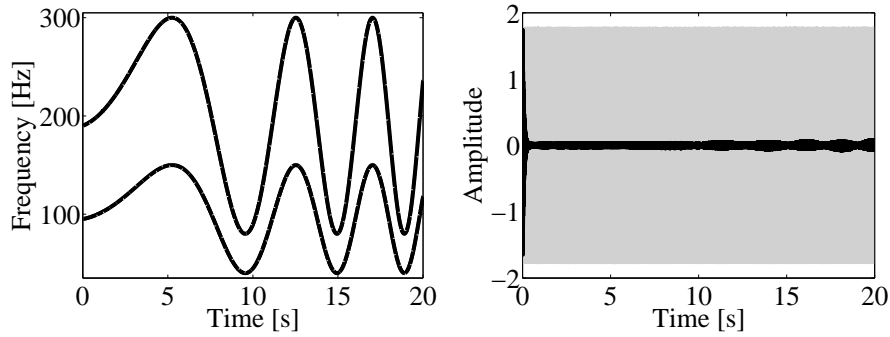


Figure 4.8: Variations of the disturbance frequencies (left) and simulation results (right) in closed loop (black) and open loop (gray)

The new eleven pLPV controllers are written as

$$\mathbf{K}_1(\tilde{\boldsymbol{\lambda}}_{1,k})^{((n_K+m_{u_p}) \times (n_K+r_{y_p}))} = \mathbf{K}_{1,\mathbf{P}_1}\tilde{\lambda}_{1,k}^{(1)} + \mathbf{K}_{2,\mathbf{P}_1}\tilde{\lambda}_{2,k}^{(1)} + \mathbf{K}_{2,\mathbf{P}_2}\tilde{\lambda}_{3,k}^{(1)}, \quad (4.216)$$

$$\mathbf{K}_2(\tilde{\boldsymbol{\lambda}}_{2,k})^{((n_K+m_{u_p}) \times (n_K+r_{y_p}))} = \mathbf{K}_{2,\mathbf{P}_1}\tilde{\lambda}_{1,k}^{(2)} + \mathbf{K}_{2,\mathbf{P}_2}\tilde{\lambda}_{2,k}^{(2)} + \mathbf{K}_{2,\mathbf{P}_3}\tilde{\lambda}_{3,k}^{(2)}, \quad (4.217)$$

⋮

$$\mathbf{K}_{10}(\tilde{\boldsymbol{\lambda}}_{10,k})^{((n_K+m_{u_p}) \times (n_K+r_{y_p}))} = \mathbf{K}_{2,\mathbf{P}_9}\tilde{\lambda}_{1,k}^{(10)} + \mathbf{K}_{2,\mathbf{P}_{10}}\tilde{\lambda}_{2,k}^{(10)} + \mathbf{K}_{2,\mathbf{P}_{11}}\tilde{\lambda}_{3,k}^{(10)}, \quad (4.218)$$

$$\mathbf{K}_{11}(\tilde{\boldsymbol{\lambda}}_{11,k})^{((n_K+m_{u_p}) \times (n_K+r_{y_p}))} = \mathbf{K}_{2,\mathbf{P}_{10}}\tilde{\lambda}_{1,k}^{(11)} + \mathbf{K}_{2,\mathbf{P}_{11}}\tilde{\lambda}_{2,k}^{(11)} + \mathbf{K}_{3,\mathbf{P}_{11}}\tilde{\lambda}_{3,k}^{(11)} \quad (4.219)$$

with the coordinate vector $\tilde{\boldsymbol{\lambda}}_{i,k}$ for $i = 1, \dots, 11$ calculated as a simple matrix multiplication and the switching between controllers is realized in intervals of 10 Hz (50 Hz, 60 Hz, ..., 140 Hz). The stability is guaranteed since a common Lyapunov function was found for all the vertices of the polygon and the switching is realized between three vertices of it. Simulation results are shown for the rejection of a harmonic disturbance with two components of frequency and a fundamental frequency $f_{0,k} \in [40, 150]$ Hz in Fig. 4.8. Excellent results are achieved in simulation results even for frequency variations of 130 Hz s^{-1} as a result of switching between the eleven pLPV controllers.

LFT Gain-scheduling Control for Harmonic Disturbances with Time-varying Frequencies

The control design to obtain an LFT controller for the rejection of harmonic disturbances with time-varying frequencies is considered in this section. The design explained here for the calculation of a gain-scheduling controller is based on Apkarian and Gahinet (1995). As explained in Sec. 3.4 this approach leads to an LFT controller with the same scheduling parameter as the generalized plant. The control structure of Fig. 3.7 is rearranged as in Fig. 4.9 leading to a more classical robust problem with the uncertainty parameter block

$$\Delta_{\text{new},k}^{(2n_d \times 2n_d)} = \begin{bmatrix} \Delta_k & \mathbf{0} \\ \mathbf{0} & \Delta_k \end{bmatrix}. \quad (4.220)$$

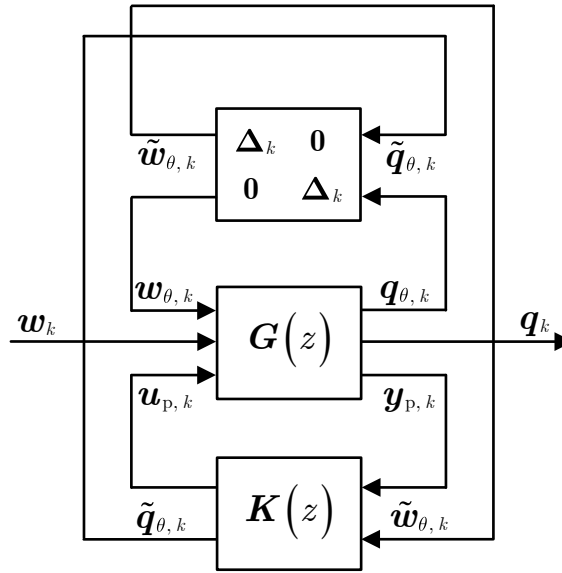


Figure 4.9: LFT control structure with a rearrangement of the parameters

The closed loop system of this control structure is obtained from the generalized plant $\mathbf{G}(z)$

$$\begin{bmatrix} \mathbf{x}_{k+1} \\ \mathbf{q}_{\theta, k} \\ \mathbf{q}_k \\ \mathbf{y}_{p, k} \end{bmatrix} = \begin{bmatrix} \mathbf{A}_0 & \mathbf{B}_\theta & \mathbf{B}_w & \mathbf{B}_u \\ \mathbf{C}_\theta & \mathbf{D}_{\theta\theta} & \mathbf{D}_{\theta w} & \mathbf{D}_{\theta u} \\ \mathbf{C}_q & \mathbf{D}_{q\theta} & \mathbf{D}_{qw} & \mathbf{D}_{qu} \\ \mathbf{C}_y & \mathbf{D}_{y\theta} & \mathbf{D}_{yw} & \mathbf{D}_{yu} \end{bmatrix} \begin{bmatrix} \mathbf{x}_k \\ \mathbf{w}_{\theta, k} \\ \mathbf{w}_k \\ \mathbf{u}_{p, k} \end{bmatrix} \quad (4.221)$$

with the matrix dimensions

$$\begin{array}{cccc} \mathbf{A}_0^{(n \times n)} & \mathbf{B}_\theta^{(n \times m_\theta)} & \mathbf{B}_w^{(n \times m_w)} & \mathbf{B}_u^{(n \times m_u)} \\ \mathbf{C}_\theta^{(r_\theta \times n)} & \mathbf{D}_{\theta\theta}^{(r_\theta \times m_\theta)} & \mathbf{D}_{\theta w}^{(r_\theta \times m_w)} & \mathbf{D}_{\theta u}^{(r_\theta \times m_u)} \\ \mathbf{C}_q^{(r_q \times n)} & \mathbf{D}_{q\theta}^{(r_q \times m_\theta)} & \mathbf{D}_{qw}^{(r_q \times m_w)} & \mathbf{D}_{qu}^{(r_q \times m_u)} \\ \mathbf{C}_y^{(r_y \times n)} & \mathbf{D}_{y\theta}^{(r_y \times m_\theta)} & \mathbf{D}_{yw}^{(r_y \times m_w)} & \mathbf{D}_{yu}^{(r_y \times m_u)} \end{array} \quad (4.222)$$

and the controller $\mathbf{K}(z)$

$$\begin{bmatrix} \mathbf{x}_{K, k+1} \\ \mathbf{u}_{p, k} \\ \tilde{\mathbf{q}}_{\theta, k} \end{bmatrix} = \begin{bmatrix} \mathbf{A}_0^{(K)} & \mathbf{B}_y^{(K)} & \mathbf{B}_\theta^{(K)} \\ \mathbf{C}_u^{(K)} & \mathbf{D}_{uy}^{(K)} & \mathbf{D}_{u\theta}^{(K)} \\ \mathbf{C}_\theta^{(K)} & \mathbf{D}_{\theta y}^{(K)} & \mathbf{D}_{\theta\theta}^{(K)} \end{bmatrix} \begin{bmatrix} \mathbf{x}_{K, k} \\ \mathbf{y}_{p, k} \\ \tilde{\mathbf{w}}_{\theta, k} \end{bmatrix} \quad (4.223)$$

with the matrices

$$\begin{array}{ccc} \mathbf{A}_0^{(K)(n_K \times n_K)} & \mathbf{B}_y^{(K)(n_K \times r_y)} & \mathbf{B}_\theta^{(K)(n_K \times r_\theta)} \\ \mathbf{C}_u^{(K)(m_u \times n_K)} & \mathbf{D}_{uy}^{(K)(m_u \times r_y)} & \mathbf{D}_{u\theta}^{(K)(m_u \times r_\theta)} \\ \mathbf{C}_\theta^{(K)(m_\theta \times n_K)} & \mathbf{D}_{\theta y}^{(K)(m_\theta \times r_y)} & \mathbf{D}_{\theta\theta}^{(K)(m_\theta \times r_\theta)} \end{array} \quad (4.224)$$

4. LPV Gain-scheduling Control for Harmonic Disturbances with Time-varying Frequencies

applying the lower LFT to

$$\left[\begin{array}{c} \mathbf{x}_{k+1} \\ \mathbf{x}_{K,k+1} \\ \tilde{\mathbf{q}}_{\theta,k} \\ \mathbf{q}_{\theta,k} \\ \mathbf{q}_k \\ \mathbf{u}_{p,k} \\ \mathbf{y}_{p,k} \end{array} \right] = \left[\begin{array}{cc|cc|cc|cc} \mathbf{A}_0 & \mathbf{0} & \mathbf{0} & \mathbf{B}_\theta & \mathbf{B}_w & \mathbf{B}_u & \mathbf{0} \\ \mathbf{0} & \mathbf{A}_0^{(K)} & \mathbf{B}_\theta^{(K)} & \mathbf{0} & \mathbf{0} & \mathbf{0} & \mathbf{B}_y^{(K)} \\ \mathbf{0} & \mathbf{C}_\theta^{(K)} & \mathbf{D}_{\theta\theta}^{(K)} & \mathbf{0} & \mathbf{0} & \mathbf{0} & \mathbf{D}_{\theta y}^{(K)} \\ \mathbf{C}_\theta & \mathbf{0} & \mathbf{0} & \mathbf{D}_{\theta\theta} & \mathbf{D}_{\theta w} & \mathbf{D}_{\theta u} & \mathbf{0} \\ \mathbf{C}_q & \mathbf{0} & \mathbf{0} & \mathbf{D}_{q\theta} & \mathbf{D}_{qw} & \mathbf{D}_{qu} & \mathbf{0} \\ \mathbf{0} & \mathbf{C}_u^{(K)} & \mathbf{D}_{u\theta}^{(K)} & \mathbf{0} & \mathbf{0} & \mathbf{0} & \mathbf{D}_{uy}^{(K)} \\ \mathbf{C}_y & \mathbf{0} & \mathbf{0} & \mathbf{D}_{y\theta} & \mathbf{D}_{yw} & \mathbf{D}_{yu} & \mathbf{0} \end{array} \right] \left[\begin{array}{c} \mathbf{x}_k \\ \mathbf{x}_{K,k} \\ \tilde{\mathbf{w}}_{\theta,k} \\ \mathbf{w}_{\theta,k} \\ \mathbf{w}_k \\ \mathbf{u}_{p,k} \\ \mathbf{y}_{p,k} \end{array} \right]. \quad (4.225)$$

The equation (4.225) can be written as

$$\left[\begin{array}{c} \mathbf{x}_{k+1} \\ \mathbf{x}_{K,k+1} \\ \tilde{\mathbf{q}}_{\theta,k} \\ \mathbf{q}_{\theta,k} \\ \mathbf{q}_k \\ \mathbf{u}_{p,k} \\ \mathbf{y}_{p,k} \end{array} \right] = \left[\begin{array}{cccc} \mathbf{A}_1 & \mathbf{B}_1 & \mathbf{B}_2 & \mathbf{B}_3 \\ \mathbf{C}_1 & \mathbf{D}_{11} & \mathbf{D}_{12} & \mathbf{D}_{13} \\ \mathbf{C}_2 & \mathbf{D}_{21} & \mathbf{D}_{22} & \mathbf{D}_{23} \\ \mathbf{C}_3 & \mathbf{D}_{31} & \mathbf{D}_{32} & \mathbf{D}_{33} \end{array} \right] \left[\begin{array}{c} \mathbf{x}_k \\ \mathbf{x}_{K,k} \\ \tilde{\mathbf{w}}_{\theta,k} \\ \mathbf{w}_{\theta,k} \\ \mathbf{w}_k \\ \mathbf{u}_{p,k} \\ \mathbf{y}_{p,k} \end{array} \right] \quad (4.226)$$

with

$$\begin{aligned} \mathbf{A}_1^{((n+n_K) \times (n+n_K))} &= \mathbf{B}_1^{((n+n_K) \times (m_\theta+r_\theta))} & \mathbf{B}_2^{((n+n_K) \times m_w)} &= \mathbf{B}_3^{((n+n_K) \times (m_u+r_y))} \\ \mathbf{C}_1^{((r_\theta+m_\theta) \times (n+n_K))} &= \mathbf{D}_{11}^{((r_\theta+m_\theta) \times (m_\theta+r_\theta))} & \mathbf{D}_{12}^{((r_\theta+m_\theta) \times m_w)} &= \mathbf{D}_{13}^{((r_\theta+m_\theta) \times (m_u+r_y))} \\ \mathbf{C}_2^{(r_q \times (n+n_K))} &= \mathbf{D}_{21}^{(r_q \times (m_\theta+r_\theta))} & \mathbf{D}_{22}^{(r_q \times m_w)} &= \mathbf{D}_{23}^{(r_q \times (m_u+r_y))} \\ \mathbf{C}_3^{((m_u+r_y) \times (n+n_K))} &= \mathbf{D}_{31}^{((m_u+r_y) \times (m_\theta+r_\theta))} & \mathbf{D}_{32}^{((m_u+r_y) \times m_w)} &= \mathbf{D}_{33}^{((m_u+r_y) \times (m_u+r_y))} \end{aligned} \quad (4.227)$$

and the lower LFT

$$\left[\begin{array}{ccc} \mathbf{A}_1 & \mathbf{B}_1 & \mathbf{B}_2 \\ \mathbf{C}_1 & \mathbf{D}_{11} & \mathbf{D}_{12} \\ \mathbf{C}_2 & \mathbf{D}_{21} & \mathbf{D}_{22} \end{array} \right] + \left[\begin{array}{c} \mathbf{B}_3 \\ \mathbf{D}_{13} \\ \mathbf{D}_{23} \end{array} \right] (\mathbf{I} - \mathbf{D}_{33})^{-1} \left[\begin{array}{ccc} \mathbf{C}_3 & \mathbf{D}_{31} & \mathbf{D}_{32} \end{array} \right] \quad (4.228)$$

is used to obtain the closed loop system. Assuming $\mathbf{D}_{yu} = \mathbf{0}$ (see Gahinet and Apkarian (1994) and Apkarian and Gahinet (1995)) the inverse

$$(\mathbf{I} - \mathbf{D}_{33})^{-1} = \left(\mathbf{I} - \left[\begin{array}{cc} \mathbf{0} & \mathbf{D}_{uy}^{(K)} \\ \mathbf{D}_{yu} & \mathbf{0} \end{array} \right] \right)^{-1} = \left[\begin{array}{cc} \mathbf{I} & -\mathbf{D}_{uy}^{(K)} \\ \mathbf{0} & \mathbf{I} \end{array} \right]^{-1} = \left[\begin{array}{cc} \mathbf{I} & \mathbf{D}_{uy}^{(K)} \\ \mathbf{0} & \mathbf{I} \end{array} \right] \quad (4.229)$$

is very simple to calculate.

A closed loop representation of the system is given as

$$\left[\begin{array}{c} \mathbf{x}_{k+1} \\ \mathbf{x}_{K,k+1} \\ \tilde{\mathbf{q}}_{\theta,k} \\ \mathbf{q}_{\theta,k} \\ \mathbf{q}_k \end{array} \right] = \left[\begin{array}{cc} \mathbf{A}_{cl} & \mathbf{B}_{cl} \\ \mathbf{C}_{cl} & \mathbf{D}_{cl} \end{array} \right] \left[\begin{array}{c} \mathbf{x}_k \\ \mathbf{x}_{K,k} \\ \tilde{\mathbf{w}}_{\theta,k} \\ \mathbf{w}_{\theta,k} \\ \mathbf{w}_k \end{array} \right] \quad (4.230)$$

with $\mathbf{A}_{cl}^{((n+n_K) \times (n+n_K))}$, $\mathbf{C}_{cl}^{((r_\theta+m_\theta+r_q) \times (n+n_K))}$, $\mathbf{B}_{cl}^{((n+n_K) \times (m_\theta+r_\theta+m_w))}$, $\mathbf{D}_{cl}^{((r_\theta+m_\theta+r_q) \times (m_\theta+r_\theta+m_w))}$

$$\mathbf{A}_{cl} = \left[\begin{array}{cc} \mathbf{A}_0 + \mathbf{B}_u \mathbf{D}_{uy}^{(K)} \mathbf{C}_y & \mathbf{B}_u \mathbf{C}_u^{(K)} \\ \mathbf{B}_y^{(K)} \mathbf{C}_y & \mathbf{A}^{(K)} \end{array} \right], \quad (4.231)$$

$$\mathbf{B}_{\text{cl}} = \begin{bmatrix} \mathbf{B}_u \mathbf{D}_{u\theta}^{(K)} & \mathbf{B}_\theta + \mathbf{B}_u \mathbf{D}_{uy}^{(K)} \mathbf{D}_{y\theta} & \mathbf{B}_w + \mathbf{B}_u \mathbf{D}_{uy}^{(K)} \mathbf{D}_{yw} \\ \mathbf{B}_\theta^{(K)} & \mathbf{B}_y^{(K)} \mathbf{D}_{y\theta} & \mathbf{B}_y^{(K)} \mathbf{D}_{yw} \end{bmatrix}, \quad (4.232)$$

$$\mathbf{C}_{\text{cl}} = \begin{bmatrix} \mathbf{D}_{\theta y}^{(K)} \mathbf{C}_y & \mathbf{C}_\theta^{(K)} \\ \mathbf{C}_\theta + \mathbf{D}_{\theta u} \mathbf{D}_{uy}^{(K)} \mathbf{C}_y & \mathbf{D}_{\theta u} \mathbf{C}_u^{(K)} \\ \mathbf{C}_q + \mathbf{D}_{qu} \mathbf{D}_{uy}^{(K)} \mathbf{C}_y & \mathbf{D}_{qu} \mathbf{C}_u^{(K)} \end{bmatrix} \quad (4.233)$$

and

$$\mathbf{D}_{\text{cl}} = \begin{bmatrix} \mathbf{D}_{\theta\theta}^{(K)} & \mathbf{D}_{\theta y}^{(K)} \mathbf{D}_{y\theta} & \mathbf{D}_{\theta y}^{(K)} \mathbf{D}_{yw} \\ \mathbf{D}_{\theta u} \mathbf{D}_{u\theta}^{(K)} & \mathbf{D}_{\theta\theta} + \mathbf{D}_{\theta u} \mathbf{D}_{uy}^{(K)} \mathbf{D}_{y\theta} & \mathbf{D}_{\theta w} + \mathbf{D}_{\theta u} \mathbf{D}_{uy}^{(K)} \mathbf{D}_{yw} \\ \mathbf{D}_{qu} \mathbf{D}_{u\theta}^{(K)} & \mathbf{D}_{q\theta} + \mathbf{D}_{qu} \mathbf{D}_{uy}^{(K)} \mathbf{D}_{y\theta} & \mathbf{D}_{qw} + \mathbf{D}_{qu} \mathbf{D}_{uy}^{(K)} \mathbf{D}_{yw} \end{bmatrix}. \quad (4.234)$$

Using the scaled bounded real lemma, a solution for this control problem exists if the LMI

$$\begin{bmatrix} -\mathbf{X}_{\text{cl}}^{-1} & \mathbf{A}_{\text{cl}} & \mathbf{B}_{\text{cl}} & \mathbf{0} \\ \mathbf{A}_{\text{cl}}^T & -\mathbf{X}_{\text{cl}} & \mathbf{0} & \mathbf{C}_{\text{cl}}^T \\ \mathbf{B}_{\text{cl}}^T & \mathbf{0} & -\gamma \mathbf{L} & \mathbf{D}_{\text{cl}}^T \\ \mathbf{0} & \mathbf{C}_{\text{cl}} & \mathbf{D}_{\text{cl}} & -\gamma \mathbf{L}^{-1} \end{bmatrix} < 0 \quad (4.235)$$

holds for some positive definite matrices $\mathbf{X}_{\text{cl}}^{((n+n_K) \times (n+n_K))}$ and $\mathbf{L}^{((r_\theta+m_\theta+r_q) \times (m_\theta+r_\theta+m_w))}$. The LMI of (4.235) can be written as

$$\psi + \mathbf{P}^T \Omega \mathbf{Q} + \mathbf{Q}^T \Omega^T \mathbf{P} < 0 \quad (4.236)$$

with the matrix

$$\psi = \begin{bmatrix} -\mathbf{X}_{\text{cl}}^{-1} & \bar{\mathbf{A}} & \bar{\mathbf{B}} & \mathbf{0} \\ \bar{\mathbf{A}}^T & -\mathbf{X}_{\text{cl}} & \mathbf{0} & \bar{\mathbf{C}}^T \\ \bar{\mathbf{B}}^T & \mathbf{0} & -\gamma \bar{\mathbf{L}} & \bar{\mathbf{D}}^T \\ \mathbf{0} & \bar{\mathbf{C}} & \bar{\mathbf{D}} & -\gamma \bar{\mathbf{J}} \end{bmatrix} \quad (4.237)$$

built with

$$\begin{aligned} \bar{\mathbf{A}}^{((n+n_K) \times (n+n_K))} &= \begin{bmatrix} \mathbf{A} & \mathbf{0} \\ \mathbf{0} & \mathbf{0} \end{bmatrix}, \quad \bar{\mathbf{B}}^{((n+n_K) \times (2m_\theta+m_w))} = \begin{bmatrix} \mathbf{0} & \mathbf{B}_\theta & \mathbf{B}_w \\ \mathbf{0} & \mathbf{0} & \mathbf{0} \end{bmatrix}, \\ \bar{\mathbf{C}}^{((2r_\theta+r_q) \times (n+n_K))} &= \begin{bmatrix} \mathbf{0} & \mathbf{0} \\ \mathbf{C}_\theta & \mathbf{0} \\ \mathbf{C}_q & \mathbf{0} \end{bmatrix}, \quad \bar{\mathbf{D}}^{((2r_\theta+r_q) \times (2m_\theta+m_w))} = \begin{bmatrix} \mathbf{0} & \mathbf{0} & \mathbf{0} \\ \mathbf{0} & \mathbf{D}_{\theta\theta} & \mathbf{D}_{\theta w} \\ \mathbf{0} & \mathbf{D}_{q\theta} & \mathbf{D}_{qw} \end{bmatrix}, \\ \bar{\mathbf{L}}^{((2r_\theta+m_w) \times (2r_\theta+m_w))} &= \begin{bmatrix} \mathbf{L} & \mathbf{0} \\ \mathbf{0} & \mathbf{I} \end{bmatrix}, \quad \bar{\mathbf{J}}^{((2r_\theta+m_w) \times (2r_\theta+m_w))} = \mathbf{L}^{-1} \end{aligned} \quad (4.238)$$

the matrices $\mathbf{P}^{((n_K+m_u+m_\theta) \times (2n+2n_K+2m_\theta+m_w+2r_\theta+r_q))}$,
 $\mathbf{Q}^{((n_K+r_y+r_\theta) \times (2n+2n_K+2m_\theta+m_w+2r_\theta+r_q))}$

$$\mathbf{P} = \begin{bmatrix} \tilde{\mathbf{B}}^T & \mathbf{0} & \mathbf{0} & \mathbf{0} & \mathbf{0} & \tilde{\mathbf{D}}_{12}^T \end{bmatrix}, \quad \mathbf{Q} = \begin{bmatrix} \mathbf{0} & \mathbf{0} & \tilde{\mathbf{C}} & \tilde{\mathbf{D}}_{21} & \mathbf{0} & \mathbf{0} & \mathbf{0} \end{bmatrix} \quad (4.239)$$

4. LPV Gain-scheduling Control for Harmonic Disturbances with Time-varying Frequencies

defined with $\tilde{\mathbf{B}}^{((n+n_K) \times (n_K+m_u+m_\theta))}$, $\tilde{\mathbf{C}}^{((n_K+r_y+r_\theta) \times (n+n_K))}$, $\tilde{\mathbf{D}}_{12}^{((2r_\theta+r_q) \times (n_K+m_u+m_\theta))}$, $\tilde{\mathbf{D}}_{21}^{((n_K+r_y+r_\theta) \times (2m_\theta+m_w))}$

$$\begin{aligned}\tilde{\mathbf{B}} &= \begin{bmatrix} \mathbf{0} & \mathbf{B}_u & \mathbf{0} \\ \mathbf{I} & \mathbf{0} & \mathbf{0} \end{bmatrix}, \quad \tilde{\mathbf{C}} = \begin{bmatrix} \mathbf{0} & \mathbf{I} \\ \mathbf{C}_y & \mathbf{0} \\ \mathbf{0} & \mathbf{0} \end{bmatrix}, \\ \tilde{\mathbf{D}}_{12} &= \begin{bmatrix} \mathbf{0} & \mathbf{0} & \mathbf{I} \\ \mathbf{0} & \mathbf{D}_{\theta u} & \mathbf{0} \\ \mathbf{0} & \mathbf{D}_{qu} & \mathbf{0} \end{bmatrix}, \quad \tilde{\mathbf{D}}_{21} = \begin{bmatrix} \mathbf{0} & \mathbf{0} & \mathbf{0} \\ \mathbf{0} & \mathbf{D}_{y\theta} & \mathbf{D}_{yw} \\ \mathbf{I} & \mathbf{0} & \mathbf{0} \end{bmatrix}\end{aligned}\tag{4.240}$$

and the controller matrix

$$\Omega^{((n_K+m_u+m_\theta) \times (n_K+r_y+r_\theta))} = \left[\begin{array}{c|cc} \mathbf{A}_0^{(K)} & \mathbf{B}_y^{(K)} & \mathbf{B}_\theta^{(K)} \\ \mathbf{C}_u^{(K)} & \mathbf{D}_{uy}^{(K)} & \mathbf{D}_{u\theta}^{(K)} \\ \mathbf{C}_\theta^{(K)} & \mathbf{D}_{\theta y}^{(K)} & \mathbf{D}_{\theta\theta}^{(K)} \end{array} \right].\tag{4.241}$$

The controller can be calculated from (4.236) if the matrices \mathbf{X}_{cl} and \mathbf{L} are known. Equivalently (see Gahinet and Apkarian (1994)), a solution Ω for (4.236) exists if and only if

$$\begin{aligned}\mathbf{N}_P^T \psi \mathbf{N}_P &< 0, \\ \mathbf{N}_Q^T \psi \mathbf{N}_Q &< 0\end{aligned}\tag{4.242}$$

where \mathbf{N}_P and \mathbf{N}_Q are the nullspaces of \mathbf{P} and \mathbf{Q} , respectively. A proof of this theorem is obtained multiplying (4.236) by \mathbf{N}_P^T and \mathbf{N}_P , then

$$\mathbf{N}_P^T \psi \mathbf{N}_P + \mathbf{N}_P^T \mathbf{P}^T \Omega \mathbf{Q} \mathbf{N}_P + \mathbf{N}_P^T \mathbf{Q}^T \Omega^T \mathbf{P} \mathbf{N}_P = \mathbf{N}_P^T \psi \mathbf{N}_P < 0.\tag{4.243}$$

The same procedure is carried out for \mathbf{N}_Q^T and \mathbf{N}_Q .

The matrix ψ can be written as

$$\psi = \begin{bmatrix} \bar{\mathbf{A}}^T \mathbf{X}_{\text{cl}} \bar{\mathbf{A}} - \mathbf{X}_{\text{cl}} & \bar{\mathbf{A}}^T \mathbf{X}_{\text{cl}} \bar{\mathbf{B}} & \bar{\mathbf{C}}^T \\ \bar{\mathbf{B}}^T \mathbf{X}_{\text{cl}} \bar{\mathbf{A}} & -\gamma \bar{\mathbf{L}} + \bar{\mathbf{B}}^T \mathbf{X}_{\text{cl}} \bar{\mathbf{B}} & \bar{\mathbf{D}}^T \\ \bar{\mathbf{C}} & \bar{\mathbf{D}} & -\gamma \bar{\mathbf{J}} \end{bmatrix}\tag{4.244}$$

or

$$\psi = \begin{bmatrix} \bar{\mathbf{A}} \mathbf{X}_{\text{cl}}^{-1} \bar{\mathbf{A}}^T - \mathbf{X}_{\text{cl}}^{-1} & \bar{\mathbf{B}} & \bar{\mathbf{A}} \mathbf{X}_{\text{cl}}^{-1} \bar{\mathbf{C}}^T \\ \bar{\mathbf{B}}^T & -\gamma \bar{\mathbf{J}} & \bar{\mathbf{D}}^T \\ \bar{\mathbf{C}} \mathbf{X}_{\text{cl}}^{-1} \bar{\mathbf{A}}^T & \bar{\mathbf{D}} & -\gamma \bar{\mathbf{L}} \end{bmatrix}\tag{4.245}$$

doing the Schur complement to \mathbf{X}_{cl} and $\mathbf{X}_{\text{cl}}^{-1}$ in (4.237), respectively.

The conditions of (4.242) can be rewritten (Apkarian and Gahinet (1995)) using (4.244)-

(4.245) and making a decomposition of the positive definite matrix \mathbf{X}_{cl} as

$$\mathbf{N}_R^T \begin{bmatrix} \mathbf{A}\mathbf{R}\mathbf{A}^T - \mathbf{R} & \mathbf{A}\mathbf{R}\mathbf{C}_\theta^T & \mathbf{A}\mathbf{R}\mathbf{C}_q^T & \mathbf{B}_\theta & \mathbf{B}_w \\ \mathbf{C}_\theta\mathbf{R}\mathbf{A}^T & -\gamma\mathbf{J}_3 + \mathbf{C}_\theta\mathbf{R}\mathbf{C}_\theta^T & \mathbf{C}_\theta\mathbf{R}\mathbf{C}_q^T & \mathbf{D}_{\theta\theta} & \mathbf{D}_{\theta w} \\ \mathbf{C}_q\mathbf{R}\mathbf{A}^T & \mathbf{C}_q\mathbf{R}\mathbf{C}_\theta^T & -\gamma\mathbf{I} + \mathbf{C}_q\mathbf{R}\mathbf{C}_q^T & \mathbf{D}_{q\theta} & \mathbf{D}_{qw} \\ \mathbf{B}_\theta^T & \mathbf{D}_{\theta\theta}^T & \mathbf{D}_{q\theta}^T & -\gamma\mathbf{L}_3 & \mathbf{0} \\ \mathbf{B}_w^T & \mathbf{D}_{\theta w}^T & \mathbf{D}_{qw}^T & \mathbf{0} & -\gamma\mathbf{I} \end{bmatrix} \mathbf{N}_R < 0$$

$$\mathbf{N}_S^T \begin{bmatrix} \mathbf{A}^T\mathbf{S}\mathbf{A} - \mathbf{S} & \mathbf{A}^T\mathbf{S}\mathbf{B}_\theta & \mathbf{A}^T\mathbf{S}\mathbf{B}_w & \mathbf{C}_\theta^T & \mathbf{C}_q^T \\ \mathbf{B}_\theta^T\mathbf{S}\mathbf{A} & -\gamma\mathbf{L}_3 + \mathbf{B}_\theta^T\mathbf{S}\mathbf{B}_\theta & \mathbf{B}_\theta^T\mathbf{S}\mathbf{B}_w & \mathbf{D}_{\theta\theta}^T & \mathbf{D}_{q\theta}^T \\ \mathbf{B}_w^T\mathbf{S}\mathbf{A} & \mathbf{B}_w^T\mathbf{S}\mathbf{B}_\theta & -\gamma\mathbf{I} + \mathbf{B}_w^T\mathbf{S}\mathbf{B}_w & \mathbf{D}_{\theta w}^T & \mathbf{D}_{qw}^T \\ \mathbf{C}_\theta & \mathbf{D}_{\theta\theta} & \mathbf{D}_{\theta w} & -\gamma\mathbf{J}_3 & \mathbf{0} \\ \mathbf{C}_q & \mathbf{D}_{q\theta} & \mathbf{D}_{qw} & \mathbf{0} & -\gamma\mathbf{I} \end{bmatrix} \mathbf{N}_S < 0$$
(4.246)

$$\begin{bmatrix} \mathbf{R} & \mathbf{I} \\ \mathbf{I} & \mathbf{S} \end{bmatrix} \geq 0$$
(4.247)

$$\begin{bmatrix} \mathbf{L}_3 & \mathbf{I} \\ \mathbf{I} & \mathbf{J}_3 \end{bmatrix} \geq 0$$
(4.248)

with

$$\bar{\mathbf{J}}^{((r_\theta+r_q)\times(r_\theta+r_q))} = \begin{bmatrix} \mathbf{J}_3 & \mathbf{0} \\ \mathbf{0} & \mathbf{I} \end{bmatrix}, \quad \bar{\mathbf{L}}^{((m_\theta+m_w)\times(m_\theta+m_w))} = \begin{bmatrix} \mathbf{L}_3 & \mathbf{0} \\ \mathbf{0} & \mathbf{I} \end{bmatrix},$$
(4.249)

the nullspace \mathbf{N}_R of the matrix

$$[\mathbf{B}_u^T \quad \mathbf{D}_{\theta u}^T \quad \mathbf{D}_{qu}^T \quad \mathbf{0} \quad \mathbf{0}]^{(m_u \times (n+r_\theta+r_q+m_\theta+m_w))}$$
(4.250)

and the nullspace \mathbf{N}_S of

$$[\mathbf{C}_y \quad \mathbf{D}_{y\theta} \quad \mathbf{D}_{yw} \quad \mathbf{0} \quad \mathbf{0}]^{(r_y \times (n+m_\theta+m_w+r_\theta+r_q))}.$$
(4.251)

If solutions for the LMI of (4.246) are found for the positive definite matrices $\mathbf{R}^{(n \times n)}$, $\mathbf{S}^{(n \times n)}$, $\mathbf{L}_3^{(m_\theta \times m_\theta)}$ and $\mathbf{J}_3^{(r_\theta \times r_\theta)}$ an LFT controller exists and it can be calculated through

$$\psi + \mathbf{P}^T \Omega \mathbf{Q} + \mathbf{Q}^T \Omega^T \mathbf{P} < 0$$
(4.252)

building a Lyapunov function $\mathbf{X}_{\text{cl}}^{((n+n_K) \times (n+n_K))}$ fulfilling

$$\mathbf{X}_{\text{cl}} \begin{bmatrix} \mathbf{I} & \mathbf{R} \\ \mathbf{0} & \mathbf{M}^T \end{bmatrix} = \begin{bmatrix} \mathbf{S} & \mathbf{I} \\ \mathbf{N}^T & \mathbf{0} \end{bmatrix}$$
(4.253)

with $\mathbf{M}^{(n \times n_K)}$ and $\mathbf{N}^{(n \times n_K)}$ calculated through the singular value decomposition of

$$\mathbf{M}\mathbf{N}^T = \mathbf{I} - \mathbf{R}\mathbf{S}$$
(4.254)

and a matrix

$$\mathbf{L}^{(2r_\theta \times 2r_\theta)} = \begin{bmatrix} \mathbf{L}_1 & \mathbf{L}_2 \\ \mathbf{L}_2^T & \mathbf{L}_3 \end{bmatrix}$$
(4.255)

4. LPV Gain-scheduling Control for Harmonic Disturbances with Time-varying Frequencies

with $\mathbf{L}_1^{(r_\theta \times r_\theta)}$ and $\mathbf{L}_2^{(r_\theta \times r_\theta)}$ calculated through

$$\mathbf{L}_3 - \mathbf{J}_3^{-1} = \mathbf{L}_2^T \mathbf{L}_1^{-1} \mathbf{L}_2 \quad (4.256)$$

using the singular value decomposition.

The controller is obtained with this control design in two steps. First, the existence of the controller is proved solving the LMI (4.246) and with these solutions a Lyapunov function \mathbf{X}_{cl} and an auxiliar matrix \mathbf{L} are built. Finally the LMI (4.236) is solved for the controller matrix $\boldsymbol{\Omega}$. From here the controller matrices can be extracted obtaining the state-space representation in LFT form

$$\begin{bmatrix} \mathbf{x}_{K,k+1} \\ \mathbf{u}_{p,k} \\ \tilde{\mathbf{q}}_{\theta,k} \end{bmatrix} = \begin{bmatrix} \mathbf{A}_0^{(K)} & \mathbf{B}_y^{(K)} & \mathbf{B}_\theta^{(K)} \\ \mathbf{C}_u^{(K)} & \mathbf{D}_{uy}^{(K)} & \mathbf{D}_{u\theta}^{(K)} \\ \mathbf{C}_\theta^{(K)} & \mathbf{D}_{\theta y}^{(K)} & \mathbf{D}_{\theta\theta}^{(K)} \end{bmatrix} \begin{bmatrix} \mathbf{x}_{K,k} \\ \mathbf{y}_{p,k} \\ \tilde{\mathbf{w}}_{\theta,k} \end{bmatrix} \quad (4.257)$$

of the controller. For the implementation of the controller, instead of calculating the LFT at each sampling time, an alternative method is presented in this thesis.

The state-space representation of the controller is given with

$$\mathbf{x}_{K,k+1} = \mathbf{A}_0^{(K)} \mathbf{x}_{K,k} + \mathbf{B}_y^{(K)} \mathbf{y}_{p,k} + \mathbf{B}_\theta^{(K)} \tilde{\mathbf{w}}_{\theta,k} \quad (4.258)$$

$$\mathbf{u}_{p,k} = \mathbf{C}_u^{(K)} \mathbf{x}_{K,k} + \mathbf{D}_{uy}^{(K)} \mathbf{y}_{p,k} + \mathbf{D}_{u\theta}^{(K)} \tilde{\mathbf{w}}_{\theta,k} \quad (4.259)$$

$$\tilde{\mathbf{q}}_{\theta,k} = \mathbf{C}_\theta^{(K)} \mathbf{x}_{K,k} + \mathbf{D}_{\theta y}^{(K)} \mathbf{y}_{p,k} + \mathbf{D}_{\theta\theta}^{(K)} \tilde{\mathbf{w}}_{\theta,k} \quad (4.260)$$

$$\tilde{\mathbf{w}}_{\theta,k} = \Delta_k \tilde{\mathbf{q}}_{\theta,k}. \quad (4.261)$$

Substituting $\tilde{\mathbf{w}}_{\theta,k}$ in (4.258)-(4.260) and manipulating (4.260) the following equations for the implementation of the controller are obtained

$$\begin{aligned} \mathbf{x}_{K,k+1} &= \mathbf{A}_0^{(K)} \mathbf{x}_{K,k} + \mathbf{B}_y^{(K)} \mathbf{y}_{p,k} + \mathbf{B}_\theta^{(K)} \Delta_k \tilde{\mathbf{q}}_{\theta,k} \\ \mathbf{u}_{p,k} &= \mathbf{C}_u^{(K)} \mathbf{x}_{K,k} + \mathbf{D}_{uy}^{(K)} \mathbf{y}_{p,k} + \mathbf{D}_{u\theta}^{(K)} \Delta_k \tilde{\mathbf{q}}_{\theta,k} \end{aligned} \quad (4.262)$$

with $\tilde{\mathbf{q}}_{\theta,k}$ calculated as

$$\tilde{\mathbf{q}}_{\theta,k} = (\mathbf{I} - \mathbf{D}_{\theta\theta} \Delta_k)^{-1} (\mathbf{C}_\theta \mathbf{x}_{K,k} + \mathbf{D}_{\theta y} \mathbf{y}_{p,k}). \quad (4.263)$$

This controller can be implemented only if

$$(\mathbf{I} - \mathbf{D}_{\theta\theta} \Delta_k) \neq 0. \quad (4.264)$$

This section introduces the general control design to obtain an LFT controller with the same scheduling parameters as the generalized plant. In the next section the control design is explained in detail and focused in the rejection of disturbances with time-varying frequencies.

LFT Control Design

Before applying the control design, the generalized plant with the plant, disturbance model and weighting functions is built as

$$\left[\begin{array}{c} \mathbf{x}_{k+1} \\ \mathbf{q}_{\theta,k} \\ \mathbf{q}_k \\ \mathbf{y}_{p,k} \end{array} \right] = \left[\begin{array}{c|ccc} \mathbf{A}_0 & \mathbf{B}_\theta & \mathbf{B}_w & \mathbf{B}_u \\ \mathbf{C}_\theta & \mathbf{D}_{\theta\theta} & \mathbf{D}_{\theta w} & \mathbf{D}_{\theta u} \\ \mathbf{C}_q & \mathbf{D}_{q\theta} & \mathbf{D}_{qw} & \mathbf{D}_{qu} \\ \mathbf{C}_y & \mathbf{D}_{y\theta} & \mathbf{D}_{yw} & \mathbf{D}_{yu} \end{array} \right] \left[\begin{array}{c} \mathbf{x}_k \\ \mathbf{w}_{\theta,k} \\ \mathbf{w}_k \\ \mathbf{u}_{p,k} \end{array} \right] \quad (4.265)$$

with

$$\mathbf{x}_k = \left[\begin{array}{c} \mathbf{x}_{p,k} \\ \mathbf{x}_{d,k} \\ \mathbf{x}_{W_u,k} \\ \mathbf{x}_{W_y,k} \end{array} \right], \quad \mathbf{A}_0^{(n \times n)} = \left[\begin{array}{cccc} \mathbf{A}_p & \mathbf{B}_p \mathbf{C}_d & \mathbf{0} & \mathbf{0} \\ \mathbf{0} & \mathbf{A}_{d,0} & \mathbf{0} & \mathbf{0} \\ \mathbf{0} & \mathbf{0} & \mathbf{A}_{W_u} & \mathbf{0} \\ \mathbf{B}_{W_y} \mathbf{C}_p & \mathbf{0} & \mathbf{0} & \mathbf{A}_{W_y} \end{array} \right], \quad (4.266)$$

$$[\mathbf{B}_\theta \quad \mathbf{B}_w \quad \mathbf{B}_u]^{(n \times (m_\theta + m_w + m_u))} = \left[\begin{array}{ccc} \mathbf{0} & \mathbf{0} & \mathbf{B}_p \\ \mathbf{B}_{d,\theta} & \mathbf{B}_d & \mathbf{0} \\ \mathbf{0} & \mathbf{0} & \mathbf{B}_{W_u} \\ \mathbf{0} & \mathbf{0} & \mathbf{0} \end{array} \right], \quad (4.267)$$

$$\left[\begin{array}{c} \mathbf{C}_\theta \\ \mathbf{C}_q \\ \mathbf{C}_y \end{array} \right]^{((r_\theta + r_q + r_y) \times n)} = \left[\begin{array}{cccc} \mathbf{0} & \mathbf{C}_{d,\theta} & \mathbf{0} & \mathbf{0} \\ \mathbf{0} & \mathbf{0} & \mathbf{C}_{W_u} & \mathbf{0} \\ \mathbf{D}_{W_y} \mathbf{C}_p & \mathbf{0} & \mathbf{0} & \mathbf{C}_{W_y} \\ \mathbf{C}_p & \mathbf{0} & \mathbf{0} & \mathbf{0} \end{array} \right], \quad (4.268)$$

$$\left[\begin{array}{ccc} \mathbf{D}_{\theta\theta} & \mathbf{D}_{\theta w} & \mathbf{D}_{\theta u} \\ \mathbf{D}_{q\theta} & \mathbf{D}_{qw} & \mathbf{D}_{qu} \\ \mathbf{D}_{y\theta} & \mathbf{D}_{yw} & \mathbf{D}_{yu} \end{array} \right]^{((r_\theta + r_q + r_y) \times (m_\theta + m_w + m_u))} = \left[\begin{array}{ccc} \mathbf{0} & \mathbf{0} & \mathbf{0} \\ \mathbf{0} & \mathbf{0} & \mathbf{D}_{W_u} \\ \mathbf{0} & \mathbf{0} & \mathbf{0} \\ \mathbf{0} & \mathbf{0} & \mathbf{0} \end{array} \right], \quad (4.269)$$

$n = n_p + 2n_d + n_{W_u} + n_{W_y}$ and $r_q = r_{q_u} + r_{q_y}$.

The matrix $\mathbf{A}_{d,k}^{(2n_d \times 2n_d)}$ of the disturbance model is calculated using the LFT relation

$$\mathbf{A}_d(\boldsymbol{\theta}_k)^{(2n_d \times 2n_d)} = \mathbf{A}_{d,0} + \mathbf{B}_{d,\theta} \Delta_k \mathbf{C}_{d,\theta} \quad (4.270)$$

for $\mathbf{A}_{d,0}^{(2n_d \times 2n_d)}$, $\mathbf{B}_{d,\theta}^{(2n_d \times m_\theta)}$, $\mathbf{C}_{d,\theta}^{(r_\theta \times 2n_d)}$, $\Delta_k^{(n_d \times n_d)}$ and $n_d = m_\theta = r_\theta$. An example was shown in Subsec. 4.1.2.

All the necessary steps carried out to obtain the LFT controller are explained here in detail.

First, the matrices

$$[\mathbf{B}_u^T \quad \mathbf{D}_{\theta u}^T \quad \mathbf{D}_{qu}^T \quad \mathbf{0} \quad \mathbf{0}]^{(m_u \times (n + r_\theta + r_q + m_\theta + m_w))}, \quad (4.271)$$

$$[\mathbf{C}_y \quad \mathbf{D}_{y\theta} \quad \mathbf{D}_{yw} \quad \mathbf{0} \quad \mathbf{0}]^{(r_y \times (n + m_\theta + m_w + r_\theta + r_q))} \quad (4.272)$$

are built and their nullspaces \mathbf{N}_R and \mathbf{N}_S are calculated.

4. LPV Gain-scheduling Control for Harmonic Disturbances with Time-varying Frequencies

Then, the LMI is built and solved for the variables $\mathbf{R}^{(n \times n)}$, $\mathbf{S}^{(n \times n)}$, $\mathbf{J}_3^{(r_\theta \times r_\theta)}$ and $\mathbf{L}_3^{(m_\theta \times m_\theta)}$

$$\mathbf{N}_R^T \begin{bmatrix} \mathbf{A}\mathbf{R}\mathbf{A}^T - \mathbf{R} & \mathbf{A}\mathbf{R}\mathbf{C}_\theta^T & \mathbf{A}\mathbf{R}\mathbf{C}_q^T & \mathbf{B}_\theta & \mathbf{B}_w \\ \mathbf{C}_\theta \mathbf{R}\mathbf{A}^T & -\gamma \mathbf{J}_3 + \mathbf{C}_\theta \mathbf{R}\mathbf{C}_\theta^T & \mathbf{C}_\theta \mathbf{R}\mathbf{C}_q^T & \mathbf{D}_{\theta\theta} & \mathbf{D}_{\theta w} \\ \mathbf{C}_q \mathbf{R}\mathbf{A}^T & \mathbf{C}_q \mathbf{R}\mathbf{C}_\theta^T & -\gamma \mathbf{I} + \mathbf{C}_q \mathbf{R}\mathbf{C}_q^T & \mathbf{D}_{q\theta} & \mathbf{D}_{qw} \\ \mathbf{B}_\theta^T & \mathbf{D}_{\theta\theta}^T & \mathbf{D}_{q\theta}^T & -\gamma \mathbf{L}_3 & \mathbf{0} \\ \mathbf{B}_w^T & \mathbf{D}_{\theta w}^T & \mathbf{D}_{qw}^T & \mathbf{0} & -\gamma \mathbf{I} \end{bmatrix} \mathbf{N}_R < 0$$

$$\mathbf{N}_S^T \begin{bmatrix} \mathbf{A}^T \mathbf{S} \mathbf{A} - \mathbf{S} & \mathbf{A}^T \mathbf{S} \mathbf{B}_\theta & \mathbf{A}^T \mathbf{S} \mathbf{B}_w & \mathbf{C}_\theta^T & \mathbf{C}_q^T \\ \mathbf{B}_\theta^T \mathbf{S} \mathbf{A} & -\gamma \mathbf{L}_3 + \mathbf{B}_\theta^T \mathbf{S} \mathbf{B}_\theta & \mathbf{B}_\theta^T \mathbf{S} \mathbf{B}_w & \mathbf{D}_{\theta\theta}^T & \mathbf{D}_{q\theta}^T \\ \mathbf{B}_w^T \mathbf{S} \mathbf{A} & \mathbf{B}_w^T \mathbf{S} \mathbf{B}_\theta & -\gamma \mathbf{I} + \mathbf{B}_w^T \mathbf{S} \mathbf{B}_w & \mathbf{D}_{\theta w}^T & \mathbf{D}_{qw}^T \\ \mathbf{C}_\theta & \mathbf{D}_{\theta\theta} & \mathbf{D}_{\theta w} & -\gamma \mathbf{J}_3 & \mathbf{0} \\ \mathbf{C}_q & \mathbf{D}_{q\theta} & \mathbf{D}_{qw} & \mathbf{0} & -\gamma \mathbf{I} \end{bmatrix} \mathbf{N}_S < 0$$
(4.273)

$$\begin{bmatrix} \mathbf{R} & \mathbf{I} \\ \mathbf{I} & \mathbf{S} \end{bmatrix} \geq 0$$
(4.274)

$$\begin{bmatrix} \mathbf{L}_3 & \mathbf{I} \\ \mathbf{I} & \mathbf{J}_3 \end{bmatrix} \geq 0.$$
(4.275)

with \mathbf{N}_R and \mathbf{N}_S .

The pair of matrices $\mathbf{M}^{(n \times n_K)}$, $\mathbf{N}^{(n \times n_K)}$ and $\mathbf{L}_1^{(r_\theta \times r_\theta)}$, $\mathbf{L}_2^{(r_\theta \times r_\theta)}$ are calculated through singular value decomposition with

$$\mathbf{M}\mathbf{N}^T = \mathbf{I} - \mathbf{R}\mathbf{S}$$
(4.276)

and

$$\mathbf{L}_3 - \mathbf{J}_3^{-1} = \mathbf{L}_2^T \mathbf{L}_1^{-1} \mathbf{L}_2,$$
(4.277)

respectively.

The Lyapunov function

$$\mathbf{X}_{\text{cl}}^{((n+n_K) \times (n+n_K))} = \begin{bmatrix} \mathbf{S} & \mathbf{I} \\ \mathbf{N}^T & \mathbf{0} \end{bmatrix} \begin{bmatrix} \mathbf{I} & \mathbf{R} \\ \mathbf{0} & \mathbf{M}^T \end{bmatrix}^{-1}$$
(4.278)

and the matrix

$$\mathbf{L}^{(2r_\theta \times 2r_\theta)} = \begin{bmatrix} \mathbf{L}_1 & \mathbf{L}_2 \\ \mathbf{L}_2^T & \mathbf{L}_3 \end{bmatrix}$$
(4.279)

are built with \mathbf{M} , \mathbf{N} , \mathbf{L}_1 , \mathbf{L}_2 and the solutions \mathbf{R} , \mathbf{S} , \mathbf{L}_3 and \mathbf{J}_3 of the previous LMI.

The matrices $\psi^{((2n+2n_K+2m_\theta+m_w+2r_\theta+r_q) \times (2n+2n_K+2m_\theta+m_w+2r_\theta+r_q))}$, $\mathbf{P}^{((n_K+m_u+m_\theta+) \times (2n+2n_K+2m_\theta+m_w+2r_\theta+r_q))}$, $\mathbf{Q}^{((n_K+r_y+r_\theta) \times (2n+2n_K+2m_\theta+m_w+2r_\theta+r_q))}$

$$\psi = \begin{bmatrix} -\mathbf{X}_{\text{cl}}^{-1} & \bar{\mathbf{A}} & \bar{\mathbf{B}} & \mathbf{0} \\ \bar{\mathbf{A}}^T & -\mathbf{X}_{\text{cl}} & \mathbf{0} & \bar{\mathbf{C}}^T \\ \bar{\mathbf{B}}^T & \mathbf{0} & -\gamma \bar{\mathbf{L}} & \bar{\mathbf{D}}^T \\ \mathbf{0} & \bar{\mathbf{C}} & \bar{\mathbf{D}} & -\gamma \bar{\mathbf{J}} \end{bmatrix},$$
(4.280)

$$\mathbf{P} = \begin{bmatrix} \tilde{\mathbf{B}}^T & \mathbf{0} & \mathbf{0} & \mathbf{0} & \mathbf{0} & \tilde{\mathbf{D}}_{12}^T \end{bmatrix}, \quad \mathbf{Q} = \begin{bmatrix} \mathbf{0} & \mathbf{0} & \tilde{\mathbf{C}} & \tilde{\mathbf{D}}_{21} & \mathbf{0} & \mathbf{0} & \mathbf{0} \end{bmatrix}$$
(4.281)

are built with

$$\begin{aligned}
 \bar{\mathbf{A}}^{((n+n_K) \times (n+n_K))} &= \begin{bmatrix} \mathbf{A} & \mathbf{0} \\ \mathbf{0} & \mathbf{0} \end{bmatrix}, \quad \bar{\mathbf{B}}^{((n+n_K) \times (2m_{\theta}+m_w))} = \begin{bmatrix} \mathbf{0} & \mathbf{B}_{\theta} & \mathbf{B}_w \\ \mathbf{0} & \mathbf{0} & \mathbf{0} \end{bmatrix}, \\
 \bar{\mathbf{C}}^{((2r_{\theta}+r_q) \times (n+n_K))} &= \begin{bmatrix} \mathbf{0} & \mathbf{0} \\ \mathbf{C}_{\theta} & \mathbf{0} \\ \mathbf{C}_q & \mathbf{0} \end{bmatrix}, \quad \bar{\mathbf{D}}^{((2r_{\theta}+r_q) \times (2m_{\theta}+m_w))} = \begin{bmatrix} \mathbf{0} & \mathbf{0} & \mathbf{0} \\ \mathbf{0} & \mathbf{D}_{\theta\theta} & \mathbf{D}_{\theta w} \\ \mathbf{0} & \mathbf{D}_{q\theta} & \mathbf{D}_{qw} \end{bmatrix}, \quad (4.282) \\
 \bar{\mathbf{L}}^{((2r_{\theta}+m_w) \times (2r_{\theta}+m_w))} &= \begin{bmatrix} \mathbf{L} & \mathbf{0} \\ \mathbf{0} & \mathbf{I} \end{bmatrix}, \quad \bar{\mathbf{J}}^{((2r_{\theta}+m_w) \times (2r_{\theta}+m_w))} = \mathbf{L}^{-1}, \\
 \tilde{\mathbf{B}}^{((n+n_K) \times (n_K+m_u+m_{\theta}))} &= \begin{bmatrix} \mathbf{0} & \mathbf{B}_u & \mathbf{0} \\ \mathbf{I} & \mathbf{0} & \mathbf{0} \end{bmatrix}, \\
 \tilde{\mathbf{C}}^{((n_K+r_y+r_{\theta}) \times (n+n_K))} &= \begin{bmatrix} \mathbf{0} & \mathbf{I} \\ \mathbf{C}_y & \mathbf{0} \\ \mathbf{0} & \mathbf{0} \end{bmatrix}, \quad (4.283) \\
 \tilde{\mathbf{D}}_{12}^{((2r_{\theta}+r_q) \times (n_K+m_u+m_{\theta}))} &= \begin{bmatrix} \mathbf{0} & \mathbf{0} & \mathbf{I} \\ \mathbf{0} & \mathbf{D}_{\theta u} & \mathbf{0} \\ \mathbf{0} & \mathbf{D}_{qu} & \mathbf{0} \end{bmatrix}
 \end{aligned}$$

and

$$\tilde{\mathbf{D}}_{21}^{((n_K+r_y+r_{\theta}) \times (2m_{\theta}+m_w))} = \begin{bmatrix} \mathbf{0} & \mathbf{0} & \mathbf{0} \\ \mathbf{0} & \mathbf{D}_{y\theta} & \mathbf{D}_{yw} \\ \mathbf{I} & \mathbf{0} & \mathbf{0} \end{bmatrix}. \quad (4.284)$$

Finally, the LMI

$$\psi + \mathbf{P}^T \boldsymbol{\Omega} \mathbf{Q} + \mathbf{Q}^T \boldsymbol{\Omega}^T \mathbf{P} < 0 \quad (4.285)$$

is solved for $\boldsymbol{\Omega}^{((n_K+m_u+m_{\theta}) \times (n_K+r_y+r_{\theta}))}$. From this solution the controller matrices are extracted

$$\boldsymbol{\Omega} = \left[\begin{array}{c|cc} \mathbf{A}_0^{(K)} & \mathbf{B}_y^{(K)} & \mathbf{B}_{\theta}^{(K)} \\ \hline \mathbf{C}_u^{(K)} & \mathbf{D}_{uy}^{(K)} & \mathbf{D}_{u\theta}^{(K)} \\ \mathbf{C}_{\theta}^{(K)} & \mathbf{D}_{\theta y}^{(K)} & \mathbf{D}_{\theta\theta}^{(K)} \end{array} \right] \quad (4.286)$$

with

$$\begin{aligned}
 \mathbf{A}_0^{(K)(n_K \times n_K)} & \quad \mathbf{B}_y^{(K)(n_K \times r_y)} \quad \mathbf{B}_{\theta}^{(K)(n_K \times r_{\theta})} \\
 \mathbf{C}_u^{(K)(m_u \times n_K)} & \quad \mathbf{D}_{uy}^{(K)(m_u \times r_y)} \quad \mathbf{D}_{u\theta}^{(K)(m_u \times r_{\theta})} \\
 \mathbf{C}_{\theta}^{(K)(m_{\theta} \times n_K)} & \quad \mathbf{D}_{\theta y}^{(K)(m_{\theta} \times r_y)} \quad \mathbf{D}_{\theta\theta}^{(K)(m_{\theta} \times r_{\theta})}
 \end{aligned} \quad (4.287)$$

and the controller can be implemented using (4.262-4.263).

As an example a controller for the rejection of a disturbance with two frequency components $n_d = 2$, $f_1 \in [40, 50]$ Hz and $f_2 \in [80, 100]$ Hz acting at the output of the plant

$$G_p(z) = \frac{1-a}{z-a} \quad (4.288)$$

with $a = 0.1$ and $T = 0.001$ s is calculated using this control design and tested in simulations with the controller implemented as in (4.262-4.263).

4. LPV Gain-scheduling Control for Harmonic Disturbances with Time-varying Frequencies

The generalized plant

$$\begin{bmatrix} \mathbf{x}_{k+1} \\ \mathbf{q}_{\theta,k} \\ \mathbf{q}_k \\ \mathbf{y}_{p,k} \end{bmatrix} = \left[\begin{array}{c|ccc} \mathbf{A}_0 & \mathbf{B}_\theta & \mathbf{B}_w & \mathbf{B}_u \\ \mathbf{C}_\theta & \mathbf{D}_{\theta\theta} & \mathbf{D}_{\theta w} & \mathbf{D}_{\theta u} \\ \mathbf{C}_q & \mathbf{D}_{q\theta} & \mathbf{D}_{qw} & \mathbf{D}_{qu} \\ \mathbf{C}_y & \mathbf{D}_{y\theta} & \mathbf{D}_{yw} & \mathbf{D}_{yu} \end{array} \right] \begin{bmatrix} \mathbf{x}_k \\ \mathbf{w}_{\theta,k} \\ \mathbf{w}_k \\ \mathbf{u}_{p,k} \end{bmatrix} \quad (4.289)$$

is built with the plant, weighting functions and disturbance model.

For this example, a constant is chosen for the weighting function of the control input

$$\begin{bmatrix} x_{W_u,k+1} \\ q_{u,k} \end{bmatrix} = \left[\begin{array}{c|c} A_{W_u} & B_{W_u} \\ C_{W_u} & D_{W_u} \end{array} \right] \begin{bmatrix} x_{W_u,k} \\ u_{p,k} \end{bmatrix} = \left[\begin{array}{c|c} 0 & 0 \\ 0 & 0.001 \end{array} \right] \begin{bmatrix} x_{W_u,k} \\ u_{p,k} \end{bmatrix} \quad (4.290)$$

with $A_{W_u}^{(n_{W_u} \times n_{W_u})}$, $B_{W_u}^{(n_{W_u} \times m_u)}$, $C_{W_u}^{(r_{qu} \times n_{W_u})}$, $D_{W_u}^{(r_{qu} \times m_u)}$, $r_{qu} = m_u = 1$, $n_{W_u} = 0$ and a low pass filter for the output of the plant

$$\begin{bmatrix} x_{W_y,k+1} \\ q_{y,k} \end{bmatrix} = \left[\begin{array}{c|c} A_{W_y} & B_{W_y} \\ C_{W_y} & D_{W_y} \end{array} \right] \begin{bmatrix} x_{W_y,k} \\ y_{p,k} \end{bmatrix} = \left[\begin{array}{c|c} 0.9813 & 0.5 \\ 0.3453 & 0.7538 \end{array} \right] \begin{bmatrix} x_{W_y,k} \\ y_{p,k} \end{bmatrix} \quad (4.291)$$

with $A_{W_y}^{(n_{W_y} \times n_{W_y})}$, $B_{W_y}^{(n_{W_y} \times r_y)}$, $C_{W_y}^{(r_{qu} \times n_{W_y})}$, $D_{W_y}^{(r_{qu} \times n_{W_y})}$ and $n_{W_y} = r_y = r_{qu} = 1$.

The low pass filter is obtained through the Tustin discretization of the continuous-time state-space representation

$$\begin{bmatrix} \dot{x}_{W_y} \\ q_y \end{bmatrix} = \left[\begin{array}{c|c} A_{W_y} & B_{W_y} \\ C_{W_y} & D_{W_y} \end{array} \right] \begin{bmatrix} x_{W_y} \\ y_p \end{bmatrix} \quad (4.292)$$

with

$$A_{W_y} = -w_b a, \quad B_{W_y} = w_b \left(1 - \frac{a}{m}\right), \quad C_{W_y} = 1 \quad \text{and} \quad D_{W_y} = \frac{1}{m} \quad (4.293)$$

for

$$w_b = 2\pi 30 \frac{\text{rad}}{\text{s}}, \quad a = 0.1 \quad \text{and} \quad m = 1.5. \quad (4.294)$$

This weighting function is proposed by Skogestad & Postlethwaite (2005) for the output of the plant $y_{p,k}$. Depending on the parameters chosen for w_b , a and m different controllers are obtained in the control design. The controller obtained with these weighting functions achieved a good performance in closed-loop.

The disturbance model is given as

$$\begin{bmatrix} \mathbf{x}_{d,k+1} \\ \mathbf{q}_{\theta,k} \\ \mathbf{y}_{d,k} \end{bmatrix} = \left[\begin{array}{c|cc} \mathbf{A}_{d,0} & \mathbf{B}_{d,\theta} & \mathbf{B}_d \\ \mathbf{C}_{d,\theta} & \mathbf{D}_{\theta\theta} & \mathbf{D}_{\theta w} \\ \mathbf{C}_d & \mathbf{D}_{y\theta} & \mathbf{D}_{yw} \end{array} \right] \begin{bmatrix} \mathbf{x}_{d,k} \\ \mathbf{w}_{\theta,k} \\ \mathbf{w}_{d,k} \end{bmatrix} \quad (4.295)$$

with

$$\mathbf{A}_{d,0}^{(2n_d \times 2n_d)} = \begin{bmatrix} 0 & 1 & 0 & 0 \\ -r^2 & a_{0,1} & 0 & 0 \\ 0 & 0 & 0 & 1 \\ 0 & 0 & -r^2 & a_{0,2} \end{bmatrix}, \quad (4.296)$$

$$[\mathbf{B}_{d,\theta} \quad \mathbf{B}_d]^{(2n_d \times (m_\theta + m_w))} = \left[\begin{array}{cc|cc} 0 & 0 & 0.001 & 0 \\ a_{1,1} & 0 & 0.001 & 0 \\ 0 & 0 & 0 & 0.001 \\ 0 & a_{1,2} & 0 & 0.001 \end{array} \right], \quad (4.297)$$

$$\left[\begin{array}{c} \mathbf{C}_{d,\theta} \\ \mathbf{C}_d \end{array} \right]^{((r_\theta + r_{y_d}) \times (2n_d))} = \left[\begin{array}{cccc} 0 & 1 & 0 & 0 \\ 0 & 0 & 0 & 1 \\ \hline 1 & 0 & 1 & 0 \end{array} \right], \quad (4.298)$$

$$\left[\begin{array}{cc} \mathbf{D}_{\theta\theta} & \mathbf{D}_{\theta w} \\ \mathbf{D}_{y\theta} & \mathbf{D}_{yw} \end{array} \right]^{((r_\theta + r_{y_d}) \times (m_\theta + m_w))} = \left[\begin{array}{cc|cc} 0 & 0 & 0 & 0 \\ 0 & 0 & 0 & 0 \\ \hline 0 & 0 & 0 & 0 \end{array} \right] \quad (4.299)$$

for

$$[a_{0,1} \quad a_{0,2}] = \left[\frac{a_{\max,1} + a_{\min,1}}{2} \quad \frac{a_{\max,2} + a_{\min,2}}{2} \right] = [1.9194 \quad 1.6852], \quad (4.300)$$

$$[a_{1,1} \quad a_{1,2}] = \left[\frac{a_{\max,1} - a_{\min,1}}{2} \quad \frac{a_{\max,2} - a_{\min,2}}{2} \right] = [-0.0175 \quad -0.0673], \quad (4.301)$$

$$[a_{\max,1} \quad a_{\max,2}] = [2r \cos(2\pi 50T) \quad 2r \cos(2\pi 100T)] = [1.9019 \quad 1.6179], \quad (4.302)$$

$$[a_{\min,1} \quad a_{\min,2}] = [2r \cos(2\pi 40T) \quad 2r \cos(2\pi 80T)] = [1.9370 \quad 1.7524], \quad (4.303)$$

$r = 0.9999$, $T = 0.001$ s, $n_d = m_w = m_\theta = r_\theta = 2$ and $r_{y_d} = 1$.

Now, combining plant, disturbance model and weighting functions the generalized plant is built as

$$\left[\begin{array}{c} \mathbf{x}_{k+1} \\ \mathbf{q}_{\theta,k} \\ \mathbf{q}_k \\ \mathbf{y}_{p,k} \end{array} \right] = \left[\begin{array}{c|ccc} \mathbf{A}_0 & \mathbf{B}_\theta & \mathbf{B}_w & \mathbf{B}_u \\ \mathbf{C}_\theta & \mathbf{D}_{\theta\theta} & \mathbf{D}_{\theta w} & \mathbf{D}_{\theta u} \\ \mathbf{C}_q & \mathbf{D}_{q\theta} & \mathbf{D}_{qw} & \mathbf{D}_{qu} \\ \mathbf{C}_y & \mathbf{D}_{y\theta} & \mathbf{D}_{yw} & \mathbf{D}_{yu} \end{array} \right] \left[\begin{array}{c} \mathbf{x}_k \\ \mathbf{w}_{\theta,k} \\ \mathbf{w}_k \\ \mathbf{u}_{p,k} \end{array} \right] \quad (4.304)$$

with

$$\mathbf{A}_0^{(n \times n)} = \left[\begin{array}{ccc} A_p & B_p \mathbf{C}_d & 0 \\ \mathbf{0} & \mathbf{A}_{d,0} & \mathbf{0} \\ B_{W_y} C_p & \mathbf{0} & A_{W_y} \end{array} \right], \quad (4.305)$$

$$[\mathbf{B}_\theta \quad \mathbf{B}_w \quad \mathbf{B}_u]^{(n \times (m_\theta + m_w + m_u))} = \left[\begin{array}{ccc} \mathbf{0} & \mathbf{0} & B_p \\ \mathbf{B}_{d,\theta} & \mathbf{B}_d & \mathbf{0} \\ \mathbf{0} & \mathbf{0} & 0 \end{array} \right], \quad (4.306)$$

$$\left[\begin{array}{c} \mathbf{C}_\theta \\ \mathbf{C}_q \\ \mathbf{C}_y \end{array} \right]^{((r_\theta + r_q + r_y) \times n)} = \left[\begin{array}{ccc} \mathbf{0} & \mathbf{C}_{d,\theta} & \mathbf{0} \\ \mathbf{0} & \mathbf{0} & 0 \\ D_{W_y} C_p & \mathbf{0} & C_{W_y} \\ C_p & \mathbf{0} & 0 \end{array} \right], \quad (4.307)$$

$$\begin{bmatrix} D_{\theta\theta} & D_{\theta w} & D_{\theta u} \\ D_{q\theta} & D_{qw} & D_{qu} \\ D_{y\theta} & D_{yw} & D_{yu} \end{bmatrix}^{((r_\theta+r_q+r_y) \times (m_\theta+m_w+m_u))} = \begin{bmatrix} \mathbf{0} & \mathbf{0} & \mathbf{0} \\ \mathbf{0} & \mathbf{0} & D_{W_u} \\ \mathbf{0} & \mathbf{0} & 0 \\ \hline \mathbf{0} & \mathbf{0} & 0 \end{bmatrix}, \quad (4.308)$$

$$\begin{bmatrix} x_{p,k+1} \\ y_{p,k} \end{bmatrix} = \left[\begin{array}{c|c} A_p & B_p \\ \hline C_p & D_p \end{array} \right] \begin{bmatrix} x_{p,k} \\ u_{p,k} \end{bmatrix} = \left[\begin{array}{c|c} 0.1 & 1 \\ \hline 0.9 & 0 \end{array} \right] \begin{bmatrix} x_{p,k} \\ u_{p,k} \end{bmatrix}, \quad (4.309)$$

$A_p^{(n_p \times n_p)}, B_p^{(n_p \times m_u)}, C_p^{(r_y \times n_p)}, D_p^{(r_y \times m_u)}$, $n_p = m_u = r_y = 1$, $n = n_p + 2n_d + n_{W_u} + n_{W_y}$ and $r_q = r_{qu} + r_{qy}$.

The LMI of (4.273-4.275) is solved for

$$\mathbf{R}^{(n \times n)} = 10^4 \begin{bmatrix} 0.3010 & 0 & 0 & 0 & 0 & -0.5910 \\ 0 & 0.0016 & 0.0015 & 0 & 0 & 0 \\ 0 & 0.0015 & 0.0016 & 0 & 0 & 0 \\ 0 & 0 & 0 & 0.0006 & 0.0005 & 0 \\ 0 & 0 & 0 & 0.0005 & 0.0006 & 0 \\ -0.5910 & 0 & 0 & 0 & 0 & 1.1611 \end{bmatrix}, \quad (4.310)$$

$$\mathbf{S}^{(n \times n)} = 10^4 \begin{bmatrix} 0.3793 & -0.3030 & 0.0564 & -0.3836 & 0.1371 & 0 \\ -0.3030 & 1.4080 & -0.9939 & 0.3039 & -0.2366 & 0 \\ 0.0564 & -0.9939 & 0.8481 & 0.0845 & -0.0474 & 0 \\ -0.3836 & 0.3039 & 0.0845 & 1.3537 & -0.9780 & 0 \\ 0.1371 & -0.2366 & -0.0474 & -0.9780 & 0.9888 & 0 \\ 0 & 0 & 0 & 0 & 0 & 1.3388 \end{bmatrix}, \quad (4.311)$$

$$\mathbf{J}_3^{(r_\theta \times r_\theta)} = 10^4 \begin{bmatrix} 8.5564 & 0 \\ 0 & 3.0146 \end{bmatrix}, \quad \mathbf{L}_3^{(m_\theta \times m_\theta)} = 10^4 \begin{bmatrix} 1.6353 & 0 \\ 0 & 1.6294 \end{bmatrix} \quad (4.312)$$

where $\mathbf{R} = \mathbf{R}^T > 0$, $\mathbf{S} = \mathbf{S}^T > 0$ and the diagonal matrices \mathbf{L}_3 and \mathbf{J}_3 .

These solutions are used with the matrices

$$\mathbf{M}^{(n \times n_K)} = 10^4 \begin{bmatrix} -0.6077 & 0.0013 & 0.0008 & -0.0007 & -0.0013 & 0.0016 \\ 0.0002 & -0.0286 & 0.0052 & 0.0039 & -0.0027 & -0.0002 \\ 0.0002 & -0.0252 & -0.0012 & -0.0037 & 0.0037 & 0.0004 \\ 0.0001 & -0.0081 & -0.0131 & -0.0042 & -0.0024 & -0.0002 \\ 0 & -0.0016 & -0.0085 & 0.0093 & 0.0014 & 0.0003 \\ 1.1938 & 0.0007 & 0.0004 & -0.0004 & -0.0007 & 0.0008 \end{bmatrix}, \quad (4.313)$$

$$\mathbf{N}^{(n \times n_K)} = 10^4 \begin{bmatrix} 0.1878 & -0.0133 & -0.0058 & 0.0043 & 0.0032 & -0.001 \\ -0.15 & 0.0222 & -0.0078 & -0.0042 & -0.0009 & -0.001 \\ 0.0279 & -0.0077 & 0.0065 & 0.0035 & -0.0033 & -0.0011 \\ -0.1899 & 0.0219 & 0.0102 & 0.0019 & 0.0026 & -0.0003 \\ 0.0679 & -0.0155 & 0.0055 & -0.0090 & 0.0012 & -0.0005 \\ -1.3021 & -0.0086 & -0.001 & 0.0004 & 0.0002 & 0 \end{bmatrix}, \quad (4.314)$$

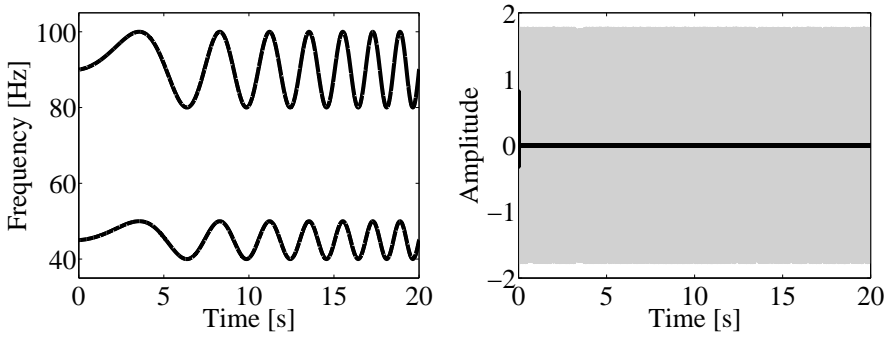


Figure 4.10: Variations of the disturbance frequencies (left) and simulation results (right) in closed loop (black) and open loop (gray)

$$\mathbf{L}_1^{(r_\theta \times r_\theta)} = \begin{bmatrix} 1 & 0 \\ 0 & 1 \end{bmatrix} \quad \text{and} \quad \mathbf{L}_2^{(r_\theta \times r_\theta)} = \begin{bmatrix} 127.878 & 0 \\ 0 & 127.6487 \end{bmatrix} \quad (4.315)$$

calculated through singular value decomposition (4.276-4.277) to build the matrices $\mathbf{X}_{\text{cl}}^{((n+n_K) \times (n+n_K))}$ and $\mathbf{L}^{(2r_\theta \times 2r_\theta)}$ as in (4.278-4.279).

Finally the basic LMI (4.285) is solved for Ω obtaining the following state-space representation of the controller in LFT-form

$$\begin{bmatrix} \mathbf{x}_{K,k+1} \\ u_{p,k} \\ \tilde{\mathbf{q}}_{\theta,k} \end{bmatrix} = \begin{bmatrix} \mathbf{A}_0^{(K)} & \mathbf{B}_y^{(K)} & \mathbf{B}_\theta^{(K)} \\ \mathbf{C}_u^{(K)} & \mathbf{D}_{uy}^{(K)} & \mathbf{D}_{u\theta}^{(K)} \\ \mathbf{C}_\theta^{(K)} & \mathbf{D}_{\theta y}^{(K)} & \mathbf{D}_{\theta\theta}^{(K)} \end{bmatrix} \begin{bmatrix} \mathbf{x}_{K,k} \\ y_{p,k} \\ \tilde{\mathbf{w}}_{\theta,k} \end{bmatrix} \quad (4.316)$$

with

$$\mathbf{A}_0^{(K)(n_K \times n_K)} = \begin{bmatrix} 1.0414 & -0.0003 & -0.0023 & 0.0018 & 0.0021 & 0.0036 \\ -8.9562 & 1.0432 & 0.3814 & -0.2643 & -0.3006 & -0.4741 \\ -2.1868 & -0.2254 & 1.2483 & -0.3017 & 0.0923 & -0.2991 \\ -1.4087 & -0.1923 & 1.1161 & 0.4414 & 0.5639 & 0.373 \\ -3.8544 & 0.2179 & 0.1762 & -0.1833 & 0.7428 & 0.6424 \\ 4.6318 & 0.0502 & 0.0216 & -0.0053 & 0.1237 & -0.4213 \end{bmatrix}, \quad (4.317)$$

$$\begin{bmatrix} \mathbf{B}_y^{(K)} & \mathbf{B}_\theta^{(K)} \end{bmatrix}^{(n_K \times (r_y + r_\theta))} = \begin{bmatrix} 0.6489 & 0 & -0.0001 \\ -20.1008 & 0.0024 & 0.015 \\ -4.9083 & -0.0068 & 0.0072 \\ -3.1609 & -0.0082 & 0.0369 \\ -8.6493 & 0.0069 & 0.0098 \\ 10.3936 & 0.0006 & 0.0013 \end{bmatrix}, \quad (4.318)$$

$$\begin{bmatrix} \mathbf{C}_u^{(K)} \\ \mathbf{C}_\theta^{(K)} \end{bmatrix}^{((m_u + m_\theta) \times n_K)} = \begin{bmatrix} -0.9911 & 0.0521 & 0.0228 & -0.0216 & -0.0205 & -0.0307 \\ -2.9998 & 6.9502 & -2.8504 & -0.0864 & -7.0382 & -9.4264 \\ -5.8742 & 0.4058 & 5.7833 & -3.4744 & 1.6679 & -2.8869 \end{bmatrix} \quad (4.319)$$

4. LPV Gain-scheduling Control for Harmonic Disturbances with Time-varying Frequencies

and

$$\begin{bmatrix} D_{uy}^{(K)} & \mathbf{D}_{u\theta}^{(K)} \\ \mathbf{D}_{\theta y}^{(K)} & \mathbf{D}_{\theta\theta}^{(K)} \end{bmatrix}^{((m_u+m_\theta) \times (r_y+r_\theta))} = \begin{bmatrix} -1.4997 & 0 & 0 \\ -6.7359 & 0 & 0 \\ -13.1841 & 0 & 0 \end{bmatrix}. \quad (4.320)$$

This controller is tested in simulations for the rejection of a disturbance containing time-varying frequencies acting at the output of the plant. The variations of the frequencies and the simulation results are shown in Fig. 4.10.

Chapter 5

Experimental Results

All the controllers designed in the previous chapters for the rejection of harmonic disturbances with time-varying frequencies are validated with experimental results in three different test beds. A MIMO AVC system built in a Golf VI Variant for the reduction of the engine-induced vibrations, a SISO AVC test bed and an ANC system.

In this chapter, the experimental setups for the three different test beds are described and results for all the LPV control structures presented in this thesis are shown. The validation of the controllers is done with experimental results for disturbances with constant frequencies and with time-varying frequencies, since the control design explained in this thesis is focused on LPV techniques. The controllers presented here, are gain-scheduling controllers with the frequency of the disturbance as gain-scheduling parameter. Therefore, it is assumed that the frequency of the disturbance is known or can be measured. The LPV controllers were extensively tested, this chapter shows only a selection of the experimental results.

AVC Golf VI Experimental Setup

An AVC system is installed in a Golf VI variant for the reduction of engine-induced vibrations. A photograph and a schematic representation of the experimental setup are shown in Fig. 5.1. This setup is used to implement MIMO LPV AVC controllers for the reduction of the engine-induced vibrations in the car body.

Two inertia mass actuators (shakers) and two accelerometers are attached to the engine mounts. The battery is moved to the trunk of the car and the resulting space is used for the power amplifiers driving the actuators. Anti-aliasing filters are applied to the accelerometer signals and reconstruction filters to the control signals. The controller is implemented on a rapid control prototyping unit (dSPACE MicroAutoBox) and it uses the sensor signals to generate the control signals of the shakers. The filters and the rapid control prototyping unit were placed on the trunk of the car. All the cables between sensors and control unit and between actuators and control unit are hidden in the car body. The engine speed (scheduling parameter $f_{0,k}$) is measured directly from the CAN Bus.

The anti-aliasing filters and the reconstruction filters are low pass filters with a cut-off frequency of 500 Hz. The filters were designed taking into account the frequency component range of the harmonic disturbances (engine-induced vibrations). Two Pololu High-Power Motor Driver 18v25 CS are used as amplifiers to drive the shakers of the engine mounts. An accelerometer of ± 1.5 g was used for the right side (drive direction) and an accelerometer of ± 13.3 g for the left side (drive direction).

The main objective of this setup is the application and validation of LPV controllers in AVC and ANC real applications. At this point, it is important to notice that the Golf VI Variant does not suffer from vibrations problems. Experimental results of LPV

5. Experimental Results

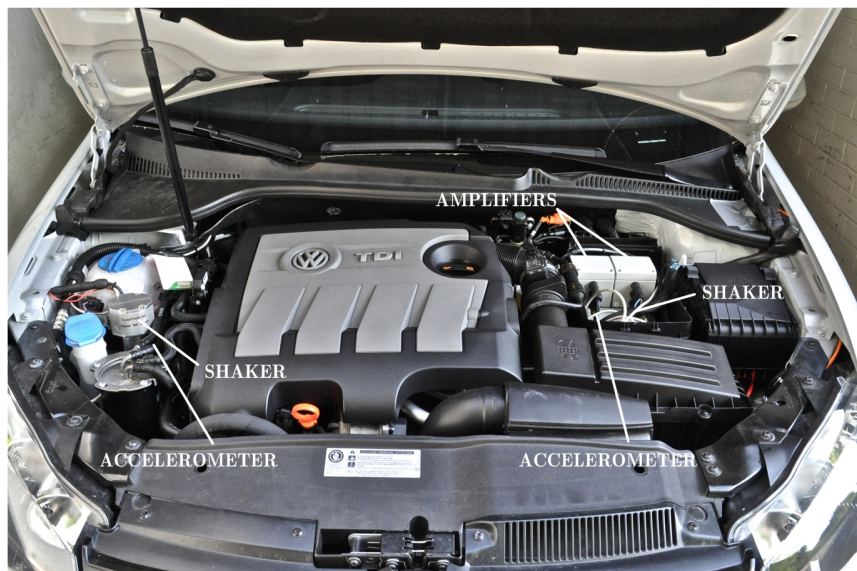
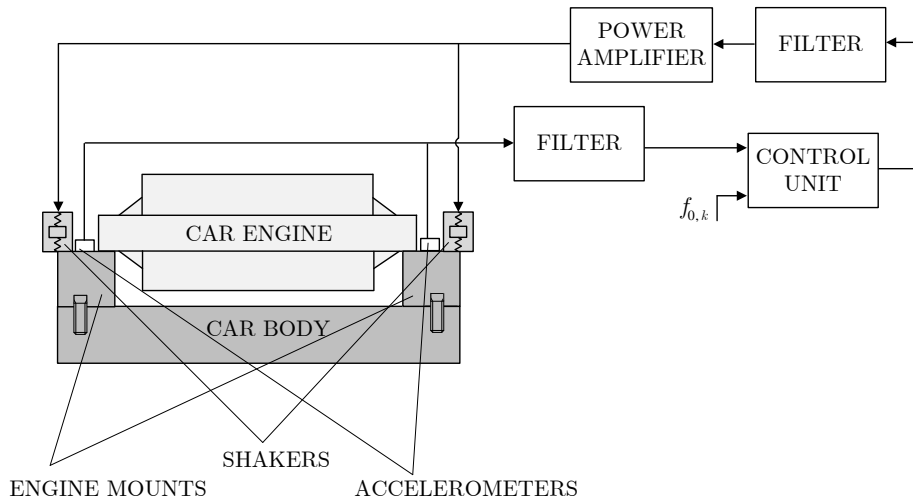


Figure 5.1: Schematic representation (top) and photograph (bottom) of the experimental setup

controllers for the reduction of engine-induced vibrations are shown in Sec. 5.3.1. This experimental setup permits the validation of MIMO LPV controllers.

AVC Test Bed Experimental Setup

The scheme and a photograph of the AVC test bed are shown in Fig. 5.2. Two shakers (inertia mass actuators) are attached to a steel cantilever beam. One shaker acts as the disturbance source and the other shaker is driven by the control signal to counteract this disturbance. An accelerometer is used to measure the output signal. An anti-aliasing filter is applied to the output signal and a reconstruction filter to the control input with a cut-off frequency of 500 Hz. The controller is also implemented in rapid tool prototyping unit (dSPACE MicroAutoBox).

Two Elmo 15/60 Violin current amplifiers are used as power amplifiers. An accelerometer of a range of ± 1.3 g is placed at the tip of the beam. This setup allows a hard test of the LPV controllers for unrealistic behaviors of the disturbance frequencies such as step changes in the frequency variations or sweep changes of the disturbance frequencies, since the disturbance shaker is driven with the MicroAutoBox. It is assumed for the controller validation that the frequency is known or it can be measured. Experimental results with this setup are shown in Secs.5.3.2 and 5.5.

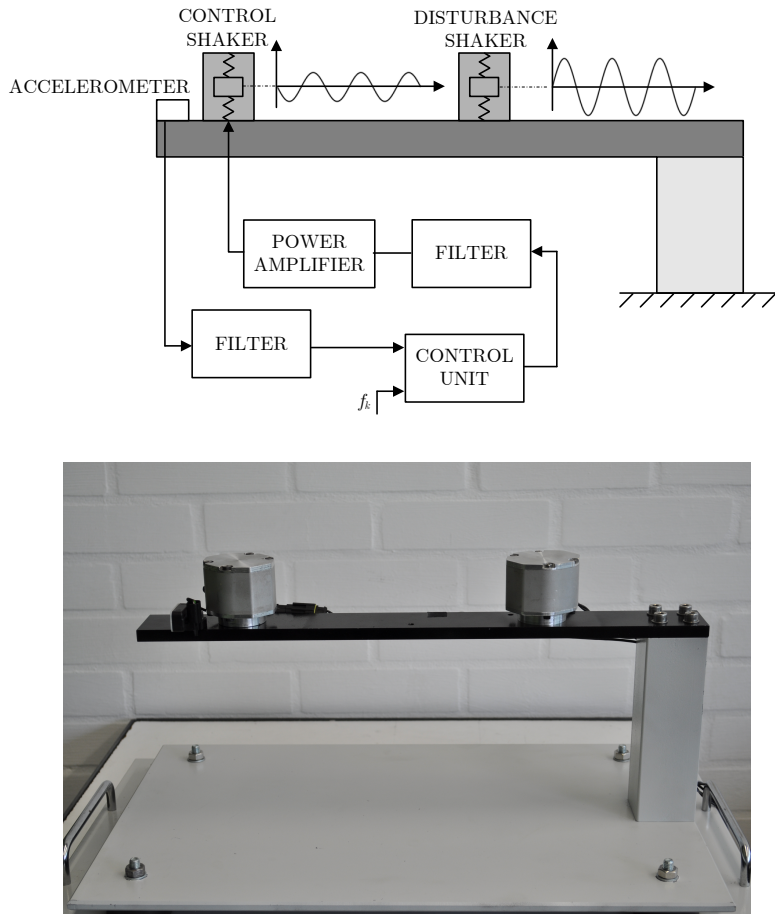


Figure 5.2: Schematic representation (top) and photograph (bottom) of the experimental setup for the AVC system

ANC Test Bed Experimental Setup

The experimental setup of the ANC system is shown schematically in Fig. 5.3. An external loudspeaker is used to generate a harmonic disturbance. A headset PXC 300 provided by Sennheiser is used. This headset has one microphone on each loudspeaker. The objective is to cancel the disturbance with the loudspeakers of the headset using the measured signals of the microphones. An anti-aliasing filter is applied to the output signal and a reconstruction filter to the control input with a cut off frequency of 500 Hz.

For the control design this setup can be considered as two independent SISO systems. One LPV controller is calculated for one side and the same LPV controller can be implemented for the other side too. The control algorithms are implemented on a MicroAutoBox from dSPACE.

The characteristics of the LPV controllers would also allow for an application without measurements of the disturbance frequency. For example, an ANC headset is possible where the frequency to be rejected can be readjusted manually by the user to the dominant frequency that is present in a noisy environment.

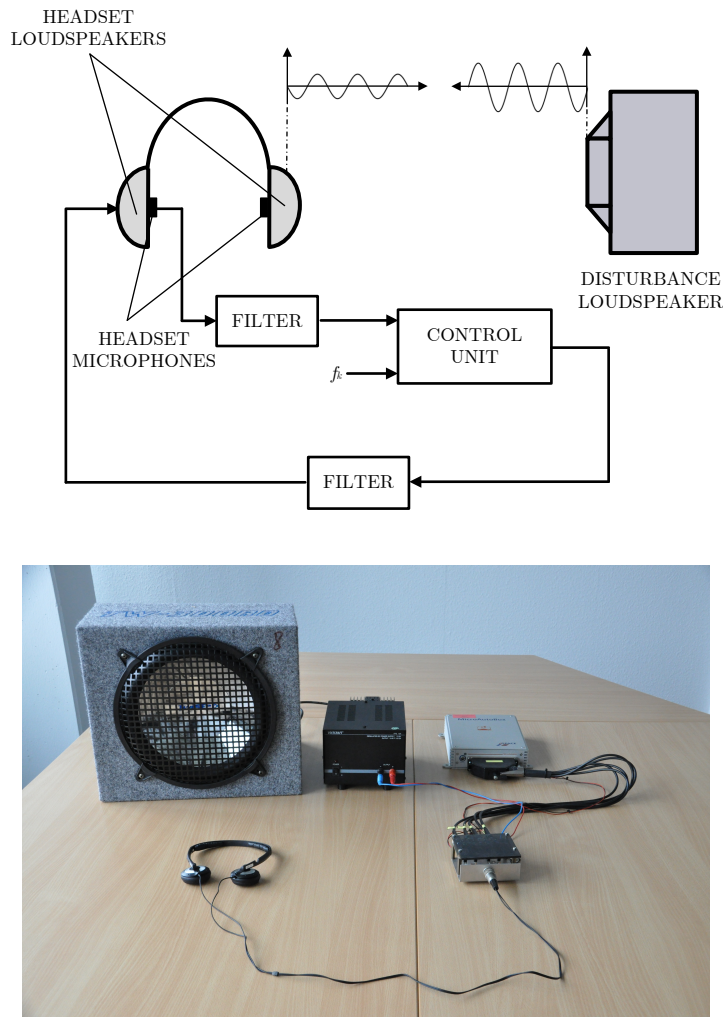


Figure 5.3: Schematic representation (top) and photograph (bottom) of the experimental setup for the ANC system

pLPV Disturbance Observer Controller Experimental Results

The pLPV disturbance-observer controller of Sec. 4.1.3 is validated in a MIMO AVC system (Golf VI Variant) and in a SISO AVC system (test bed). In these applications, the polynomial approximation (4.11) and a triangle as polytope is used to reduce the complexity of the interpolation and to reduce the number of gain-scheduling parameters to two. Excellent results are achieved for the reduction of vibrations for disturbances with harmonically related frequency components. Nine frequency components of the engine-induced vibrations are reduced in the Golf VI Variant and 26 frequency components are reduced in the AVC test bed.

Golf VI Variant

Black-box system identification techniques with a sampling frequency of 2 kHz are used to obtain a state-space representation of the 2x2 MIMO system between outputs and inputs of the control unit. The identified system of order 22 is used with the control design explained in Sec. 4.1.3 to obtain a pLPV gain-scheduling controller with the frequency of the disturbance as gain-scheduling parameter. The engine-induced vibrations are harmonically related therefore, the polynomial approximation (4.11) can be used with a triangle as polytope to reduce the number of vertices and to simplify the interpolation. The control algorithm is implemented on a rapid control prototyping unit. The controller obtained with the pLPV control design is interpolated using the fundamental frequency $f_{0,k}$ (half engine order) taken from the CAN bus with a very simple matrix multiplication from three controller vertices, see (4.53).

In this section, experimental results obtained with a 2x2 MIMO controller designed with the methods described in Sec. 4.1.3 is validated experimentally in a Golf VI Variant. The controller is designed for the rejection of nine frequency components $f_{0,k}[4 \ 5 \dots 12]$ with $f_{0,k} \in [25, 28.75]$ Hz being the half engine order. Controllers for an engine speed range of 1200 rpm were designed and they worked well in practice, but the stability was not guaranteed. Before testing the controllers in the car, test drives to record the accelerations and the engine speed from the CAN bus were realized. These recorded signals were used in simulations to test that the control signals were not saturated and to test the stability of the closed-loop system. The controller was validated in the Golf VI Variant once it was successfully tested in simulations with the real measurements for the designed frequencies.

The amplitude frequency responses in closed loop and open loop are shown in Fig. 5.4 for a constant engine speed of 3000 rpm (corresponding to $f_{0,k} = 25$ Hz). The upper left amplitude frequency response corresponds to the transfer function between shaker and accelerometer of the driver side. The lower right amplitude frequency response is the transfer function between shaker and accelerometer of the rider side. The upper right amplitude frequency response is the transfer function from shaker of the rider side to accelerometer of the driver side. The lower left amplitude frequency response corresponds to the transfer function from shaker of the driver side to accelerometer of the rider side. From the amplitude frequency responses in closed loop a very good disturbance rejection is expected for a disturbance containing the constant frequency components $f_{0,k}[4 \ 5 \dots 12]$ with a fundamental frequency $f_{0,k} = 25$ Hz.

5. Experimental Results

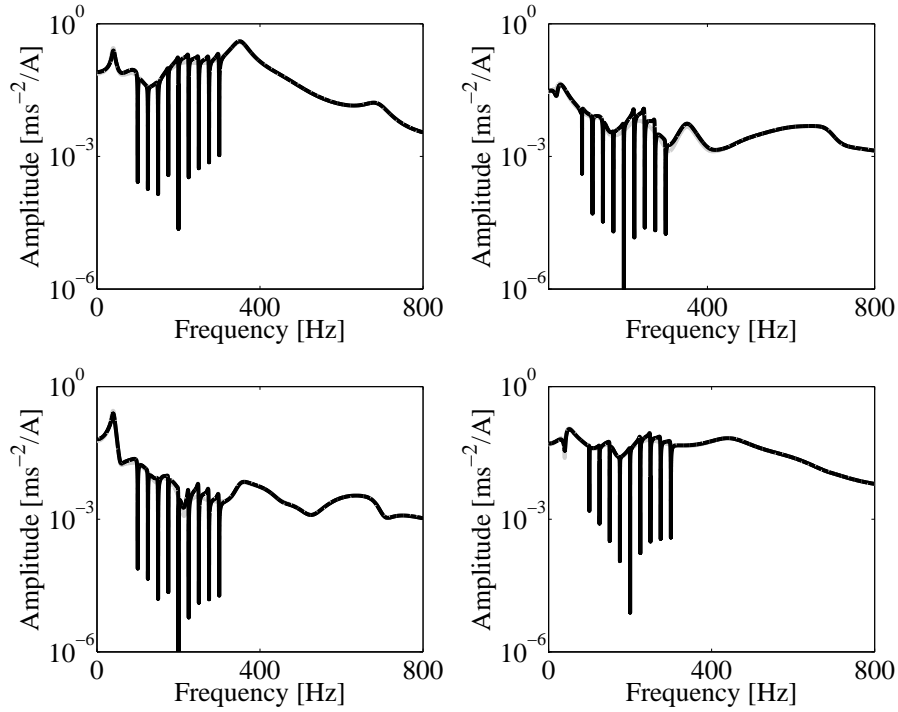


Figure 5.4: Open loop (gray) and closed loop (black) amplitude frequency responses for a sampling frequency of 2 kHz

The controller has been validated experimentally with all the car gears. In the following, results in third gear are shown. Accelerations measured in test drives for a constant engine speed of approximately 3420 rpm are shown in Fig. 5.5 for a control sequence off/on/off. Excellent results are achieved as shown by the spectra of the measured accelerations. The frequency components $f_{0,k}[4 \ 5 \ \dots \ 12]$ with the fundamental frequency $f_{0,k} = 28.5$ Hz are suppressed.

Further test drives are realized to test the MIMO LPV controller with time-varying engine speeds. The variations of the engine speed and the accelerations measured on the driver and rider side for time-varying engine speeds are shown in Fig. 5.6. The controller is switched on for the first one hundred seconds and switched off for the next one hundred seconds.

The effectiveness of the controller for the reduction of the engine-induced vibrations with time-varying engine speeds is shown with the time-frequency diagrams in Fig. 5.7. The frequency components ($f_{0,k}[4 \ 5 \ \dots \ 12]$) of the accelerations are suppressed during the first hundred seconds. Excellent results are achieved for the reduction of the engine-induced vibrations with the discrete-time MIMO LPV observer-based controller for constant and time-varying engine speeds. The controller remained stable even for fast changes of the engine speed since LPV gain-scheduling control design techniques are used.

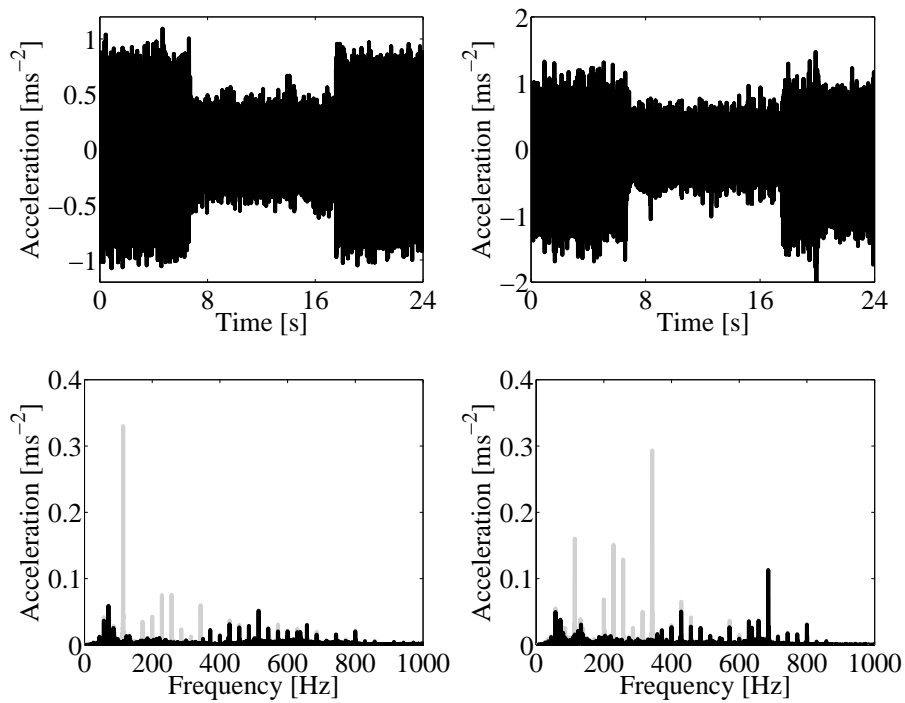


Figure 5.5: Acceleration measured by the accelerometers (top) for approximately 3420 rpm and fourier transformation (bottom) in open loop (gray) and closed loop (black). The control sequence is off/on/off

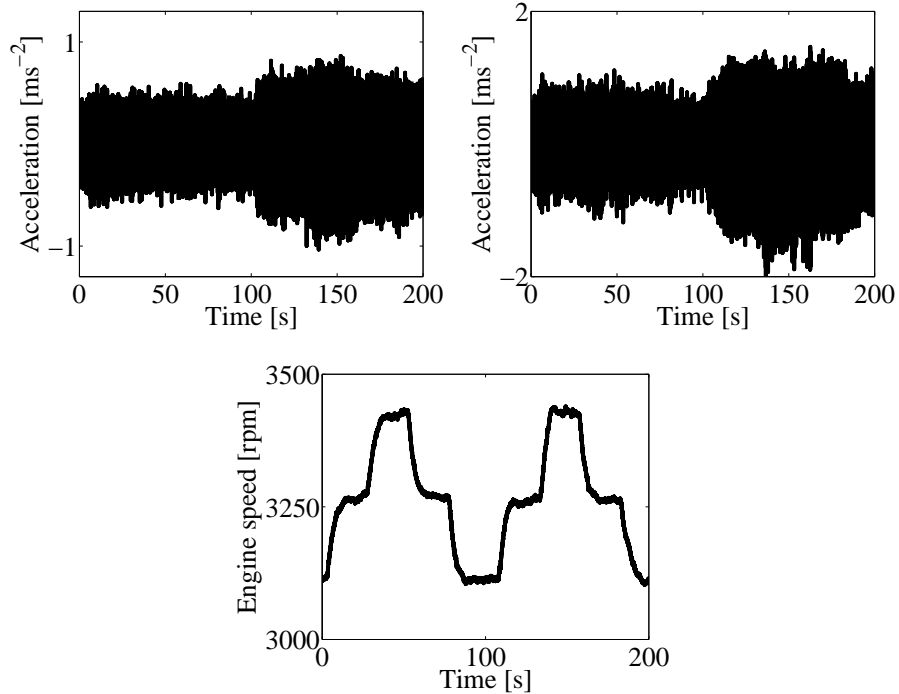


Figure 5.6: Acceleration measured by the accelerometers (top) and variations of the engine speed (bottom) for a control sequence on/off

5. Experimental Results

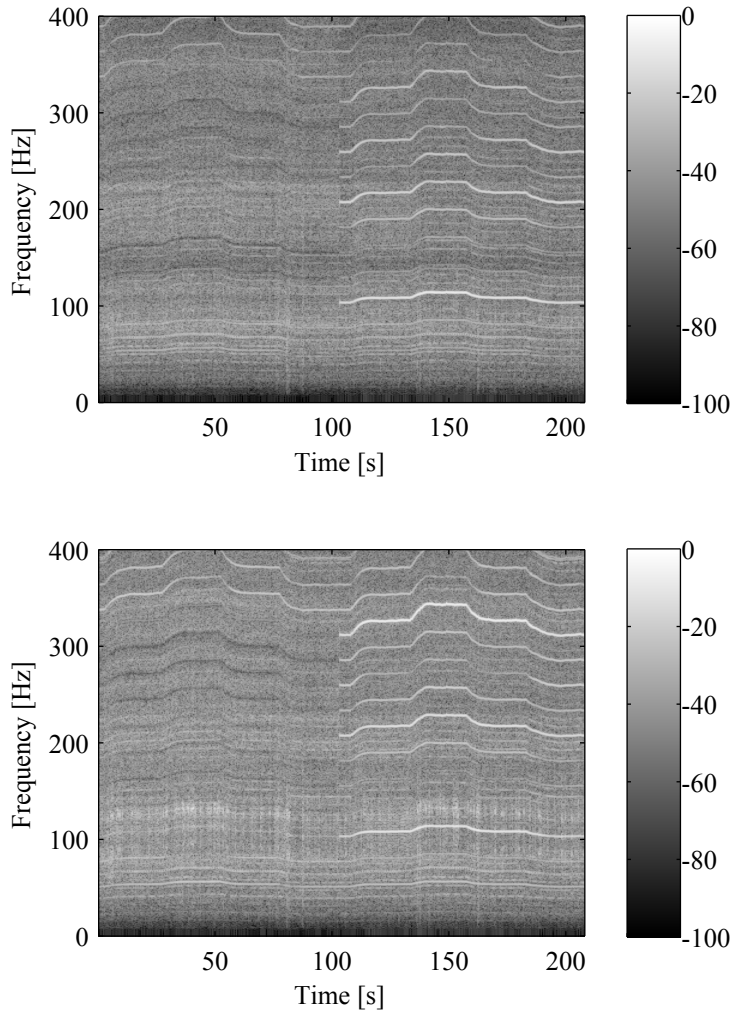


Figure 5.7: Spectrograms for the acceleration measured by the accelerometers on the left side (top) and right side (bottom) for a sampling frequency of 2 kHz

AVC Test Bed

A pLPV disturbance-observer controller with the polynomial approximation and sampling frequency of 1 kHz is validated experimentally on the AVC test bed. The controller is implemented on the MicroAutoBox from dSPACE.

The transfer function between output and input of the control unit is obtained with standard black-box identification techniques, resulting in a transfer function of order 10. The controller is designed for the rejection of a harmonic disturbance with 26 frequency components with a fundamental frequency $f_{0,k}$ between 100 Hz and 110 Hz. The disturbance frequency components are $\mathbf{f} = [f_{0,k} \ 1.1f_{0,k} \ \dots \ 3.5f_{0,k}]$. At each sampling time the controller is interpolated from only three controller vertices. The disturbance frequencies are harmonically related and the polynomial approximation can be used with a triangle as polytope to reduce the number of vertices.

Amplitude frequency responses in closed loop and open loop are shown in Fig. 5.8 for constant fundamental frequencies $f_{0,k}$ of 100 Hz and 110 Hz. A constant state-feedback gain \mathbf{K}_p is calculated to damp the resonance frequencies as it can be seen in Fig. 5.8.

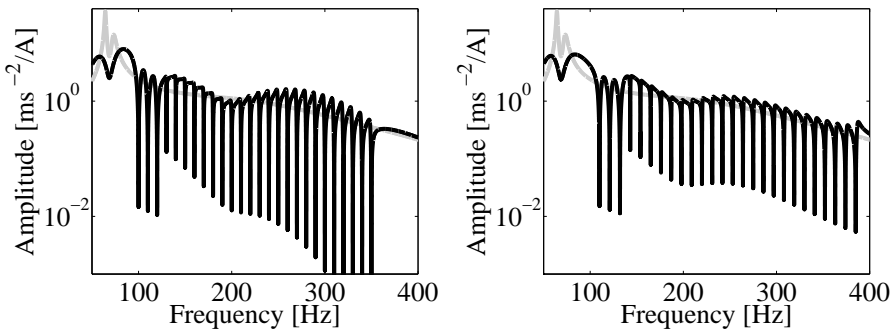


Figure 5.8: Amplitude frequency responses in open loop (gray) and closed loop (black) for a fundamental frequency of 100 Hz (left) and 110 Hz (right) for a sampling frequency of 1 kHz

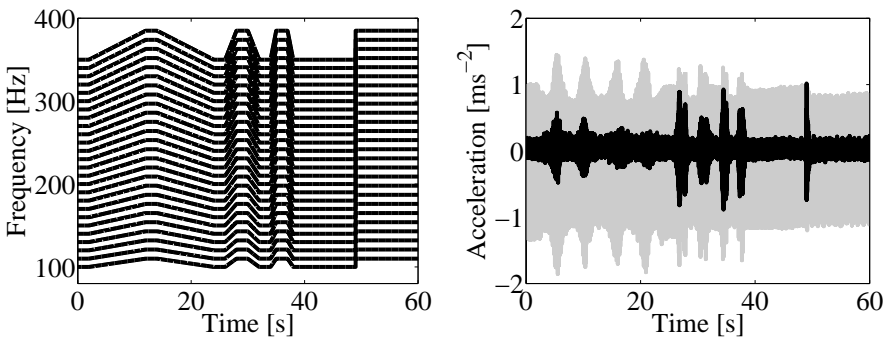


Figure 5.9: Time-varying frequencies behavior (top) and accelerations measured (bottom) in open loop (gray) and closed loop (black)

Experimental results for a disturbance with time-varying frequencies are shown in Fig. 5.9. Excellent disturbance rejection is achieved for 26 frequency components with only two gain-scheduling parameters. As predicted by theory, the controller remained stable even for fast variations of the frequency components (step changes, which is not very realistic).

In this section, experimental results for the disturbance-observer controller are shown. The error-filter controller also achieved excellent results with 26 frequency components and a sampling frequency of 1 kHz for exactly the same range of frequencies (see next section). It is extremely difficult to compare all the approaches presented in this thesis. A different controller is obtained with a small change of the weighting functions or the weighting matrices. It can not be assured that the calculated controller using some weighting matrices is the best controller of the pLPV observer-based control design. The main advantage of the LPV approaches compared with adaptive filtering (FxLMS) is that the stability can be guaranteed even for unrealistic changes of the gain-scheduling parameters since one Lyapunov function was found for the whole range of variation of the gain-scheduling parameters (Lyapunov stability).

pLPV Error Filter Controller Experimental Results

The pLPV error-filter controller is validated experimentally in the AVC test bed. The controller is designed for the rejection of $\mathbf{f}_k = [f_{0,k} \ 1.1f_{0,k} \ \dots \ 3.5f_{0,k}]$ (26 frequency components) with a fundamental frequency $f_{0,k} \in [100, 110]$ Hz. Since the frequencies of the disturbances are harmonically related, the polynomial approximation and a triangle as polytope are here used. This leads to a controller calculated at each sampling time as a result of a simple matrix multiplication. Amplitude frequencies responses for a fundamental frequency of $f_{0,k} = 100$ Hz and $f_{0,k} = 110$ Hz are shown in Fig. 5.10. From this figure it is expected a very good disturbance rejection for the case of constant disturbance frequencies. Some frequency components are amplified, if this is tolerable or not depends on the frequency components of the disturbance.

Experimental results for a disturbance with time-varying frequencies are shown in Fig. 5.11. Here it is confirmed what was expected from Fig. 5.10. Very good results are achieved for constant and time-varying frequencies using only two gain-scheduling parameters since the polynomial approximation was used. Here it is important to notice that the LFT approaches or the pLPV approaches without polynomial approximation need the same number of scheduling parameters as frequency components contained in the disturbance.

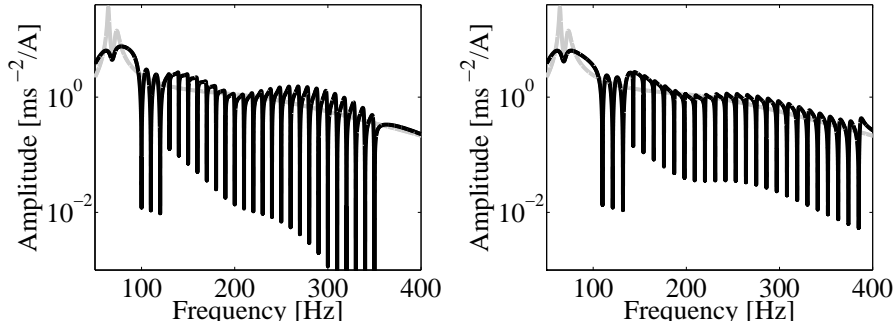


Figure 5.10: Amplitude frequency responses in open loop (gray) and closed loop (black) for a fundamental frequency of 100 Hz (left) and 110 Hz (right) for a sampling frequency of 1 kHz

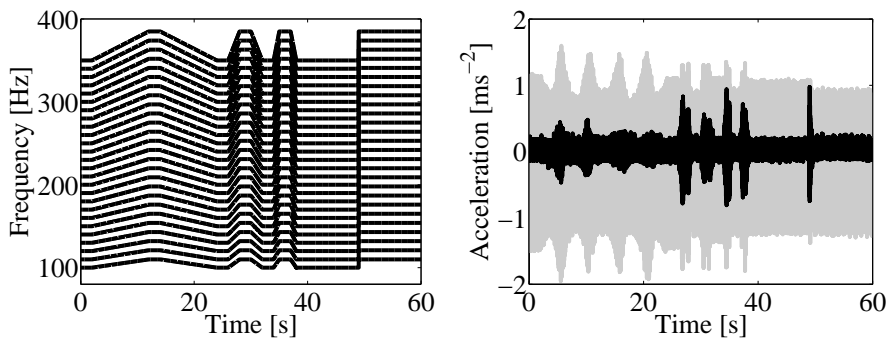


Figure 5.11: Time-varying frequencies behavior (top) and accelerations measured (bottom) in open loop (gray) and closed loop (black)

The main advantage of the pLPV error-filter controller using the polynomial approximation compared with another approaches is the reduction of the number of gain-scheduling parameters to two. The calculation of the controller is then a simple matrix multiplication. A normal pLPV controller for the application presented in this section needs 26 gain-scheduling parameters and 2^{26} vertices. A huge number of vertices complicates the interpolation of the controller. The pLPV controller of this section has two gain-scheduling parameters and three vertices.

pLPV Output Feedback Controller Experimental Results

The pLPV gain-scheduled output-feedback controller is validated with experimental results on the ANC headset. The controller is designed to reject a disturbance signal which contains four harmonically related sine signals $\mathbf{f}_k = [f_{0,k} \ 2f_{0,k} \ 3f_{0,k} \ 4f_{0,k}]$ with a fundamental frequency $f_{0,k}$ between 80 and 90 Hz. The controller obtained is of 21st order. The pLPV controller of this section has four gain-scheduling parameters and 2^4 vertices. The calculation of the controller is not so simple as other pLPV approaches using the polynomial approximation (two gain-scheduling parameters and three vertices).

Amplitude frequency responses and pressure measured when the fundamental frequency rises suddenly from 80 to 90 Hz are shown in Figs. 5.12 and 5.13. A very good disturbance rejection is achieved even for unrealistic changes of the disturbance frequencies. In Fig. 5.14, results for time-varying frequencies are shown. The performance attenuation decreases with fast changes of the fundamental frequency but the controller remained stable.

The interpolation of the pLPV controller of this section is more complicated as other pLPV approaches using the polynomial approximation. The performance of the pLPV controller for the reduction of disturbances with time-varying frequencies was not affected by the complicated interpolation of the controller.

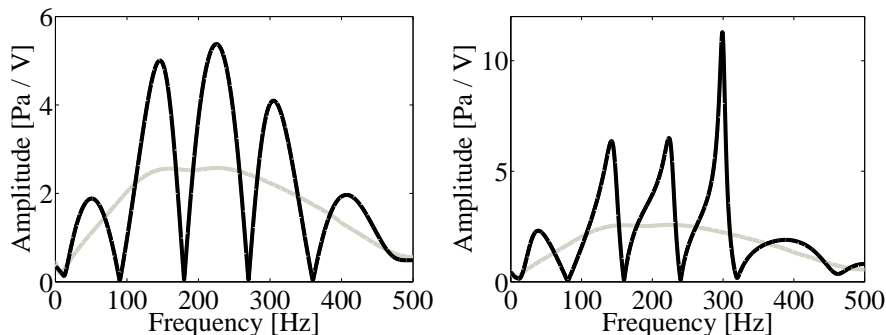


Figure 5.12: Open-loop (gray) and closed-loop (black) amplitude frequency responses for fixed disturbance frequencies of 80, 160, 240 and 320 Hz (left) and of 90, 180, 270 and 360 Hz (right) for a sampling frequency of 1 kHz

5. Experimental Results

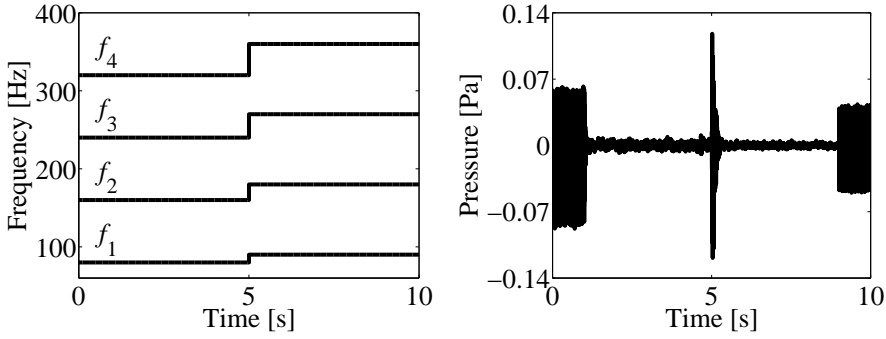


Figure 5.13: Results for a disturbance with time-varying frequencies. Variation of the frequencies (left) and pressure measured (right). The control sequence is off/on/off

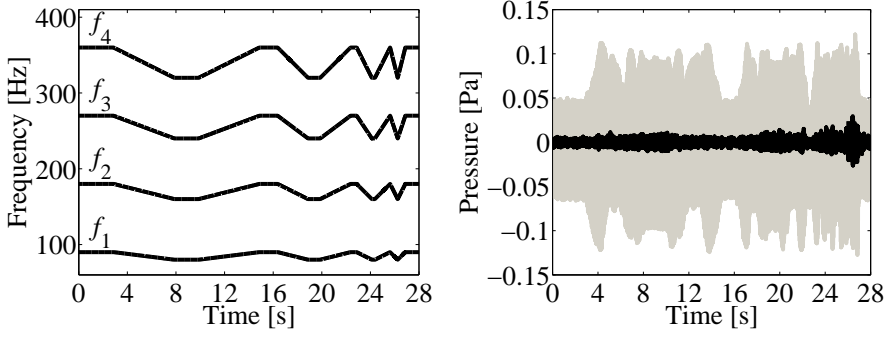


Figure 5.14: Results for a disturbance with time-varying frequencies. Variation of the frequencies (left) and pressure measured (right) in open loop (gray) and closed loop (black)

LFT Controller Experimental Results

The AVC test bed is used to test the LFT gain-scheduled controller experimentally. The controller is designed to reject a disturbance with eight harmonic components which are selected to be uniformly distributed from 80 to 380 Hz in intervals of 20 Hz. The resulting controller is of 27th order and a sampling frequency of 1 kHz is used. The LFT controller presented in this section uses eight gain-scheduling parameters.

Amplitude frequency responses are shown in Fig. 5.15 and results for an experiment where the frequencies change drastically as a step function in Fig. 5.16. Experiments with time-varying frequencies are shown in Fig. 5.17. The controller rejected the disturbance even with eight time-varying frequencies.

The LFT control design approach needs the same number of gain-scheduling parameters as the number of frequency components contained in the disturbance, even if the frequency components of the disturbance are harmonically related. This is the main disadvantage of this method compared with the pLPV control design methods. The polynomial approximation can only be used in the pLPV control design approach.

Excellent results were achieved using eight gain-scheduling parameters for the reduction of a disturbance with eight time-varying frequency components. The calculation of the controller with this method is easier as the traditional pLPV approach. A pLPV controller can be calculated for this application through interpolation between 2^8 vertices

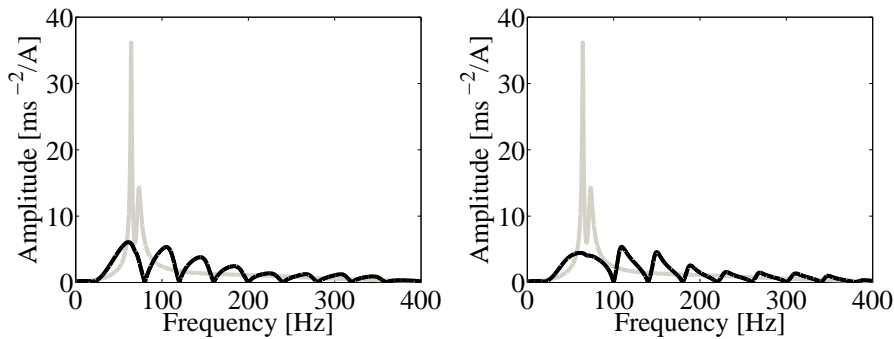


Figure 5.15: Open-loop (gray) and closed-loop (black) amplitude frequency responses for fixed disturbance frequencies of 80, 120, 160, 200, 240, 280, 320 and 360 Hz (left) and of 100, 140, 180, 220, 260, 300, 340 and 380 Hz (right) for a sampling frequency of 1 kHz

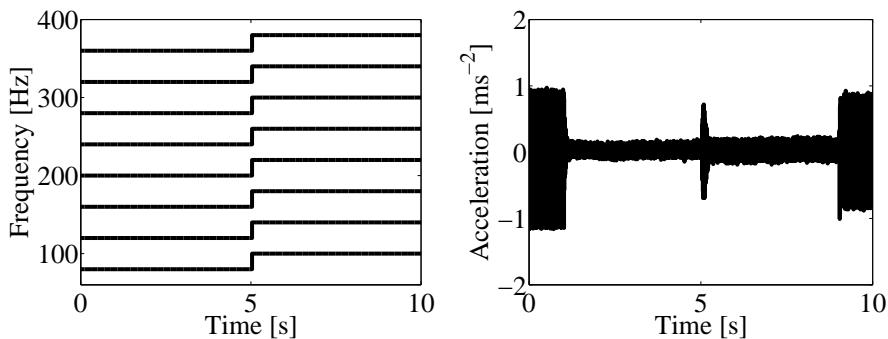


Figure 5.16: Results for a disturbance with time-varying frequencies. Variation of the frequencies (left) and acceleration measured (right). The control sequence is off/on/off

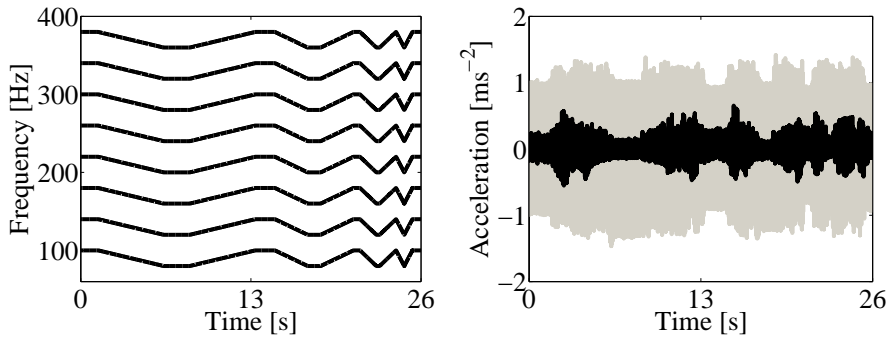


Figure 5.17: Results for a disturbance with time-varying frequencies. Variation of the frequencies (left) and acceleration measured (right) in open loop (gray) and closed loop (black)

5. Experimental Results

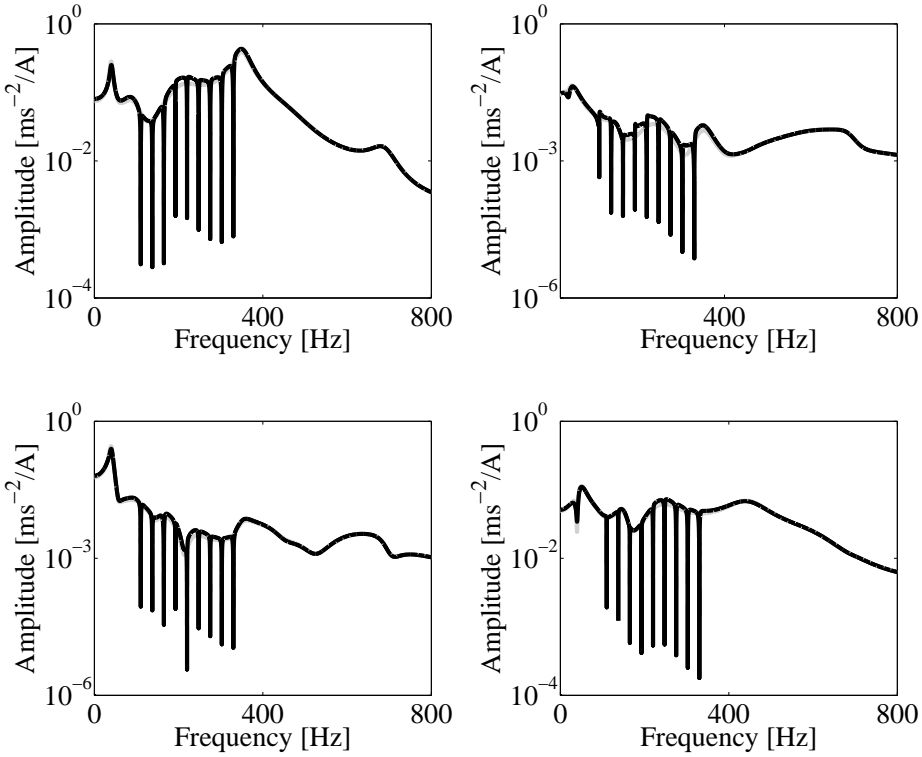


Figure 5.18: Open loop (gray) and closed loop (black) amplitude frequency responses for a sampling frequency of 2 kHz

using eight gain-scheduling parameters. The controller obtained applying the control design of this section is directly an LFT controller with the frequencies of the disturbance as gain-scheduling parameters.

Switching Control Strategy Results

Two MIMO pLPV controllers obtained with the control design from Sec. 4.1.3 and the switching strategy of Sec. 4.1.6 are used for the reduction of the engine-induced vibrations in a Golf VI Variant. The experimental setup of Sec. 5.1 is used. The controllers are designed to reject nine frequency components of the engine-induced vibration in a range of 750 rpm. The controller is calculated as a very simple interpolation (matrix multiplication) with three vertices using only two gain-scheduling parameters as a result of applying the polynomial approximation.

Black-box system identification techniques are used to obtain a MIMO state-space representation of the system between output and input of the control unit using a sampling frequency of 2 kHz. The controllers are capable of reducing nine frequency components $f_{0,k} \in [4 \ 5 \ \dots \ 12]$ of the engine-induced vibration for a fundamental frequency (half engine order) $f_{0,k} \in [22.5 \ 28.75]$ Hz. The switch between the pLPV controllers is realized for a fundamental frequency of 25 Hz. Amplitude frequency responses in open loop and closed loop for a fundamental frequency of $f_{0,k} = 27.6$ Hz (engine speed of approximately 3320 rpm) are shown in Fig. 5.18.

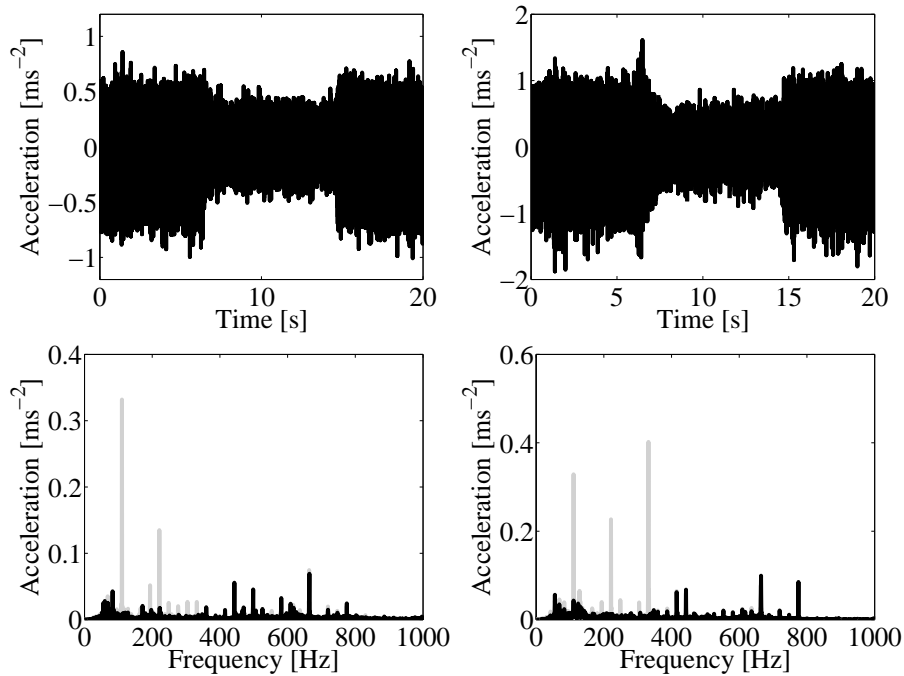


Figure 5.19: Acceleration measured by the accelerometers (top) for approximately 3320 rpm and fourier transformation (bottom) in open loop (gray) and closed loop (black). The control sequence is off/on/off

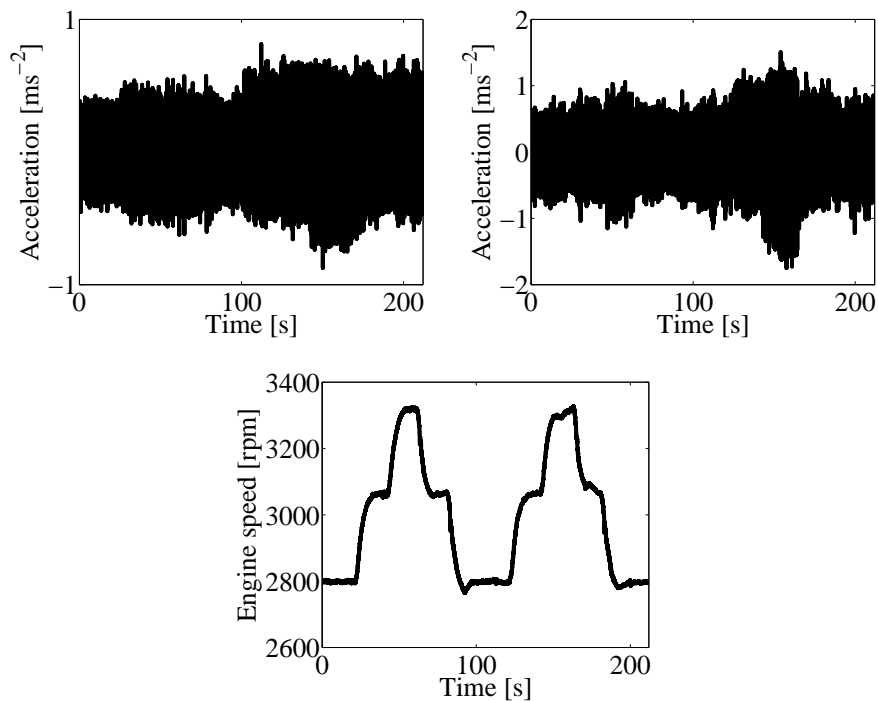


Figure 5.20: Acceleration measured by the accelerometers (top) and variations of the engine speed measured from the CAN bus (bottom) for a control sequence on/off

5. Experimental Results

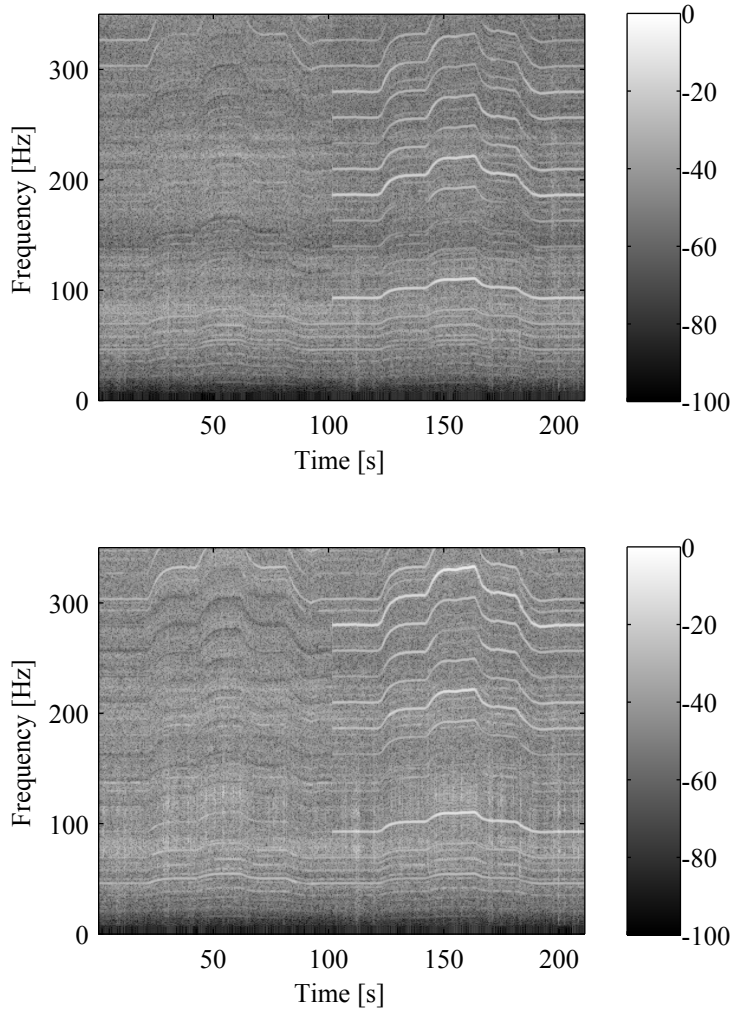


Figure 5.21: Spectrograms of the accelerations measured on the driver side (top) and rider side (bottom) for a sampling frequency of 2 kHz. The control sequence is on/off

The controllers were tested in drives with all the gears. In the following only results in third gear are shown. Results and spectrums for an engine speed of approximately 3320 rpm are shown for a control sequence off/on/off are shown in Fig. 5.19. Excellent results were achieved for constant engine speeds as the spectrums of the acceleration in closed loop and open loop show.

Further experiments were realized in test drives for time-varying engine speeds. The accelerations measured on the driver and rider side and the engine-speed variations are shown in Fig. 5.20. The controller is switched on for the first one hundred seconds and switched off for the next one hundred seconds.

Excellent results are achieved for the reduction of nine frequency components of the engine-induced vibration for time-varying engine speed as the time-frequency diagrams of Fig. 5.21 show. The switching control strategy augmented the frequency range of actuation for the reduction of the engine-induced vibrations and the switch between controllers did not affect the performance of this approach. Nine frequency components are reduced using only two gain-scheduling parameters and a triangle as polytope.

Chapter 6

Summary and Conclusions

This dissertation focuses on the rejection of disturbances with time-varying frequencies using LPV control design techniques. The use of LPV control design assures the stability of the controllers for arbitrarily fast changes of the gain-scheduling parameters. All the controllers are designed in discrete time and no discretization is needed to test the controllers in real time. Therefore the implementation of all the LPV controllers presented here is straightforward.

The four LPV controllers presented here are based on the IMP (Francis & Wonham (1976)). For the reduction of a harmonic disturbance, the controller must contain a model of it. Since the frequencies of the disturbance are the time-varying parameters the controllers containing the model of these disturbances are LPV.

Two discrete-time observer-based pLPV controllers are designed and validated with experimental results. The first control structure is based on the controller of Bohn et al. (2003, 2004) where a SISO state-feedback observer-based controller is built through state-augmentation combining plant and disturbance model. The stability is not guaranteed in Bohn et al. (2003, 2004) for changes of the gain-scheduling parameters but this approach worked well in practice for the reduction of a disturbance up to 17 frequency components. In the work presented in this dissertation and in Heins et al. (2012a, 2012b) pLPV control design techniques are used to guarantee the stability for changes in the gain-scheduling parameters. The second observer-based controller structure is based on Kinney & de Callafon (2006a) where the controller is an observer for the plant combined with a state-feedback gain of plant and a model of the disturbance (error filter). In Kinney & de Callafon (2006a) the controller is designed in continuous time and only simulation results are shown. In the work presented in this dissertation the whole control design is carried out in discrete-time and the controller is validated with experimental results.

Two output-feedback LPV control structures are also used for the reduction of disturbances with time-varying frequencies. The disturbance model is introduced in the generalized plant through the weighting functions at the input of the plant. One output-feedback controller uses LFT techniques and the other pLPV control design techniques. The controllers for the reduction of non stationary harmonic disturbances are calculated using the control design of Gahinet & Apkarian (1994) applying the pLPV control design and Apkarian & Gahinet (1995) for the LFT controller.

For the classical pLPV approach, the number n_d of gain-scheduling parameters results in a polytope with 2^{n_d} vertices, resulting in a complicated interpolation at each sampling time. A very useful idea is introduced by Füger et al. (2012, 2013) in the case where the frequencies of the disturbance are harmonically related. A polynomial approximation is used to approximate the cosine function (model of constant frequencies) of the disturbance model to reduce the number of gain-scheduling parameters and a rectangle is used as polytope. The approach of Füger et al. (2012, 2013) uses a model for constant frequencies to reduce time-varying frequencies. In this dissertation, the polynomial approximation is used for the sine and cosine function (model for time-varying frequencies) reducing

6. Summary and Conclusions

the number of gain-scheduling parameters to two and a triangle is used as polytope. This approach leads to a very simple interpolation strategy (a matrix multiplication) to calculate the controller at each sampling time. For harmonically related disturbance frequencies only two gain-scheduling parameters are needed independently of the number of disturbance frequencies.

In some applications, one controller is not capable to cover all the range of variation of the gain-scheduling parameter (e.g., reduction of the engine-induced vibrations in an automotive vehicle or an ANC headphone). In this work, a switch between discrete-time MIMO pLPV controllers based on parameter-independent Lyapunov functions is presented and validated with experimental results in a Golf VI Variant for the reduction of the engine-induced vibrations. The main objective of this switch is to augment the range of variation of the gain-scheduling parameter not to reduce the conservatism of the control design. The control design presented in this work is conservative because variations of the gain-scheduling parameters are considered that they do not take place. For example in the polytopic approaches a triangle is used as polytope but the relation of the gain-scheduling parameters is quadratic.

All the controllers are obtained applying LPV control design techniques in discrete-time, this is an advantage compared to those methods where the control design is realized in continuous-time and then the controller has to be discretized (Balini et al. (2011), Ruderman et al. (2014) and Witte et al. (2010)). In Balini et al. (2011), Ruderman et al. (2014) and Witte et al. (2010) very high sampling frequencies were used for the reduction of disturbance frequencies up to 48 Hz (Balini et al. (2011) used 50 kHz for time-varying frequencies and Ruderman et al. (2014) used 11kHz for disturbances with constant frequencies). This dissertation uses sampling frequencies of 1 kHz to 2 kHz for the reduction of disturbance frequencies up to 500 Hz. The controllers presented here are validated with experimental results in three different test benches. Excellent results were achieved even for arbitrarily fast changes of the gain-scheduling parameters. To the best author knowledge, it is the first time that a MIMO LPV controller is implemented in an automotive vehicle for the reduction of the engine-induced vibrations.

The future work is focused on reducing the conservatism of the control design through the use of parameter-dependent Lyapunov functions augmenting at the same time the range of variation of the gain-scheduling parameters for the LPV controllers.

Appendix A

LTI Control Design

Linear Fractional Transformation

Let $\mathbf{M}^{(n_1+n_2) \times (m_1+m_2)}$ be a matrix defined with

$$\mathbf{M} = \begin{bmatrix} \mathbf{M}_{11} & \mathbf{M}_{12} \\ \mathbf{M}_{21} & \mathbf{M}_{22} \end{bmatrix} \quad (\text{A.1})$$

and a matrix given as $\Delta^{(m_2 \times n_2)}$. The lower LFT of the matrix \mathbf{M} respect to the matrix Δ is defined (Zhou and Doyle (1998)) with

$$\mathcal{F}_l(\mathbf{M}, \Delta) = \mathbf{M}_{11} + \mathbf{M}_{12}\Delta(\mathbf{I} - \mathbf{M}_{22}\Delta)^{-1}\mathbf{M}_{21}. \quad (\text{A.2})$$

The upper LFT of the matrix $\mathbf{M}^{(n_1+n_2) \times (m_1+m_2)}$ respect to Δ is defined as

$$\mathcal{F}_u(\mathbf{M}, \Delta) = \mathbf{M}_{22} + \mathbf{M}_{21}\Delta(\mathbf{I} - \mathbf{M}_{11}\Delta)^{-1}\mathbf{M}_{12} \quad (\text{A.3})$$

with $\Delta^{(m_1 \times n_1)}$.

Let a general system written in LFT form be defined by

$$\begin{bmatrix} \mathbf{x}_{k+1} \\ \mathbf{y}_{p,k} \\ \hline \mathbf{q}_{\theta,k} \end{bmatrix} = \left[\begin{array}{cc|c} \mathbf{A}_0 & \mathbf{B}_u & \mathbf{B}_\theta \\ \mathbf{C}_y & \mathbf{D}_{yu} & \mathbf{D}_{y\theta} \\ \hline \mathbf{C}_\theta & \mathbf{D}_{\theta u} & \mathbf{D}_{\theta\theta} \end{array} \right] \begin{bmatrix} \mathbf{x}_k \\ \mathbf{u}_{p,k} \\ \hline \mathbf{w}_{\theta,k} \end{bmatrix} \quad (\text{A.4})$$

with

$$\Delta_k^{(m_\theta \times r_\theta)} = \begin{bmatrix} \theta_{1,k} & & 0 \\ & \ddots & \\ 0 & & \theta_{n_d,k} \end{bmatrix} \quad (\text{A.5})$$

and the matrices dimensions

$$\begin{array}{ccc} \mathbf{A}_0^{(n \times n)} & \mathbf{B}_u^{(n \times m_u)} & \mathbf{B}_\theta^{(n \times m_\theta)} \\ \mathbf{C}_y^{(r_y \times n)} & \mathbf{D}_{yu}^{(r_y \times m_u)} & \mathbf{D}_{y\theta}^{(r_y \times m_\theta)} \\ \mathbf{C}_\theta^{(r_\theta \times n)} & \mathbf{D}_{\theta u}^{(r_\theta \times m_u)} & \mathbf{D}_{\theta\theta}^{(r_\theta \times m_\theta)} \end{array}. \quad (\text{A.6})$$

The system

$$\begin{bmatrix} \mathbf{x}_{k+1} \\ \mathbf{y}_{p,k} \end{bmatrix} = \left[\begin{array}{c|c} \mathbf{A} & \mathbf{B} \\ \hline \mathbf{C} & \mathbf{D} \end{array} \right] \begin{bmatrix} \mathbf{x}_k \\ \mathbf{u}_{p,k} \end{bmatrix} \quad (\text{A.7})$$

is obtained as a result of applying the lower LFT respect to the parameter Δ_k

$$\left[\begin{array}{c|c} \mathbf{A} & \mathbf{B} \\ \hline \mathbf{C} & \mathbf{D} \end{array} \right] = \left[\begin{array}{cc} \mathbf{A}_0 & \mathbf{B}_u \\ \mathbf{C}_y & \mathbf{D}_{yu} \end{array} \right] + \left[\begin{array}{c} \mathbf{B}_\theta \\ \mathbf{D}_{y\theta} \end{array} \right] \Delta_k \left[\begin{array}{cc} \mathbf{C}_\theta & \mathbf{D}_{\theta u} \end{array} \right] \quad (\text{A.8})$$

A. LTI Control Design

assuming $\mathbf{D}_{\theta\theta} = \mathbf{0}$ with

$$\begin{aligned}\mathbf{A}^{(n \times n)} &= \mathbf{A}_0 + \mathbf{B}_\theta \Delta_k \mathbf{C}_\theta, \\ \mathbf{B}^{(n \times m_u)} &= \mathbf{B}_u + \mathbf{B}_\theta \Delta_k \mathbf{D}_{\theta u}, \\ \mathbf{C}^{(r_y \times n)} &= \mathbf{C}_y + \mathbf{D}_{yu} \Delta_k \mathbf{C}_\theta\end{aligned}\tag{A.9}$$

and

$$\mathbf{D}^{(r_y \times m_u)} = \mathbf{D}_{yu} + \mathbf{D}_{yu} \Delta_k \mathbf{D}_{\theta u}.\tag{A.10}$$

Schur Complement

The block matrix

$$\left[\begin{array}{cc} \mathbf{Q} & \mathbf{S} \\ \mathbf{S}^T & \mathbf{R} \end{array} \right] > 0\tag{A.11}$$

is positive definite if and only if

$$\mathbf{Q} > 0 \text{ and } \mathbf{R} - \mathbf{S}^T \mathbf{Q}^{-1} \mathbf{S} > 0\tag{A.12}$$

or, if and only if

$$\mathbf{R} > 0 \text{ and } \mathbf{Q} - \mathbf{S} \mathbf{R}^{-1} \mathbf{S}^T > 0.\tag{A.13}$$

H_2 -norm for discrete-time systems

The H_2 -norm of a discrete-time system

$$\mathbf{G} = \left[\begin{array}{c|c} \mathbf{A} & \mathbf{B} \\ \hline \mathbf{C} & \mathbf{0} \end{array} \right]\tag{A.14}$$

with

$$\begin{array}{cc} \mathbf{A}^{(n \times n)} & \mathbf{B}^{(n \times m_u)} \\ \mathbf{C}^{(r_y \times n)} & \mathbf{0}^{(r_y \times m_u)} \end{array}\tag{A.15}$$

is bounded by γ

$$\|\mathbf{G}\|_2 < \gamma\tag{A.16}$$

if exist solutions of the LMIs

$$\mathbf{A} \mathbf{P} \mathbf{A}^T - \mathbf{P} + \mathbf{B} \mathbf{B}^T < 0,\tag{A.17}$$

$$\mathbf{W} - \mathbf{C} \mathbf{P} \mathbf{C}^T > 0,\tag{A.18}$$

$$\text{trace}(\mathbf{W}) < \gamma^2\tag{A.19}$$

for the positive definite matrices $\mathbf{P}^{(n \times n)}$ and $\mathbf{W}^{(n \times n)}$ (Zhou et al., 1996) or equivalently if exist solutions for the LMIs

$$\mathbf{A}^T \mathbf{X} \mathbf{A} - \mathbf{X} + \mathbf{C}^T \mathbf{C} < 0,\tag{A.20}$$

$$\mathbf{Z} - \mathbf{B}^T \mathbf{X} \mathbf{B} > 0,\tag{A.21}$$

$$\text{trace}(\mathbf{Z}) < \gamma^2\tag{A.22}$$

for the positive definite matrices $\mathbf{X}^{(n \times n)}$ and $\mathbf{Z}^{(n \times n)}$.

Using the Schur complement the LMIs of (A.17)-(A.19)

$$\begin{aligned}\mathbf{R} - \mathbf{S}^T \mathbf{Q}^{-1} \mathbf{S} &= (\mathbf{P} - \mathbf{B} \mathbf{B}^T) - \mathbf{A} \mathbf{P} \mathbf{P}^{-1} \mathbf{P} \mathbf{A}^T > 0, \\ \mathbf{Q} - \mathbf{S} \mathbf{R}^{-1} \mathbf{S}^T &= \mathbf{W} - \mathbf{C} \mathbf{P} \mathbf{P}^{-1} \mathbf{P} \mathbf{C}^T > 0\end{aligned}\quad (\text{A.23})$$

and (A.20)-(A.22)

$$\begin{aligned}\mathbf{R} - \mathbf{S}^T \mathbf{Q}^{-1} \mathbf{S} &= (\mathbf{X} - \mathbf{C}^T \mathbf{C}) - \mathbf{A}^T \mathbf{X} \mathbf{X}^{-1} \mathbf{X} \mathbf{A} > 0, \\ \mathbf{R} - \mathbf{S}^T \mathbf{Q}^{-1} \mathbf{S} &= \mathbf{Z} - \mathbf{B}^T \mathbf{X} \mathbf{X}^{-1} \mathbf{X} \mathbf{B} > 0\end{aligned}\quad (\text{A.24})$$

can be rewritten as

$$\begin{aligned}\left[\begin{array}{cc} \mathbf{P} & \mathbf{P} \mathbf{A}^T \\ \mathbf{A} \mathbf{P} & \mathbf{P} - \mathbf{B} \mathbf{B}^T \end{array} \right] &> 0, \\ \left[\begin{array}{cc} \mathbf{W} & \mathbf{C} \mathbf{P} \\ \mathbf{P} \mathbf{C}^T & \mathbf{P} \end{array} \right] &> 0, \\ \text{trace}(\mathbf{W}) < \gamma^2\end{aligned}\quad (\text{A.25})$$

and

$$\begin{aligned}\left[\begin{array}{cc} \mathbf{X} & \mathbf{X} \mathbf{A} \\ \mathbf{A}^T \mathbf{X} & \mathbf{X} - \mathbf{C}^T \mathbf{C} \end{array} \right] &> 0, \\ \left[\begin{array}{cc} \mathbf{X} & \mathbf{X} \mathbf{B} \\ \mathbf{B}^T \mathbf{X} & \mathbf{Z} \end{array} \right] &> 0, \\ \text{trace}(\mathbf{Z}) < \gamma^2.\end{aligned}\quad (\text{A.26})$$

H_2 state-feedback control for discrete-time systems

The H_2 -norm can be used to obtain a state-feedback gain $\mathbf{K}^{(m_u \times n)}$ for a discrete-time system. The objective is to minimize the H_2 -norm between performance input \mathbf{w}_k and performance output \mathbf{q}_k of the closed-loop system given by

$$\left[\begin{array}{c} \mathbf{x}_{k+1} \\ \mathbf{q}_k \\ \mathbf{y}_{p,k} \end{array} \right] = \left[\begin{array}{c|cc} \mathbf{A} & \mathbf{B}_w & \mathbf{B}_u \\ \hline \mathbf{C}_q & \mathbf{D}_{qw} & \mathbf{D}_{qu} \\ \mathbf{C}_y & \mathbf{D}_{yw} & \mathbf{D}_{yu} \end{array} \right] \left[\begin{array}{c} \mathbf{x}_k \\ \mathbf{w}_k \\ \mathbf{u}_{p,k} \end{array} \right] \quad (\text{A.27})$$

with

$$\begin{aligned}\mathbf{A}^{(n \times n)} & \quad \mathbf{B}_w^{(n \times m_w)} \quad \mathbf{B}_u^{(n \times m_u)} \\ \mathbf{C}_q^{(r_q \times n)} & \quad \mathbf{D}_{qw}^{(r_q \times m_w)} \quad \mathbf{D}_{qu}^{(r_q \times m_u)} \\ \mathbf{C}_y^{(r_y \times n)} & \quad \mathbf{D}_{yw}^{(r_y \times m_w)} \quad \mathbf{D}_{yu}^{(r_y \times m_u)}\end{aligned}\quad (\text{A.28})$$

$\mathbf{u}_{p,k} = -\mathbf{K} \mathbf{x}_k$, $\mathbf{D}_{qw} = \mathbf{0}$, $\mathbf{D}_{yu} = \mathbf{0}$, $\mathbf{B}_w = \mathbf{I}$ and the matrices $\mathbf{Q}^{(n \times n)}$ to weight the states and $\mathbf{R}^{(m_u \times m_u)}$ to weight the control input. The closed loop system is written as

$$\left[\begin{array}{c} \mathbf{x}_{k+1} \\ \mathbf{q}_k \end{array} \right] = \left[\begin{array}{c|c} \mathbf{A} - \mathbf{B}_u \mathbf{K} & \mathbf{I} \\ \hline \mathbf{C}_q - \mathbf{D}_{qu} \mathbf{K} & \mathbf{0} \end{array} \right] \left[\begin{array}{c} \mathbf{x}_k \\ \mathbf{w}_k \end{array} \right] \quad (\text{A.29})$$

A. LTI Control Design

with

$$\mathbf{C}_q^{((n+m_u) \times n)} = \begin{bmatrix} \mathbf{Q}^{\frac{1}{2}} \\ \mathbf{0} \end{bmatrix} \quad \text{and} \quad \mathbf{D}_{qu}^{((n+m_u) \times m_u)} = \begin{bmatrix} \mathbf{0} \\ \mathbf{R}^{\frac{1}{2}} \end{bmatrix}. \quad (\text{A.30})$$

The H_2 -norm of the closed-loop system is bounded by γ (see A.3) if solutions for the LMIs

$$\begin{bmatrix} \mathbf{P} & (\mathbf{AP} - \mathbf{B}_u \mathbf{Y})^T \\ \mathbf{AP} - \mathbf{B}_u \mathbf{Y} & \mathbf{P} - \mathbf{B}_w \mathbf{B}_w^T \end{bmatrix} > 0, \quad (\text{A.31})$$

$$\begin{bmatrix} \mathbf{W} & \mathbf{C}_q \mathbf{P} - \mathbf{D}_{qu} \mathbf{Y} \\ (\mathbf{C}_q \mathbf{P} - \mathbf{D}_{qu} \mathbf{Y})^T & \mathbf{P} \end{bmatrix} > 0, \quad (\text{A.32})$$

$$\text{trace}(\mathbf{W}) < \gamma^2 \quad (\text{A.33})$$

are found for the positive definite matrices $\mathbf{P}^{(n \times n)}$, $\mathbf{W}^{((m_u+n) \times (m_u+n))}$ and $\mathbf{Y}^{(m_u \times n)} = \mathbf{K} \mathbf{P}$. The state-feedback gain $\mathbf{K}^{(m_u \times n)}$ is calculated through

$$\mathbf{K} = \mathbf{Y} \mathbf{P}^{-1}. \quad (\text{A.34})$$

The same procedure can be realized to calculate an observer gain $\mathbf{L}^{(n \times r_y)}$ minimizing the H_2 -norm of the transfer function between \mathbf{w}_k and the observer error $\tilde{\mathbf{x}}_k$. The observer error is obtained from

$$\begin{bmatrix} \mathbf{x}_{k+1} \\ \mathbf{q}_k \\ \mathbf{y}_{p,k} \end{bmatrix} = \left[\begin{array}{c|cc} \mathbf{A} & \mathbf{B}_w & \mathbf{B}_u \\ \hline \mathbf{C}_q & \mathbf{D}_{qw} & \mathbf{D}_{qu} \\ \mathbf{C}_y & \mathbf{D}_{yw} & \mathbf{D}_{yu} \end{array} \right] \begin{bmatrix} \mathbf{x}_k \\ \mathbf{w}_k \\ \mathbf{u}_{p,k} \end{bmatrix} \quad (\text{A.35})$$

and

$$\begin{bmatrix} \hat{\mathbf{x}}_{k+1} \\ \hat{\mathbf{q}}_k \\ \hat{\mathbf{y}}_{p,k} \end{bmatrix} = \left[\begin{array}{c|cc} \mathbf{A} - \mathbf{LC}_y & \mathbf{L} & \mathbf{B}_u \\ \hline \mathbf{C}_q & \mathbf{0} & \mathbf{D}_{qu} \\ \mathbf{C}_y & \mathbf{0} & \mathbf{D}_{yu} \end{array} \right] \begin{bmatrix} \hat{\mathbf{x}}_k \\ \mathbf{y}_k \\ \mathbf{u}_{p,k} \end{bmatrix} \quad (\text{A.36})$$

as

$$\begin{bmatrix} \tilde{\mathbf{x}}_{k+1} \\ \tilde{\mathbf{q}}_k \end{bmatrix} = \left[\begin{array}{c|c} \mathbf{A} - \mathbf{LC}_y & \mathbf{B}_w - \mathbf{LD}_{yw} \\ \hline \mathbf{I} & \mathbf{0} \end{array} \right] \begin{bmatrix} \tilde{\mathbf{x}}_k \\ \mathbf{w}_k \end{bmatrix} \quad (\text{A.37})$$

with

$$\mathbf{B}_w^{(n \times (n+r_y))} = \begin{bmatrix} \mathbf{Q}^{\frac{1}{2}} \\ \mathbf{0} \end{bmatrix}^T, \quad \mathbf{D}_{yw}^{(r_y \times (n+r_y))} = \begin{bmatrix} \mathbf{0} \\ \mathbf{R}^{\frac{1}{2}} \end{bmatrix}^T, \quad \mathbf{C}_q = \mathbf{I} \quad \text{and} \quad \mathbf{D}_{qw} = \mathbf{0}. \quad (\text{A.38})$$

The matrices $\mathbf{Q}^{(n \times n)}$ and $\mathbf{R}^{(r_y \times r_y)}$ are used to weight the states and the output, respectively. If solutions for the LMIs

$$\begin{bmatrix} \mathbf{X} & \mathbf{XA} - \mathbf{YC}_y \\ (\mathbf{XA} - \mathbf{YC}_y)^T & \mathbf{X} - \mathbf{C}_q^T \mathbf{C}_q \end{bmatrix} > 0, \quad (\text{A.39})$$

$$\begin{bmatrix} \mathbf{X} & \mathbf{XB}_w - \mathbf{YD}_{yw} \\ (\mathbf{XB}_w - \mathbf{YD}_{yw})^T & \mathbf{Z} \end{bmatrix} > 0, \quad (\text{A.40})$$

$$\text{trace}(\mathbf{Z}) < \gamma^2 \quad (\text{A.41})$$

are found for $\mathbf{X}^{(n \times n)}$, $\mathbf{Z}^{((n+r_y) \times (n+r_y))}$ and $\mathbf{Y}^{(n \times r_y)}$ the system has an H_2 -norm bounded by γ . The observer gain $\mathbf{L}^{(n \times r_y)}$ is finally calculated with

$$\mathbf{L} = \mathbf{X}^{-1} \mathbf{Y}. \quad (\text{A.42})$$

H_∞ -norm for discrete-time systems

The H_∞ -norm of a discrete-time system

$$\mathbf{G} = \left[\begin{array}{c|c} \mathbf{A} & \mathbf{B} \\ \hline \mathbf{C} & \mathbf{0} \end{array} \right] \quad (\text{A.43})$$

with

$$\begin{array}{cc} \mathbf{A}^{(n \times n)} & \mathbf{B}^{(n \times m_u)} \\ \mathbf{C}^{(r_y \times n)} & \mathbf{0}^{(r_y \times m_u)} \end{array} \quad (\text{A.44})$$

is bounded by γ (Gahinet and Apkarian (1994), Vaidyanathan (1985))

$$\|\mathbf{G}\|_\infty < \gamma \quad (\text{A.45})$$

if exists a positive definite matrix $\mathbf{X}^{(n \times n)}$ for the LMI

$$\begin{bmatrix} -\mathbf{X}^{-1} & \mathbf{A} & \mathbf{B} & \mathbf{0} \\ \mathbf{A}^T & -\mathbf{X} & \mathbf{0} & \mathbf{C}^T \\ \mathbf{B}^T & \mathbf{0} & -\gamma \mathbf{I} & \mathbf{D}^T \\ \mathbf{0} & \mathbf{C} & \mathbf{D} & -\gamma \mathbf{I} \end{bmatrix} < 0, \quad (\text{A.46})$$

based on the Bounded Real Lemma (BRL) or equivalently using the Schur complement to (A.46)

$$\mathbf{R} - \mathbf{S}^T \mathbf{Q}^{-1} \mathbf{S} \quad (\text{A.47})$$

with

$$\mathbf{Q} = -\mathbf{X}^{-1}, \quad \mathbf{S}^T = \begin{bmatrix} \mathbf{A}^T \\ \mathbf{B}^T \\ \mathbf{0} \end{bmatrix}, \quad \mathbf{S} = [\mathbf{A} \ \mathbf{B} \ \mathbf{0}] \quad (\text{A.48})$$

and

$$\mathbf{R} = \begin{bmatrix} -\mathbf{X} & \mathbf{0} & \mathbf{C}^T \\ \mathbf{0} & -\gamma \mathbf{I} & \mathbf{D}^T \\ \mathbf{C} & \mathbf{D} & -\gamma \mathbf{I} \end{bmatrix} \quad (\text{A.49})$$

if exists a solution $\mathbf{X} = \mathbf{X}^T > 0$ for the LMI

$$\begin{bmatrix} \mathbf{A}^T \mathbf{X} \mathbf{A} - \mathbf{X} & \mathbf{A}^T \mathbf{X} \mathbf{B} & \mathbf{C}^T \\ \mathbf{B}^T \mathbf{X} \mathbf{A} & \mathbf{B}^T \mathbf{X} \mathbf{B} - \gamma \mathbf{I} & \mathbf{D}^T \\ \mathbf{C} & \mathbf{D} & -\gamma \mathbf{I} \end{bmatrix} < 0 \quad (\text{A.50})$$

derived from (A.47)-(A.49).

H_∞ output-feedback control design for discrete-time systems

The H_∞ control design of Gahinet and Apkarian (1994) for discrete-time systems is in this section reviewed and all the necessary steps for an easier calculation of the controller are written and enumerated with matrices dimensions.

A. LTI Control Design

1. Build the generalized plant

$$\begin{bmatrix} \mathbf{x}_{k+1} \\ \mathbf{q}_k \\ \mathbf{y}_{p,k} \end{bmatrix} = \left[\begin{array}{c|cc} \mathbf{A} & \mathbf{B}_w & \mathbf{B}_u \\ \hline \mathbf{C}_q & \mathbf{D}_{qw} & \mathbf{D}_{qu} \\ \mathbf{C}_y & \mathbf{D}_{yw} & \mathbf{D}_{yu} \end{array} \right] \begin{bmatrix} \mathbf{x}_k \\ \mathbf{w}_k \\ \mathbf{u}_{p,k} \end{bmatrix} \quad (\text{A.51})$$

with plant and weighting functions. An example to build the generalized plant is given in Sec. 2.1.2.

2. Next, the matrices dimensions

$$\begin{array}{ccc} \mathbf{A}^{n \times n} & \mathbf{B}_w^{n \times m_w} & \mathbf{B}_u^{n \times m_u} \\ \mathbf{C}_q^{r_q \times n} & \mathbf{D}_{qw}^{r_q \times m_w} & \mathbf{D}_{qu}^{r_q \times m_u} \\ \mathbf{C}_y^{r_y \times n} & \mathbf{D}_{yw}^{r_y \times m_w} & \mathbf{D}_{yu}^{r_y \times m_u} \end{array} \quad (\text{A.52})$$

are obtained for all the matrices of the generalized plant.

3. Solve the LMIs

$$\begin{aligned} \begin{bmatrix} \mathbf{N}_X & \mathbf{0} \\ \mathbf{0} & \mathbf{I} \end{bmatrix}^T \begin{bmatrix} \mathbf{A}^T \mathbf{X}_1 \mathbf{A} - \mathbf{X}_1 & \mathbf{A}^T \mathbf{X}_1 \mathbf{B}_w & \mathbf{C}_q^T \\ \mathbf{B}_w^T \mathbf{X}_1 \mathbf{A} & -\gamma \mathbf{I} + \mathbf{B}_w^T \mathbf{X}_1 \mathbf{B}_w & \mathbf{D}_{qu}^T \\ \mathbf{C}_q & \mathbf{D}_{qu} & -\gamma \mathbf{I} \end{bmatrix} \begin{bmatrix} \mathbf{N}_X & \mathbf{0} \\ \mathbf{0} & \mathbf{I} \end{bmatrix} < 0, \\ \begin{bmatrix} \mathbf{N}_Y & \mathbf{0} \\ \mathbf{0} & \mathbf{I} \end{bmatrix}^T \begin{bmatrix} \mathbf{A} \mathbf{Y}_1 \mathbf{A}^T - \mathbf{Y}_1 & \mathbf{A} \mathbf{Y}_1 \mathbf{C}_q^T & \mathbf{B}_w \\ \mathbf{C}_q \mathbf{Y}_1 \mathbf{A}^T & -\gamma \mathbf{I} + \mathbf{C}_q \mathbf{Y}_1 \mathbf{C}_q^T & \mathbf{D}_{qu} \\ \mathbf{B}_w^T & \mathbf{D}_{qu}^T & -\gamma \mathbf{I} \end{bmatrix} \begin{bmatrix} \mathbf{N}_Y & \mathbf{0} \\ \mathbf{0} & \mathbf{I} \end{bmatrix} < 0, \\ \begin{bmatrix} \mathbf{X}_1 & \mathbf{I} \\ \mathbf{I} & \mathbf{Y}_1 \end{bmatrix} \geq 0 \end{aligned} \quad (\text{A.53})$$

for $\mathbf{X}_1^{(n \times n)}$ and $\mathbf{Y}_1^{(n \times n)}$ with the matrices $\mathbf{N}_X^{((n+m_w) \times (n+m_w))}$ and $\mathbf{N}_Y^{((n+r_q) \times (n+r_q))}$ calculated through

$$\begin{aligned} \mathbf{N}_X &= \text{null}([\mathbf{C}_y \quad \mathbf{D}_{yw}]) \\ \mathbf{N}_Y &= \text{null}([\mathbf{B}_u \quad \mathbf{D}_{qu}^T]). \end{aligned} \quad (\text{A.54})$$

4. The auxiliar matrix $\psi^{((4n+m_w+r_q) \times (4n+m_w+r_q))}$

$$\psi = \begin{bmatrix} -\mathbf{X}^{-1} & \bar{\mathbf{A}} & \bar{\mathbf{B}} & \mathbf{0} \\ \bar{\mathbf{A}}^T & -\mathbf{X} & \mathbf{0} & \bar{\mathbf{C}}^T \\ \bar{\mathbf{B}}^T & \mathbf{0} & -\gamma \mathbf{I} & \mathbf{D}_{qw}^T \\ \mathbf{0} & \bar{\mathbf{C}} & \mathbf{D}_{qw} & -\gamma \mathbf{I} \end{bmatrix} \quad (\text{A.55})$$

is built with

$$\bar{\mathbf{A}}^{(2n \times 2n)} = \begin{bmatrix} \mathbf{A} & \mathbf{0} \\ \mathbf{0} & \mathbf{0} \end{bmatrix}, \quad \bar{\mathbf{B}}^{(2n \times m_w)} = \begin{bmatrix} \mathbf{B}_w \\ \mathbf{0} \end{bmatrix}, \quad \bar{\mathbf{C}}^{(r_q \times 2n)} = [\mathbf{C}_q \quad \mathbf{0}] \quad (\text{A.56})$$

and the matrix $\mathbf{X}^{(2n \times 2n)}$

$$\mathbf{X} = \begin{bmatrix} \mathbf{X}_1 & \mathbf{X}_2 \\ \mathbf{X}_2^T & \mathbf{I} \end{bmatrix} \quad (\text{A.57})$$

with $\mathbf{X}_2^{(n \times n)}$ obtained through

$$\mathbf{X}_2 = (\mathbf{X}_1 - \mathbf{Y}_1^{-1})^{\frac{1}{2}}. \quad (\text{A.58})$$

5. Build the matrices $\mathbf{P}^{((n+m_u) \times (4n+m_w+r_q))}$ and $\mathbf{Q}^{((r_y+n) \times (4n+m_w+r_q))}$

$$\begin{aligned}\mathbf{P} &= \left[\begin{array}{cccc} \underline{\mathbf{B}}^T & \mathbf{0} & \mathbf{0} & \underline{\mathbf{D}}_{qu}^T \end{array} \right] \\ \mathbf{Q} &= \left[\begin{array}{cccc} \mathbf{0} & \underline{\mathbf{C}} & \underline{\mathbf{D}}_{yw} & \mathbf{0} \end{array} \right]\end{aligned}\tag{A.59}$$

with

$$\begin{aligned}\underline{\mathbf{B}}^{(2n \times (n+m_u))} &= \left[\begin{array}{cc} \mathbf{0} & \mathbf{B}_u \\ \mathbf{I} & \mathbf{0} \end{array} \right], \underline{\mathbf{C}}^{((n+r_y) \times 2n)} = \left[\begin{array}{cc} \mathbf{0} & \mathbf{I} \\ \mathbf{C}_y & \mathbf{0} \end{array} \right], \\ \underline{\mathbf{D}}_{qu}^{(r_q \times (n+m_u))} &= \left[\begin{array}{cc} \mathbf{0} & \mathbf{D}_{qu} \end{array} \right] \text{ and } \underline{\mathbf{D}}_{yw}^{((n+r_y) \times m_w)} = \left[\begin{array}{c} \mathbf{0} \\ \mathbf{D}_{yw} \end{array} \right].\end{aligned}\tag{A.60}$$

6. Solve the LMI

$$\psi + \mathbf{P}^T \Omega \mathbf{Q} + \mathbf{Q}^T \Omega^T \mathbf{P} < 0\tag{A.61}$$

for $\Omega^{((n+m_u) \times (n+r_y))}$ with the matrices ψ , \mathbf{P} and \mathbf{Q} calculated before.

7. Finally, the controller matrices are extracted from Ω

$$\Omega = \left[\begin{array}{c|c} \mathbf{A}_{\text{of}} & \mathbf{B}_{\text{of}} \\ \hline \mathbf{C}_{\text{of}} & \mathbf{D}_{\text{of}} \end{array} \right]\tag{A.62}$$

with $\mathbf{A}_{\text{of}}^{(n \times n)}$, $\mathbf{B}_{\text{of}}^{(n \times r_y)}$, $\mathbf{C}_{\text{of}}^{(m_u \times n)}$ and $\mathbf{D}_{\text{of}}^{(m_u \times r_y)}$.

A. LTI Control Design

References

- Amato, F. 2006. *Robust control of linear systems subject to uncertain time-varying parameters*. Berlin: Springer.
- Apkarian, P. 1997. On the discretization of LMI-synthesized linear parameter-varying controllers. *Automatica* 33:655-61.
- Apkarian, P. and P. Gahinet. 1995. A convex characterization of gain scheduled H_∞ controllers. *IEEE Transactions on Automatic Control*, 40:853-64.
- Apkarian, P., P. Gahinet and G. Becker. 1995. Self-scheduled control of linear parameter-varying systems: A design example. *Automatica* 31:1251-61.
- Ardekani, I. T. 2012. *Stability analysis of adaptation process in FxLMS-based active noise control*. PhD thesis. University of Auckland.
- Balini, H. M. N. K., C. W. Scherer and J. Witte. 2011. Performance enhancement for AMB systems using unstable H_∞ controllers. *IEEE Transactions on Control Systems Technology* 19:1479-92.
- Ballesteros, P and C. Bohn. 2010. Ein LPV Ansatz für die aktive Schwingungsregelung. *Proceedings of the Workshop des GMA FA 1.40*. Salzburg, Sept. 2010. 168-85. (In German, An LPV approach for active vibration control.)
- Ballesteros, P. and C. Bohn. 2011a. A frequency-tunable LPV controller for narrowband active noise and vibration control. *Proceedings of the American Control Conference*. San Francisco, June 2011. 1340-45.
- Ballesteros, P. and C. Bohn. 2011b. Disturbance rejection through LPV gain-scheduling control with application to active noise cancellation. *Proceedings of the IFAC World Congress*. Milan, August 2011. 7897-902.
- Ballesteros, P., X. Shu and C. Bohn. 2014a. Active control of engine induced vibrations in automotive vehicles through LPV gain-scheduling. *SAE 2014 World Congress*. Detroit, April 2014. 264-72.
- Ballesteros, P., X. Shu and C. Bohn. 2014b. A discrete-time MIMO LPV controller for the rejection of nonstationary harmonically related multisine disturbances. *Proceedings of the American Control Conference*. Portland, June 2014. 4464-69.
- Ballesteros, P., X. Shu and C. Bohn. 2014c. Discrete-time switching MIMO LPV gain-scheduling control for the reduction of engine-induced vibrations in vehicles. *Proceedings of the IFAC World Congress*. Cape Town, August 2014. 7572-78.
- Ballesteros, P., X. Shu, W. Heins, and C. Bohn. 2012. LPV gain-scheduling output feedback for active control of harmonic disturbances with time-varying frequencies. In: M. Zapateiro and F. Pozo (eds.), *Advances on Analysis and Control of Vibrations Theory and Applications*. Rijeka, Croatia: InTech. 65-86. Available: <http://dx.doi.org/10.5772/50294>.
- Ballesteros, P., X. Shu, W. Heins and C. Bohn. 2013. Reduced-order two-parameter pLPV controller for the rejection of nonstationary harmonically related multisine disturbances. *Proceedings of the European Control Conference*. Zurich, July 2013. 1835-42.
- Bein, T., S. Elliot, L. Ferralli, M. Casella, J. Meschke, E. U. Saemann, F. K. Nielsen and W. Kropp. 2012. Integrated solutions for noise and vibration control in vehicles.

References

- Procedia - Social and Behavioral Sciences* 48:919-31.
- Bohn, C., A. Cortabarria, V. Härtel and K. Kowalczyk. 2003. Disturbance-observer-based active control of engine-induced vibrations in automotive vehicles. *Proceedings of the SPIE's 10th Annual International Symposium on Smart Structures and Materials*. San Diego, March 2003. 5049-68.
- Bohn, C., A. Cortabarria, V. Härtel and K. Kowalczyk. 2004. Active control of engine-induced vibrations in automotive vehicles using disturbance observer gain scheduling. *Control Engineering Practice* 12:1029-39.
- Cauet, S., P. Coirault and M. Njeh. 2013. Diesel engine torque ripple reduction through LPV control in hybrid electric vehicle powertrain: Experimental results. *Control Engineering Practice* 21:1830-40.
- Daafouz, J., G. I. Bara, F. Kratz and J. Ragot. 2000. State observers for discrete-time LPV systems: an interpolation based approach. *Proceedings of the 39th IEEE Conference on Decision and Control* 5:4571-72.
- Darengosse, C., P. Chevrel. 2000. Linear parameter-varying controller design for active power filters. *Proceedings of the IFAC Conference on Control Systems Design*. Bratislava, June 2000. 65-70.
- Du, H. and X. Shi. 2002. Gain-scheduled control for use in vibration suppression of system with harmonic excitation. *Proceedings of the American Control Conference*. Anchorage, May 2002. 4668-69.
- Du, H., L. Zhang and X. Shi. 2003. LPV technique for the rejection of sinusoidal disturbance with time-varying frequency. *IEE Proceedings on Control Theory and Applications* 150:132-38.
- Duan, J., M. Li and T. C. Lim. 2013. Virtual Secondary Path Algorithm for Multichannel Active Control of Vehicle Powertrain Noise. *Journal of Vibration and Acoustics* 135: 0510141-48.
- Duarte, F., P. Ballesteros and C. Bohn. 2013a. H_∞ and state-feedback controllers for vibration suppression in a single-link flexible robot. *Proceedings of the 2013 IEEE/ASME International Conference on Advanced Intelligent Mechatronics*. Wollongong, July 2013. 1719-24.
- Duarte, F., P. Ballesteros, X. Shu and C. Bohn. 2012. Active Control of the Harmonic and Transient Response of Vibrating Flexible Structures with Piezoelectric Actuators. *Proceedings of the International Conference and Exhibition of New Actuators and Drive Systems ACTUATOR 12*. Bremen, June 2012. 447-50.
- Duarte, F., P. Ballesteros, X. Shu and C. Bohn. 2013b. An LPV discrete-time controller for the rejection of harmonic time-varying disturbances in a lightweight flexible structure. *Proceedings of the American Control Conference*. Washington, D.C., June 2013. 4092-97.
- Duarte, F., P. Ballesteros, X. Shu and C. Bohn. 2013c. Rejection of harmonic and transient disturbances of a smart structure with piezoelectric actuators. *Mechanics and Control* 32:41-51.
- Feintuch, P. L., N. J. Bershad and A. K. Lo. 1993. A frequency-domain model for filtered LMS algorithms - Stability analysis, design, and elimination of the training mode. *IEEE Transactions on Signal Processing* 41:1518-31.
- Francis, B. and W. Wonham. 1976. The internal model principle of control theory. *Automatica* 12:457-65.
- Füger, T., N. Lachhab and F. Svaricek. 2012. Parameterreduktion zur Störunterdrückung mit einem diskreten LPV-Regler. *Proceedings of the Workshop of the GMA FA*

- 1.40. Salzburg, September 2012. (In German, Parameter reduction for disturbance rejection with a discrete-time LPV controller.)
- Füger, T., N. Lachhab and F. Svaricek. 2013. Parameter reduction for disturbance attenuation with a discrete-time LPV controller. *Proceedings of the IFAC 5th Symposium on System Structure and Control (Joint Conference)*. Grenoble, France, February 2013. 791-96.
- Gahinet, P. and P. Apkarian. 1994. A linear matrix inequality approach to H_∞ control. *International Journal of Robust and Nonlinear Control* 40:421-448.
- Hanifzadegan, M. and R. Nagamune. 2014. Smooth switching LPV controller design for LPV systems. *Automatica* 50:1481-88.
- Heins, W., P. Ballesteros and C. Bohn. 2011. Gain-scheduled state-feedback control for active cancellation of multisine disturbances with time-varying frequencies. *Mechanics and Control* 30:127-37. Available: http://journals.bgu.ac.il/p1/MECHANICS-CTRL/2011-03/Mechanics_2011_03_03.pdf.
- Heins, W., P. Ballesteros and C. Bohn. 2012a. Experimental evaluation of an LPV-gain-scheduled observer for rejecting multisine disturbances with time-varying frequencies. *Proceedings of the American Control Conference*. Montreal, June 2012. 768-74.
- Heins, W., P. Ballesteros, X. Shu and C. Bohn. 2012b. LPV gain-scheduled observer-based state feedback for active control of harmonic disturbances with time-varying frequencies. In: M. Zapateiro and F. Pozo (eds.), *Advances on Analysis and Control of Vibrations-Theory and Applications*. Rijeka, Croatia: InTech. 35-64. Available: <http://dx.doi.org/10.5772/50293>.
- Horn, R. A. and C. R. Johnson. 1985. *Matrix Analysis*. Cambridge: Cambridge UP.
- Inoue, T., A. Takahashi, H. Sano, M. Onishi and Y. Nakamura. 2004. NV countermeasure technology for a cylinder-on-demand engine- development of active booming noise control system applying adaptive notch filter. *Proceedings of the SAE World Congress and Exhibition*. Detroit, March 2004. SAE Technical Paper 2004-01-0411.
- Kajiwara, H., P. Apkarian and P. Gahinet. 1999. LPV techniques for control of an inverted pendulum. *IEEE Control Systems* 19:44-54.
- Karimi, A. and Z. Emedi. 2013. H_∞ gain-scheduled controller design for rejection of time-varying narrow-band disturbances applied to a benchmark problem. *European Journal of Control* 19:279-88.
- Kinney, C. E. and R. A. de Callafon. 2006a. Scheduling control for periodic disturbance attenuation. *Proceedings of the American Control Conference*. Minneapolis, June 2006. 4788-93.
- Kinney, C. E. and R. A. de Callafon. 2006b. An adaptive internal model-based controller for periodic disturbance rejection. *Proceedings of the 14th IFAC Symposium on System Identification*. Newcastle, Australia, March 2006. 273-78.
- Kinney, C. E. and R. A. de Callafon. 2007. A comparison of fixed point designs and timevarying observers for scheduling repetitive controllers. *Proceedings of the 46th IEEE Conference on Decision and Control*. New Orleans, December 2007. 2844-49.
- Kinney, C. E. and R. A. de Callafon. 2009. *Realtime Controller tuning for Periodic Disturbance Rejection*. Saarbrücken: VDM.
- Köroğlu, H. and C. W. Scherer. 2008. LPV control for robust attenuation of non-stationary sinusoidal disturbances with measurable frequencies. *Proceedings of*

References

- the 17th IFAC World Congress. Seoul, July 2008, 4928-33.
- Kuo, S. M. and D. R. Morgan. 1996. *Active Noise Control Systems*. New York: Wiley.
- Landau, I. D., A. Castellanos Silva, T. B. Airimitoiae, G. Buche and M. Noë. 2013. Benchmark on adaptive regulation-rejection of unknown/time-varying multiple narrow band disturbances. *European Journal of Control* 19:237-52.
- Matsuoka, H., T. Mikasa, and H. Nemoto. 2004. NV countermeasure technology for a cylinder-on-demand engine-development of active control engine mount. *Proceedings of the SAE World Congress and Exhibition*. Detroit, March 2004. SAE Technical Paper 2004-01-0413.
- Ruderman, M., A. Ruderman and T. Bertram. 2013. Observer-based compensation of additive periodic torque disturbances in permanent magnet motors. *IEEE Transactions on Industrial Informatics* 9:1130-38.
- Rugh, W. J. and J. S. Shamma. 2000. Research on gain scheduling. *Automatica* 36:1401-25.
- Sano, H., T. Inoue, A. Takahashi, K. Terai, and Y. Nakamura. 2001. Active control system for low-frequency road noise combined with an audio system. *IEEE Transactions on Speech and Audio Processing* 9:755- 63.
- Sano, H., T. Yamashita and M. Nakamura. 2002. Recent application of active noise and vibration control to automobiles. *Proceedings of the ACTIVE 2002*. Southampton, July 2002. 29-42.
- Shimomura, T. 2003. Hybrid control of gain-scheduling and switching: a design example of aircraft control. *Proceedings of the American Control Conference*. Denver, June 2003. 4639:44.
- Shoureshi, R. and T. Knurek. 1996. Automotive applications of a hybrid active noise and vibration control. *IEEE Control Systems Magazine* 16:7278.
- Shoureshi, R. A., R. Gasser, and J. Vance. 1997. Automotive applications of a hybrid active noise and vibration control. *Proceedings of the IEEE International Symposium on Industrial Electronics*. Guimaraes, December 1997. 107176.
- Shu, X., P. Ballesteros and C. Bohn. 2011. Active vibration control for harmonic disturbances with time-varying frequencies through LPV gain scheduling. *Proceedings of the 23rd Chinese Control and Decision Conference*. Mianyang, China, May 2011. 728-33.
- Shu, X., P. Ballesteros, W. Heins and C. Bohn. 2013. Design of structured discrete-time LPV gain-scheduling controllers through state augmentation and partial state feedback. *Proceedings of the American Control Conference*. Washington, D.C., June 2013. 6090-95.
- Skogestad, S. and I. Postlethwaite. 2005. *Multivariable Feedback Control: Analysis and Design*. New York: Wiley.
- Svaricek, F., T. Füger, H. J. Karkosch, P. Marienfeld and C. Bohn. 2010. *Automotive applications of active vibration control*. In: M. Lallart (ed.), *Vibration Control*. Scio, Croatia: InTech. 303-18. Available: <http://dx.doi.org/10.5772/10149>.
- Unbehauen, H. 2011. *Regelungstechnik III*. Wiesbaden: Vieweg. (In German, Control theory III.)
- Vaidyanathan, P. P. 1985. The discrete-time bounded-real lemma in digital filtering. *IEEE Transactions on Circuits and Systems*, 32:918-24.
- Veenman., J. and C. W. Scherer. 2014. A synthesis framework for robust gain-scheduling controllers. *Automatica* 50:2799-12.

- White, A. P., G. Zhu and J. Choi. 2013. *Linear parameter-varying control for engineering applications*. London: Springer.
- Witte, J., H. M. N. K. Balini and C. W. Scherer. 2010. Experimental results with stable and unstable LPV controllers for active magnetic bearing systems. *Proceedings of the IEEE International Conference on Control Applications*. Yokohama, September 2010. 950-55.
- Zhou, K., J. C. Doyle and K. Glover. 1996. *Robust and Optimal Control*. Englewood Cliffs: Prentice Hall.
- Zhou, K. and J. C. Doyle. 1998. *Essentials of Robust Control*. Englewood Cliffs: Prentice Hall.